THE SYNTHESIS, CHARACTERISATION, PHOTOCHEMICAL AND PHOTOPHYSICAL PROPERTIES OF RUTHENIUM (II) AND OSMIUM (II) POLYPYRIDYL COMPLEXES CONTAINING TRIAZOLE LIGANDS

by

Helen P Hughes, B Sc (Hons)

A Thesis presented to Dublin City University for the degree of Doctor of Philosophy

Supervisor Dr Johannes G Vos

School of Chemical Sciences

Dublin City University

September 1993

To my parents and Peter

This thesis has not previously been submitted as an exercise for a degree at this or at any other university Except as otherwise indicated, this work has been carried out by the author alone

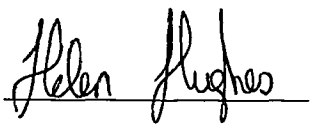

Helen Hughes

ACKNOWLEDGEMENTS

I wish to thank my supervisor, Dr Han Vos for his help, encouragement and patience over the past few years His assistance in the preparation of this manuscript is greatly appreciated

In my own research group, I would like to express my gratitude to Dr Ellie Ryan and Dr Renyi Wang for all their help when I started my thesis Thanks especially to Tia Keyes for many useful chemistry discussions and for putting up with me in Italy and in Belfast Thanks also to Frances, Karen, Miriam, Dave, Margaret, Alan, Andy and Boris, my fellow ruthenium researchers!

I would also like to acknowledge the project students that helped me in my work over the past three years, i e Peter, Juan, Frances, Itxaso, Pascal, Gonzalo, Henning, and Reinhart

I wish to thank Dr J J McGarvey and Tanya Martin of the Chemistry Department at Queens University, Belfast for their help with the resonance Raman measurements I would also like to thank Dr Francesco Barigelletti for carrying out some luminescent lifetime measurements and for his kindness during my stay in Italy Special thanks to Dr Ronald Hage for synthesising a lot of the ligands used in this work and for many useful discussions

To my fellow postgraduates both past and present for their friendship and encouragement particularly Tia, Fiona, Ellie, Catherine, Eithne, Frances, Mick, Mary, Maureen, Barry, Gerry, Eamonn, John, Maureen, Conor, Celia, Mark, James, Ciaran, Pat, Shane, Margaret and many more.

Many thanks also to Dr Conor Long for his assistance with the temperature dependent lifetime measurements and to the members of his research group whom I asked millions of questions, i e Mick, Mary, Maureen and Celia

Thanks to Dr Padraic James for his help with the printing of this document and for his help with the interpretation of some of the NMR data

Thanks also to Eolas and Mayo Co Co for their financial assistance over the past three years and to the Chemistry Department at DCU for the use of their facilities Thanks also to the technical staff for all their help, especially Damien for his NMR expertise and Veronica for her continuous help with the HPLC

Finally, I would like to express my thanks to Peter for his patience, kindness, support and love Also, to my parents for financial assistance, their support and encouragement and to my sister, Mary and my brother, Anthony for their help

ABSTRACT

The synthesis, characterisation, photochemical and photophysical properties of ruthenium (II) and osmium (II) polypyridyl complexes containing 1,2,4-triazole ligands are described These complexes were characterised using HPLC, UV/vis spectroscopy, electrochemistry, NMR, fluorimetry, spectroelectrochemistry, laser flash photolysis and resonance Raman spectroscopy

Firstly, the photochemistry of a series of mononuclear Ru(II) polypyridyl complexes has been investigated Evidence for the existence of a mononuclear photolysis intermediate during the irradiation of $[Ru(bpy)_2(4Mepytr)]^{2+}$ (where 4Mepytr = 4-methyl-3-(pyridin-2-yl)-1,2,4-triazole) was found Photoisomerisation from the N4-bound isomer to the N2-bound isomer of complexes containing the ligand Hpztr (where Hpztr = 3-(pyrazin-2-yl)-1,2,4-triazole) was noted, while the deprotonated species remained photostable

In the main section of the thesis, the photophysical and photochemical properties of a series of dinuclear Ru(II) and Os(II) polypyridyl complexes containing bridging 1,2,4-triazole ligands were examined Investigation into the nature of the lowest emitting state was carried out using mixed-ligand dinuclear Ru(II) polypyridyl complexes, containing the Hbpt ligand (where Hbpt = 3,5-bis-(pyridin-2-yl)-1,2,4-triazole) The nature of the lowest emitting state was found to depend on the polypyridyl ligand, whereas that of the reactive excited state (the ^{3}MC excited state) depended on the asymmetric properties of the bridging ligand The effect of replacing pyridine by the stronger π-accepting pyrazine ring was examined using the ligand Hbpzt (where Hbpzt = 3,5-bis-(pyrazin-2-yl)-1,2,4-triazole) and it was found that the emitting state was bpy-based in the mononuclear species, whereas a switch-over to a pyrazine-based emission occurred upon formation of the dinuclear species A combination of these properties were obtained using the Hppt ligand (where Hppt = 3-(pyrazin-2-yl)-5-(pyridin-2-yl)-1,2,4-triazole) and the photophysical properties investigated in detail Its properties were compared with those obtained for the more symmetrical Hbpt and Hbpzt ligands Again, a switch-over to a pyrazine-based emission occurred upon formation of the dinuclear species and upon protonation of the pyrazine-bound monomer, whereas a bpy-based emission was observed for the pyridine-bound mononuclear complex

Finally, the replacement of the strong σ-donor 1,2,4-triazole ligands by the more strongly π-accepting 1,2,4-triazine ligands was examined The lowest emitting state was found to be pyridyltriazine-based and the effect of substituents on the physical properties of these complexes was evaluated

CONTENTS

CHAPTER 1

GENERAL INTRODUCTION

1.1 NATURAL PHOTOSYNTHESIS

Solar energy captured by the process of photosynthesis is the source of well over 90% of all the energy used by man for heat, light and power, since coal, petroleum ether and natural gas, the fuels for most man-made machines, are all decomposition products of biological material generated millions of years ago by photosynthetic organisms Life on earth, therefore, depends on the flow of energy from the thermonuclear reaction taking place at the heart of the sun However, living cells cannot use solar energy directly Green plants absorb a small fraction of this light energy and transform it into chemical energy This process of photosynthesis is the vital link between the vast energy resources of the sun and the energy needs of the living world[1]

The overall equation for photosynthesis can be written as follows[2]

$$6CO_2 + 6H_2O + \text{light} + \text{chlorophyll} \text{ -----> } C_6H_{12}O_6 \text{ (glucose)} \qquad \textbf{1.1.1}$$

Photosynthetically produced carbohydrates serve as an energy source for the organism that produced them as well as for nonphotosynthetic organisms that directly or indirectly consume photosynthetic plants[3] Therefore, photosynthesis can be defined as the utilisation of solar light energy by plant cells for the biosynthesis of cell components

1 1 1 *Light absorption*

The process of photosynthesis depends upon the efficient capture of light quanta by aggregates of pigments present in photosynthetic tissues Light has to be

absorbed before it can be of any use in a photobiological reaction[2] By far the most important and most abundant of these pigments are the chlorophylls The structure of chlorophyll is illustrated in Figure 1 1 1 Higher plants contain two forms of chlorophyll, designated chlorophyll a (Chl a) and chlorophyll b (Chl b) They are magnesium-porphyrin complexes The four central nitrogen atoms are co-ordinated with a Mg^{2+} ion to form an extremely stable essentially planar complex, with a long hydrophobic side chain[5] It absorbs light principally in the violet and blue wavelengths and also in the red

Photosynthetic cells may contain pigments of two other classes carotenoids (yellow) and phycobilins (red and blue) These pigments serve as supplementary light receptors for portions of the visible spectrum not covered by chlorophyll[4] These pigments are known as the light harvesting complexes

The pigment molecules of the light-trapping apparatus are assembled into arrays that funnel absorbed energy into photoreactive centres These arrays are called photosystems The photosystems are located on the inner membranes of organelles called chloroplasts Chloroplasts must, therefore, be the site of light-induced O_2 evolution

In addition to pigments, electron transport systems are present These carriers form an electron-transport chain that covers the potential span from about -0 1 V to +0 4 V [4]

1 1 2 *Light Reactions*

Chloroplasts contain two photosystems, designated Photosystem I and Photosystem II Photosystem I, with a maximum near 710 nm, is associated with those forms of chlorophyll a absorbing at longer wavelengths and is not responsible for oxygen evolution It raises the energy of the absorbed electrons

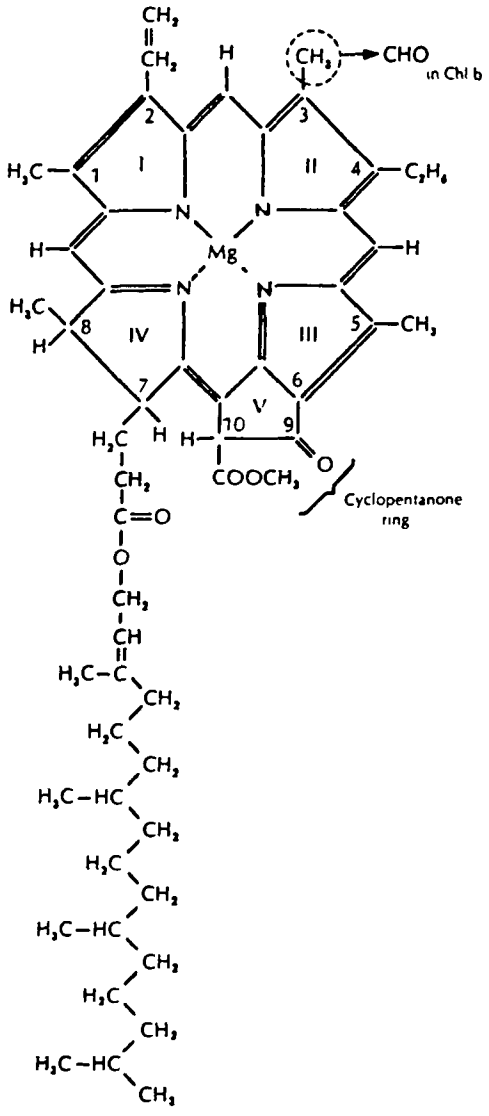

Figure 1 1 1

Structure of chlorophyll [5]

from about +0 4 V to -0 6 V A similar photosystem is found in the membranes of all photosynthetic bacteria Photosystem II, found only in oxygen-evolving photosynthetic bacteria, is activated by shorter wavelengths, 670 nm and below, and it is required for oxygen evolution It raises the energy of an absorbed electron

from about +0 9 V to -0 2 V The two photosystems work together in chloroplasts but have different functions[4]

Light energy first enters Photosystem II (PS-II), where it is responsible for two major events

(1) Electrons transportation

(2) The splitting of water into protons, electrons and oxygen gas (see Figure 1 1 2)

Excitation by absorbed light quanta result in excited electrons which are channelled to P680, the reactive centre of PS-II From here the electrons are passed uphill at increasingly higher energy levels to a primary electron acceptor Some of these electron acceptors are cytochromes[6] The electron is then passed downhill along an electron transport chain to P700, the reactive centre of PS-I In the course of this reaction, ATP (adenosine triphosphate) is formed from ADP (adenosine diphosphate) and phosphate (P_i) This process is known as photophosphorylation

System II probably has a second light reaction that generates a stronger oxidant capable of extracting electrons from water and liberating oxygen The acceptor of the electrons from water would then provide the reducing power needed to reduce the cytochromes after they have been oxidised with the simultaneous reduction of ferredoxin[7]

In photosystem I (PS-I), light energy induces the electronic excitation of pigments This excitation is then channelled by energy transfer to a special chlorophyll a species, named P700, which in turn gets excited and boosts electrons to an electron carrier from which they are passed downhill to the electron acceptor molecule with the consequent formation of $P700^+$ (see Figure 1 1 2) Electrons for the re-reduction of $P700^+$ come from excited PS-II via a central electron transport chain Electrons required to fill the electron holes in PS-II come

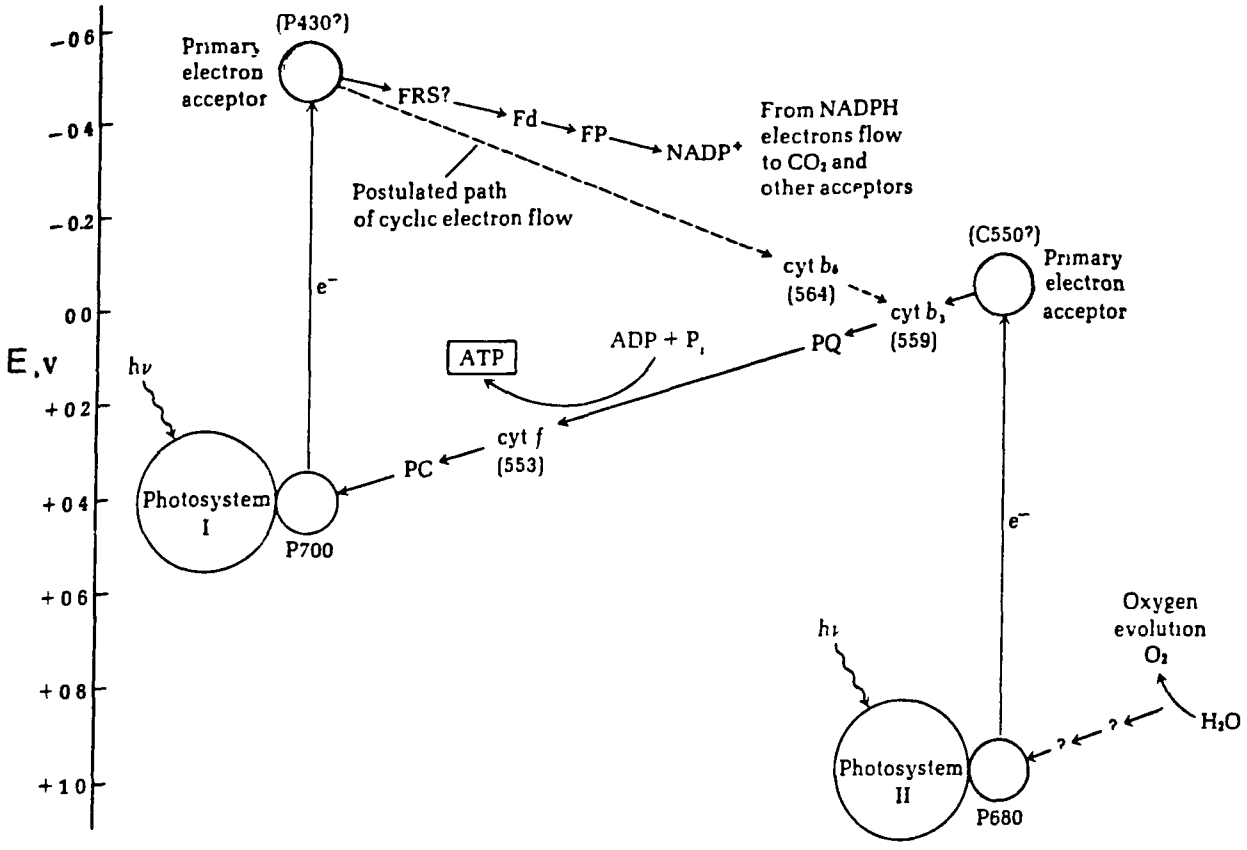

Figure 1 1 2

Mechanism of electron transfer in PS-II and PS-I [5]

from H_2O, which is dehydrogenated and yields O_2 [5] Reduced ferredoxin produced by electron transfer from the primary electron acceptor in PS-I, serves for the reduction of $NADP^+$ (nicotinamide adenine dinucleotide phosphate), a coenzyme which functions as an electron acceptor, and for the reduction of other chloroplast components such as thioredoxin[8] Ferredoxin is also involved in the cyclic electron flow around PS-I, a process which is coupled to proton translocation and ATP synthesis The precise mechanism of which is still poorly understood[9]

These two systems working together result in the conversion of light energy into electrical energy, followed by a flow of electrons, resulting in the electron energy being converted to chemical energy stored in the form of NADPH and ATP

The general equation for the first phase of photosynthesis, i e the light reactions, can be written in the following form

$$2H_2O + NADP^+ + P_i + ADP + h\nu \text{ ----> } \tfrac{1}{2}O_2 + NADPH + H^+ + ATP + H_2O \quad \textbf{1.1.2}$$

The water molecule on the left-hand side of the equation is the donor of the two electrons required to reduce $NADP^+$ and of the oxygen atom that is released as $\tfrac{1}{2}O_2$ The water molecule on the right-hand side of the equation arises from the formation of ATP from ADP and phosphate

As we have already seen, the heart of the photosynthetic process is a photochemical oxidation / reduction reaction in which the energy of a photon is utilised for producing a charge-separated pair capable of acting as reductant in biological processes The process of charge separation takes place in the photosynthetic reaction centres (see Figure 1 1 3)[10] Two of the Bchl b molecules, the so-called "special pair" are closely associated, they are nearly parallel and have an Mg - Mg distance of 7 Å The primary photochemical event of bacterial photosynthesis is absorption of a photon by the special pair This event is nearly instantaneous occupying < 1 fs (10^{-12} s) The excited electron is delocalised over both of them Within 4 ps, the electron has been transferred to the Bpheo a on the right By some 200 ps later, the electron has further migrated to the menaquinone or Q_A, to form the anionic semiquinone radical Q_A^- In fact, this sequence of electron transfers is so efficient that its overall quantum yield is virtually 100% Within approximately 10 µs after its formation Q_A^- transfers its excited electron to the more solvent exposed ubiquinone, Q_B, to form Q_B^- This anionic quinol takes up two protons from the solution on the cytoplasmic side of the plasma membrane for form Q_BH_2 Thus, Q_B is a molecular transducer that converts two light-driven one electron excitations to a two electron chemical reduction The electrons taken

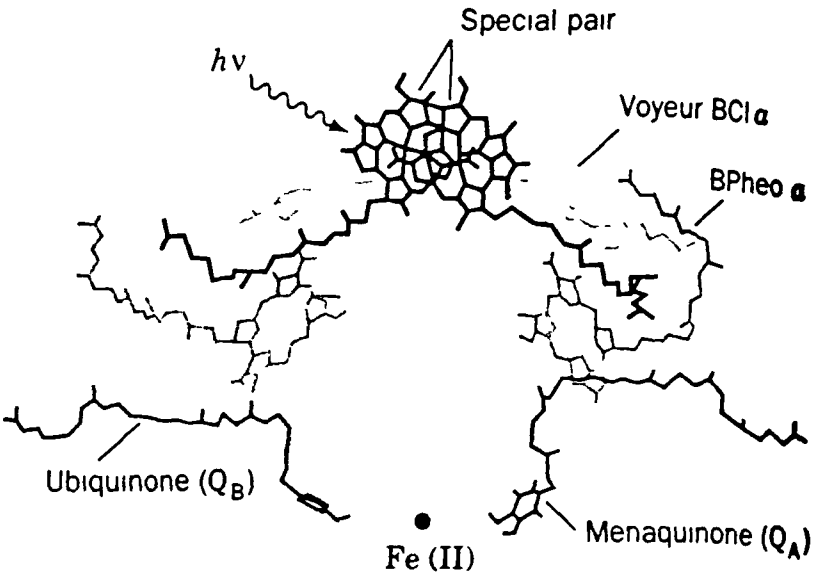

Figure 1 1 3

A bacterial photosynthetic reaction centre[3]

up by Q_BH_2 are eventually returned to $P870^+$ via a complex electron transport chain[3]

1 1 3 *Dark reactions*

In the second stage of photosynthesis, the energy generated by the light reactions is used to incorporate carbon into organic molecules These reactions take place in the stroma of the chloroplasts and do not need light, and so they are often referred to as the "dark reactions" They involve a cycle called "The Calvin Cycle" The dark reactions convert the chemical energy produced by the light reactions in the form of ATP (a compound that has been called the universal energy currency of living cells) and NADPH (the carrier of energy-rich electrons that, together with protons, provide the hydrogen atoms used in the biosynthesis of organic compounds) into forms more suitable for storage and transport and also build the basic carbon structures from which all the other organic molecules of living systems are produced This last process is known as carbon fixation[11]

The Calvin cycle as shown in Figure 1 1 4, begins when carbon dioxide enters the cycle and is incorporated into ribulose-1,5-bis-phosphate (RuBP, a five-carbon sugar with two phosphates attached) RuBP then splits to form two molecules of 3-phosphoglycerate (PGA) The enzyme responsible for this reaction is RuBP carboxylase Each step is regulated by a specific enzyme At each full turn of the cycle, a molecule of CO_2 enters the cycle, is reduced, and a molecule of RuBP is regenerated Six revolutions of the cycle, with the introduction of six atoms of carbon are necessary to produce a 6-C sugar, such as glucose The overall equation is[1]

$$6RuBP + 6CO_2 + 18ATP + 12NADPH \text{ -----> } 6RuBP + glucose + 18P_i + 18ADP + 12NADP^+ \qquad \textbf{1.1.3}$$

During the day, plants satisfy their energy needs via the light and dark

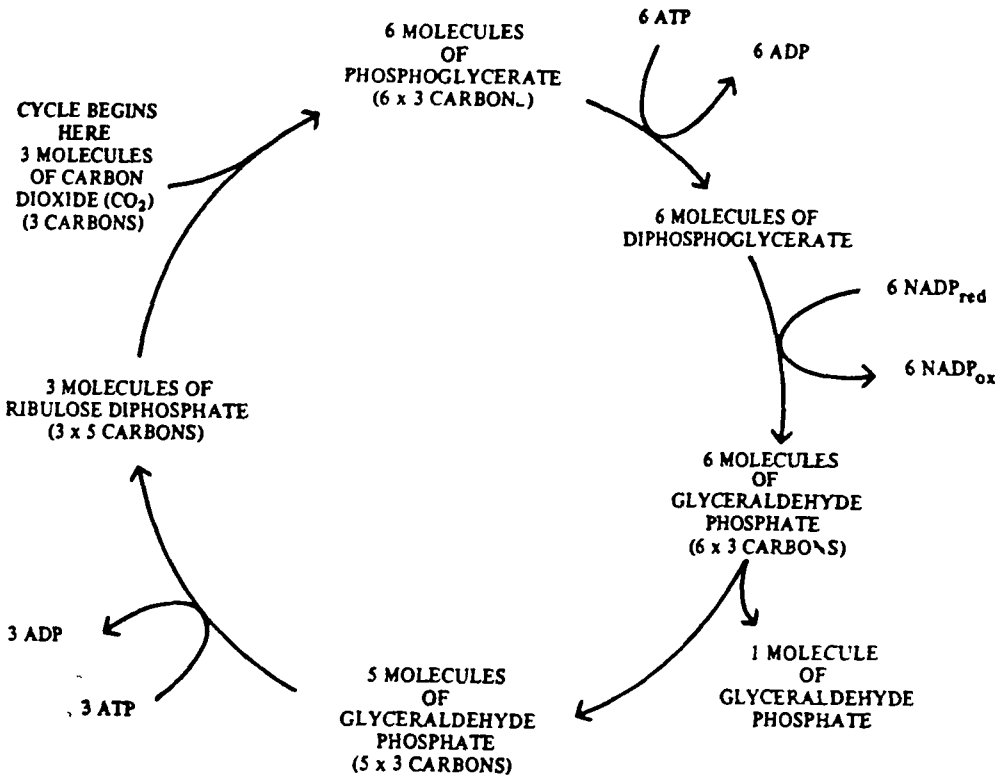

Figure 1 1 4

The Calvin cycle [1]

reactions of photosynthesis At night, however, like other organisms, they must use their nutritional reserves to generate their required ATP and NADPH through glycolysis, oxidative phosphorylation and the pentose phosphate pathway Plants, therefore, have a light-sensitive control mechanism to prevent the Calvin cycle from consuming the catabolically produced ATP and NADPH The activity of RuBP carboxylase responds to four light-dependent factors

(1) It varies with pH Upon illumination, the pH of the stroma increases from around 7 0 to about 8 0 as protons are pumped from the stroma into the

thylakoid space RuBP carboxylase has a sharp pH optimum near pH 8 0

(2) It is stimulated by Mg^{2+} Light-induced influx of protons to the thylakoid space is accompanied by the efflux of Mg^{2+} to the stroma

(3) It is activated by NADPH, which is produced by illuminated PS-I.

(4) It is strongly inhibited by 2-carboxylarabinitol-1-phosphate, which many plants synthesise only in the dark

Thus, in plants light stimulates the Calvin cycle while deactivating glycolysis, whereas darkness has the opposite effect (that is, the so-called dark reactions do not occur in the dark)[3]

1 1 4 *Summary*

In summary, water is used as an electron donor and from it oxygen is evolved during photosynthesis The first stage of photosynthesis (the light reactions) results in the reduction of $NADP^+$ and the phosphorylation of ADP In the second state (the dark reactions), NADPH and ATP are used to reduce CO_2 to hexose

Phosphorylation of ADP is coupled to photoinduced electron transport in the chain between PS-I and PS-II Photoinduced electron transport is occurring during the net transfer of electrons from water to $NADP^+$ At least one molecule of ATP is generated per pair of electrons passing from H_2O to $NADP^+$ Apparently, eight light quanta are required to evolve each molecule of O_2 and to reduced one molecule of CO_2, for which two molecules of NADPH and three molecules of ATP are necessary[5]

1.2 ARTIFICIAL PHOTOSYNTHESIS

The elucidation of the structure of the bacterial photosynthetic reaction centre caused a marked change in direction for fundamental research aimed at constructing artificial photosynthetic devices[12] The study of photoinduced electron-transfer reactions within large macromolecular units has dominated the subject of artificial photosynthesis for the past number of years[13-15]

Considerable effort has been expended to develop artificial models that mimic various aspects of natural photosynthesis[16] A main goal is the use of solar photons to split water into hydrogen and oxygen, thereby converting solar energy into electrical energy Hydrogen is very energy-rich, it is a clean-burning fuel, giving only water as the product Pollution problems, an integral part of other energy producing systems, would be reduced tremendously if hydrogen was burned instead of hydrocarbons Furthermore, the direct conversion of sunlight and very abundant raw materials into high energy chemicals, which can be further converted to fuels that can be used to heat homes, make electricity, run cars, etc , is a very attractive prospect[17]

In analogy to the structure of the photosynthetic reaction centre, efficient electron transfer in artificial photosynthetic systems has been accomplished in organised micro-heterogeneous media and also in sensitizer relay assemblies possessing a covalent linkage of donor, sensitizer and electron acceptor (relay)[18]

1 2 1 *Supramolecular complexes*

In the last few years, a trend to study artificial assemblies of two or more molecular components has emerged with the dual aim of making progress towards the understanding of photobiological processes and the design of artificial systems

capable of performing useful functions These species are known as supramolecular compounds[19-20] In the area of co-ordination chemistry, one can distinguish three types of supramolecular systems

(1) Second-sphere co-ordination compounds, i e complexes associated to other species by electrostatic interactions, hydrogen bonds, or other intramolecular forces

(2) Cage-type co-ordination compounds, i e complexes in which a metal ion is encapsulated in a single, polydentate ligand

(3) Molecular building blocks linked via bridging units by means of covalent or co-ordination bonds[19]

What is clear from photobiology is that any valuable photochemical function requires a complex elaboration in time of the absorbed light energy input by a system suitably organised in the dimensions of space and energy The complexity of the natural systems, however, makes immediately clear that any synthetic effort aimed at their exact duplication would be hopeless The assembly of suitable molecular components into an appropriate supramolecular structure so as to obtain an organised sequence of chemical acts leading to the desired function is the real aim of supramolecular chemistry An appropriate assembly of these molecular components capable of performing light-induced functions can be called a "photochemical molecular device" (PMD)[21]

A PMD can have a number of functions which have been summarised as follows

(1) Generation and migration of electronic energy,

(2) Photoinduced vectorial transport of electric charge,

(3) Photoinduced conformational changes,

(4) Control and tuning of the photochemical and photophysical properties of molecular components[21]

The area of supramolecular photochemistry is currently active along three research lines

(1) Photochemical and photophysical studies on adducts of transition metal complexes with organic or inorganic species

(2) Photoinduced electron and energy-transfer processes in covalently-linked molecular building blocks (e g polynuclear metal complexes)

(3) Photochemical and photophysical studies on rotaxanes, catenanes, and related species[22].

We will be dealing mostly with the first two applications

1 2 2 *Metal co-ordination complexes*

For d^6 metal complexes, synthetic control and tuning of important properties such as excited-state energy and lifetime, emission yields, photoreactivity and excited-state redox potentials is now feasible Particularly interesting from the point of view of artificial photosynthetic systems are molecular systems that contain two or more metal centres connected by bridging ligands, i e supramolecular species To obtain a photochemically interesting polynuclear complex, an "assembling procedure" is usually followed, i e starting with mononuclear complexes having well-defined individual properties and then making the appropriate chemical connections between these units[23-24]

The extensive use of complexes as luminescent species, electron transfer photosensitizers and chemiluminescence inducers has evidenced the need for compounds that, while exhibiting the desired spectroscopic properties, do not undergo dissociation when they are photoexcited, oxidised and/or reduced[25].

One of the most interesting and extensively studied co-ordination compounds is $[Ru(bpy)_3]^{2+}$ and its derivatives The unique combination of

chemical stability, redox properties, excited state reactivity, luminescent emission and excited state lifetime has attracted the attention of many research workers The results show that in polynuclear systems, fast (subnanosecond) intramolecular electron transfer between adjacent $[Ru(bpy)_2]^{2+}$ chromophores always leads to 100% efficient population of the lowest energy chromophore. Systems of this type exhibit an "antenna effect" similar (though probably different in mechanism) to that by which the antenna pigments increase the effective absorption cross-section of the special pair in natural photosynthetic reaction centres[23] It is conceivable that artificial antennas of this type, but of larger size can be constructed by replacing the terminal units with polymeric chromophoric chains[26-27]

The conclusions that have been reached concerning energy transfer processes in polynuclear systems are as follows

(1) The energy of the donor state must be higher than the energy of the acceptor state

(2) The participation of bridging ligand orbitals in the excited states involved in energy transfer are essential, and

(3) The efficiency of energy transfer is attenuated by distance to a greater degree than what is observed for excited-state, electron-transfer reactions, which are reasonably efficient over relatively long distances[23]

1 2 3 *Photochemical water decomposition*

Tris(2,2'-bipyridine)ruthenium(II) has been recognised as a potential catalyst for the decomposition of water by irradiation of solar light[28] The photodecomposition can be regarded as two half-cell reactions

$$H_2O + e^- \text{-----> } \tfrac{1}{2}H_2 + OH^- \qquad \textbf{1.2.1}$$

$$\tfrac{1}{2}H_2O \text{-----> } \tfrac{1}{4}O_2 + H^+ + e^- \qquad \textbf{1.2.2}$$

This reaction cannot occur in the dark as it is endothermic by 1 23 eV In principle, excitation with visible light should make the process thermodynamically favourable However, as H_2O is unable to absorb the exciting light, the reaction cannot occur[28] This "potential" photochemical reaction can be induced (or sensitised) by a species which possesses specific redox, spectroscopic and excited-state properties Such species are called light absorption sensitizers (LAS) Similarly, "potential" chemiluminescent reactions can be induced by suitable species that can be called light emission sensitizers (LES) Figure 1 2 1 shows the method of operation of these sensitizers

As early as 1975, Creutz and Sutin[29] discovered that using absorption of light in the visible region, $[Ru(bpy)_3]^{2+}$ yields $^*[Ru(bpy)_3]^{2+}$ which is, in principle, capable of reducing water or hydrogen ion to dihydrogen in the pH range 0-14, with concomitant production of $[Ru(bpy)_3]^{3+}$ This latter species may be reduced by hydroxide according to the following equation

$$[Ru(bpy)_3]^{3+} + OH^- \text{------> } [Ru(bpy)_3]^{2+} + \tfrac{1}{4}O_2 + \tfrac{1}{2}H_2O \qquad \textbf{1.2.3}$$

to form dioxygen and regenerate the starting material It was later found[30] that a redox catalyst such as ruthenium dioxide, RuO_2, markedly effected the rate of oxygen formation, and was, therefore, a necessary part of the water-splitting process

Further investigation into the use of catalysts in this reaction lead Gratzel et al [31] to study colloidal TiO_2 particles loaded with ultrafine deposits of Pt and RuO_2 Such a catalyst is surprisingly efficient in coupling H_2 and O_2 production to a

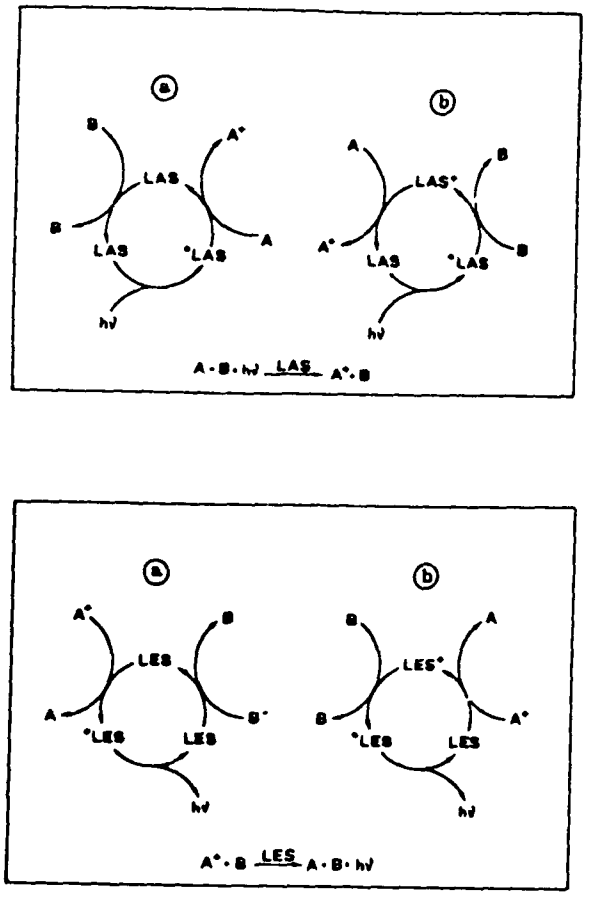

Figure 1 2 1

Operation of LAS and LES[28]

light-driven redox reaction in which an electron relay such as methyl viologen (MV^{2+}) is reduced by the CT excited state of $[Ru(bpy)_3]^{2+}$ The electron relay is reduced on light excitation, and the photoreaction is coupled with catalytic steps generating H_2 and O_2 from water[32] At this stage, sustained photochemical cleavage of water by photocatalysts has been achieved, but still remains fairly inefficient

Subsequent studies[33] involved addition of a suitable quencher to prevent back-reaction of $[Ru(bpy)_3]^{3+}$ to $[Ru(bpy)_3]^{2+}$ Both EDTA (ethylenediaminetetraacetate) and TEOA (triethanolamine) proved to be suitable reducing agents

Various other attempts at improving the efficiency of the photoinduced decomposition of water included optimisation of pH conditions[34] and changing the redox catalysts[35] Two redox schemes for (a) the reduction of water into H_2 on platinum using TEOA as the sacrificial electron donor and (b) oxidation of H_2O to O_2 on ruthenium dioxide using $[Co(NH_3)_5Cl]^{2+}$ as a sacrificial electron acceptor are presented in Figures 1 2 2 and 1 2 3 respectively[36]

Gratzel et al have succeeded in constructing a photovoltaic cell with an energy conversion efficiency that is commercially realistic[37-38] A thin transparent film of TiO_2 particles coated with a single molecular layer of a ruthenium complex is used, and allows the conversion of more than 80 % of incident light photons to electrical current Other studies involved incorporating $[Ru(bpy)_3]^{2+}$ and MV^{2+} in micellar microenvironments in an attempt to increase the reaction rate by increasing the local reagents concentration[39] and tuning the excited-state properties in the Ru(II) polypyridyl family[28] in an attempt to overcome problems associated with using $[Ru(bpy)_3]^{2+}$ as a photosensitizer This latter method has extensive possibilities, however, as to date no other complex has been produced with properties to exceed those of the Ru(II) polypyridyl complexes in the photochemical decomposition of water

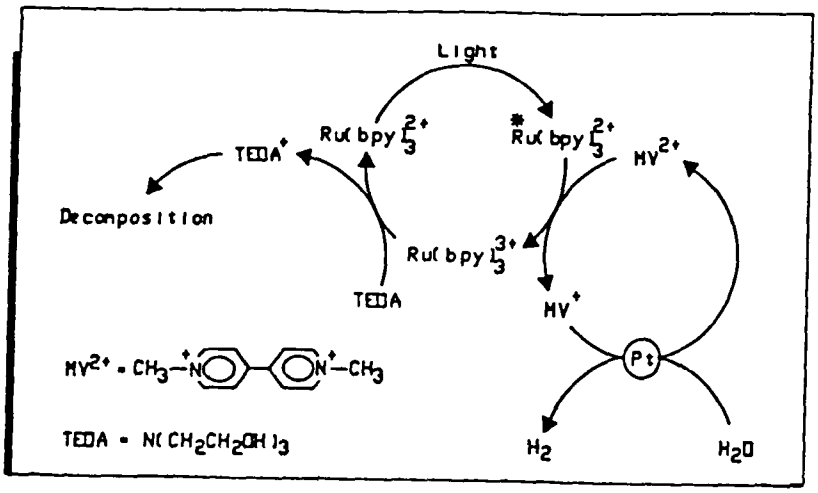

Figure 1 2 2

Redox scheme for the conversion of H_2O into H_2 [36]

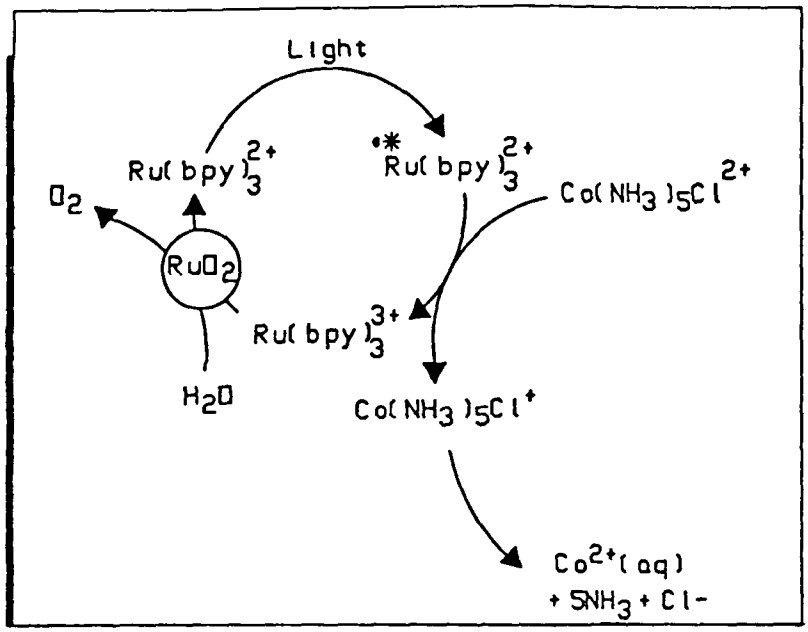

Figure 1 2 3

Redox scheme for the conversion of H_2O into O_2 [36]

1.3 THE PHOTOPHYSICAL PROPERTIES OF $[Ru(bpy)_3]^{2+}$

As already mentioned, Ru^{2+} is a stable, low-spin d^6 system and the polypyridyl ligands are usually colourless molecules possessing σ-donor orbitals localised on the nitrogen atoms and π-donor and π*-acceptor orbitals more or less delocalised on the aromatic rings Figure 1 3 1 contains a schematic representation of the structure of $[Ru(bpy)_3]^{2+}$ [28]

1 3 1 *Absorption and Emission properties*

Visible light absorption in $[Ru(bpy)_3]^{2+}$ is dominated by intense absorption bands arising from dπ(Ru) - π*(bpy) metal-to-ligand charge-transfer (MLCT) transitions[40-41] These transitions have significant absorptions in the visible region The maximum wavelength of absorption for $[Ru(bpy)_3]^{2+}$ is 452 nm Transitions within the ligand π-bonding orbital to the π*-antibonding orbital, labelled π-π* or ligand-centred transitions usually lie at higher energies (185 and 285 nm), have high extinction coefficients and are substantially ligand in character In addition, transitions such as promotion of an electron from a t_2 orbital to an e orbital are possible and such d-d or metal-centred transitions give rise to weak (Laporte forbidden) absorption bands (322 and 344 nm)[42] Figure 1 3 2 contains the electronic absorption spectrum of $[Ru(bpy)_3]^{2+}$, showing the various electronic transitions occurring upon excitation with visible light

The upper excited states of transition metal complexes can participate either in a chemical reaction or undergo efficient radiationless deactivation to the lowest excited state[28] Figure 1 3 3 contains a diagrammatic representation of the photophysical properties of $[Ru(bpy)_3]^{2+}$ For $[Ru(bpy)_3]^{2+}$, the lowest excited-state is a ^{3}MLCT excited-state[43] In fact, the efficiency of intersystem crossing

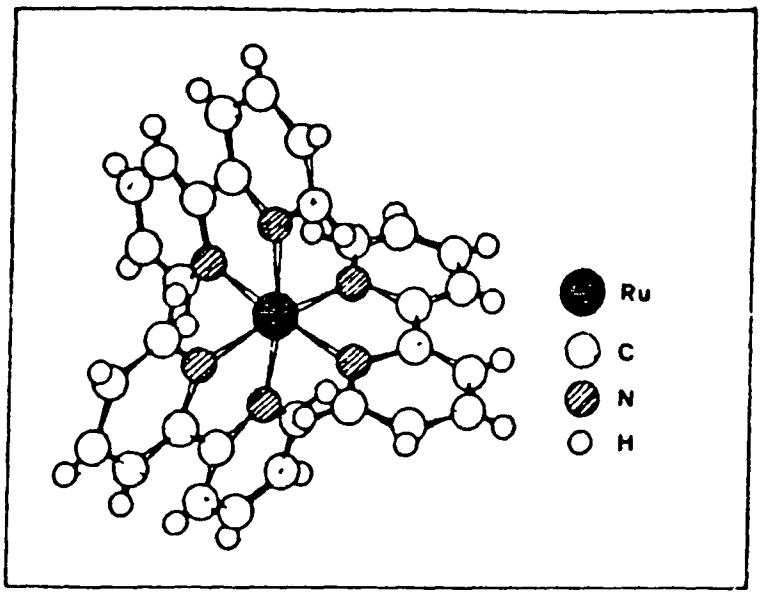

Figure 1 3 1

Schematic representation of the structure of $[Ru(bpy)_3]^{2+}$ [28]

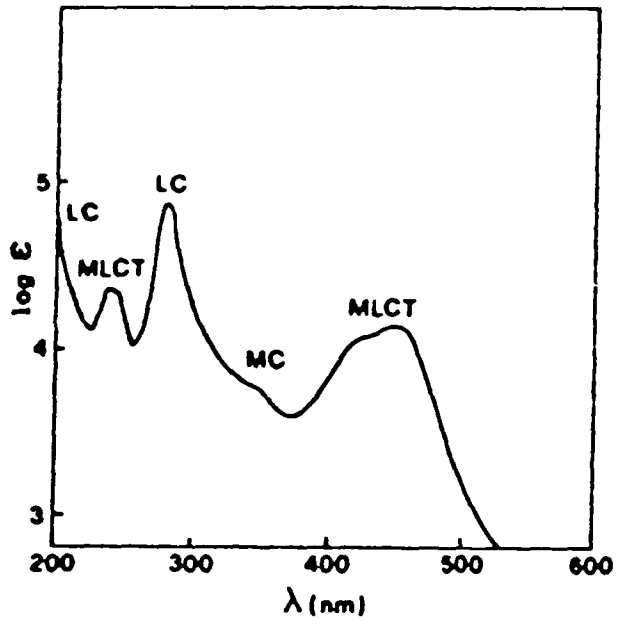

Figure 1 3 2

The electronic absorbance spectrum of $[Ru(bpy)_3]^{2+}$ [28]

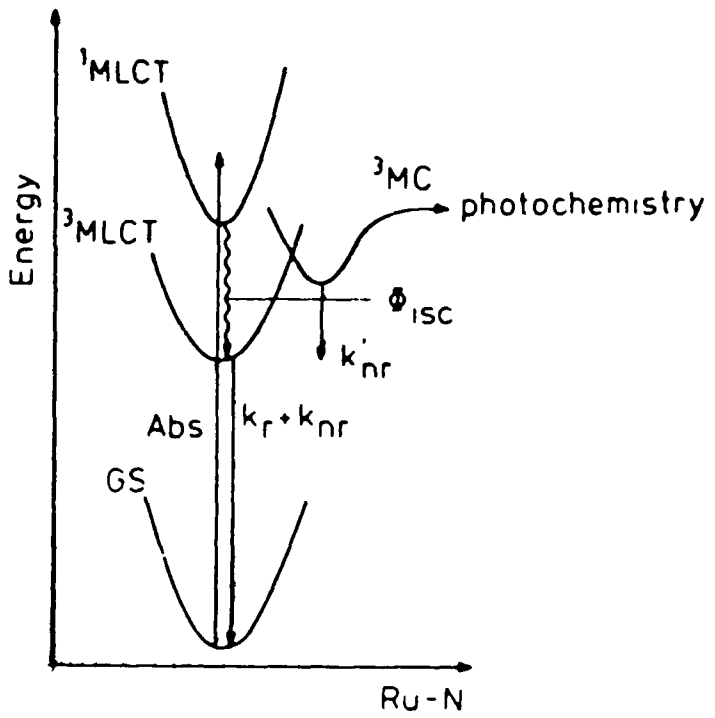

Figure 1 3 3

The photophysical properties of $[Ru(bpy)_3]^{2+}$ [43]

from the upper singlets (^{1}MLCT) obtained by excitation to the lowest triplet is essentially unity The large spin-orbital coupling present in this complex makes this spin-forbidden transition allowed[44] This ^{3}MLCT excited-state is the emissive excited-state Low temperature (4 - 77 K) measurements of the banded emission

of $[Ru(bpy)_3]^{2+}$, including its phosphorescence quantum yield (ϕ_p) and lifetime (τ) indicate the presence of three electronic components in the emitting state with the upper two members situated approximately 10 and 60 cm^{-1} above the lowest[45] The excited-state lifetime is temperature dependent and increases rather dramatically as the temperature is increased[46] This behaviour has been successfully interpreted in terms of a thermally equilibrated Boltzmann population of several low-lying excited states with lifetimes which are temperature independent From the temperature dependent lifetime measurements, evidence for localisation of the excited electron on one of the bpy ligands is found, although electron hopping from one ligand to another occurs on a rapid timescale[47] Evidence also exists for the presence of a fourth low-lying ^{3}MLCT state about 800 cm^{-1} higher in energy Unfortunately, the ability to observed the fourth MLCT state for $[Ru(bpy)_3]^{2+}$ is probably masked by a surface-crossing process to low-lying dd states However, since the dd state does not appear to luminesce appreciably, the fourth MLCT state may be detectable from changes in emission spectra as a function of temperature[48]

1 3 2 *Lifetime of the emitting state*

The large energy-gap between the lowest excited states and the ground-state allows radiative processes (emission) to compete with non-radiative ones (quenching)[49] The fraction of the luminescent set of excited states which undergo radiative decay may be expressed as follows

$$\phi_r = k_r / k_r + k_{nr} \qquad \textbf{1.3.1}$$

where k_r and k_{nr} represent the rate constants for radiative and non-radiative decay of this luminescent set of states, respectively[50] As mentioned previously, there are additional, low-lying MLCT states (in particular the fourth MLCT excited-state) which can play a role in non-radiative decay Population of dd states following MLCT excitation by internal conversion from the ^{3}MLCT to the ^{3}MC excited states, can lead to at best non-radiative decay, but can also lead to ligand-loss photochemistry[51], which is a major problem for utilisation of this complex in solar-energy conversion systems

When the lifetime of the excited-state is sufficiently long (non-radiative decay is inefficient), the excited molecule may have a chance to encounter a molecule of another solute For $[Ru(bpy)_3]^{2+}$, only the lowest spin-forbidden excited-state satisfies this requirement (0 6 μs at room temperature in degassed aqueous solution)[28] Energy-transfer or electron-transfer (either by the oxidation or the reduction of the excited-state) may occur as follows

$^*A + B \text{ ------> } A + {}^*B$	Energy transfer	**1.3.2**
$^*A + B \text{ ------> } A^+ + B^-$	Oxidative electron transfer	**1.3.3**
$^*A + B \text{ ------> } A^- + B^+$	Reductive electron transfer	**1.3.4**

The ability to undergo energy transfer is related to the 0 - 0 spectroscopic energy levels (the energy gap between the ground-state and the ^{1}MLCT excited state) of the donor-acceptor pair and that of electron transfer is related to the redox potentials[42] These processes can be used in the following manner

(1) To utilise well defined MLCT excited-states to explore the fundamental details of how electron and energy-transfer occur

(2) To learn how to prepare molecular assemblies in which long range energy or electron-transfer can occur and, in doing so, to mimic, for example, the reaction centre in photosynthesis

(3) To prepare assemblies which can act as interfaces between simple excited state electron-transfer and the multi-electron catalysts that are required to carry out such small molecular redox reactions as the oxidation of water to O_2 or the reduction of CO_2

(4) To translate the solution based photochemistry to polymeric films where it may be possible to utilise molecular level photochemistry in device-like applications[29]

Therefore, the ease of energy and electron-transfer in the excited state associated with $[Ru(bpy)_3]^{2+}$ and its derivatives make it an ideal candidate for investigating these processes

1 3 3 *Photochemical properties*

As mentioned previously, the high chemical stability of $[Ru(bpy)_3]^{2+}$ in more than one oxidation state and its high light absorptivity in the visible made it an attractive candidate for exploiting solar energy conversion possibilities However, at higher temperatures additional temperature-dependent processes such as population of low-lying ^3MC excited states which can lead to ligand-loss photochemistry and, therefore, to loss of the useful properties associated with $[Ru(bpy)_3]^{2+}$ can occur These temperature dependent processes play a role in dictating the photochemical and photophysical applications of the complex

The mechanism of the observed photochemistry is not fully understood, but it is thought to occur in the following manner (see Figure 1 3 4)[52] The photochemical reaction is initiated by thermal activation to an upper, presumably

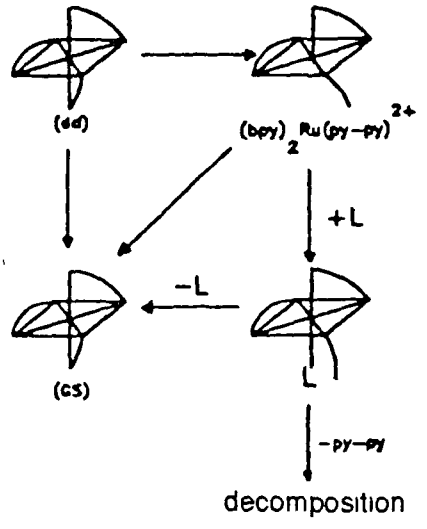

Figure 1 3 4

Mechanism of ligand-loss photochemistry occurring in $[Ru(bpy)_3]^{2+}$ [52]

dd state, following population of the ^3CT state From available evidence, it is expected that the ^3MLCT and the ground-state are probably structurally related, at least in terms of the Ru - N co-ordination environment For a dd excited state, an antibonding, metal-based orbital of e symmetry is occupied which is expected to lead to significant distortions along the Ru - N bonding axes Substitution appears to occur from the dd state by a thermally activated dissociative mechanism, with

the formation of a five co-ordinate intermediate, which is square pyramidal in structure There is then direct evidence for the six co-ordinate unidentate intermediate shown in Figure 1 3 4 (where L = the co-ordinating anion, Cl^- or a solvent molecule such as MeCN)[53] There is at this stage competition between chelate ring closure to give $[Ru(bpy)_3]^{2+}$ and loss of bpy to give $[Ru(bpy)_2L_2]$ The former is favoured in aqueous solutions, whereas the latter is favoured in more non-polar solutions such as CH_2Cl_2

1 3 4 *Redox properties*

Oxidation of Ru(II) polypyridyl complexes usually involves a metal-centred orbital, with formation of genuine Ru(III) complexes, which are inert to ligand substitution

$$[Ru^{II}(bpy)_3]^{2+} \text{ -----> } [Ru^{III}(bpy)_3]^{3+} + e^- \qquad \textbf{1.3.5}$$

Ru(II) / Ru(III) potentials in the complexes usually fall in a rather narrow range around +1 25 V versus NHE Substitution of one or more polypyridine ligands by another similar type ligand can drastically change their potentials

Reduction of Ru(II) polypyridyl complexes usually takes place on a ligand π^* orbital

$$[Ru^{II}(bpy)_3]^{2+} + e^- \text{ -----> } [Ru^{II}(bpy)_2(bpy^-)]^+ \qquad \textbf{1.3.6}$$

Up to six electrons can be pumped into $[Ru(bpy)_3]^{2+}$, yielding a highly reduced complex which can be formulated as $[Ru^{II}(bpy^{2-})_3]^{4-}$ [28] The π^*_L orbital that is involved in the reduction processes is usually the same orbital which is involved in

the MLCT transition Correlations exist between the electrochemical and spectroscopic data

Because of its higher energy content, the excited state is both a stronger reductant and a stronger oxidant than the corresponding ground-state[29] In other words, the excited state can be formulated as $[Ru^{III}(bpy)_2(bpy^-)]^{2+}$ The electron deficient Ru^{III} centre is a strong oxidising agent and the electron proficient bpy^- acts as a strong reducing agent In fact, the 3+ ion is capable of oxidising water to O_2 (E_0 (O_2 / H_2O) = +1 23 V) and the 1+ state is also capable of reducing water to H_2 (E_0 (H^+ / H_2) = 0 0 V)

Excited state redox potentials can be tuned by changing the ground-state redox potentials and / or the excited state energy Since reduction usually takes place on a ligand, the ground-state reduction potential will be roughly related to the reduction potential of the free ligand However, the ability of a co-ordinated ligand to accept an electron also depends on the amount of charge transferred to the metal or received from the metal via the σ and π bonding by the other ligands Similarly, the oxidation potential depends on the amount of charge localised on the metal A change in the oxidation potential of the ground state causes a change in the excited state oxidation potential[48]

1.4 FINE TUNING OF THE EXCITED STATE

In catalytic photoredox applications, photochemical substitutions can be suppressed by the addition of sufficient quencher to capture the ^{3}MLCT excited state before surface crossing to the ^{3}MC excited-state can occur[54] Also, it would be desirable to control the factors involved in determining the relative ordering of the ^{3}MLCT and dd excited-state energies in Ru(II) polypyridyl complexes For a

series of $[Ru^{II}(bpy)_2(L)]^{n+}$ complexes, variations in L can significantly affect the relative position of the dd state and, hopefully, increase the energy-gap between the ^{3}MLCT and ^{3}MC excited states, thus preventing population of the deactivating state[55] Therefore, control of the luminescence properties of complexes hinges on control of the relative state energies and the nature and energy of the lowest excited-state[56]

We have already seen that the σ-donor and π-donor / π-acceptor properties of the co-ordinating ligand significantly influence the redox potentials of these compounds As the spectroscopic and redox properties are closely related, changes in the co-ordinating ligands can also influence to a larger degree the positions of the CT bands and the ^{3}MC excited state With an appropriate combination of ligands, it should be possible to increase the ^{3}MLCT -^{3}MC energy gap to a sufficiently large extent that population of the ^{3}MC excited state is prevented Thus, ligand loss photochemistry is eliminated[57]

In fact, these complexes are also strongly influenced by both solvent and by ion-pair formation Both the emission energies and the emission lifetimes were found to vary on changing the anion[58] As the emission energy increases, the emission lifetime also increases This ion-pair effect may be useful to produce a fine-tuning of the excited-state properties Changing the central metal ion, for example, turning to osmium complexes which have larger spin-orbital coupling constants, can also prevent population of this ^{3}MC excited state

1 4 1 *The effect of specific co-ordinating ligands*

Apart from $[Ru(bpy)_3]^{2+}$, most attention has been focused on systems containing at least one strong π-accepting ligand Specific examples of such ligands are 2,2'-bipyrazine (bpz)[59-65], 2,2'-bipyrimidine (bpm)[66-69], 2,2'-biquinoline (biq)[70-72] and

2,3-bis-(2-pyridyl)-pyrazine (dpp)[73-78] The structure of these ligands and the rest of the ligands cited in the text is given in Figure 1 4 1 The attraction of replacing one bpy ligand by a strong π-acceptor ligand lies in the ability of this ligand to red-shift the absorption and emission energies, thereby, facilitating a larger portion of the energy of the sun to be harvested As the number of these ligands increase, the potential of the $Ru^{III}Ru^{II}$ couple also increases, indicating that these ligands are also weaker σ-donors than bpy, which has the effect of stabilisation of the Ru^{II} metal ion[79] Further stabilisation of Ru(II) could then occur by backbonding of the dπ orbitals with the π* level of the co-ordinating ligands This interpretation would suggest that the lower π* levels in a ligand like bipyrazine would result in more effect mixing with the metal dπ energy levels and result in stabilisation of the $(d\pi)^6$ configuration for Ru(II)[63], but also destabilisation of the ligand π* level As a result, the ligand-field splitting of Ru(II) is much smaller and after excitation of the complex, the ^{3}MC state becomes very easily populated and the emission yield is diminished

Alternatively, the lower π* levels for these ligands leads to changes in the excited and ground-state redox potentials as a consequence of changes in electronic structure, but the photophysical properties of the emitting ^{3}MLCT states are largely unaffected[62] As a result, in some cases the energy gap between the ^{3}MLCT and ^{3}MC excited states is larger than in $[Ru(bpy)_3]^{2+}$ and photostable complexes have been obtained[62]

Recently, there has been increased interest in systems containing at least one strong σ-donating ligand Specific examples of such ligands include bibenzimadazoles[80-86], pyrazoles (pz)[87-89], imidazoles[90-91] and 1,2,4-triazoles[92-98] Because of their stronger σ-donor ability compared with bpy, the π* levels are much higher in energy and, therefore, in mixed-ligand chelates, the emission is always bpy-based Larger ligand-field splitting may result, thus, preventing

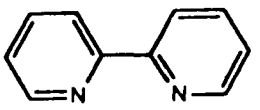

2 2 bipyridine (bpy)

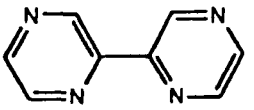

2 2 bipyrazine (bpz)

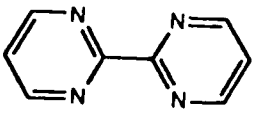

2 2 -bipyrimidine (bpm)

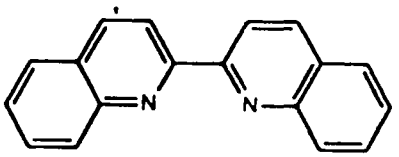

2 2 biquinoline (biq)

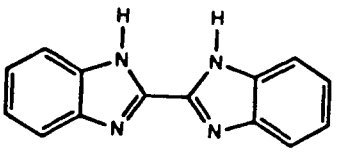

H_2bim

2,2'-bisbenzimidazole

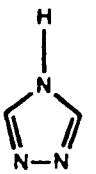

1 2 4 triazole (Htrz)

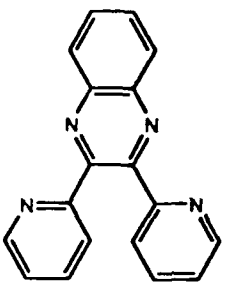

bpq

2,3-bis(2-pyridyl)quinoxaline

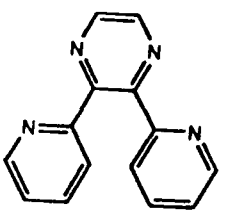

dpp

2,3-bis(2-pyridyl)pyrazine

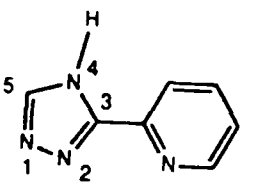

Hptr

3-(pyridin-2-yl)-1,2,4-triazole

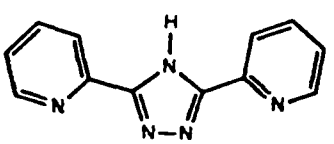

Hbpt

3,5-bis(pyridin-2 yl)-1,2,4-triazole

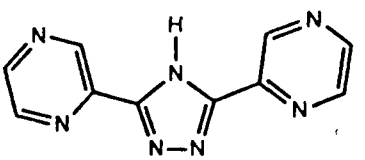

Hbpzt

3,5 bis(pyrazin-2-yl) 1,2,4-triazole

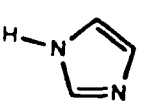

imidazole (Him)

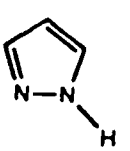

pyrazole(Hpz)

Figure 1 4 1

Structures of the ligands cited in the text

photodecomposition occurring A blue shift of the MLCT band energies also results, which may be a disadvantage for solar energy capture

1 4 2 *Dinuclear complexes*

Dimeric Ru(II) complexes are of interest because, if certain lifetime constraints are satisfied, they could in principle act as a two-electron transfer reagent when excited by two photons and are the first step to a more indepth understanding of the potential applications of supramolecular species However, many of the dinuclear species prepared containing strong π-accepting ligands do not satisfy the criteria of ligand-field strength and/or co-ordination about each Ru(II) ion necessary for luminescence Luminescence is not necessarily a prerequisite for photoredox behaviour, but its presence is a desired property as a convenient probe of the excited state[74]

Studies with previously synthesised Ru(II) dimers, suggest that, in general, deviations from a bipyridine-like structure in the bridging ligand cause a loss of the dπ* luminescence characteristic of $[Ru(bpy)_3]^{2+}$ and its homologues For example, the monomer $[Ru(bpy)_2(bpm)]^{2+}$ is luminescent when dissolved in acetonitrile at room temperature, but the corresponding bridged dimer $[Ru(bpy)_2(bpm)Ru(bpy)_2]^{4+}$ is not[73,76,78] Similar results for dinuclear complexes containing the ligands 2,2'-bibenzimidazole or 2,3-bis(2-pyridyl)-quinoxaline were also reported[74] Weak emissions were observed from ambient temperature fluid solutions for the monometallic complexes, whereas the bimetallic species do not emit under such conditions

Consequently, preparation of luminescent bimetallic Ru(II) complexes demands a bridging ligand that resembles, as closely as possible, 2,2'-bipyridine, so that the co-ordination and field strength about each Ru(II) ion is essentially

equivalent to that in $[Ru(bpy)_3]^{2+}$ In fact, studies on binuclear complexes containing 2,3-bis-(2-pyridyl)-pyrazine (dpp) by Braunstein et al [74] and on 3,5-bis-(pyridin-2-yl)-1,2,4-triazole (Hbpt) by Barigelletti et al [99-100], showed that upon co-ordination of the second $Ru(bpy)_2$ moiety, luminescence was still present at room temperature

1 4 3 *1,2,4-triazole ligands*

1,2,4-triazole ligands are a particularly interesting type of co-ordination ligand, because by the combination of a 5- and 6-membered ring in a ligand such as 3-(pyridin-2-yl)-1,2,4-triazole, co-ordinating nitrogen atoms are created which have quite different electronic properties[95] In general, they are stronger σ-donors and weaker π-acceptors than 2,2'-bipyridine The central triazole ring binds one metal centre through N2 and the other one through N4 of the triazole ring[101] Furthermore, the co-ordinated ligand is a much stronger acid than the free ligand[102]

As already mentioned, the Hbpt ligand allows formation of dinuclear species which retain their luminescent properties Contrary to most of the previously studies bridges, Hbpt carries a negative charge This negative charge has only a minor effect on the excited-state and redox properties of the building $Ru(bpy)_2$ blocks and may allow the occurrence of vectorial energy or electron-transfer along a suitably organised sequence of components Because of the stronger σ-donor power of bpt^-, the MC levels are expected to lie at higher energy than for $[Ru(bpy)_3]^{2+}$ Coupled with the lower energy of the luminescent ^{3}MLCT level , this leads to the conclusion that the ^{3}MLCT - ^{3}MC energy gap for $[Ru(bpy)_2(bpt)]^+$ is considerably higher than for $[Ru(bpy)_3]^{2+}$, resulting in a photostable mononuclear species The dimer is, however, photoactive, as the ligand-field strength is much

lower upon co-ordination of the second metal unit, due to a sharing of the negative charge on the bpt$^-$ ligand between two metal units in this case[99]

Both the mononuclear and dinuclear osmium-containing species were found to be photostable, due to the greater spin-orbital coupling constant for Os(II), increasing the ^{3}MLCT -^{3}MC energy gap, so that this state is inaccessible at room temperature It was found that the bpt$^-$ ligand was not a trap for energy and electron transfer and, thus, appears to be a convenient bridge for polynuclear complexes which can exhibit photoinduced electron or energy migration[100].

Mixed-metal ruthenium-osmium complexes containing this ligand exhibit efficient energy-transfer processes from the Ru-based ^{3}MLCT to the Os-based ^{3}MLCT states[103] As a result, these compounds are found to be photostable[104] Electron delocalisation was also found to be significant for these complexes[105] In heteronuclear ruthenium-rhodium and ruthenium-iridium complexes, efficient energy transfer was found to occur from higher energy excited states centred on the rhodium (or iridium) component to the lowest energy excited state, which is a MLCT level localised on the Ru(bpy)$_2$ component[106]

Replacement of the pyridyl ring by pyrazine to give (pyrazin-2-yl)-1,2,4-triazole ligands gave very interesting complexes The lowest unoccupied molecular orbitals (LUMO) are now pyrazyltriazole based when protonated and bpy-based when deprotonated[98] The presence of the pyrazine ring leads to an increased basicity of the excited state and, therefore, the excited electron is located on the pyrazyltriazole ligand[107] The bridging 3,5-bis-(pyrazin-2-yl)-1,2,4-triazole (Hbpzt) ligand showed a bpy-based emission upon formation of the mononuclear species and a bpzt-based emission upon protonation of the mononuclear species and upon formation of the dinuclear species However, considerable metal-metal interaction does exist for this dimer This suggests that for triazolate containing

systems, hole transfer (via the HOMO (highest occupied molecular orbital) levels) is the main pathway for electron transfer in these systems[108]

Therefore, 1,2,4-triazole ligands are an interesting type of bridging ligand, Because of the synthetic control available in the preparation of these dinuclear species, it should be possible to utilise the different co-ordinating properties of the two sides of these asymmetric ligands in order to get some detailed information regarding the localisation of the emission state in these systems

1.5 SCOPE OF THIS THESIS

The aim of this present study is to synthesis and characterise mononuclear and dinuclear ruthenium(II) complexes containing various 1,2,4-triazole and 1,2,4-triazine ligands This work is part of a wider research programme on triazole-containing complexes[109-110] Particular emphasis on their photophysical and photochemical properties is given, due to their potential application as sensitizers in solar energy conversion systems The dinuclear species are studied with respect to their metal-metal interaction, photochemical stability and localisation of the lowest emitting excited state Variations in the bridging ligand and the auxiliary polypyridyl ligands are investigated with a view to find-tuning the excited state properties of the complexes The influence of the different co-ordination sites of the triazole ring on the electrochemical and electronic properties of the complexes is also investigated

In Chapter 2, a description of the physical measurements which are common to all complexes are given In Chapter 3, mononuclear complexes containing pyridyl and pyrazyl-1,2,4-triazole ligands are discussed, with emphasis on their photochemical properties In Chapter 4, mononuclear and dinuclear

complexes containing the ligand 3,5-bis-(pyridin-2-yl)-1,2,4-triazole are studied with a view to pinpointing the nature of the lowest emitting state in these complexes and the effect of the different co-ordination environments of the asymmetric bridging ligand Chapter 5 investigates the effect of replacing pyridine rings with pyrazine rings using the analogous 3,5-bis-(pyrazin-2-yl)-1,2,4-triazole ligand Chapter 6 examines the effect of increased asymmetry using a combination of both pyridine and pyrazine rings incorporated into the 3-(pyrazin-2-yl)-5-(pyridin-2-yl)-1,2,4-triazole ligand Finally, Chapter 7 looks at the effect of the 6-membered 1,2,4-triazine ring on the physical properties of mononuclear Ru(II) polpyridyl complexes and how substitutions on the triazine ring can be used to fine-tune these properties

1.6 REFERENCES

1 P H Raven, R F Evert, and H Curtis, *Biology of plants*, 2nd Edition, **1976**, Worth Publishing, Inc , 108

2 R M Devlin and A V Barker, *Photosynthesis*, **1971**, VNR Publishers, 27-123

3 D Voet and J G Voet, *Biochemistry*, **1990**, John Wiley and Sons, Inc , 586-617

4 W B Wood, J H Wilson, R M Benbois, and L E Hood (Eds), *Biochemistry*, 2nd Edition, **1981**, 242

5 A L Leninger, *Biochemistry*, 2nd Edition, **1975**, Worth Publishers, Inc , 587

6 R C Jennings, G Zucchelli, F M Garlaschi, and A Vianelli, *Proc EPA Summer School*, **1992**, Italy, 101

7 D B Knaff and D I Arnon, *Biochem* , **1969**, *64*, 715

8 B Lagoutte and P Mathis, *Photochem and Photobiol* , **1989**, *49*, 6, 833

9 D B Knaff, *TIBS*, **1988**, 461

10 B A Melandri, *Proc EPA Summer School*, **1992**, Italy, 151

11 D I Arnon, *The Sciences*, **1982**, *22*, 7, 22

12 A Harriman, *J Photochem and Photobiol , A Chem* , **1990**, *51*, 41

13 N Sutin and C Creutz, *J Chem Ed* , **1993**, *60*, 10, 809

14 M A Fox, *Photochem and Photobiol* , **1990**, *53*, 3, 617

15 R A Marcus and N Sutin, *Biochim and Biophys Acta*, **1985**, *811*, 265

16 J R Norris and P Gast, *J Photochem* , **1985**, *29*, 185

17 H B Gray, *C&EN*, **1991**, 17

18 S Bobmann, M Seiler, and H Durr, *J Phys Org Chem* , **1992**, *5*,2, 63

19 V Balzani, *Pure & Appl Chem* , **1990**, *62*, 6, 1099

20 V Balzani, (Ed) *Supramolecular Photochemistry*, Reidel, Dortrecht, **1987**

21 V Balzani, L Moggi, and F Scandola, *Supramolecular Photochemistry*, Reidel, Dordrecht, **1987**, 1-28

22 R Ballardini, M T Gandolfi, M L Moya, L Prodi, and V Balzani, *Isr. J Chem*, **1992**, *32*, 1, 47

23 J D Peterson, L W Morgan, I Hsu, M A Billadeau, and S E Ronco, *Coord. Chem Rev*, **1991**, *111*, 319

24 F Scandola, C A Bignozzi, C Chiroboli, M T Indelli, and M A Rampi, *Coord Chem Rev*, **1990**, *97*, 299

25 V Balzani and L Moggi, *Coord Chem Rev*, **1990**, *97*, 313,

26 G Denti, S Serroni, S Campagna, V Ricevuto, and V Balzani, *Inorg Chim Acta*, **1991**, *182*, 127

27 S Bossmann and D Heinz, *EPA Newsl*, **1992**, *45*, 17

28 A Juris, V Balzani, F Barigelletti, S Campagna, P Belser, and A von Zelewsky, *Coord Chem Rev*, **1988**, *84*, 85

29 C Creutz and N Sutin, *Proc Nat Acad Sci, USA*, **1975**, *72*, 8, 2858

30 J M Lehn, J P Sauvage, and R Ziessel, *Nouv J de Chimie*, **1979**, *3*, 7, 423

31 E Borgarello, J Kiwi, E Pelizzetti, M Visca, and M Gratzel, *J Am Chem Soc*, **1981**, *103*, 6324

32 E Borgarello, J Kiwi, E Pelizzetti, M Visca, and M Gratzel, *Nature*, **1981**, *289*, 158

33 S F Chan, M Chou, C Creutz, T Matsumara, and N Sutin, *J Am Chem Soc*, **1981**, *103*, 369

34 P K Ghosh, B S Brunschwig, M Chou, C Creutz, and N Sutin

35 P A Christensen, W Erbs, and A Harriman, *J Chem Soc, Faraday Trans 2*, **1985**, *81*, 575

36 J K Nagle and D M Roundhill, *Chemtracts Inorg Chem*, **1992**, *41*, 3, 144

37 (a) B O'Regan and M Gratzel, *Nature*, **1991**, *353*, 737 (b) M K Nazeeruddin, P Liska, J Moser, N Vlachopoulos, and M Gratzel, *Helv Chim Acta*, **1990**, *73*, 1788

38 K Kalyanasundaram, M K Nazeeruddin, M Gratzel, G Viscardi, and P. Savarino, *Inorg Chim Acta*, 1992, *198-200*, 831

39 N J Turro, I V Khudyakov, and K R Gopidas, *Chem Phys* , **1992**, *162*, 131

40 T J Meyer, *Pure & Appl Chem* , **1990**, *62*, 6, 1003

41 T J Meyer, *Pure & Appl Chem* , **1986**, *58*, 9, 1193

42 K Kalyanasundaram, *Coord Chem Rev* , **1982**, *46*, 159

43 R Hage, J G Haasnoot, J Reedijk, and J G Vos, *Chemtracts - Inorg Chem* , **1992**, *4*, 75

44 E R Carraway, J N Demas, B A DeGraaff, and J R Bacon, *Anal Chem* , **1991**, *63*, 337

45 S R Allsopp, A Cox, T J Kemp, and W J Reed, *Inorg Photophys in Soln* , **1977**, *1-41*, 1275

46 F E Lytle and D M Hercules, *J Am Chem Soc* , **1969**, *91*, 2, 253

47 J E Baggot, G K Gregory, M J Pilling, S Anderson, K R Seddon, and J E Turp, *J Chem Soc , Faraday Trans 2*, **1983**, *79*, 195

48 E M Kober and T J Meyer, *Inorg Chem* , **1984**, *23*, 3877

49 G A Crosby and W H Elfring Jr , *J Phys Chem* , **1976**, *80*, 20, 2206

50 R J Watts, *J Chem Ed* , 1983, *60*, 10, 835

51 T J Meyer, *Photochem Processes in Organized Molecular Systems*, K Honda (Ed), Elsevier Publishing Inc , **1991**, 133

52 B Durham, J V Caspar, J K Nagle, and T J Meyer, *J Am Chem Soc* , **1982**, *104*, 4803

53 J Van Houten and R J Watts, *Inorg Chem* , **1978**, *17*, 12, 3381

54 C Lin and N Sutin, *J Phys Chem*, **1976**, *80*, 2, 97

55 G H Allen, R P White, D P Rillema, and T J Meyer, *J Am Chem Soc*, **1984**, *106*, 2613

56 J N Demas and B A DeGraaff, *Anal Chem*, **1991**, *63*, 17, 829A

57 V Balzani, A Juris, F Barigelletti, P Belser, and A von Zelewsky, *Sci Papers, I P.C R*, **1984**, *78*, 4, 78

58 V Balzani, N Sabbatini, and F Scandola, *Chem Rev*, **1986**, *86*, 319

59 M Venturi, Q G Mulazzani, M Ciano, and M Z Hoffman, *Inorg Chem*, **1986**, *25*, 4493

60 G D Danzer and K R Kincaid, *J Phys Chem*, **1990**, *94*, 3976

61 R J Crutchley, N Kress, and A B P Lever, *J Am Chem Soc*, **1983**, *105*, 1170

62 G H Allen, R P White, D P Rillema, and T J Meyer, *J Am Chem Soc*, **1984**, *106*, 2613

63 D P Rillema, G Allen, T J Meyer, and D Conrad, *Inorg Chem*, **1988**, *22*, 1617

64 H E Toma, P S Santos, and A B P Lever, *Inorg Chem*, **1988**, *27*, 3850

65 K Maruszewski, D P Strommen, K Handrich, and J R Kincaid, *Inorg Chem*, **1991**, *30*, 4579

66 M Hunziker and A Ludi, *J Am Chem Soc*, **1977**, *99*, 22, 7370

67 S Ernst, V Kasack, and W Kaim, *Inorg Chem*, **1988**, *27*, 1146

68 E V Dose and L J Wilson, *Inorg Chem*, **1978**, *17*, 9, 2660

69 T S Akasheh, P C Beaumont, B J Parsons, and G O Phillips, *J Phys. Chem*, **1986**, *90*, 5651

70 K Kalyanasundaram, M Gratzel, and M K Nazeeruddin, *J Chem Soc, Dalton Trans*, **1991**, 343,

71 F Barigelletti, A Juris, V Balzani, P Belser, and A von Zelewsky, *Inorg Chem*, **1983**, *22*, 3335

72 A T Cocks, R D Wright, and K R Seddon, *Chem Phys Letts*, **1982**, *85*, 3, 369

73 R M Berger, *Inorg Chem*, **1990**, *29*, 1920

74 C H Braunstein, A D Baker, T C Strekas, and H D Gafney, *Inorg Chem*, **1984**, *23*, 857

75 G Denti, S Serroni, S Campagna, V Ricevuto, and V Balzani, *Inorg Chim Acta*, **1991**, *182*, 127

76 G Di Marco, A Bartolotta, V Ricevuto, S Campagna, G Denti, L Sabatino, and G De Rosa, *Inorg Chem*, **1991**, *30*, 270

77 K R Barqawi, T S Akasheh, P C Beaumont, B J Parsons, and G O Phillips, *J Phys Chem*, **1988**, *92*, 291

78 S Serroni and G Denti, *Inorg Chem*, **1992**, *31*, 4251

79 R J Crutchley and A B P Lever, *Inorg Chem*, **1982**, *21*, 2276

80 T Ohno, K Nozaki, and M Haga, *Inorg Chem*, **1992**, *31*, 548

81 M Haga and A Tsunemitsu, *Inorg Chim Acta*, **1989**, *164*, 137

82 M Haga, *Inorg Chim Acta*, **1980**, *45*, L183

83 M Haga, T Ano, K Kano, and S Yamabe, *Inorg Chem*, **1991**, *30*, 3843

84 M Haga, T Matsumura-Inoue, and S Yamabe, *Inorg Chem*, **1987**, *26*, 4148

85 T Ohno, K Nozaki, and M Haga, *Inorg Chem*, **1992**, *31*, 4256

86 A M Bond and M Hagga, *Inorg Chem*, **1986**, *25*, 4507

87 P J Steel, F Lahousse, D Lerner, and C Marzin, *Inorg Chem*, **1983**, *22*, 1488

88 B P Sullivan, D J Salmon, T J Meyer, and J Peedin, *Inorg Chem*, **1979**, *18*, 12, 3369

89 A J Downard, G E Honey, and P J Steel, *Inorg Chem*, **1991**, *30*, 3733

90 C R Johnson, W W Henderson, and R E Shepherd, *Inorg Chem*, **1984**, *23*, 2745

91 W Tang, D Chen, Z Liu, and A Dai, *Sci China, Ser B*, **1991**, *34*, 8, 897

92 B D J R Fennema, R Hage, J G Haasnoot, J Reedijk, and J G Vos, *Inorg Chim Acta*, **1990**, *171*, 223

93 R Hage, J G Haasnoot, J Reedijk, R Wang, E M Ryan, J G Vos, A L Spek, and A J M Duisenberg, *Inorg Chim Acta*, **1990**, *174*, 77

94 G Giuffrida, G Calogero, G Guglielmo, V Ricevuto, M Ciano, and S Campagna, *Inorg Chem*, **1993**, *23*, 1179

95 R Hage, R Prins, J G Haasnoot, J Reedijk, and J G Vos, *J Chem Soc, Dalton Trans*, **1987**, 1389

96 J M de Wolf, R Hage, J G Haasnoot, J Reedijk, and J G Vos, New J Chem, 1991, 15, 501

97 B E Buchanan, J G Vos, M Kaneko, W J M van der Putten, J M Kelly, R Hage, R A G de Graaff, R Prins, J G Haasnoot, and J Reedijk, *J Chem Soc, Dalton Trans*, **1990**, 2425

98 H A Nieuwenhuis, J G Haasnoot, R Hage, J Reedijk, T L Snoek, D J Stufkens, and J G Vos, *Inorg Chem*, **1991**, *30*, 48

99 F Barigelletti, L De Cola, V Balzani, R Hage, J G Haasnoot, J Reedijk, and J G Vos, *Inorg Chem*, **1989**, *28*, 4344

100 F Barigelletti, L De Cola, V Balzani, R Hage, J G Haasnoot, J Reedijk, and J G Vos, *Inorg Chem*, **1991**, *30*, 641

101 B E Buchanan, R Wang, J G Vos, R Hage, J G Haasnoot, and J Reedijk, *Inorg Chem*, **1990**, *29*, 3263

102 R Hage, J G Haasnoot, J Reedijk, R Wang, E M Ryan, J G Vos, A L Spek, and A J M Duisenberg, *Inorg Chim Acta*, **1990**, *174*, 77.

103 R Hage, *Coord Chem Rev*, **1991**, *111*, 161

104 L De Cola, F Barigelletti, V Balzani, R Hage, J G Haasnoot, J Reedijk, and J G Vos, *Chem Phys Letts*, **1991**, *178*, 5-6, 491

105 R Hage, J G Haasnoot, H A Nieuwenhuis, J Reedijk, D J A De Ridder, and J G Vos, *J Am Chem Soc*, **1990**, *112*, 9245

106 J H van Diemen, R Hage, J G Haasnoot, H E B Lempers, J Reedijk, J G Vos, L De Cola, F Barigelletti, and V Balzani, *Inorg Chem*, **1992**, *31*, 3518

107 R Hage, J G Haasnoot, H A Nieuwenhuis, J Reedijk, R Wang, and J G Vos, *J Chem Soc, Dalton Trans*, **1991**, 3271

108 R Hage, J G Haasnoot, J Reedijk, R Wang, and J G Vos, *Inorg Chem*, **1991**, *30*, 3262

109 R Hage, *Ph D Thesis*, **1991**, Leiden University, The Netherlands

110 R Wang, *Ph D Thesis*, **1992**, Dublin City University, Ireland

CHAPTER 2

EXPERIMENTAL PROCEDURES

The synthesis of the ligands and the complexes made during the course of this thesis are described in detail in the appropriate chapters. Unless otherwise stated, all starting materials and solvents were of commercial grade.

2.1 *Absorption and emission spectroscopy*

UV-vis spectra were obtained on a Waters 990 photodiode array spectrometer or on a Shimadzu UV240 instrument. Absorption coefficients are accurate to 5%. Emission spectra were obtained both at room temperature and at lower temperatures, (77K, cooled with liquid nitrogen) using a Perkin-Elmer LS50 luminescence spectrometer equipped with an Epsom PC, which utilises the Fluorescence Data Manager software. An emission slitwidth of 5 nm was used at room temperature and 2.5 nm at 77 K. The excitation slit width was 5 nm at both temperatures. The results obtained were not corrected for photomultiplier response.

Titrations in the pH range from 1 to 10 were carried out in a Britton-Robinson buffer solution (0.04 M H_3BO_3, 0.04 M H_3PO_4, 0.04 M H_3CCOOH). The pH of the solutions was adjusted using concentrated sulphuric acid, or 2 M NaOH. The emission titrations were carried out using an appropriate isosbestic point (from the absorption titration data) as the excitation wavelength.

Quantum yields of emission were carried out using optically dilute measurements as described by Demas and Crosby[1] and are accurate to ± 10%. $[Ru(bpy)_3]^{2+}$ was used as the standard as it is known to have a quantum yield of 0.028 in aqueous solutions at room temperature[2]. The normalisation of the absorption spectra were carried out using the Shimadzu UV240 spectrometer and the emission spectra was carried out in the normal manner.

2.2 *Nuclear Magnetic Resonance spectroscopy*

Proton nuclear magnetic resonance (NMR) spectra were obtained using a Bruker AC 400 MHz spectrometer or using a Jeol JNM-FX 200 MHz

spectrometer Measurements were carried out in acetone-d^6 or in deuterated acetonitrile, unless otherwise stated The peak positions are relative to TMS For the COSY (correlated spectroscopy) experiments, 128 FID'S of sixteen scans each consisting of 1 K data points were accumulated After digital filtering (sine-bell squared), the FID was zero filled to 512 W in the F1 dimension. Acquisition parameters were F1 = +/- 500 Hz, F2 = 1000 Hz and $t_{1/2}$ = 0 001 sec The cycle delay was 2 s

2 3 *Resonance Raman Spectroscopy*

Time resolved Resonance Raman measurements were carried out using a Q-switched Nd/Yag laser (Quanta-Ray GCR2, pulse width ca 9 ns) to populate and probe the excited states of the various complexes at an excitation wavelength of 355 nm Ground state spectra were also obtained for comparison purposes using a Spectra Physics Argon ion laser at 363 8 nm, 457 9 nm, 465 8 nm, 472 7 nm, 476 5 nm, 488 0 nm, 496 5 nm and 504 9 nm All measurements were carried out in acetone/H_2O (1/5 v/v) solvent mixtures, degassed by bubbling with argon throughout the measurement These measurements were carried out in Queens University, Belfast under the supervision of Dr J J McGarvey

2 4 *Electrochemical measurements*

Cyclic voltammetric (CV) measurements were carried out using an EG & G Princeton applied research 362 Scanning Potentiostat Differential pulse voltammetric (DPV) measurements were carried out using an EG & G Princeton applied research 265 polarographic analyser / stripping voltammeter A saturated calomel electrode (SCE) was used as the reference electrode Measurements were carried out in spectroscopic grade acetonitrile with 0 1 M TEAP as the supporting electrolyte Glassy carbon and platinum electrodes were used as the working and counter electrodes respectively The scan-rate

used was 100 mV/sec for CV and 10 mV/sec for DPV. In order to carry out reduction measurements for both techniques, it was necessary to deoxygenate the solution by bubbling nitrogen through it for fifteen minutes prior to scanning. The oxidation potentials were measured in the range 0 -----> 1.6 V and the reduction potentials in the range 0 -----> -2.0 V. Protonation of the complexes took place by adding two drops of 0.1 M $HClO_4$ to the electrolyte solution.

2.5 *Luminescent lifetime measurements*

The lifetime measurements were carried out using a Q-switched Nd-YAG spectrum laser system. They were carried out either in analytical grade acetonitrile at room temperature (aerated and degassed by bubbling with argon), or in ethanol / methanol (4/5 v/v) for the measurements at 77 K and for the temperature dependent lifetime experiments. The temperature dependent lifetime experiments were performed by bubbling a dilute solution of the complex (10^{-4} - 10^{-5} M) with argon for thirty minutes prior to use. The results obtained were the same within experimental error to those obtained for the freeze-pump-thaw method of degassing. The cell was placed inside a Thor C600 nitrogen flow cryostat, equipped with a Thor 3030 temperature controller. The absolute error on the temperature is estimated at ± 2 K. The single exponential analysis was performed with modified non-linear programs. The experimental lifetime error is estimated to be < 8%. Standard iterative non-linear programs were used to obtain the parameters for the temperature dependence of the lifetime.

2.6 *Chromatographic techniques*

High performance liquid chromatography (HPLC) was carried out using a Waters 990 photo-diode array HPLC system, equipped with a NEC PAC III computer, a Waters pump model 6000 A, a 20 µl injector loop and a partisil SCX radial PAK cartridge. The detection wavelength used was 280 nm. The

chromatography was achieved using a mobile phase which consisted of acetonitrile water (4 1 v/v) containing 0 08 M lithium perchlorate, unless otherwise stated The flowrate used was 1 5 - 3 0 cm^3/min depending on the elution of the complexes

Semi-preparative HPLC was carried out using an Applied Chromatography services pump (model RR066) and detector (ACS model 353 / UV/vis), a 1 ml injection loop and a Magnum 9 partisil cation exchange column (10 mm / 25 cm) The mobile phase in this system consisted of acetonitrile water (80 20 v/v) containing 1 0 M potassium nitrate The flowrate used was 2 0 - 3 0 ml/min depending on the elution of the complexes

2 7 *Photochemical measurements*

Photochemical experiments were carried out using a Kodak carousel S AV 2020 projector equipped with two medium pressure 250 W tungsten lamps The sample was placed in a quartz cuvette (path length 1 cm^3) The light was focused by means of two glass lenses, a filter (> 390 nm) was used to prevent any ultra-violet light from reaching the sample A transparent water bath was placed in front of the sample to prevent any thermal reactions occurring Any large scale experiments were carried out using a double walled Pyrex glass vessel (cooled) and a medium pressure mercury lamp (400 W)

2 8 *Elemental analyses*

Elemental analyses on C, H and N were carried out at the Microanalytical laboratory of University College Dublin (UCD)

2 9 *Kinetics*

All kinetic experiments were carried out using the Shimadzu UV 240 spectrophotometer connected to a thermostat bath, recycling water at the

correct temperature (accurate to 1%) The calculations were carried out based on the equation

$$\ln[OD(t) - OD(max) / OD(0) - OD(max)] = kt$$

where OD = absorbance (or optical density), and t = time For a first order equation, this plot would be linear, with a slope, k, in min^{-1} This is the rate of the reaction This slope can subsequently be used in an Arrhenius plot in order to calculate the activation energy of the reactions

$$\text{slope} = A \exp(-E_a/RT) \quad \text{-----} > \quad \ln k = \ln A - E_a/RT$$

where R is the gas constant, 8 314 $JK^{-1}Mol^{-1}$ and A is the pre-exponential factor (which is independent of temperature) Therefore the activation energy, E_a, can be determined from a plot of lnk versus 1/T

2 10 *Spectroelectrochemical measurements*

Spectroelectrochemistry in the range 900 nm - 200 nm was carried out on the Shimadzu UV240 spectrophotometer attached to an EG & G Princeton applied research 265 polarographic analyser / stripping voltammeter connected to a thermostat bath, recycling water @ 20°C Electrochemical oxidation was carried out in a home-made cell with a platinum sheet as the working electrode, a platinum wire as the auxiliary electrode and a coated silver wire electrode as the reference electrode The electrolyte used was acetonitrile containing 0 1 M tetraethyl ammonium perchlorate Near infra-red spectra were obtained using a Perkin-Elmer 9 UV/Vis/NIR spectrometer, and were also carried out in acetone, benzonitrile and dichloromethane containing 0 5 M $TBABF_4$ These NIR measurements were carried out at the University of Edinburgh, under the supervision of Dr Lesley Yellowlees

The potentials applied for the preparation of the mixed valence species were 1 15 for RuRu complexes, 0 75 for OsOs and 1 00 V versus SCE for RuOs complexes These potentials varied slightly according to the solvent used in the solvent dependence studies

2 11 *References*

1 J N Demas and G A Crosby, *J Phys Chem*, **1971**, *75*, 8, 991

2 K Nakamuru, *Bull Chem Soc, Japn*, **1982**, *55*, 2697

CHAPTER 3

THE PHOTOCHEMICAL AND PHOTOPHYSICAL PROPERTIES OF MONONUCLEAR Ru(II) COMPLEXES CONTAINING 1,2,4-TRIAZOLE LIGANDS

3.1 INTRODUCTION

Originally, it was thought that compounds such as $[Ru(bpy)_3]^{2+}$ were photochemically inert towards ligand substitution in aqueous solutions[1]. However, subsequently this was found not to be the case and one of the problems associated with their application to solar energy conversion systems is the small, but significant, photodecomposition of these complexes[2-5]. A detailed mechanism for the ligand photosubstitution reaction for $[Ru(bpy)_3]^{2+}$ has been proposed and can be seen in Figure 3.1.1 [2].

Absorption of a photon of light gives rise to the excited ^{3}MLCT (metal-to-ligand charge-transfer) state. If the energy gap between the ^{3}MLCT and the ^{3}MC (metal-centred) excited state is relatively small, then thermally activated formation of this (d-d) ^{3}MC excited state can occur. This can undergo further thermal activation, leading to cleavage of a Ru-N bond, with formation of a five-co-ordinate square pyramidal species. This species is unstable and in the absence of co-ordinating ions, such as when the ammonium hexafluorophosphate salt is present, this square pyramidal species returns to its ground state i.e. $[Ru(bpy)_3]^{2+}$. If, however, co-ordinating anions are present, such as Cl^- ions or acetonitrile, a hexacoordinate monodentate bpy intermediate is formed, where both chlorine (or acetonitrile) and bpy are bonded to ruthenium. Once formed, this monodentate bpy species can undergo loss of bpy with formation of a $[Ru(bpy)_2X_2]$ species (where X = Cl^- or MeCN). Alternatively, chelate ring closure (otherwise known as a "self-annealing" process) can occur with formation of the ground-state species. The latter is favoured in aqueous solutions due to stabilisation of the cationic $[Ru(bpy)_3]^{2+}$ species, whereas formation of the neutral $[Ru(bpy)_2X_2]$ complex is favoured in low polarity solvents[2]. It was found that, unlike previously proposed, the apparent photochemical stability of $[Ru(bpy)_3]^{2+}$ in water is a result of the dominance of chelate ring closure and not of inherently low

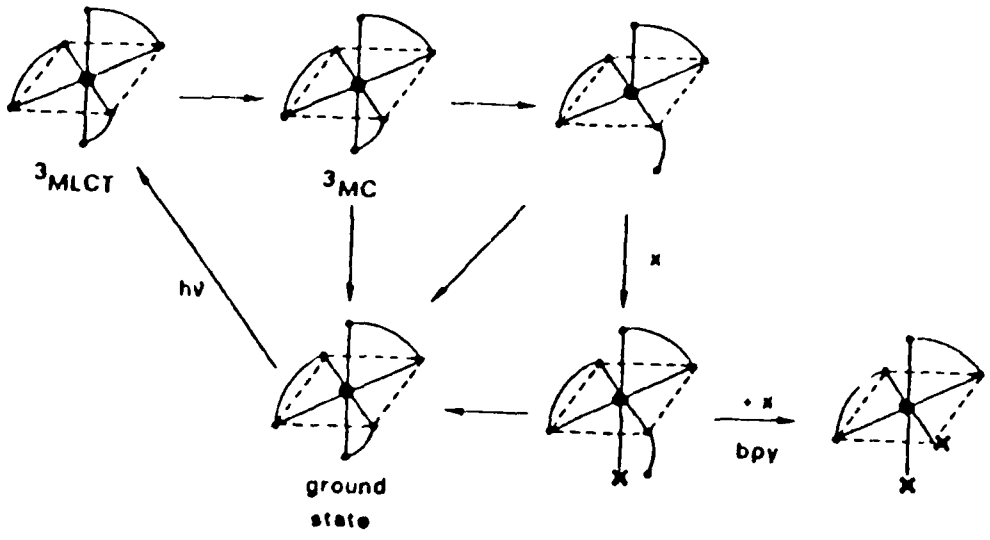

Figure 3 1 1

Proposed mechanism for the ligand photosubstitution reaction of $[Ru(bpy)_3]^{2+}$ [2]

photochemical reactivity[3] However, no direct structural evidence proving this mechanism and the presence of such monodentate co-ordinated chelating ligands has so far been published

One method of overcoming the problems associated with the use of $[Ru(bpy)_3]^{2+}$ for the conversion of water into its molecular components using sunlight, would be to replace one of the bpy ligands by another ligand with deliberately modified chemical and physical behaviour in an attempt to fine-tune the various photoredox and photosubstitution properties of these complexes, thus, creating a $[Ru(bpy)_2(LL')]^{n+}$ complex Examples of such LL' ligands are 1,10-phenanthroline[6], 2,2'-bisbenzimidazole[7], and 2,2'-bipyrazine[8]. If LL' is a good π-acceptor ligand, back-bonding from Ru(II) to LL' results in stabilisation of the dπ levels relative to π*(bpy) and an increase in the MLCT

band energy[10] If LL' is a good σ-donor ligand, the oxidation potential of the complex is now lower and the emission properties of the mixed ligand systems are now bpy-based[11]

In this chapter, we concentrate on the effect of replacing a bpy ligand by a 1,2,4-triazole ligand has on the photochemical properties of ruthenium polypyridyl complexes 1,2,4-triazole ligands are known to be better σ-donors than bpy They are particularly interesting ligands because with the combination of a six--membered ring such as pyridine or pyrazine into a bidentate ligand, two different types of co-ordinating nitrogen atoms are created It is anticipated that such asymmetric bidentate ligands which contain a σ-donor and a π-acceptor site may produce ruthenium compounds with unusual excited-state properties and may facilitate the formation of monodentate intermediates

The photochemical and photophysical properties of $Ru(bpy)_2$ complexes containing the ligands 4-methyl-3-(pyridin-2-yl)-1,2,4-triazole (4Mepytr), 3-(pyrazin-2-yl)-1,2,4-triazole (Hpztr) and 1-methyl-3-(pyrazin-2-yl)-1,2,4-triazole (1Mpztr) is reported (for structures see Figure 3 1 2) The effect of replacing a pyridine ring by a pyrazine ring is examined by comparing the physical properties of the complexes containing the pyrazine ligands with those of the analogous 3-(pyridin-2-yl)-1,2,4-triazole (Hptr) and 1-methyl-3-(pyridin-2-yl)-1,2,4-triazole (1Mpytr) compounds already studied by Wang et al[12] and 2-(pyridin-2-yl)-pyrazole (pnp)[13]

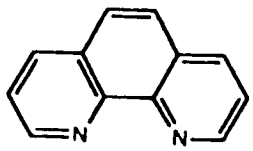

1 10-phenanthroline (phen)

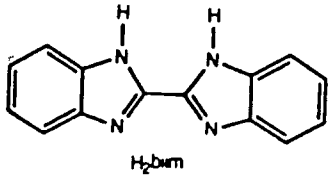

H_2bim

2,2'-bisbenzimidazole

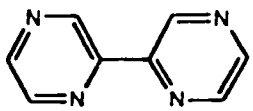

2 2' bipyrazine (bpz)

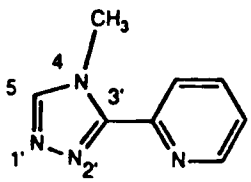

4-methyl-3-(pyridin-2-yl)-1,2,4-triazole

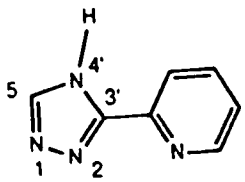

3-(pyridin-2 yl)-1,2,4 triazole

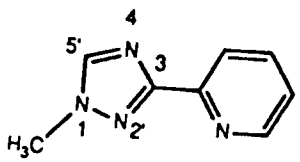

1-methyl-3-(pyridin-2 yl)-1,2,4 triazole

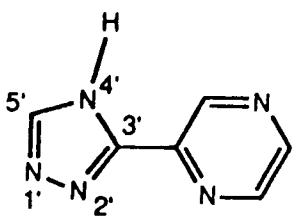

3-(pyrazin-2-yl) 1,2,4-triazole

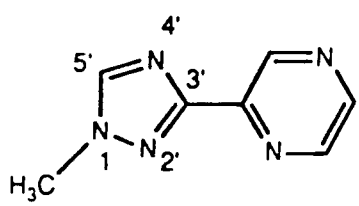

1 methyl-3-(pyrazin-2-yl) 1,2,4 triazole

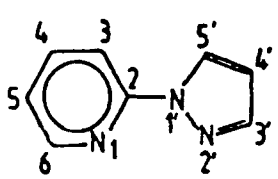

PNP

2-(pyridin-2 yl)-pyrazole

Figure 3.1.2

Structures of the ligands cited in the text

3.2 EXPERIMENTAL

3.2.1 *Preparation of the ligands.*

The synthesis of 4-methyl-3-(pyridin-2-yl)-1,2,4-triazole (4Mepytr), 1-methyl-3-(pyrazin-2-yl)-1,2,4-triazole (1Mpztr), 1-methyl-3-(pyridin-2-yl)-1,2,4-triazole (1Mpytr) and 2-(pyridin-2-yl)-pyrazole (pnp) were carried out by Dr. Ronald Hage, University of Leiden, The Netherlands[14].

3-(pyrazin-2-yl)-1,2,4-triazole:
This ligand was prepared according to literature methods[15] in the following manner: An equimolar mixture of 5 g of 2-cyanopyridine (0.048 mol) and 2.4 g of hydrazine hydrate were added to 20 cm^3 ethanol and stirred at room temperature for 1 hour. The yellow crystals of 2-pyrazylamidrazone were collected by filtration. This was dissolved in a 10-fold excess of cold formic acid at 0°C in an ice-bath, and stirred for 3 hours. After heating to 120°C, the ligand precipitated and was recrystallised from hot ethanol. Yield: 38 %. M.p. 213 °C. ^1H NMR data [$CDCl_3$]: H^3, 9.47; H^5, 8.71; H^6, 8.65; $H^{5'}$, 8.24.

3.2.2 *Preparation of the ruthenium complexes.*

The complexes $[Ru(bpy)_2(1Mpytr)](PF_6)_2$ and $[Ru(bpy)_2(pnp)](PF_6)_2$ were prepared by Dr. B.E. Buchanan, Dublin City University[13].

$[Ru(bpy)_2Cl_2].2H_2O$
This complex was prepared according to literature methods[16]. 7.8 g $RuCl_3.3H_2O$, 9.4 g 2,2'-bipyridine and 1.2 g LiCl were heated at reflux for 8 h in 50 cm^3 DMF. After cooling, 250 cm^3 of acetone were added and the solution

was left at -4 °C overnight The resulting product was collected by vacuum filtration Yield 9 g (60 %)

$[Ru(bpy)_2(4Mepytr)](PF_6)_2$ **(1)**

This compound was prepared according to the literature[17] Yield 601 mg (84%) Found C, 38 7, H, 2 8, N, 12 5 $C_{28}H_{24}F_{12}N_8P_2Ru$ requires C, 39 0, H, 2 8, N, 13 0%

$[Ru(bpy)_2(4Mepytr)Cl]PF_6\ H_2O$ Method A **(2)**

The complex cis-$[Ru(bpy)_2Cl]\ 2H_2O$ (520 mg, 1 mmol) was heated under reflux in acetone ethanol (50 50 cm^3) The ligand 4Mepytr (190 mg, 1 2 mmol) was dissolved in acetone (5 cm^3) and added to the reaction mixture over a period of ten minutes and heated at reflux for a further thirty-five minutes The solvent was removed by rotary evaporation and the remaining residue dissolved in methanol diethyl ether (3 1) and purified by column chromatography using neutral alumina and methanol diethyl ether (3 1) containing 1% acetone as eluent The first dark red fraction which eluted, later found to be the monodentate species, was isolated by addition to an aqueous solution of NH_4PF_6 Yield 460 mg (60%) Found C, 43 3, H, 3 2, Cl 4 4, N, 14 1 $C_{28}H_{26}ClF_6N_8OPRu$ requires C, 43 5, H, 3 2, Cl, 4 6, N, 14 8 %

$[Ru(bpy)_2(4Mepytr)Cl]PF_6\ H_2O$ Method B

This compound was also obtained in small quantities by photochemical means 100 mg of $[Ru(bpy)_2(4Mepytr)]^{2+}$ was irradiated in 300 cm^3 MeCN / 0 01 mol dm^{-3} LiCl in an immersion well at room temperature The solution was continuously purged with nitrogen The reaction progress was followed by HPLC (see section 2 7) The optimum irradiation time was typically 20 minutes The solvent was then evaporated *in vacuo* at room temperature and the monodentate intermediate was separated by semi-preparative HPLC The

material was found to be unstable in water, but it was possible to isolate small quantities of it by freezing out the aqueous component The material was found to be NMR pure, but a substantial amount of KNO_3, originally in the mobile phase, was present Therefore, elemental analysis was not successful. Attempts at further purification failed, but the proton NMR spectrum obtained was identical to that of compound **2**, as prepared by method A

$[Ru(bpy)_2(4Mepytr)MeCN](PF_6)_2$ **(3)**

This compound was prepared in a similar fashion to compound **3**, except that 30 mg of **1** was irradiated in 300 cm^3 of acetonitrile, with an optimum irradiation time of six minutes The monodentate intermediate was isolated by semi-preparative HPLC and the product precipitated using aqueous ammonium hexafluorophosphate (0 5 g in 10 cm^3) giving an overall yield of 60% Recrystallisation did not improve the purity of the sample, as a small amount of the starting material was always found (about 2 - 5%) No elemental analysis was therefore carried out

$[Ru(bpy)_2(pztr)]PF_6\ H_2O$ **(4)**

This complex was prepared as described in the literature[15] Two isomers were formed which were separated by semi-preparative HPLC The first compound isolated from the HPLC will be termed as isomer 1 and the second as isomer 2. Yield 52% Found C, 43 6, H, 3 1, N, 17 3 $C_{26}H_{22}F_6N_9OPRu$ requires C, 44 3, H, 2 9, N, 17 9%

$[Ru(bpy)_2(1Mpztr)](PF_6)_2\ 2H_2O$ **(5)**

This complex was synthesised as for compound (**5**) Only one isomer was formed as evidenced by ^1H NMR and from HPLC data Yield 68% Found C, 36 1, H, 2 8, N, 13.7 $C_{27}H_{26}F_{12}N_9O_2P_2Ru$ requires C, 36.0; H, 3 0; N, 14 0%

3.3 RESULTS AND DISCUSSION.

3 3 1 *General characterisation*

3 3 1 1 ^{1}H NMR spectroscopy

Proton NMR has proved to be a powerful technique in elucidation of the structure of ruthenium diimine complexes, as they are diamagnetic low-spin d^6 species [18-25] The relevant ^{1}H NMR data of all complexes is present in Table 3 3 1 The chemical shifts of the bpy protons all fall in the normal range for these systems and so are not discussed in detail here Assignments of the resonances are made using COSY techniques, by comparison with other related compounds and with the free ligand The co-ordination mode of the ligands can therefore be determined by examination of these spectra

$[Ru(bpy)_2(4Mepytr)]^{2+}$

In the case of $[Ru(bpy)_2(4Mepytr)]^{2+}$, no ambiguity exists concerning the co-ordination mode of the triazole ring, as the only possible co-ordination mode available is via N2 of the triazole ring The methyl group (δ 4 35) and H^3 proton (δ 8 59) are shifted considerably downfield upon co-ordination to the $Ru(bpy)_2$ moiety This is caused by the moderate steric influence between these groups when the ligand is bound to the metal centre In the assignment of this and the other complexes, the positions of the H^6 protons of the various pyridine rings enables the identification of most protons, as H^6 is very sensitive to interaction through space with neighbouring ligands, such as Cl^- or triazole[26]

$[Ru(bpy)_2(4Mepytr)Cl]PF_6$ and $[Ru(bpy)_2(4Mepytr)(MeCN)](PF_6)_2$

In the case of the monodentate complexes, assignment of the co-ordinating site of the triazole ring is not straightforward From the

Compound	H^3	H^4	H^5	H^6	$H^{5'}$	CH_3
$[Ru(bpy)_2(4Mepytr)]^{2+}$	8.59 d	8.13 m	7.57 m	8.05 d	8.74 s	4.35 s
$[Ru(bpy)_2(4Mepytr)Cl]^{+}$	7.70 d	8.00 m	7.55 q	8.80 d	9.00 s	3.98 s
$[Ru(bpy)_2(4Mepytr)(MeCN)]^{2+}$	7.80 d	7.90 m	7.50 q	8.69 d	9.24 s	4.12 s 2.55 s
$[Ru(bpy)_2(pztr)]^{+}$ iso 1	9.54 s	----	8.08 d	8.63 d	7.37 s	----
$[Ru(bpy)_2(pztr)]^{+}$ iso 2	9.44 s	----	8.11 d	8.54 d	8.58 s	----
$[Ru(bpy)_2(1Mpztr)]^{2+}$	9.47 s	----	8.06 d	8.60 d	8.75 s	4.10 s

Table 3.3.1:

400 MHz ^1H NMR resonances for the mononuclear complexes. All measurements were carried out in acetone-d^6. (s = singlet, d = doublet, t = triplet, q = quartet and m = multiplet).

resonances observed for the pyridine ring, it can be concluded that most likely the monodentate co-ordinated pyridyltriazole ligands are bound via the triazole ring. This assumption is based on the fact that for the pyridine ring of the monodentate species, the resonance of the H^5 proton appears, like in the free ligand, as a quartet (see Figure 3.3.1, 7.50 ppm). Also, the position of the H^3 and H^6 protons of this ring are quite different than that observed in the bidentate case. Because of the absence of any interaction with adjacent bpy rings (the diamagnetic anisotrophic effect) the H^6 proton is shifted to a much lower field (δ, 8.70) than when the pyridine ring is co-ordinated [17]. Due to the absence of steric interaction of the H^3 proton from other protons, a shift to a rather high field is observed (δ, 7.80). Also, the presence of methyl resonances at (δ, 4.12) of the pyridyltriazole ligand suggests that the ligand is co-ordinated to the metal via the triazole ring, due to the considerable downfield shift of the

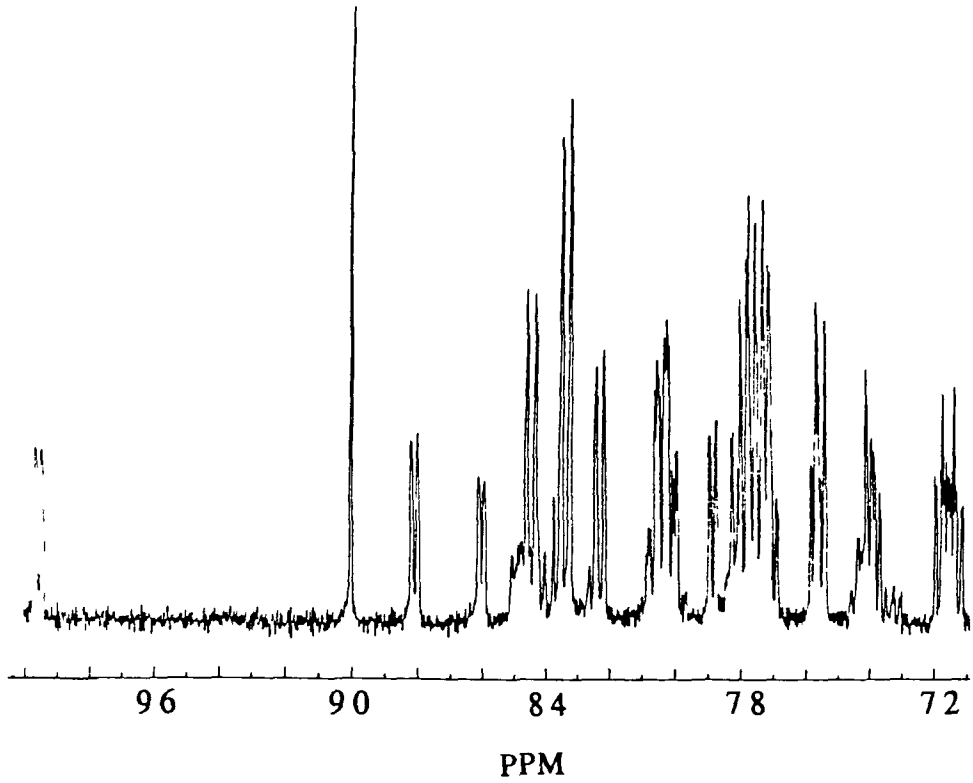

Figure 3 3 1

200 MHz ^{1}H NMR spectrum of [Ru(bpy)$_2$(4Mepytr)Cl]$^+$ in acetone-d^6

methyl protons In the [Ru(bpy)$_2$(4Mepytr)MeCN]$^{2+}$ monodentate species, an acetonitrile resonance at δ, 2 55 clearly indicates that this molecule is co-ordinated to the ruthenium (II) centre, as free acetonitrile is found at (δ, 1 95)[27]

[Ru(bpy)$_2$(pztr)]$^+$ and [Ru(bpy)$_2$(1Mpztr)]$^{2+}$

The ^{1}H NMR resonances of the two isomers of [Ru(bpy)$_2$(pztr)]$^+$ are significantly different as already shown by Hage et al[28] The H$^{5'}$ proton is influenced by its proximity to an adjacent bpy ring If the triazole ring binds via

N4 to the Ru(II) centre, then the $H^{5'}$ proton is shifted considerably upfield If the triazole ring binds via N2 to the Ru(II) centre, then the bpy rings do not influence the chemical shift of this proton By examination of the chemical shifts of both isomers, it can be clearly seen that isomer 1 is bound via N4 to the metal centre and isomer 2 is bound via N2

The ^1H NMR resonances of $[Ru(bpy)_2(1Mpztr)]^{2+}$ indicate the presence of only one isomer for this complex, in agreement with the results obtained by Hage[14] The methyl group on the N1 position in this ligand causes some sort of steric hindrance which prohibits binding via the N2 of the triazole ring occurring When co-ordination takes place via N4, the methyl group is completely free and has no interactions with other ligands However, when bound via N2, the methyl group is close to one of the bpy ligands and a large upfield shift is expected for the methyl group compared with the free ligand[29] This large upfield shift is not present in the NMR spectrum of this compound and therefore co-ordination most probably takes place via N4 of the triazole ring

3 3 1 2 Electronic and redox properties

The electronic and redox properties of the Ru(II) polypyridyl complexes and their protonated analogues are given in Table 3 3 2 and Table 3 3 3 respectively As in other ruthenium(II) diimine compounds, the lowest energy absorption band is in the correct region to be assigned to a metal-to-ligand charge-transfer (MLCT) transition[30] This MLCT band is formed by promotion of an electron from a $d\pi(Ru)$ orbital to a $\pi^*(L)$ orbital[31] It should be noted that very little difference exists between the absorption spectra for compounds **1** and **4**

The position of the MLCT band in compounds **2** and **3** is in agreement

COMPOUND	[a]Absorption log ε	[a]Emission (τ/μs) (300K)	[b]Emission (τ/μs) (77K)
$[Ru(bpy)_2(pztr)]^+$ iso 1	440 (457) (3 94)	658 (659) 0 29 (0 08)	630 (603) 4 6 (4 3)
$[Ru(bpy)_2(Hpztr)]^{2+}$ iso 1	429 (439) (4 14)	657 (657) 0 04 (0 13)	603 (596) 6 7 (4 1)
$[Ru(bpy)_2(pztr)]^+$ iso 2	438 (456) (3 80)	677 (680) 0 28 (0 08)	607 (618) 4 1 (4 9)
$[Ru(bpy)_2(Hpztr)]^{2+}$ iso 2	430 (440) (4 12)	652 (662) 0 03 (0 01)	603 (612) 7 1 (4 1)
$[Ru(bpy)_2(1Mpztr)]^{2+}$	440 (440) (4 16)	645 (630) 0 06 (0 07)	593 (575) 6 9 (7 8)
$[Ru(bpy)_2(4Mepytr)]^{2+}$	440 (4 16)	600 (---)	584 (---)
$[Ru(bpy)_2(4Mepytr)Cl]^+$	508 (3 69)	710 (---)	655 (---)
$[Ru(bpy)_2(4Mepytr)(MeCN)]^{2+}$	440 (---)	[d]	[d]

Table 3 3 2

Electronic properties of the mononuclear complexes [a]Measured in acetonitrile, [b]Measured in ethanol [d]Due to impurity in sample All protonated measurements were carried out by addition of 1 drop of concentrated H_2SO_4 Values in parenthesis are those obtained by Hage[14] (77 K lifetime measurements carried out in propionitrile / butyronitrile (4/5 v/v))

with the presence of a $[RuN_5Cl]$ moiety[32-33] The presence of the chloride ion is also confirmed by the emission energies and the low oxidation potential observed As expected the $[Ru(bpy)_2(4Mepytr)Cl]^+$ compound emits at a longer wavelength than its bidentate analogue[33] It is probable that the stronger σ-donor ability of the Cl^- ion results in a red shift of the lowest dπ-π* absorption band as seen in similar situations with other co-ordinated ligands[34] The emission is thought to originate from bpy-based ^{3}MLCT states for all complexes containing the 4Mepytr ligand[35], whereas it was shown to be bpy-based for the deprotonated complexes containing the $pztr^-$ ligand and pyrazyltriazole-based

COMPOUND	Ru (II/III) oxidation	Ligand based reduction
$[Ru(bpy)_2(pztr)]^+$ iso 1	1.01 (1.00)	-1.43 -1.67 (-1.44 -1.66)
$[Ru(bpy)_2(Hpztr)]^{2+}$ iso 1	1.33 (1.31)	Not measured
$[Ru(bpy)_2(pztr)]^+$ iso 2	0.97 (0.95)	-1.44 -1.68 (-1.44 -1.66)
$[Ru(bpy)_2(Hpztr)]^{2+}$ iso 2	1.22 (1.20)	-1.21 -1.54 (-1.23 -1.53)
$[Ru(bpy)_2(1Mpztr)]^{2+}$	1.32 (1.30)	-1.24 -1.50 (-1.26 -1.52)
$[Ru(bpy)_2(4Mepytr)]^{2+}$	1.21	-1.42 -1.64
$[Ru(bpy)_2(4Mepytr)Cl]^+$	0.66	-1.34
$[Ru(bpy)_2(4Mepytr)(MeCN)]^{2+}$	1.16	(----)
$[Ru(bpy)_3]^{2+}$	1.23	-1.36 -1.54 -1.79

Table 3.3.3

Electrochemical data of the Ru(II) complexes obtained in MeCN containing 0.1 M TEAP. Values obtained by using differential pulse polarography. Potentials in Volts versus SCE. Protonation occurred via addition of 1 drop of H_2SO_4. Values in parenthesis are those obtained by Hage[14].

for the protonated complexes[28]. This is confirmed by the reduction potentials observed for these species.

The reduction processes for all compounds containing the 4Mepytr ligand are most likely bpy-based, whereas the first reduction potential is bpy-based for the deprotonated $pztr^-$ complexes and pyrazyltriazole-based for the protonated Hpztr complexes and the complex containing the 1Mpztr ligand.

Oxidation of these complexes involves a metal-centred orbital with formation of genuine Ru(III) complexes [36] Again the presence of chlorine in the compound effects its redox properties Upon co-ordination to the ruthenium centre, the Cl^- ion causes a higher electron density on the metal centre and therefore a much lower oxidation potential is observed [34]

Compounds **1** and **3** also show similarities between their electronic and redox properties Because of the presence of small amounts of compound **1** (less than five percent) in samples obtained for compound **3**, an exact extinction coefficient could not be obtained From the UV/vis spectra taken during the photolysis of **1** in acetonitrile, it is estimated that the extinction coefficient at the maximum wavelength of compound **3** is about 60% of that of compound **1** (vide infra) The presence of **1** also caused problems in the measurement of the emission spectra for compound **3**, as only weak emission was observed, which can be attributed to the spectra obtained for compound **1**

The electronic properties of both isomers of $[Ru(bpy)_2(pztr)]^+$ are very similar and therefore no additional information could be obtained from them concerning the effect of the co-ordination mode on the physical properties of the complexes The pK_a's of the two isomers are, however, significantly different A pK_a of 5 1 was observed for isomer 1, whereas a pK_a of 3 2 was found for isomer 2 This suggests that the $pztr^-$ ligand is considerably more acidic when co-ordination via the N2 position of the triazole ring takes place Therefore, the N2 site is a better σ-donor than the N4 site[33] The $pztr^-$ ligand is a stronger σ-donor and π-acceptor compared to bpy, as reflected by the lower energy of the absorption maxima and the lower Ru(II/III) oxidation potentials for the two $[Ru(bpy)_2(pztr)]^+$ isomers compared to that of $[Ru(bpy)_3]^{2+}$ The higher oxidation potentials of the protonated species compared to $[Ru(bpy)_3]^{2+}$ suggest that the Hpztr ligand is a weaker σ-donor than bpy That the Hpztr ligand is a stronger π-acceptor compared with bpy is reflected by the less negative reduction potentials for the Hpztr complexes

3 3 2 *Photochemistry*

3 3 2 1 Photochemistry of pyridyltriazole complexes

The compound $[Ru(bpy)_2(4Mepytr)](PF_6)_2$ was photolysed in both pure acetonitrile and in acetonitrile containing 0 01 mol/dm^{-3} lithium chloride The purpose of these experiments was to try to isolate a possible intermediate formed containing monodentate co-ordinated ligands UV/vis spectra taken during the photolysis of **1** in both acetonitrile and in acetonitrile / lithium chloride do not show clear isosbestic points (see Figure 3 3 2), indicating that more than more than two species are present in solution

Photolysis in acetonitrile

During the photolysis of $[Ru(bpy)_2(4Mepytr)]^{2+}$ in acetonitrile, the absorption maximum of the reaction mixture eventually shifts from 450 nm to 425 nm In order to further investigate this photochemical process, HPLC analysis was carried out at specified intervals during the photolysis An example of the HPLC data is depicted in Figure 3 3 3 From the HPLC traces it is clear that upon photolysis of compound **1** (peak 4 in Figure 3 3 3) three main photoproducts are formed The first product, peak 2, has a retention time of 3 05 minutes and an absorption maximum at 445 nm This product formed solely without any evidence for the presence of free ligand Because of this feature, this species was tentatively assigned as $[Ru(bpy)_2(4Mepytr)(MeCN)]^{2+}$, in which the pyridyltriazole ligand is bound in a monodentate fashion

The product peak 3, obtained in conjunction with peak 1, and found to be the final product after a period of one hour photolysis, has a retention time 6 8 minutes and an absorption maximum of 425 nm This species was identified as $[Ru(bpy)_2(MeCN)_2]^{2+}$, by comparison with an authentic sample and with literature data[37] This compound is also the expected final photoproduct The

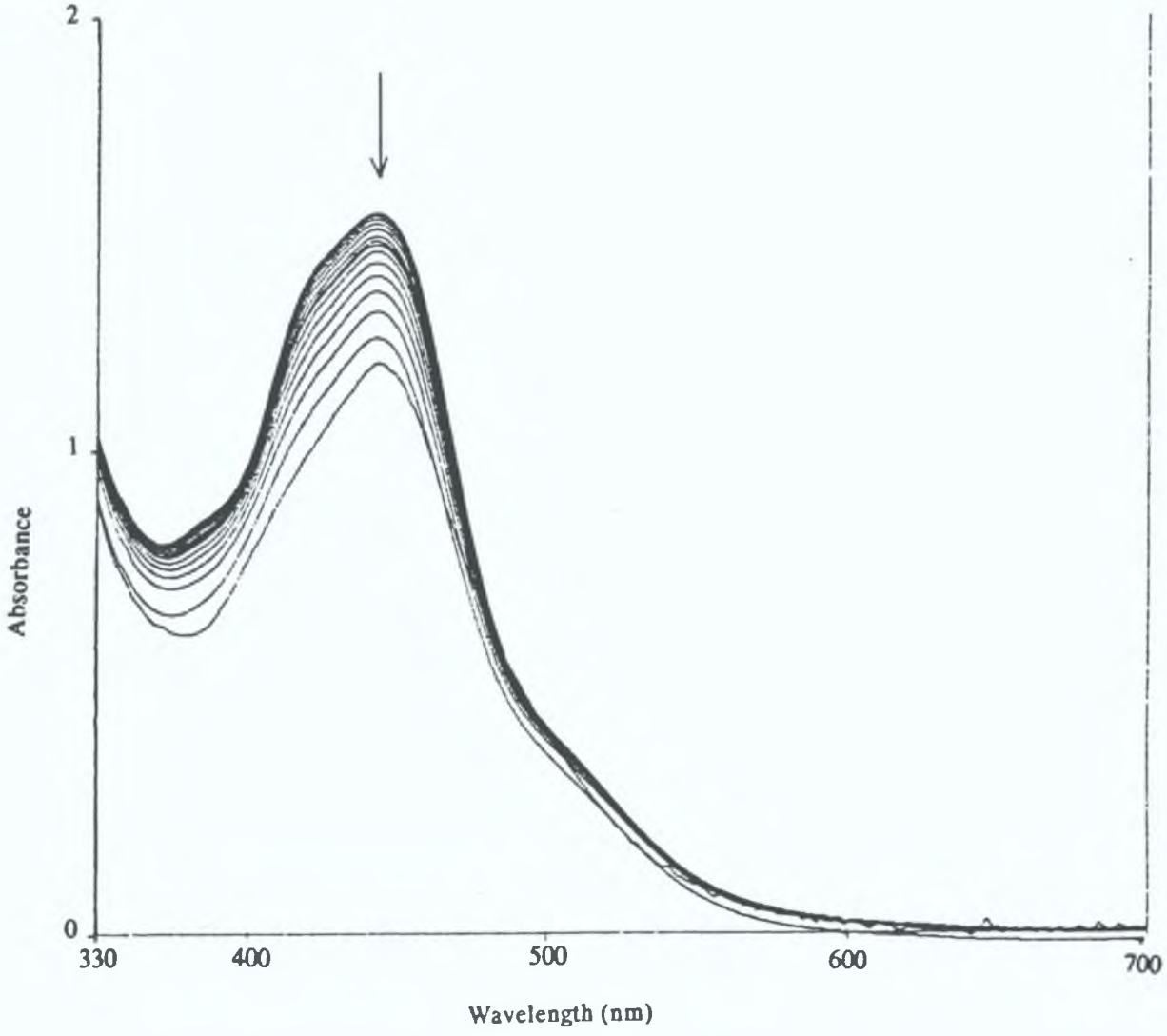

Figure 3.3.2

UV/vis absorption spectra taken during the photolysis of $[Ru(bpy)_2(4Mepytr)]^{2+}$ in acetonitrile.

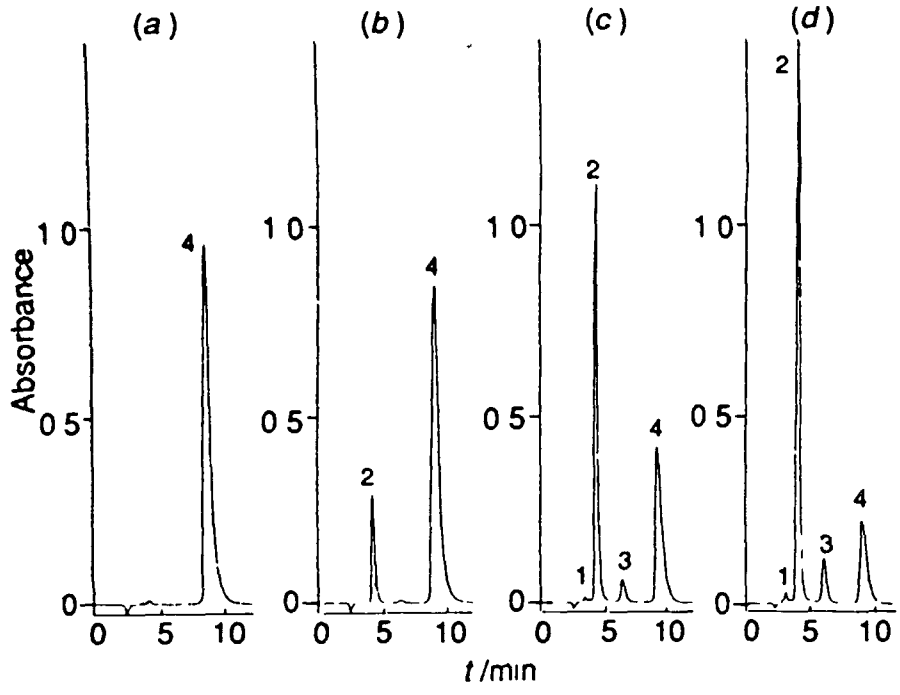

Figure 3 3 3

HPLC traces taken during the photolysis of $[Ru(bpy)_2(4Mepytr)]^{2+}$ in acetonitrile Photolysis times are (a) 0, (b) 60, (c) 360 and (d) 660 s Flowrate 2 0 cm^3 min^{-1}, mobile phase MeCN H_2O (80 20) containing 0 1 mol dm^{-3} $LiClO_4$, detection wavelength 280 nm For peak numbering see text

third species, peak 1, retention time 1 65 minutes was identified as free ligand also by comparison with an authentic sample

A preparative scale photolysis was carried out and the proposed monodentate species was isolated by semi-preparative HPLC Proton NMR spectra substantiated the above interpretation of the identity of the first photoproduct (see Section 3 2)

Further evidence about the nature of the intermediate was obtained by a study of its thermal properties The compound was heated at 80°C in acetonitrile and NMR spectroscopy shows the formation of the starting

bidentate species as the sole product (see Figure 3 3 4) The resonances observed for **3** disappear and are replaced by signals which can be attributed to **1**, with complete loss of the acetonitrile resonance at δ, 2 55

Kinetic and thermodynamic studies were carried out on the $[Ru(bpy)_2(4Mepytr)(MeCN)]^{2+}$ complex in order to investigate the thermal back reaction

$$[Ru(bpy)_2(4Mepytr)]^{2+} \quad <\text{---------} \quad [Ru(bpy)_2(4Mepytr)(MeCN)]^{2+} \quad \mathbf{3.1}$$

The thermal decomposition of compound **3** in acetonitrile, methanol and acetone was followed by UV/vis spectroscopy over a range of temperatures between 70 and 90°C As can be seen in Figure 3 3 5, the reaction proceeds showing no change in the maximum wavelength of absorption However, there is an increase in the amount of light absorbed as the reaction proceeds The reactions fit a first order equation of the form

$$\ln[OD(t) - OD(max) \ / \ OD(0) - OD(max)] = kT \qquad \mathbf{3.2}$$

A typical first order plot is presented in Figure 3 3 6, as used to calculate the rate constant, k, in acetonitrile at 80°C The activation energy of the reaction in acetonitrile, obtained from measurements carried out over the 70 - 90°C temperature range, is 100 (+/- 10) kJ/mol and an entropy change of close to zero was obtained In methanol the activation energy over the same temperature range was the same However, in acetone a value of 70 (+/- 10) kJ/mol was found This discrepancy could be due to the difficulty observed in acetone to keep a constant volume The Arrhenius plot for acetonitrile is presented in Figure 3 3 7

Durham et al [3] have proposed that upon photolysis of ruthenium (II) tris(diimine) complexes, intermediates are formed which contain one of the

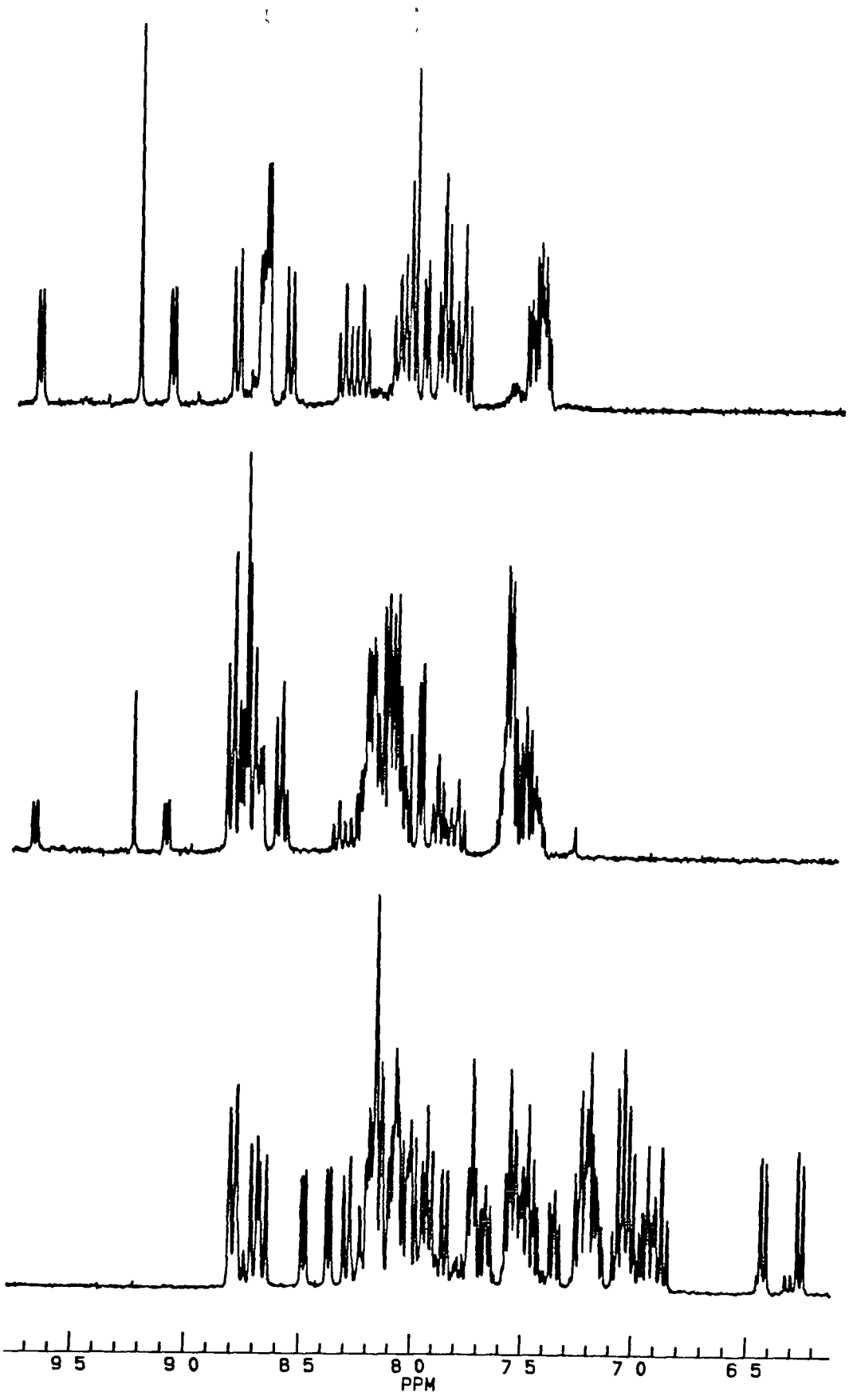

Figure 3 3 4

^1H NMR spectrum in CD_3CN of $[Ru(bpy)_2(4Mepytr)(MeCN)]^{2+}$ at (a) time 0, (b) after 2 h at 80°C, and (c) after 5 h at 80°C

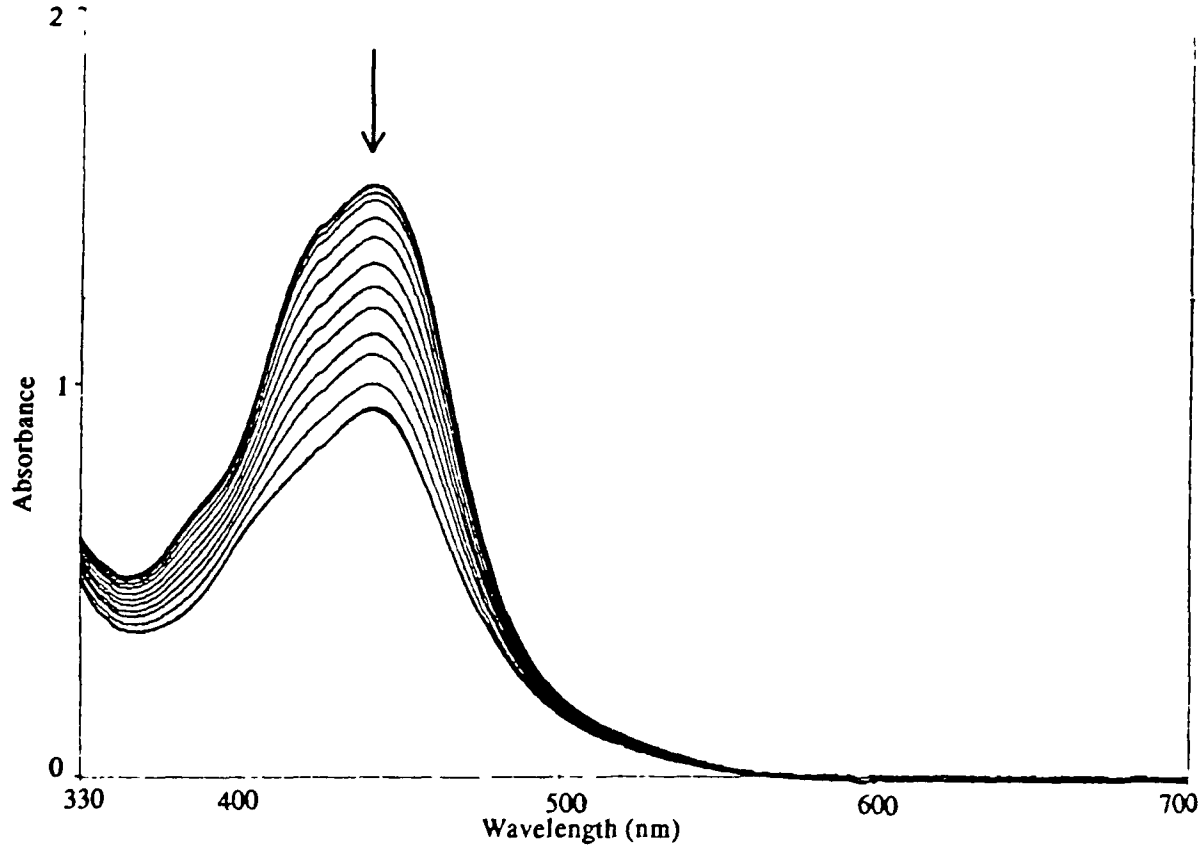

Figure 3 3 5

Thermal decomposition of $[Ru(bpy)_2(4Mepytr)(MeCN)]^{2+}$ at 80°C in acetonitnle

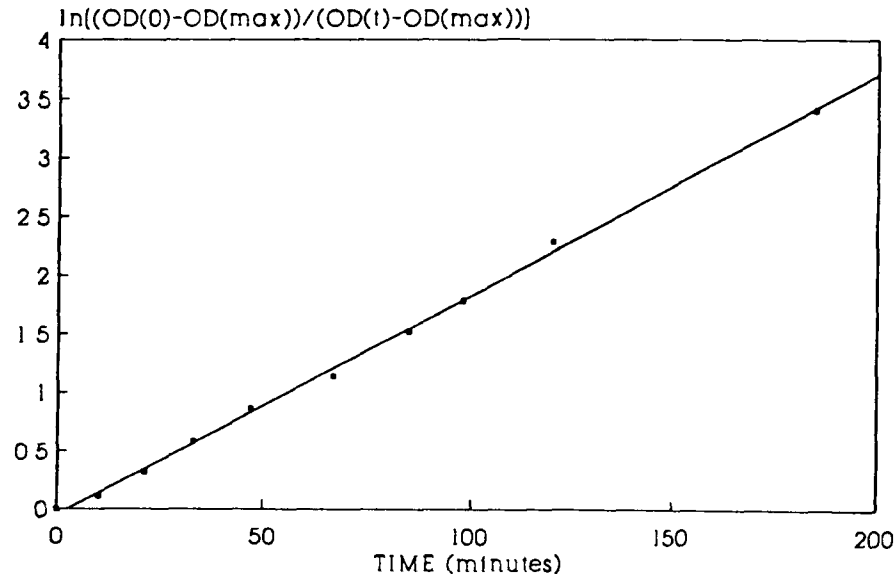

Figure 3 3 6

First order plot used to calculate the rate constant, k, in acetonitrile at 80°C, for $[Ru(bpy)_2(4Mepytr)(MeCN)]^{2+}$

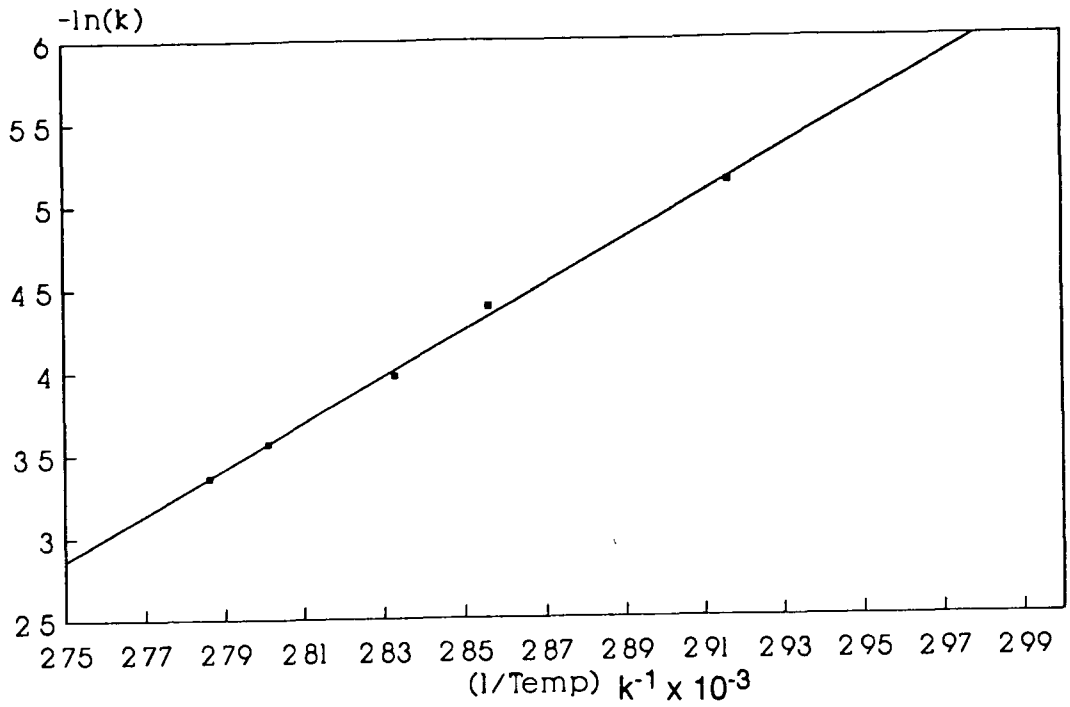

Figure 3 3 7

The Arrhenius plot in acetonitrile of $[Ru(bpy)_2(4Mepytr)(MeCN)]^{2+}$ over a range of temperatures

chelating ligands co-ordinated in a monodentate fashion according to the following equation

$$[Ru(bpy)_2(L\text{-}L')]^{2+} + MeCN \quad <=====> \quad [Ru(bpy)_2(L\text{-}L')(MeCN)]^{2+} \quad \textbf{3.3}$$

They furthermore proposed that thermal ring closure, as in equation 3 1, occurs to regenerate the starting material This has been clearly seen to occur in our situation, with the $[Ru(bpy)_2(4Mepytr)]^{2+}$ complex

Further photochemical experiments were carried out on the isolated monodentate $[Ru(bpy)_2(4Mepytr)(MeCN)]^{2+}$ species Photolysis in acetonitrile causes the formation of one photoproduct, which has been identified as the bis-acetonitrile species, $[Ru(bpy)_2(MeCN)_2]^{2+}$ Clearly, photodecomposition of the monodentate species has occurred However, photolysis in both acetone and methanol, from HPLC and UV/vis data, clearly show the formation of the original bidentate starting material $[Ru(bpy)_2(4Mepytr)]^{2+}$ (peak 3) (see Figure 3 3 8) A fast reaction occurs first in which the monodentate species disappears and forms what is possibly its methanol analogue (peak 2) This in turn disappears in a much slower reaction to form the bidentate species It appears that in solvents that are weaker ligands, photochemically induced ring closure is observed There is no evidence for any free ligand formed throughout the photolysis

Photolysis in acetonitrile / 0 01 M Lithium Chloride

Photolysis of $[Ru(bpy)_2(4Mepytr)]^{2+}$ in acetonitrile and 0 01 M lithium chloride shows a more complicated picture Again UV/vis spectra taken during the photolysis do not show isosbestic points HPLC traces taken during the photolysis are presented in Figure 3 3 9 At photolysis times of up to 170 seconds, the main photoproduct obtained is peak 3, which has a retention time of 3 12 minutes and an absorption maximum of 445 nm This was found to be the previously isolated $[Ru(bpy)_2(4Mepytr)(MeCN)]^{2+}$ monodentate species The formation of this compound reaches a maximum at a photolysis time of 540 seconds and subsequently decreases Another intermediate, peak 1, with a retention time of 1 30 minutes and an absorption maximum of 500 and 340 nm is also formed early in the reaction

This species was again isolated using a preparative scale photolysis experiment and semi-preparative HPLC NMR spectroscopy has shown that this material is $[Ru(bpy)_2(4Mepytr)Cl]^{+}$ This compound was also made by

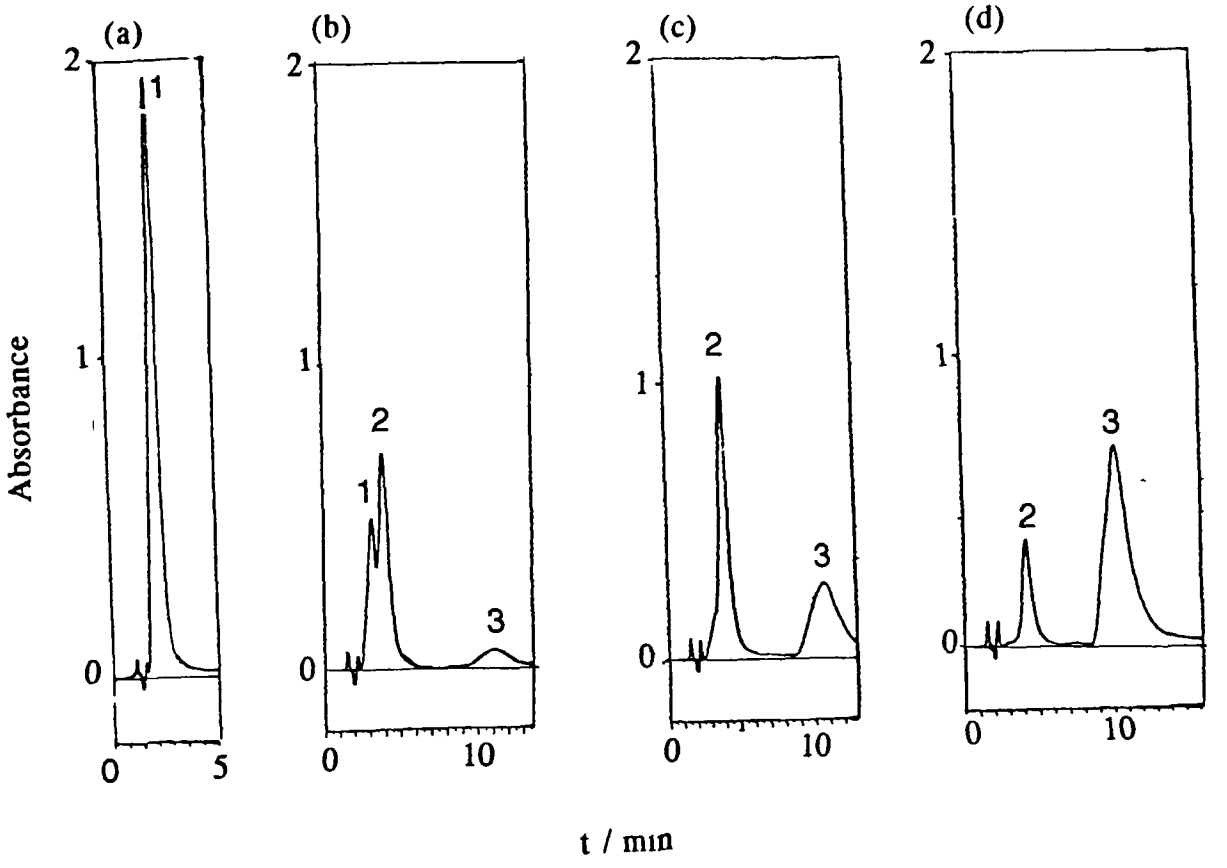

Figure 3 3 8 HPLC traces taken during the photolysis of $[Ru(bpy)_2(4Mepytr)(MeCN)]^{2+}$ in methanol Photolysis times are (a) 0 sec, (b) 10 sec, (c) 1 min and (d) 20 min For photolysis conditions see Figure 3 3 3.

thermal means as seen in the experimental section A striking observation is that according to the NMR data, the resonances observed for the thermally and photochemically prepared compounds are essentially identical An X-ray crystal structure of the related complex $[Ru(bpy)_2(3Mpytr)(Cl)]^+$ (where 3Mpytr = 3-methyl-1-(pyridin-2-yl)-1,2,4-triazole) revealed that the monodentate

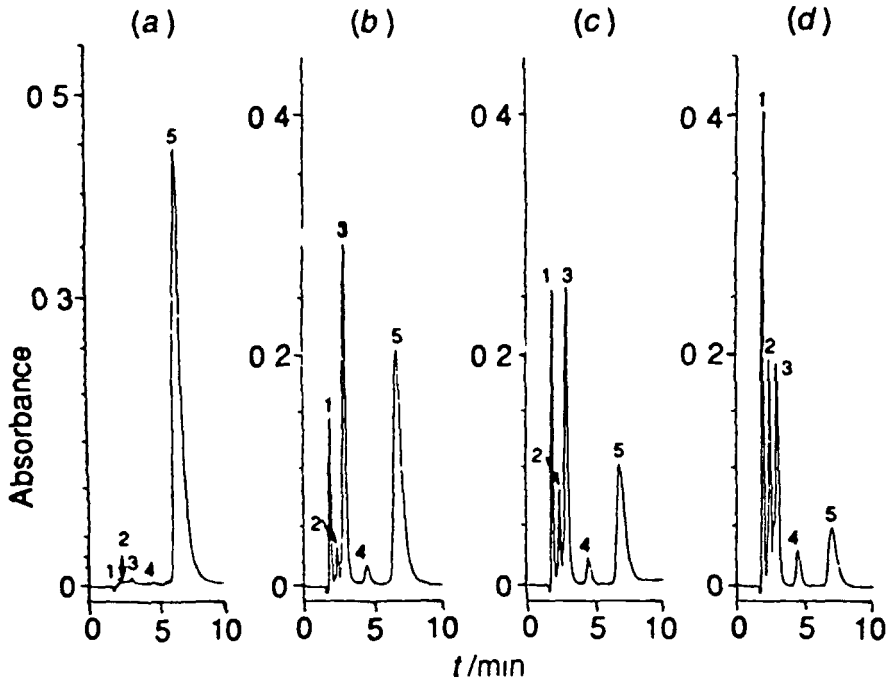

Figure 3 3 9

HPLC traces during the photolysis of $[Ru(bpy)_2(4Mepytr)]^{2+}$ in acetonitrile and 0 01 M LiCl Photolysis times are (a) 0 sec, (b) 200 sec, (c) 400 sec and (d) 700 sec For HPLC conditions as in Figure 3 3 3

co-ordination mode observed was via N4 of the triazole ring, or the non-chelating co-ordination site This suggests that in thermally produced products the co-ordination site that offers the least steric hindrance is favoured [28]

The other photoproducts obtained were identified, by comparison with authentic samples, to be $[Ru(bpy)_2(MeCN)_2]^{2+}$, peak 4, retention time 7 minutes, maximum wavelength 425 nm, and $[Ru(bpy)_2(MeCN)Cl]^{+}$, peak 2, retention time 1 95 minutes, and maximum wavelength at 475 nm It is possible to make a comparison between the peak areas of each photoproduct (including the decay of the starting material) and the photolysis time A plot of such data is presented in Figure 3 3 10

Photolysis experiments carried out on $[Ru(bpy)_2(pnp)]^{2+}$ (where pnp = 2-

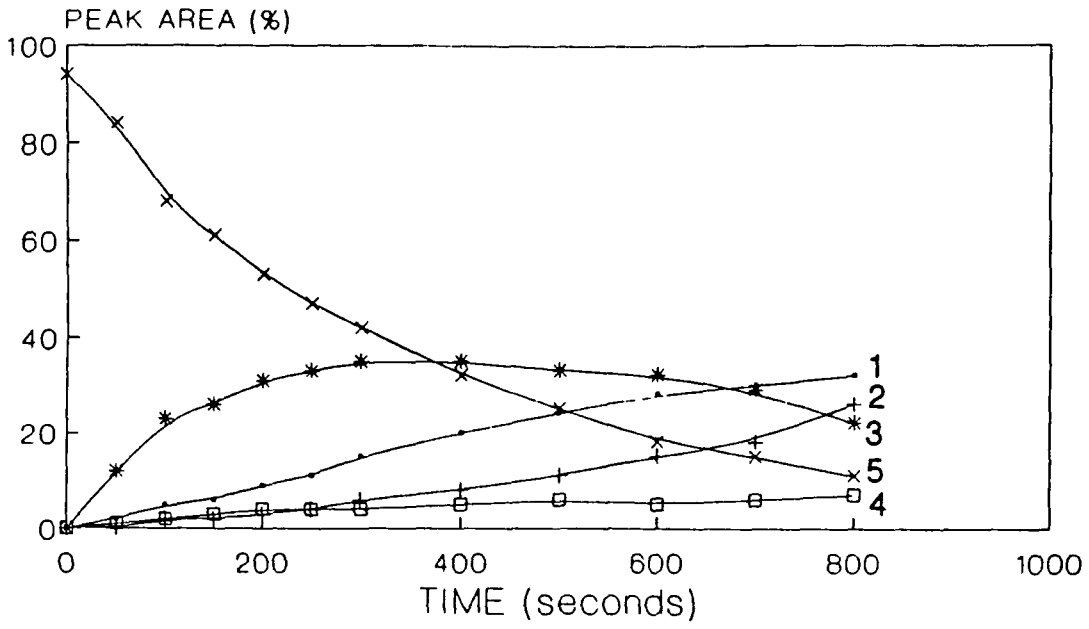

Figure 3 3 10

Plot of the formation of the photoproducts and decay of the $[Ru(bpy)_2(4Mepytr)]^{2+}$ during its photolysis in MeCN containing 0 01 M LiCl

(pyridin-2-yl)-pyrazole) and $[Ru(bpy)_2(1Mpytr)]^{2+}$ (where 1Mpytr = 1-methyl-3-(pyridin-2-yl)-1,2,4-triazole), which only contain nitrogens at chelating positions, gave quite different results Photolysis in acetonitrile of $[Ru(bpy)_2(pnp)]^{2+}$ gave two main photoproducts (see Figure 3 3 11) The main photoproduct, peak 2, retention time 9 20 minutes, maximum wavelength 425 nm, was found to be the bis-acetonitrile $[Ru(bpy)_2(MeCN)_2]^{2+}$ complex The other main photoproduct, peak 1, retention time 1 60 minutes was identified as free ligand No photolysis intermediates were detected The same result was found for $[Ru(bpy)_2(1Mpytr)]^{2+}$

It therefore seem clear that when co-ordination would have to take place via a chelating site of the triazole ring, then bidentate co-ordination results Because of these observations, it is suggested that in both monodentate species, co-ordination is taking place via the non-chelating N1 atom This is

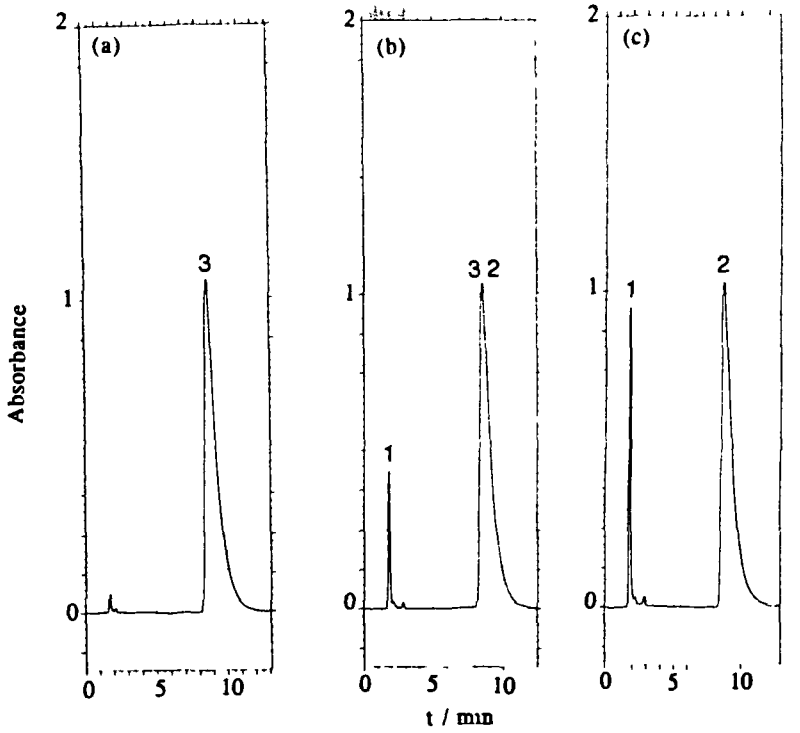

Figure 3 3 11

Photolysis in acetonitrile of $[Ru(bpy)_2(pnp)]^{2+}$ Photolysis times are (a) 0 min, (b) 135 min, and (c) 225 min Mobile phase MeCN H_2O (80 20) containing 0 08 M $LiClO_4$ Flowrate 2 5 cm^3 min^{-1} For peak numbering see text

quite an interesting observation as it suggests that in the photochemically obtained compounds, **2** and **3**, co-ordination of the central ruthenium atom to the triazole ring has changed from the chelating N2 position to the non-chelating N1 atom The proposed structures for the monodentate tnazole complexes are given in Figure 3 3 12

3 3 3 2 Photochemistry of pyrazyltriazole complexes

The complexes containing the pyrazine ligands, 3-(pyrazin-2-yl)-1,2,4-triazole (Hpztr) and 1-methyl-3-(pyrazin-2-yl)-1,2,4-triazole (1Mpztr) were photolysed in pure MeCN, in MeCN containing 0 01 mol/dm^{-3} lithium chloride,

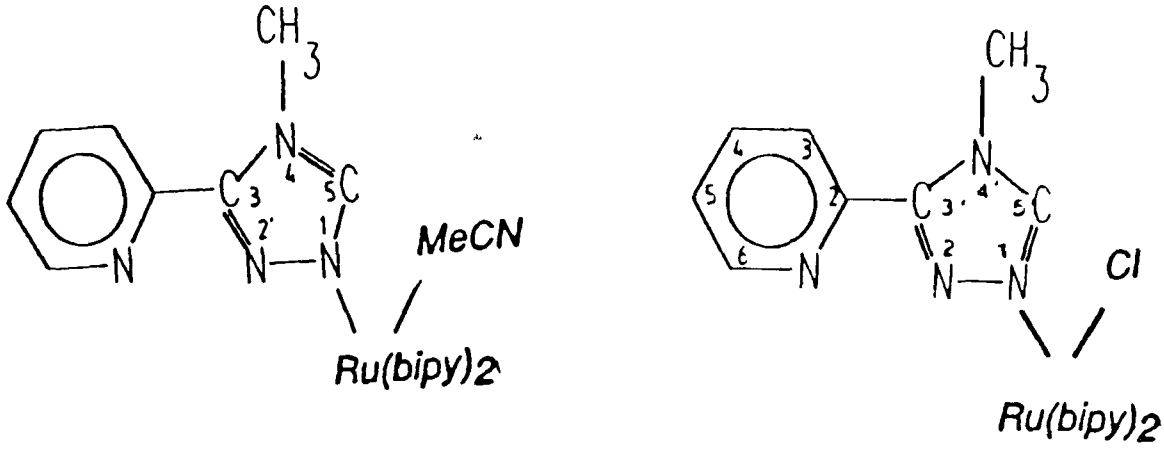

Figure 3 3 12

Proposed structures of the photochemically produced monodentate triazole complexes

in dichloromethane containing 0 005 mol/dm^{-3} benzyl tetraethyl ammonium chloride and in dichloromethane containing 1 drop of trifluoroacetic acid The purpose of these experiments was to examine the effect of the stronger π-accepting pyrazine ring on the photochemical properties of the Ru(II) complexes Photochemical studies of their pyridine analogues carried out by Wang et al[38] have already been analysed and have produced some interesting results The most important difference between the two types of complexes is that for the Hptr complexes the emitting state is bpy-based, whereas for the pyrazyltriazole complexes studied here, the emitting state is pyrazyltriazole-based. It is interesting to study the effect of the lower π* level of the Hpztr ligand on the photochemical properties of these complexes

$[Ru(bpy)_2(1Mpztr)]^{2+}$

The 1Mpztr ligand has no non-chelating site available for co-ordination and during synthesis only one isomer formed Photolysis of $[Ru(bpy)_2(1Mpztr)]^{2+}$ in pure MeCN gave rise to only two main photoproducts, Peak 1, retention time 2 5 min, was identified as free ligand by comparison with an authentic sample

and Peak 2, retention time 5 5 min, λ_{max} 425 nm was identified as $[Ru(bpy)_2(MeCN)_2]^{2+}$ Complete photodecomposition of the complex occurred upon irradiation with visible light without any evidence for the formation of photolysis intermediates Similarly in the other solvent systems studied, irradiation of the ^{1}MLCT band gave rise to a rupture of the Ru-N bond at the triazole ring with formation of free ligand and $[Ru(bpy)_2Cl_2]$ In pure dichloromethane or in dichloromethane containing 1 drop of trifluoroacetic acid photochemical stability was observed Since the ligand 1Mpztr has no N-H proton, protonation of the complex is not necessary However, the fact that no reaction occurs when acid is present in the solution, suggests that the presence of acid itself is not leading to any photochemistry

$[Ru(bpy)_2(pztr)]^+$

Photolysis of both isomers of $[Ru(bpy)_2(pztr)]^+$ in MeCN or in chloride containing solvents were photostable, similar to the results obtained by Wang et al for the corresponding $[Ru(bpy)_2(ptr)]^+$ complexes, where Hptr = 3-(pyridin-2-yl)-1,2,4-triazole under such conditions[12] Even upon prolonged irradiation (> 8 h) no evidence for photoanation is observed It should be noted that injection of a mixture of the two isomers onto the cation exchange column yields two well resolved peaks occurring at retention times of 5 08 min (isomer 1) and 6 25 min (isomer 2)

However, photolysis of both isomers of $[Ru(bpy)_2(Hpztr)]^{2+}$ (obtained by addition of one drop of trifluoroacetic acid) in MeCN gave rise to two main photoproducts which were identified as follows Peak 1, retention time 2 58 min was identified as free ligand and peak 2, retention time 9 34 min, λ_{max} 425 nm was identified as $[Ru(bpy)_2(MeCN)_2]^{2+}$ Figure 3 3 13 shows the HPLC traces taken at different times during the photolysis of isomer 1 in MeCN Photolysis in chloride-containing solvents gave similar results, with rupture of the Ru-N bond at the co-ordinating site occurring, giving rise to photodecomposition of the

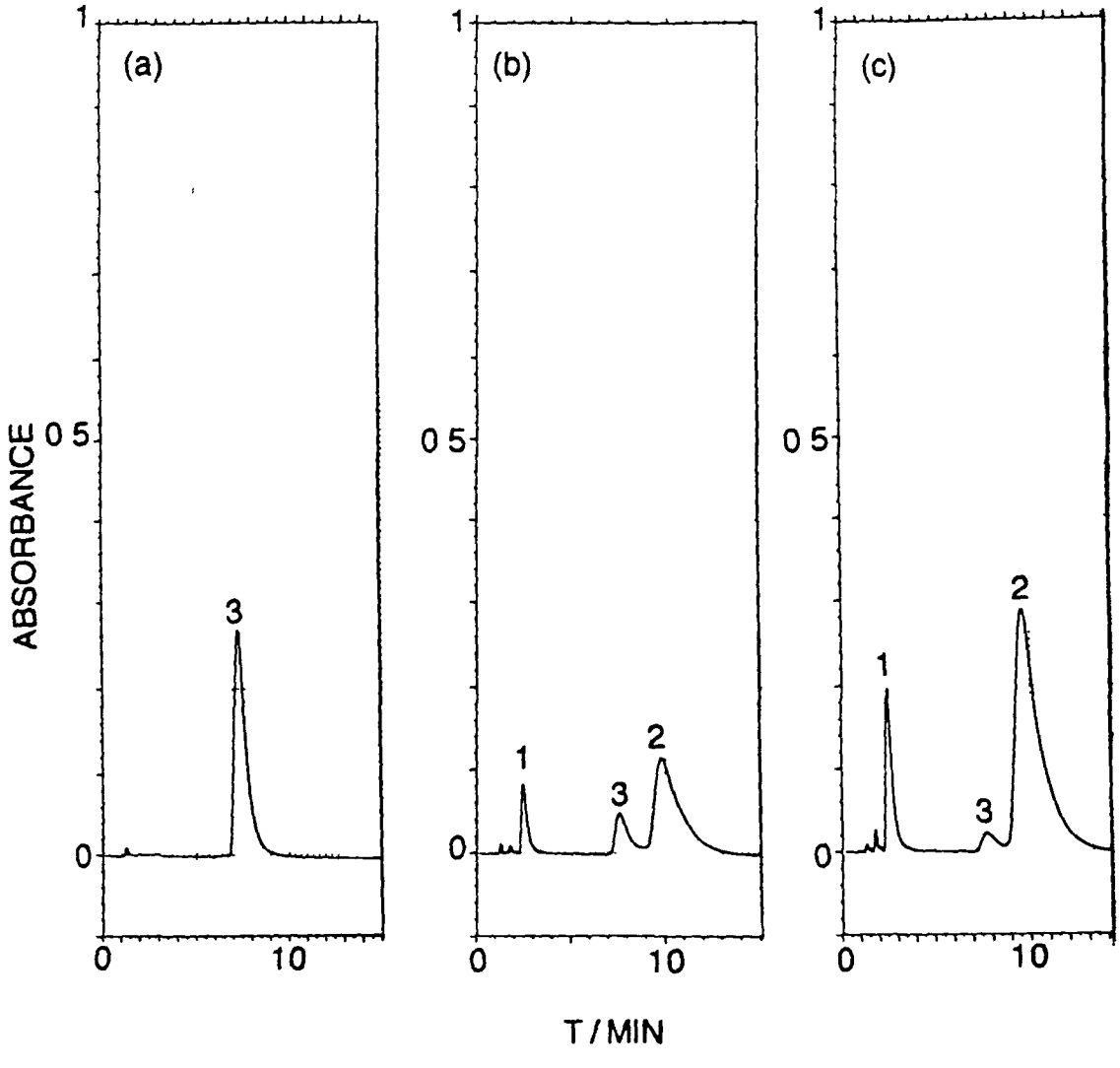

Figure 3 3 13

HPLC traces taken during the photolysis in MeCN of $[Ru(bpy)_2(Hpztr)]^{2+}$ isomer 1 Photolysis times are (a) 0 min, (b) 45 min, and (c) 75 min Flowrate 2 0 cm^3 min^{-1} Mobile phase MeCN H_2O (60 40) containing 0 08 M $LiClO_4$

protonated complexes Again, the protonated complexes containing the analogous Hptr ligand showed complete photodissociation of the compounds[12].

Photolysis of the N4-bound isomer (isomer 1) of $[Ru(bpy)_2(Hpztr)]^{2+}$ in dichloromethane with trifluoroacetic acid results in the formation of a small amount (~ 20%) of the N2 isomer However, irradiation of the N2 isomer (peak 2) under the same conditions results in approx 80 % conversion to the N4-

bound isomer (peak 1) Figure 3 3 14 shows the HPLC traces obtained during this photolysis This phenomenon has already been encountered for the Ru(II) compounds containing the corresponding pyridine ligand (Hptr)[12] It would therefore seem likely that a monodentate form of the pyrazyltriazole complex is formed during the photolysis which anneals to the starting complex while undergoing linkage isomerism to form the N4-bound isomer The actual equilibrium established between both isomers is similar to that in the pyridyltriazole case in which an equilibrium of 4 1 $[Ru(bpy)_2(Hptr)]^{2+}$ (N4) . $Ru(bpy)_2(Hptr)]^{2+}$ (N2) was found[12]

3 3 3 *Luminescent lifetime measurements*

The room temperature and low temperature (77 K) luminescent lifetimes of the two isomers of $[Ru(bpy)_2(pztr)]^+$ and $Ru(bpy)_2(Hpztr)]^{2+}$ are listed in Table 3 3 2 At room temperature, the lifetimes for the protonated complexes are much shorter than those of the deprotonated ones However, at 77 K, an opposite behaviour was observed both protonated isomers have larger emission lifetimes Upon protonation, the Hpztr ligand becomes a better π-acceptor and a weaker σ-donor compared with the deprotonated form This results in stabilisation of the t_{2g} orbitals which further results in an increase in the t_{2g} - ^{3}MLCT energy gap Table 3 3 2 shows that the protonated forms have higher emission energies In agreement with the energy-gap law[39-40], this results in longer emission lifetimes of the protonated species at 77 K

At room temperature, however, the luminescent lifetimes of both isomers decrease upon protonation, in disagreement with the energy-gap law Therefore, non-radiative decay of the ^{3}MLCT state is occurring via a pathway other than radiationless deactivation of the ^{3}MLCT excited state to the ground state of the complex This competing pathway could be the thermally activated

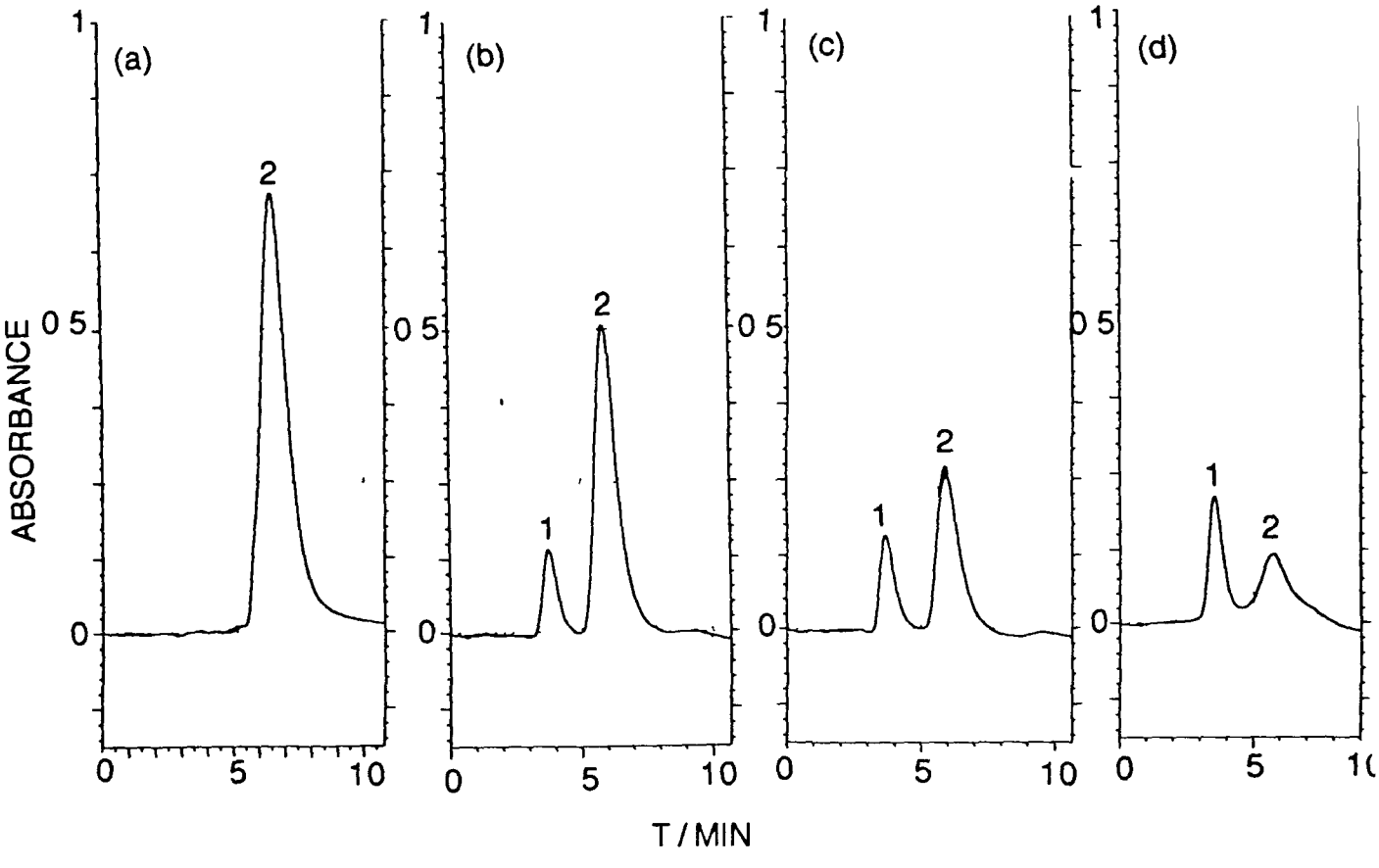

Figure 3 3 14

HPLC traces taken during the photolysis of $[Ru(bpy)_2(Hpztr)]^{2+}$ isomer 2 in dichloromethane containing trifluoroacetic acid Photolysis times are (a) 0 min, (b) 10 min, (c) 20 min, and (d) 60 min Mobile phase 60 20 MeCN H_2O containing 0 06 M $LiClO_4$ Flowrate 2 0 cm^3 min^{-1}

population of a ^3MC state close in energy to the ^3MLCT state (vide supra) This ^3MC state is much more difficult to populate at very low temperatures (< 150 K)[38] As mentioned previously, upon protonation of the co-ordinated

pyrazyltriazole ligand, it becomes a weaker σ-donor and a stronger π-acceptor The weaker σ-donating ability causes a smaller splitting of the t_{2g} - e_g^* energy gap, while the strong π-acceptor ability reduces the t_{2g} - ^{3}MLCT gap Both effects result in decreasing the energy gap between the ^{3}MLCT - ^{3}MC excited states Thus, population of the ^{3}MC state becomes more feasible upon protonation, resulting in faster non-radiative decay or photodecomposition of the protonated species, leading to shorter luminescent lifetime measurements compared to the deprotonated species[41-42]

Temperature dependent lifetime measurements of the deprotonated and protonated Hpztr complexes and of $[Ru(bpy)_2(1Mpztr)]^{2+}$ have been carried out in order to further investigate the photochemical processes occurring with these complexes The temperature dependence of the lifetime of the ^{3}MLCT state has been explained by several workers as due to a close-lying ligand field (d-d) state that may be responsible for photochemistry[43-45]

The temperature dependent lifetime data in the 150 - 300 K temperature range were analysed by assuming that the excited state decay consists of a temperature independent intrinsic decay from the ^{3}MLCT state and a single thermally activated non-radiative decay process according to the equation

$$1/\tau_{obs} = k_0 + A\exp^{(-E_a/RT)} \qquad \textbf{3.4}$$

where $k_0 = k_{nr} + k_r$ (the sum of the temperature independent radiative and non-radiative decays), A is the frequency factor and E_a is the activation energy from the ^{3}MLCT to the ^{3}MC excited levels

The radiative rate constant can be obtained by measuring the luminescent quantum yield and lifetime at room temperature according to the equation

$$k_r = \Phi_{em}/\tau \qquad \textbf{3.5}$$

This constant is obtained at room temperature because it is generally accepted that k_r is temperature independent above 77 K[46] The temperature independent non-radiative rate constant, k_{nr}, can be obtained from the lifetime at 77 K according to the equation

$$k_{nr} = 1/\tau_{77K} - k_r \qquad \textbf{3.6}$$

At 77 K, no extra deactivating processes are present (like population of the ^{3}MC states) and now the value of k_{nr} is only governed by radiationless deactivation of the ^{3}MLCT states

From the activation parameters obtained in this manner, it is possible to calculate the efficiency of population of the ^{3}MC state from the ^{3}MLCT state (η_{ic}) using the following equation

$$\eta_{ic} = A\exp^{(-E_a/RT)} / (k_0 + A\exp^{(E_a/RT)}) \qquad \textbf{3.7}$$

Activation parameters obtained for ruthenium polypyridyl complexes usually fall into two categories

(1) Small activation energies (< 800 cm^{-1}) and low prefactors (< 10^9 s^{-1})

(2) Large activation energies (> 2000 cm^{-1}) and large prefactors (> 10^{11} s^{-1})[47]

Complexes exhibiting the former behaviour are typically unreactive towards photosubstitution[47-48] The low prefactor suggests the process involves the population of a state only weakly coupled to the ^{3}MLCT state Based on these observations, Kober and Meyer have suggested that this activated process corresponds to the population of an MLCT state of largely singlet character[49]

Complexes exhibiting the second type of behaviour are typically photochemically active and the activation process has be ascribed to

population of a ^{3}MC state[47,49]. If relaxation of the ^{3}MC state is rapid relative to crossover from the ^{3}MC state back to the ^{3}MLCT state, the measured E_a represents the activation energy for ^{3}MLCT - ^{3}MC internal conversion. Since the process is viewed as an electron transfer in a strongly coupled system, the prefactor is expected to be large (10^{13} - 10^{14}) [2,47,50]. The complexes are not photostable in this situation.

Table 3.3.4 lists the activation energies (E_a) and pre-exponential factors (A) parameters obtained for the pyrazyltriazole complexes. The high activation energies and prefactors obtained for $[Ru(bpy)_2(Hpztr)]^{2+}$ isomer 1 and for $[Ru(bpy)_2(1Mpztr)]^{2+}$ suggest photochemically unstable complexes. Both of the protonated $[Ru(bpy)_2(Hpztr)]^{2+}$ complexes and $[Ru(bpy)_2(1Mpztr)]^{2+}$ exhibit photolability. The weaker σ-donor capacities of the protonated pyrazyltriazole ligand cause a decrease in the ligand field strength, and a lower ^{3}MC state is expected. Therefore, a decrease in the quantum yield of the emission is noted[2]. The N2 isomer of $[Ru(bpy)_2(Hpztr)]^{2+}$ exhibits intermediate behaviour, with an activation barrier of 2190 cm^{-1} and a prefactor of 9.0×10^{11}. This could conceivably be attributable to ^{3}MLCT and ^{3}MC states in equilibrium. The measured activation energy corresponds approximately to the energy gap between the two states[51]. For the complexes containing the Hptr ligand, this intermediate behaviour was also observed for the protonated N2-bound isomer[12].

The $\ln(1/\tau)$ versus $1/T$ plots for the protonated isomers over the temperature range 150 - 300 K are illustrated in Figure 3.3.15. The N4-bound isomer (isomer 1) exhibits a steep decrease in lifetime above 250 K. At this stage, an activated surface crossing to a ^{3}MC excited state is occurring[47,49]. The population of such an excited state causes a fast deactivation to the ground state of the excited state and/or to a decomposition of the complex[52-54], as seen in the photochemical experiments. The N2-bound isomer (isomer 2) also contains this step at 240 K which may also be attributable to population of

Compound	E_a (cm^{-1})	A (s^{-1})	k_r (s^{-1})	k_{nr} (s^{-1})	k_0 (s^{-1})
$[Ru(bpy)_2(1Mpztr)]^{2+}$	2128	1.7×10^{12}	3.8×10^4	1.1×10^5	1.5×10^5
$[Ru(bpy)_2(pztr)]^{+}$ iso 1	1287	5.1×10^9	5.9×10^3	2.1×10^5	2.2×10^5
$[Ru(bpy)_2(Hpztr)]^{2+}$ iso 1	2935	1.5×10^{13}	1.2×10^3	1.5×10^5	1.5×10^5
$[Ru(bpy)_2(pztr)]^{+}$ iso 2	1217	3.6×10^9	1.5×10^4	2.3×10^5	2.4×10^5
$[Ru(bpy)_2(Hpztr)]^{2+}$ iso 2	2190	9.0×10^{11}	7.6×10^2	1.4×10^5	1.4×10^5
$[Ru(bpy)_2(ptr)]^{+}$ iso 1	600	3.1×10^7	3.7×10^5	8.8×10^4	4.6×10^5
$[Ru(bpy)_2(Hptr)]^{2+}$ iso 1	2860	9.2×10^{13}	3.1×10^4	6.1×10^5	6.4×10^5
$[Ru(bpy)_2(ptr)]^{+}$ iso 2	550	4.7×10^7	8.6×10^4	1.9×10^5	2.8×10^5
$[Ru(bpy)_2(Hptr)]^{2+}$ iso 2	1710	6.0×10^{10}	2.1×10^4	3.9×10^5	4.1×10^5

Table 3.3.4

Activation parameters and kinetic data for mononuclear Ru(II) complexes in ethanol / methanol (4/1) at temperatures 250 - 300 K. Rate constant errors ± 5%, activation parameters ± 10 %. Hptr data from ref. 38.

the deactivating ^{3}MC state.

Both deprotonated isomers have low activation energies and pre-exponential factors and are typically unreactive towards ligand photosubstitution. The slight temperature dependence observed for these complexes above 250 K may be attributable to population of other MLCT excited states only weakly coupled to the ^{3}MLCT excited state. As mentioned previously, this may be a MLCT band of largely singlet character[49].

Figure 3.3.16 illustrates the $\ln(1/\tau)$ versus 1/T plots for both deprotonated isomers in the temperature range 77 - 300 K. Both complexes exhibit an activation step at around 110 K, which is attributable to the melting of the solvent. At this temperature, the solvent molecules around the cation and the metal-ligand bonds can relax to their most favourable position after

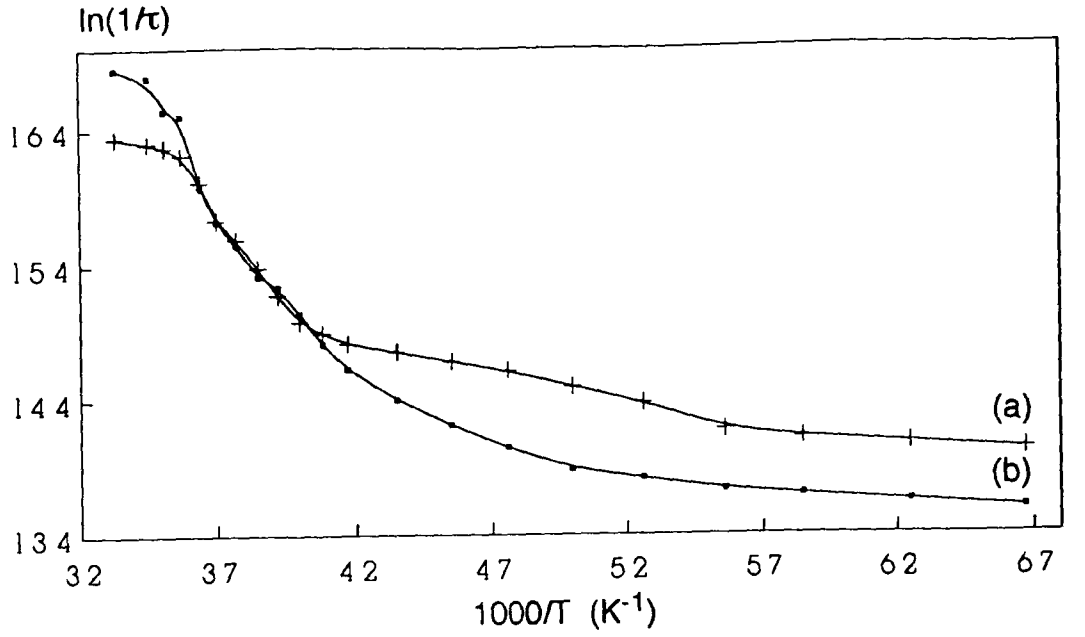

Figure 3 3 15

Temperature dependent luminescent measurements for (a) $[Ru(bpy)_2(Hpztr)]^{2+}$ isomer 1 and (b) $[Ru(bpy)_2(Hpztr)]^{2+}$ isomer 2 in ethanol / methanol (4/1 v/v)

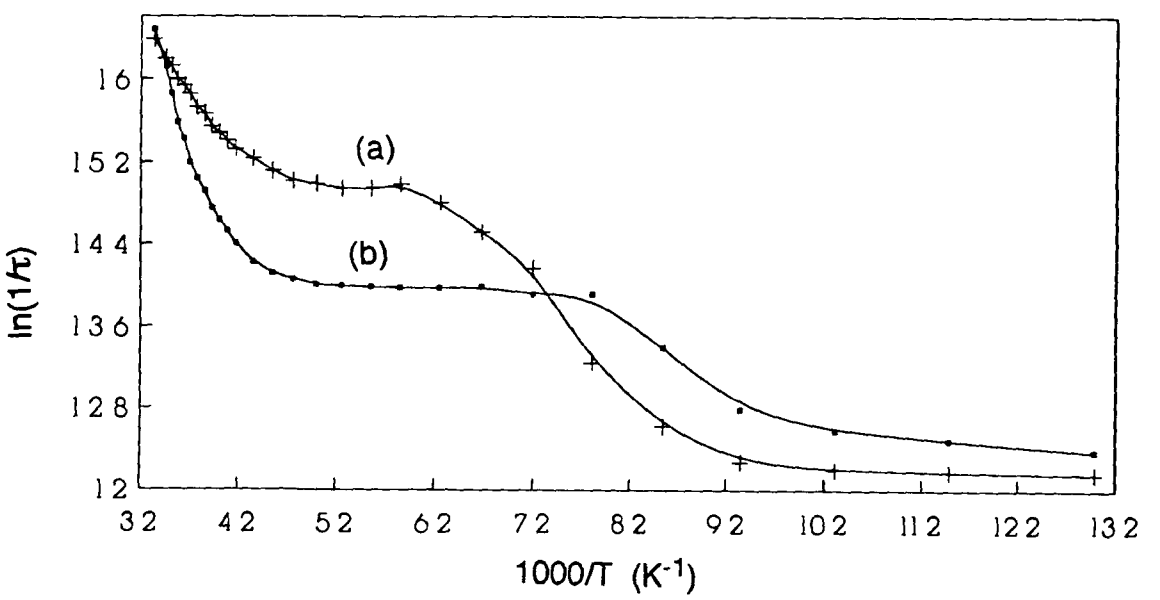

Figure 3 3 16

Temperature dependence for the luminescent lifetimes of (a) $[Ru(bpy)_2(pztr)]^{+}$ isomer 1 and (b) $[Ru(bpy)_2(pztr)]^{+}$ isomer 2 in ethanol / methanol (4/1 v/v)

excitation[2] No other activation step is noted for these complexes It is worth noting, however, that isomer 1 is considerably more sensitive to the melting of the solvent than isomer 2

For both isomers, the activation energy is higher in its protonated form Scandola et al postulated that protonation of $[Ru(bpy)_2(CN)_2]$ results in a decrease in the ^{3}MLCT - ^{3}MC gap and a subsequent increase in the non-radiative relaxation rate[55] and this phenonomen was also observed for the analogous $[Ru(bpy)_2(Hptr)]^{2+}$ complexes[12] This can be explained by taking into account the stronger π-accepting and weaker σ-donor abilities of the protonated Hpztr ligand with respect to its deprotonated form Assuming an average ligand field environment for both protonated and deprotonated complexes, the Ru($d\pi$) ---> Ru(e_g^*) (^{3}MC state) energy should be larger for the deprotonated complex Thus, changes in the metal-ligand interaction which occur upon protonation should serve to decrease the energy gap between the ^{3}MLCT and ^{3}MC excited states, thus increasing the possibility of population of the ^{3}MC state for the protonated complex

Population of the ^{3}MC state is a necessary step in the photochemistry of the protonated pyrazyltriazole complexes The N2 site is a stronger σ-donor (from pK_a data) Therefore, a larger splitting between the t_{2g} and e_g^* levels should occur for the N2 isomer relative to the N4 isomer Therefore, the activation energy for population of the ^{3}MC state from the ^{3}MLCT state is expected to be higher for the N2 isomer This was, however, not found to be the case for the protonated complexes or for the compounds containing the protonated Hptr ligand[12], suggesting that population of the ^{3}MC excited state is not the rate limiting step in the photochemistry of the protonated pyrazyltriazole complexes Perhaps, in this situation, the rate-limiting step is governed by the formation of the monodentate species during the photoisomerisation and the subsequent self-annealing process

By considering redox and luminescent data, approximate relative state energies for these complexes can be calculated, as shown in Figure 6 3 17 These energies are compared to those obtained for the analogous complexes containing the Hptr ligand The relative ground-state energies are obtained from the $Ru^{II/III}$ potentials, while the ^{3}MLCT state energies are obtained from the room temperature luminescent maxima[56] The ^{3}MC state energies can be approximated from the activation energies obtained for population of this state[57] For the protonated forms where population of this state is occurring, the energy gap between the t_{2g} and e_g^* can be estimated using

$$E(t_{2g} - e_g^*) = E_{em} + E_a(^3MLCT - ^3MC) \qquad \textbf{3.8}$$

For the deprotonated species, where population of the ^{3}MC state is not occurring, it is assumed that the ^{3}MLCT - ^{3}MC energy gap is taken to be the same for both protonated and deprotonated complexes (although, it is expected that the energy gap is much larger due to the stronger σ-donor ability of the $pztr^-$ ligand) This value will, therefore, be only a minimum value for this energy gap for the deprotonated species

Values of the ^{3}MLCT - ^{3}MC energy gap for the protonated Hpztr complexes agree reasonably well with those obtained for the Hptr complexes[38] The values obtained for the deprotonated species are only limiting values, but nevertheless indicate that the $pztr^-$ complexes have a lower ^{3}MLCT - ^{3}MC energy gap compared with the ptr^- complexes This suggests that replacement of a pyridine ring by a pyrazine ring in a Ru(II) polypyridyl complex, results in a lowering of the LUMO (it is pyrazyltriazole-based in the protonated complexes) but also results in a greater lowering of the energy of the ^{3}MC excited state, thus reducing this energy gap These complexes are, therefore, less useful as photosensitizers than the ptr^- complexes.

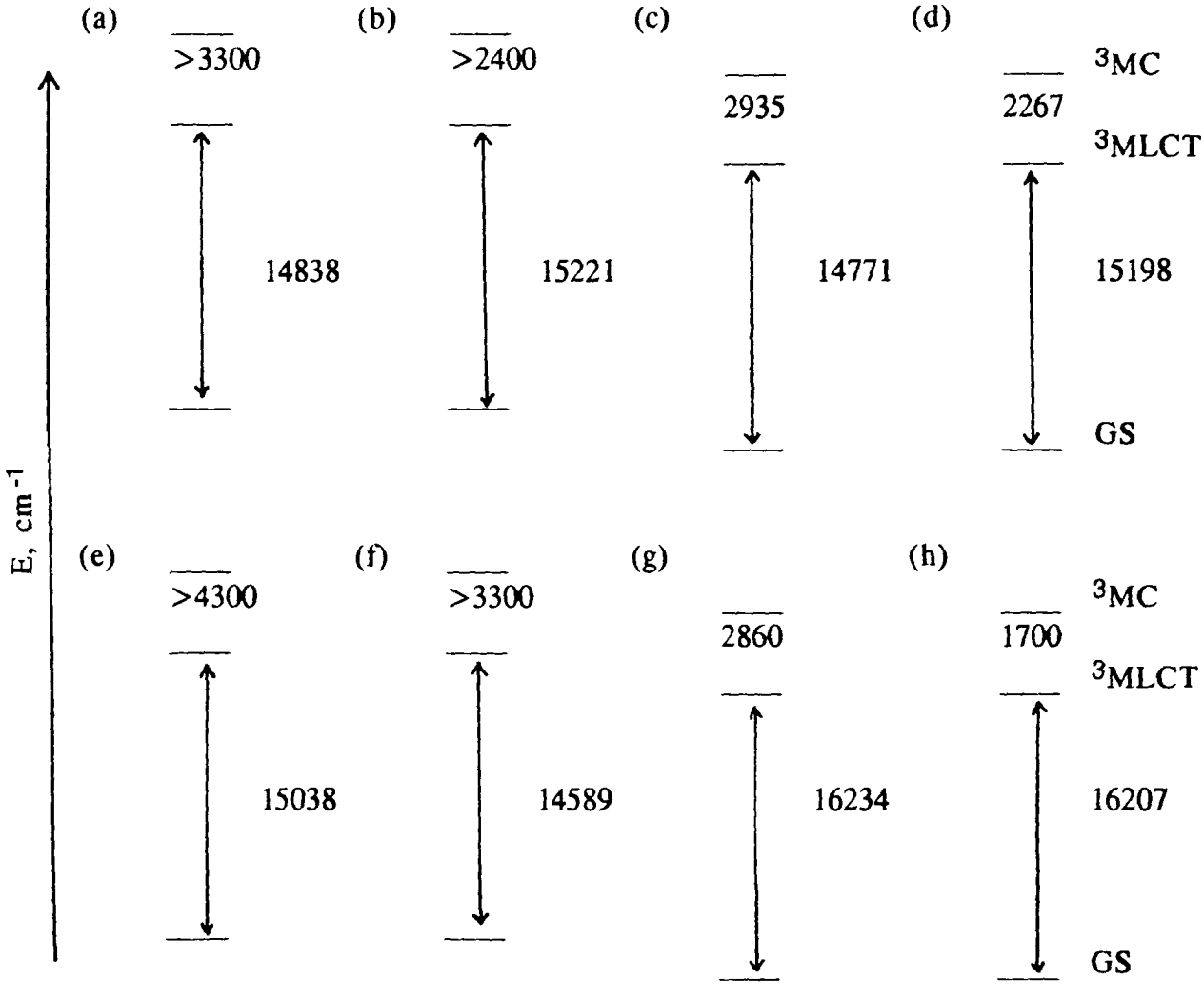

Figure 3 3 17

Approximate relative state energies for (a) $[Ru(bpy)_2(pztr)]^+$ isomer , (b) $[Ru(bpy)_2(pztr)]^+$ isomer 2, (c) $[Ru(bpy)_2(Hpztr)]^{2+}$ isomer 1, (d) $[Ru(bpy)_2(Hpztr)]^{2+}$ isomer 2, (e) $[Ru(bpy)_2(ptr)]^+$ isomer 1, (f) $[Ru(bpy)_2(ptr)]^+$ isomer 2, (g) $[Ru(bpy)_2(Hptr)]^{2+}$ isomer 1 and (h) $[Ru(bpy)_2(Hptr)]^{2+}$ isomer 2

3.4 CONCLUSION

The isolation and characterisation of two complexes containing potentially chelating pyridyltriazole ligands, bound in a monodentate fashion has been achieved. The complexes were obtained by both thermal and photochemical means and in both cases, the monodentate co-ordinated ligands were found to be bound through the non-chelating nitrogen of the triazole ring. Clearly, a photochemically induced slippage of the co-ordination bond from the N2 to the N1 atom of the triazole ring occurs. This change in co-ordination site occurring under photolysis can be removed not only by heating, but also by photochemical means. Normally, photolysis of ruthenium diimine complexes leads to loss of ligands. The regeneration of a bidentate co-ordination mode has so far not been observed with other complexes. It can be concluded that the results achieved in this section agree with the proposal which was put forward for the ligand photosubstitution reaction in the introduction. The results obtained also agree with Durham et al.'s mechanism for thermal ring closure in these triazole ligands[3].

The complex $[Ru(bpy)_2(pztr)]^+$ exhibits interesting photochemical behaviour. In its deprotonated form, photochemical stability is observed, i.e. the deprotonated complexes do not efficiently populate the deactivating ^3MC state at or below room temperature.

According to the results of the temperature dependent luminescent lifetime data, the protonated complexes decay via population of a ^3MC state. Photolysis of either isomer of $[Ru(bpy)_2(Hpztr)]^{2+}$ in CH_2Cl_2 results in linkage isomerism from the N2-bound isomer (isomer 2) to the N4-bound isomer (isomer 1). Photolysis in the presence of co-ordinating anions results in complete photoanation occurring. Therefore, the substitutional photolability of these complexes can be controlled by (de)protonation of the ground state of the compound.

3.5 REFERENCES

[1] J.P. Paris and W.W. Brandt, *J. Am. Chem. Soc.*, **1959**, *81*, 5001.

[2] A. Juris, V. Balzani, F. Barigelletti, S. Campagna, P. Belser and A. von Zelewsky, Elsevier, *Coord. Chem. Rev.*, **1988**, *84*, 85.

[3] B. Durham, J.V. Caspar, J.K. Nagle, and T.J. Meyer, *J. Am. Chem. Soc.*, **1982**, *104*, 4803.

[4] P.V. Pinnick and B. Durham, *Inorg. Chem.*, **1984**, *23*, 1440.

[5] J. Van Houten and R.J. Watts, *Inorg. Chem.*, **1978**, *17*, 3381.

[6] T. Ohno, K. Nozaki, N. Ikeda, and M. Haga, *ET in Inorg. Org. and Biol. Systems, Adv. in Chem.*, **1991**, *228*, 215.

[7] T. Ohno, K. Nozaki, and M. Haga, *Inorg. Chem.*, **1992**, *31*, 548.

[8] R.J. Crutchley, N. Kress, and A.B.P. Lever, *J. Am. Chem. Soc.*, **1983**, *105*, 1170.

[9] R. Hage, A.H.J. Dijkhuis, J.G. Haasnoot, R. Prins, J. Reedijk, B.E. Buchanan, and J.G. Vos, *Inorg. Chem.*, **1988**, *27*, 2185.

[10] B.P. Sullivan, D.J. Salmon, T.J. Meyer, and J. Peedin, *Inorg. Chem.*, **1979**, *18*, 12, 3369.

[11] M. Haga, T. Matsumura-Inoue, K. Shimizu, G.P. Sato, *J. Chem. Soc., Dalton Trans.*, **1989**, 371.

[12] R. Wang, J.G. Vos, R.H. Schmehl, and R. Hage, *J. Am. Chem. Soc.*, **1992**, *114*, 6, 1964.

[13] B.E. Buchanan, Ph. D. thesis, **1989**, Dublin City University, Ireland.

[14] R. Hage, Ph.D thesis, **1991**, Leiden University, The Netherlands.

[15] H.A. Nieuwenhuis, J.G. Haasnoot, R. Hage, J. Reedijk, T.L. Snoeck, D.J. Stufkens, and J.G. Vos, *Inorg. Chem.*, **1991**, *30*, 48.

[16] B.P. Sullivan, D.J. Salmon, and T.J. Meyer, *Inorg. Chem.*, **1978**, *17*, 3334.

[17] R. Hage, R. Prins, J.G. Haasnoot, J. Reedijk, and J.G. Vos, *J. Chem. Soc., Dalton Trans.*, **1987**, 1389.

[18] P J Steel and E C Constable, *J Chem Soc , Dalton Trans* , **1990**, 1389.

[19] R Hage, J G Haasnoot, J Reedijk, and J G Vos, *Inorg Chim Acta*, **1986**, *118*, 73

[20] J M Kelly, C Long, C M O'Connell, J G Vos, and A H A Tinnemans, *Inorg. Chem* , **1983**, *22*, 2818

[21] R P Thummel and Y Jahng, *Inorg Chem* , **1987**, *27*, 1025

[22] S Chirayil and R P Thummel, *Inorg Chem* , **1989**, *28*, 812

[23] R Hage, A H J Dijkhuis, J G Haasnoot, R Prins, J Reedijk, B E Buchanan, and J G Vos, *Inorg Chem* , **1988**, *27*, 2185

[24] E C Constable, S M Elder, J Healy, and D A Tocher, *J Chem Soc , Dalton Trans* , **1990**, 1669

[25] C J Cathey, E C Constable, M J Hannon, D A Tocher, and M D Ward, *J. Chem Soc , Chem Commum* , **1990**, 621

[26] P J Steel and E C Constable, J Chem Soc , Dalton Trans , **1990**, 1389

[27] R J Crutchly and A B P Lever, *Inorg Chem* , **1982**, *21*, 2276

[28] B E Buchanan, P Degn, J M P Velasco, H Hughes, B S Creavan, C Long, J G Vos, R A Howie, R Hage, J H van Diemen, J G Haasnoot, and J Reedijk, *J Chem Soc , Dalton Trans* , **1992**, 1177

[29] P J Steel, F Lahousse, D Lerner, and C Marzin, *Inorg Chem* , **1983**, *22*, 1488

[30] C R Bock, T J Meyer, and D G Whitten, *J Am Chem Soc* , **1974**, *96*, 4710

[31] C Creutz and N Sutin, *Inorg Chem* , **1976**, *15*, 496

[32] J M Clear, J M Kelly, C M O'Connell, and J G Vos, *J Chem Research, (M)*, **1981**, 3039

[33] S M Geraty and J G Vos, *J Chem Soc , Dalton Trans* , **1987**, 3073.

[34] B Fennema, R Hage, J G Haasnoot, J Reedijk, and J G Vos, *Inorg Chim Acta*, **1990**, *171*, 223

[35] J M Calvert, J V Caspar, R A Binstead, T D Moreland, and T J. Meyer, *J. Am Chem Soc* , **1982**, *104*, 6620

[36] Lippard, "Progress in Inorganic Chemistry" Vol 30

[37] D V Pinnick and B Durham, *Inorg Chem*, **1984**, *23*, 1440

[38] R Wang, Ph D thesis, **1991**, Dublin City University, Ireland

[39] J V Caspar, E M Kober, B P Sullivan, and T J Meyer, *J Am Chem Soc.*, **1982**, *104*, 630

[40] J V Caspar and T J Meyer, *J Phys Chem*, **1983**, *87*, 952

[41] J V Caspar and T J Meyer, *J Am Chem Soc*, **1983**, *105*, 5583

[42] L J Henerson, Jr, F R Fronczek, and W R Cherry, *J Am Chem Soc*, **1984**, *106*, 5876

[43] W M Walcholtz, R A Auerback, R H Schmehl, M Ollino, and W R Cherry, *Inorg Chem*, **1985**, *24*, 1758

[44] G H Allen, R P White, D P Rillema, and T J Meyer, *J Am Chem Soc*, **1984**, *106*, 2613

[45] F Barigelletti, A Juris, V Balzani, P Belser, A von Zelewsky, *Inorg Chem*, **1983**, *22*, 3335

[46] J V Caspar and T J Meyer, *Inorg Chem*, **1983**, *22*, 2444

[47] T,J, Meyer, *Pure Appl Chem*, **1986**, *58*, 1193

[48] Y Kawanishi, N Kitamura, and S Tazuke, *Inorg Chem*, **1989**, *28*, 2968

[49] E M Kober and T J Meyer, *Inorg Chem*, **1982**, *21*, 3967

[50] J Davila, C A Bignozzi, and F Scandola, *J Phys Chem*, **1989**, *93*, 1373

[51] W F Wacholtz, R A Auerbach, and R H Schmehl, *Inorg Chem*, **1986**, *90*, 2285

[52] J van Houten and R J Watts, *J Am Chem Soc*, **1976**, *98*, 4853

[53] B Durhan, J V Caspar, J K Nagle, and T J Meyer, *J Am Chem Soc*, **1982**, *104*, 4803

[54] F Barigelletti, L De Cola, V Balzani, R Hage, J G Haasnoot, J Reedijk, and J G Vos, *Inorg Chem*, **1989**, *28*, 4344

[55] J Davila, C A Bignozzi, and F Scandola, *J Phys Chem*, **1989**, *93*, 1373

[56] B E Buchanan, R Wang, J G Vos, R Hage, J G Haasnoot, and J. Reedijk, *Inorg Chem*, **1990**, *29*, 3263

[57] W F Wacholtz, R A Auerbach, and R H Schmehl, *Inorg Chem*, **1987**, *26*, 2989

CHAPTER 4

THE NATURE OF THE LOWEST ENERGY EXCITED STATE IN MIXED LIGAND POLYPYRIDYL COMPLEXES OF RUTHENIUM (II)

4.1 INTRODUCTION

Following the current "supramolecular" tendency of chemical research, inorganic photochemistry is evolving from the study of simple co-ordination complexes to that of more complex systems[1-5] These oligonuclear metal complexes have been extensively studied due to their potential application for light induced energy and electron transfer[6-15]

An appropriate assembly of molecular components capable of performing light-induced functions can be called a photomolecular device In a photochemical molecular device there must be an appropriate energy ordering of the lowest (longest lived, redox active, and / or luminescent) excited state and of the first oxidation and reduction potentials of the various components[16] In these complexes, the bridging ligand is an important parameter, as it often controls the physical properties of these compounds[17] Therefore, it is necessary that the bridge (or connecting component) fulfils a number of important criteria

(1) It must ensure a correct spatial arrangement of the entire system

(2) It must provide an appropriate degree of electronic communication between the components, and

(3) It must not compromise the useful properties of the components[16]

In the case of bridging ligands between ruthenium(II) polypyridine type components, it is well known that even minor changes in the co-ordination about the Ru(II) centre can lead to the loss of valuable properties of the original component[18] For example, by replacing one of the polypyridine ligands in $[Ru(biq)_3]^{2+}$ (where biq = 2,2'-biquinoline) by Cl^- ions, it is possible to change the orbital nature of the lowest excited state, i e by decreasing the ligand field strength, the ^{3}MLCT emission is altered to an emission from the ^{3}MC excited state[19]

Many different bridging ligands have already been co-ordinated to ruthenium(II) polypyridyl complexes, such as pyrazole[20], 4,4'-bipyridine[21-23], 2,2'-bis(benzimidazole)[24] and 4-cyanopyridine[25] As mentioned in the introduction, these chelating ligands can be split into two types The first type involves the usage of a strong π-accepting ligand such as 2,3-bis(2-pyridyl)pyrazine (dpp)[26], azo-2,2-bipyridine (abpy)[27-29] and 2 2'-bipyrimidine (bpm)[30-31] These ligands offer extremely low-lying π^* orbitals for interaction with occupied transition-metal d-levels, which offers increased stabilisation of the filled d-orbitals The lowest unoccupied molecular level (LUMO) in ruthenium(II) complexes containing these ligands is therefore centred upon the bridging ligand and is directly involved in the electrochemical reduction and emission processes The bridging ligand can then act as an electron-transfer or energy-transfer trap and this may result in a decrease in the emission yield and decay lifetime for the complexes

In the second class of compounds, the bridging ligands acts as a strong σ-donor Examples of such ligands are 3-(pyridin-2-yl)-1,2,4-triazole[32], 2,2'-bis(benzimidazole)[33] and bisimidazolate[34] In this situation the bridging ligand acts as a spectator ligand and does not get involved in the emission process The LUMO still remains on the bpy ligand and luminescence takes place from the lowest ^{3}MLCT level located on the auxiliary bpy ligands The bridging ligand may, however, allow energy-transfer or electron-transfer along a suitably organised (in spectroscopic energy or redox potential) sequence of components

The synthesis and properties of mononuclear and dinuclear $Ru(bpy)_2$ complexes with the potentially chelating bridging ligand 3,5-bis-(pyridin-2-yl)-1,2,4-triazole (Hbpt) will be discussed in this chapter Ru(II) polypyridyl complexes containing bpt^- belong to the second class of compounds The anion, bpt^-, is a particularly interesting bridge because, contrary to most of the previously used polypyridyl bridges, it carries a negative charge, which results in a high σ-donor

and low π-acceptor ability Furthermore, its two bidentate functions are chemically distinct, because the central triazole ring uses the N1 (or N2) and N4 nitrogen atoms for co-ordination (see Figure 4 1 1)[35] Also interaction between the two metal centres is very efficient[36]

As shown in previous work, in the bpt⁻ ligand, the σ-donor ability on the N1 (or N2) position is greater than that on the N4 position On the basis of this observation, the lowest energy luminescent ^{3}MLCT excited state (of Ru ---> bpy origin as the lowest π* level is bpy-based) is expected to be centred on the Ru-containing unit attached to the N1 (or N2) position[37], as the LUMO at this position has been lowered significantly due to its stronger σ-donor ability compared with the N4 co-ordination site Such a unit should also experience a ligand field stronger than the N4 unit because it involves the strong σ-donor N1 nitrogen of the triazole ring It was postulated that as a result in dinuclear complexes of the type $[Ru(L)_2(bpt)Ru(L_2)]^{3+}$, the emitting excited state is located on the ruthenium centre bound to the N1 site of the triazole ring, whereas photosubstitution is occurring at the N4 site of the bridging ligand[16] To verify this is important for the application of such compounds in molecular devices, since these differences might be used to effect the aforementioned vectorial energy or electron-transfer However, since the differences between the two states are small, it is very difficult to fully assess the impact of this asymmetric co-ordination upon the photophysical properties of these compounds

In this chapter, a series of dinuclear mixed polypyridyl compounds containing 2,2'-bipyridyl (bpy), 1,10-phenanthroline (phen), and 4,7-diphenyl-1,10-phenanthroline (dpphen) (see Figure 4 1 1) have been prepared, along with their mononuclear analogues Using the synthetic approach recently developed in these laboratories[38], bis(phen), bis(dpphen) and bis(bpy) units can be co-ordinated in a controlled manner to either the N1 or the N4 site of the triazole ring It was thought

that with such mixed polypyridyl compounds (especially bpy and phen), additional information regarding the excited state and redox processes can be obtained, since the UV/vis spectra of the phen and bpy moieties are significantly different It was further hoped that the use of dinuclear complexes would be beneficial in establishing differences between the photophysical properties of the polypyndyl ligands, bpy and phen The redox and excited state properties of all the complexes are reported

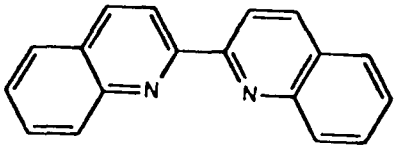

2 2 biquinoline (biq)

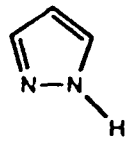

pyrazole(Hpz)

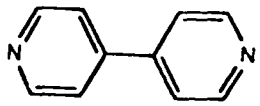

4 4 bipyridine (4 4 bpy)

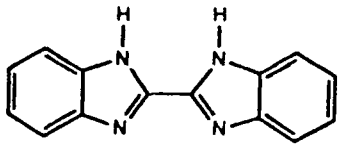

H_2bim

2,2'-bisbenzimidazole

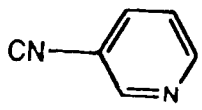

4-cyanopyridine

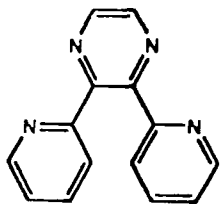

dpp

2,3-bis(2-pyridyl)pyrazine

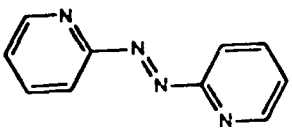

abpy

azo-2,2-bipyridine

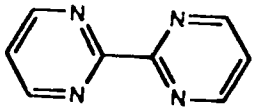

2 2'-bipyrimidine (bpm)

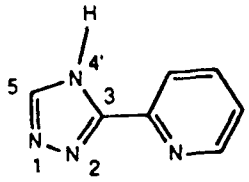

3-(pyridin 2 yl)-1,2,4 triazole

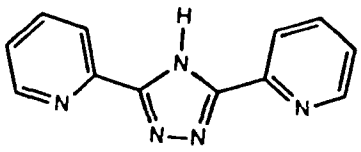

Hbpt

3,5-bis(pyridin-2 yl)-1,2,4 triazole

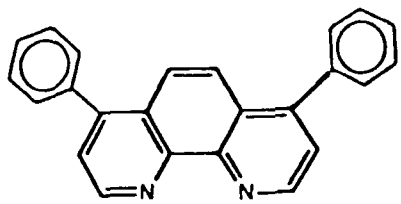

dpphen

4,7-diphenyl-1,10-phenanthroline

Figure 4 1 1

Structures of the ligands cited in the text

4.2 EXPERIMENTAL

All starting materials and solvents used were of commercial grade unless otherwise stated cis-$[Ru(bpy)_2Cl_2]$ $2H_2O$ was prepared as described in section 3 3 2 and in the literature[40] cis-$[Ru(phen)_2Cl_2]$ $2H_2O$ was also prepared according to literature methods[41] cis-$[Ru(dpphen)_2Cl_2]$ $2H_2O$ was prepared in a similar manner to cis-$[Ru(phen)_2Cl_2]$ $2H_2O$

4 2 1 *Preparation of the ligand*

The synthesis of the bridging ligand 3,5-bis-(pyridin-2-yl)-1,2,4-triazole (Hbpt)[39] was carried out by Dr R Hage, Leiden University, The Netherlands

4 2 2 *Preparation of the complexes*

$[Ru(bpy)_2(bpt)]PF_6$ H_2O **(1)**

This compound was prepared as described in the literature[39] Hbpt (2 mmol, 440 mg) was dissolved in 50 cm^3 of hot ethanol water (2 1 v\v) and heated under reflux with cis-$[Ru(bpy)_2Cl_2]$ $2H_2O$ [40] (520 mg, 1 mmol) for 8 h The hot solution was filtered and the solvent removed by rotary evaporation to dryness 10 cm^3 of water was added to the filtrate and the dark red product was subsequently precipitated by addition of a concentrated solution of aqueous NH_4PF_6 The compound was purified by semi-preparative HPLC, using a mobile phase of 80 20 acetonitrile water containing 0 1 M KNO_3 and a flowrate of 2 0 cm^3/min Further purification took place by recrystallisation from acetone water (1 1 v\v) Yield 260 mg (33%)

$[Ru(phen)_2(bpt)]PF_6\ H_2O$ (2)

This compound was prepared in a similar manner to compound (1), 1 mmol cis-$[Ru(phen)_2Cl_2]\ 2H_2O$ [41] and 2 mmol Hbpt (440 mg) were heated under reflux in 50 cm^3 ethanol water (2 1 v\v) for 8 h The compound was again isolated and purified using semi-preparative HPLC Yield 440 mg (52%) Anal found C, 50 0, H, 3 0, N, 14 8% Calcd for $C_{36}H_{26}F_6N_9OPRu$ C, 51 0, H, 3 0, N, 14 8%

$[Ru(bpy)_2(bpt)Ru(bpy)_2](PF_6)_3$ (3)

This compound was prepared as described in the literature[39] using the same procedure as for compound (1), except that 0 5 mmol of the ligand Hbpt (110 mg) was added to a refluxing mixture of 572 mg (1 1 mmol) of cis-$[Ru(bpy)_2Cl_2]\ 2H_2O$ in 100 cm^3 ethanol water (1 1 v\v) for 8 h The residue was again isolated as a PF_6^- salt and purified by recrystallisation from 1 1 acetone water Yield 600 mg (37%)

$[Ru(phen)_2(bpt)Ru(phen)_2](PF_6)_3$ (4)

This compound was prepared from $[Ru(phen)_2Cl_2]\ 2H_2O$ as described for (3) Yield 1 18 g (74 6%) Anal found C, 43 1, H, 2 5, N, 11 5% Calcd for $C_{60}H_{48}F_{18}N_{13}P_3Ru_2$ C, 42 9, H, 2 4, N, 11 7

$[Ru(bpy)_2(bpt)Ru(phen)_2](PF_6)_3\ 2H_2O$ (5)

1 mmol of $[Ru(bpy)_2(bpt)]PF_6\ H_2O$ (786 mg) was heated under reflux for 8 h with 1 2 mmol $[Ru(phen)_2Cl_2]\ 2H_2O$ (577 mg) in 50 cm^3 ethanol water (1 1 v\v) and purified by recrystallisation from acetone water (1 1 v\v) and semi-preparative HPLC Yield 1 g (65 5%) Anal found C, 43 0, H, 2 7, N, 11 4% $C_{56}H_{44}F_{18}N_{13}O_2P_3Ru_2$ requires C, 42 9, H, 2 8, N, 11 6%

$[Ru(phen)_2(bpt)Ru(bpy)_2](PF_6)_3\ 2H_2O$ **(6)**

This complex was prepared as described for (5), using 1 mmol $[Ru(phen)_2(bpt)]PF_6\ H_2O$ (846 mg) and 1 2 mmol $[Ru(bpy)_2Cl_2]\ 2H_2O$ (520 mg) These were refluxed for eight hours in ethanol water (1 1 v\v) and purified by semi-preparative HPLC and by recrystallisation from acetone water (1 1 v\v) Yield 1 2 g (78 6%) Anal found C, 42 7, H, 2 6, N, 11 2% $C_{56}H_{44}F_{18}N_{13}O_2P_3Ru_2$ requires C, 42 9, H, 2 8, N, 11 6%

$[Ru(bpy)_2(bpt)Ru(dpphen)_2](PF_6)_3\ 2H_2O$ **(7)**

This complex was prepared as for (5), using 0 5 mmol $[Ru(bpy)_2(bpt)]PF_6\ H_2O$ (393 mg) and 0 6 mmol $[Ru(dpphen)_2Cl_2]\ 2H_2O$ (523 mg) Yield 800 mg (86 %) Anal found C, 52 6, H, 3 3, N, 9 6 $C_{80}H_{60}F_{18}N_{13}O_2P_3Ru_2$ requires C, 51 3, H, 3 2, N, 9 7%

4.3 RESULTS AND DISCUSSION

4 3 1 ^1H NMR spectroscopy

An outline of the synthetic scheme used to prepare the complexes is presented in Scheme 4 1 For the dinuclear complexes two geometrical isomers may be present, depending on the relative orientation of the bpy (or phen) ligands It is also possible that each geometrical isomer has a corresponding optical isomer, although these are not expected to further complicate the NMR spectra[42-43] One of the most important applications of the ^1H NMR spectra is to verify the co-ordination mode of the bpt$^-$ ligand in the mixed-ligand dinuclear complexes We have already seen, in the previous chapter, that proton NMR spectroscopy can provide useful information regarding the structure of the ruthenium complexes 2-dimensional COSY techniques have been employed in all cases in order to elucidate the structure of the complexes[44]

A listing of the chemical shifts observed for these complexes is presented in Table 4 3 1 As the protons of the polypyridine ligands fall into the normal range for these types of complexes, they are not included

Mononuclear compounds

Both pyridine rings of the bpt$^-$ ligand give two distinct sets of protons An x-ray structure of $[Ru(bpy)_2(bpt)]^+$ has already been determined[45], and this revealed that one pyridine ring is bound to the $Ru(bpy)_2$ moiety together with N1 of the triazole ring (ring A) and that the other ring is free (ring B) The most important information concerning the co-ordination mode of the bpt$^-$ ligand comes from a study of the position of the H^6 proton in the co-ordinated and uncoordinated ligand

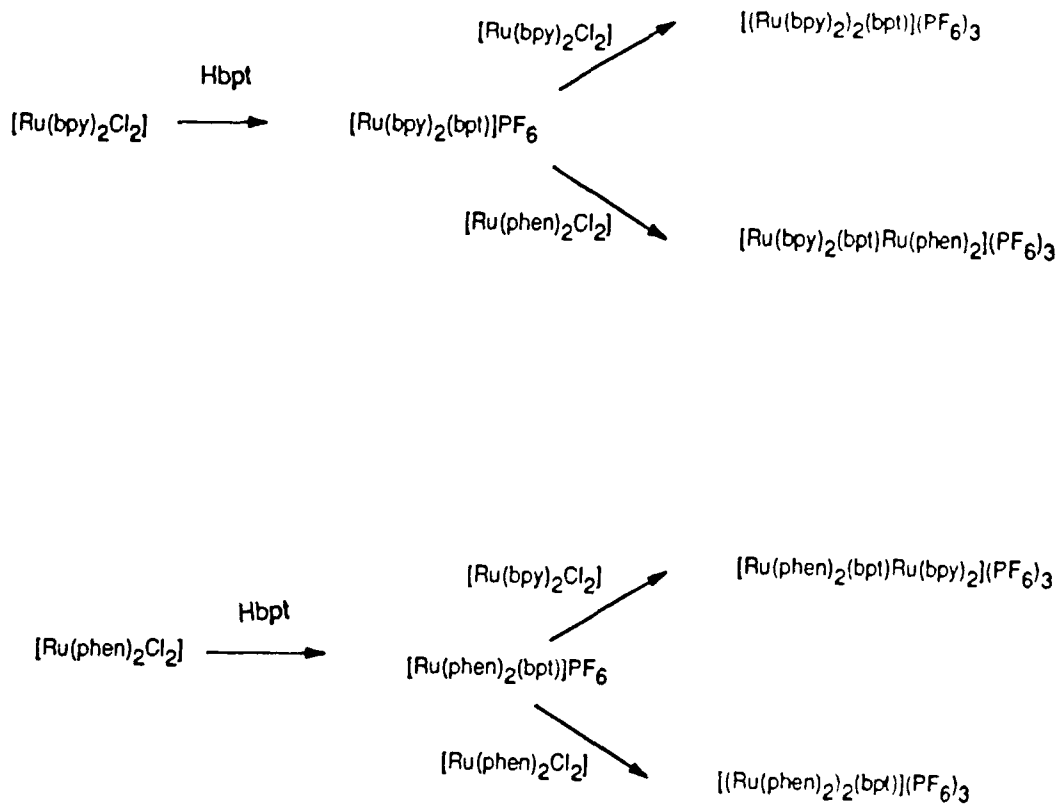

Scheme 4 1

Synthetic scheme used for the preparation of the bpt$^-$ complexes

From Table 4 1, it can be seen that for $[Ru(bpy)_2(bpt)]^+$, one H^6 proton is found at 7 74 ppm for ring A, whereas the other H^6 proton is found at 8 45 ppm for ring B This large difference between ring A and ring B for this proton indicates that the H^6 proton at 7 74 ppm has to be assigned to the metal bound pyridine ring, as it is strongly shifted upfield This is due to the fact that the H^6 proton of the pyridine ring feels the ring current of an adjacent bpy ligand (magnetic anisotrophic effect) and hence becomes shifted upfield[46] By using 2-dimensional COSY techniques, it is now possible to assign the other protons of the bpt$^-$ ligand

COMPOUND		H^3	H^4	H^5	H^6
$[Ru(bpy)_2(bpt)]^+$	Ring A	8 23 (+0 08)	7 99 (-0 01)	7 26 (-0 26)	7 74 (-0 97)
	Ring B	8 06 (-0 09)	7 74 (-0 26)	7 20 (-0 32)	8 45 (-0 22)
$[Ru(phen)_2(bpt)]^+$	Ring A	8 24 (+0 09)	7 88 (-0 12)	7 04 (-0 40)	7 49 (-1 22)
	Ring B	7 95 (-0 20)	7 72 (-0 28)	7 21 (-0 31)	8 45 (-0 22)
$[(Ru(bpy)_2)_2(bpt)]^{3+}$	Ring A	6 69 (-1 46)	7 33 (-0 67)	7 21 (-0 31)	7 82 (-0 85)
	Ring B	8 73 (+0 58)	8 08 (+0 08)	7 29 (-0 23)	7 11 (-1 56)
$[(Ru(phen)_2)_2(bpt)]^{3+}$	Ring A				
Isomer 1	Ring B	6 22 (-1 93)	6 88 (-1 12)	6 79 (-0 73)	7 43 (-1 28)
Isomer 2	Ring A	8 52 (+0 37)	7 79 (-0 21)	7 03 (-0 49)	7 15 (-1 56)
	Ring B	6 34 (-1 81)	6 93 (-1 07)	6 73 (-0 79)	7 27 (-1 44)
		8 55 (+0 40)	7 87 (-0 13)	7 04 (-0 48)	7 21 (-1 50)
$[Ru(bpy)_2(bpt)Ru(phen)_2]^{3+}$					
	Ring A	6 43 (-1 72)	7 00 (-1 00)	6 88 (-0 64)	7 33 (-1 38)
	Ring B	8 64 (+0 49)	7 63 (-0 37)	7 33 (-0 19)	6 86 (-1 81)
$[Ru(phen)_2(bpt)Ru(bpy)_2]^{3+}$					
	Ring A	6 49 (-1 66)	7 12 (-0 88)	6 96 (-0 56)	7 56 (-1 15)
	Ring B	8 67 (+0 52)	7 84 (-0 16)	7 18 (-0 33)	7 34 (-1 33)
$[Ru(bpy)_2(bpt)Ru(dpphen)_2]^{3+}$					
		6 62 (-1 53)	7 16 (-0 84)	6 97 (-0 55)	7 44 (-1 23)
	Ring A	9 02 (+0 87)	7 85 (-0 15)	7 03 (-0 49)	6 95 (-1 72)
	Ring B				
Hbpt	Ring A and Ring B	8 15	8 00	7 52	8 71

Table 4 3 1 ^1H NMR resonances for the bpt^- complexes in acetone d^6, and for the free ligand in deuterated DMSO Chemical shifts compared with those of the free ligand are given in parenthesis (H^3 and H^6 = doublets, H^4 and H^5 = multiplets)

The H^6 proton of ring B of the pyridine triazole ligand also experiences an upfield shift, but this time of only 0 22 ppm This is due to the fact that upon co-ordination the Hbpt ligand becomes deprotonated and more electron density is now present at the pyridine ring This causes and upfield shift, although no direct interaction with adjacent bpy groups is present From these observations, it can be concluded that the $Ru(bpy)_2$ moiety for $[Ru(bpy)_2(bpt)]^+$ complex is bound via ring A of the bpt^- ligand Co-ordination takes place via N1 of the triazole ring as observed from the X-ray structure analysis

^1H NMR data for the mononuclear $[Ru(phen)_2(bpt)]^+$ complex (see Figure 4 3 1) reveals an upfield shift of 1 22 ppm for the H^6 proton of ring A, compared with an upfield shift of only 0 22 ppm for ring B In both species co-ordination takes place via the same co-ordination site at the triazole ring It does appear, however, that the presence of adjacent phen ligands shifts the H^6 proton to a much higher field that with the corresponding bpy ligands The variation in resonances of Ring A between phen and bpy can be because of two reasons

1 Larger electron density on the bpt^- ligand

2 Larger anisotrophic effect for phen

If the phenanthroline ligand is a less good π-acceptor than bpy, it would drain less electron density from the bpt^- ligand Hence, there would be a higher electron density on the bpt^- ligand, causing the NMR resonances to shift to higher field Also the phen ligand has a "larger" π-system and may, therefore, have stronger ring currents These electronic effects could cause the upfield shift of the bpt^- protons

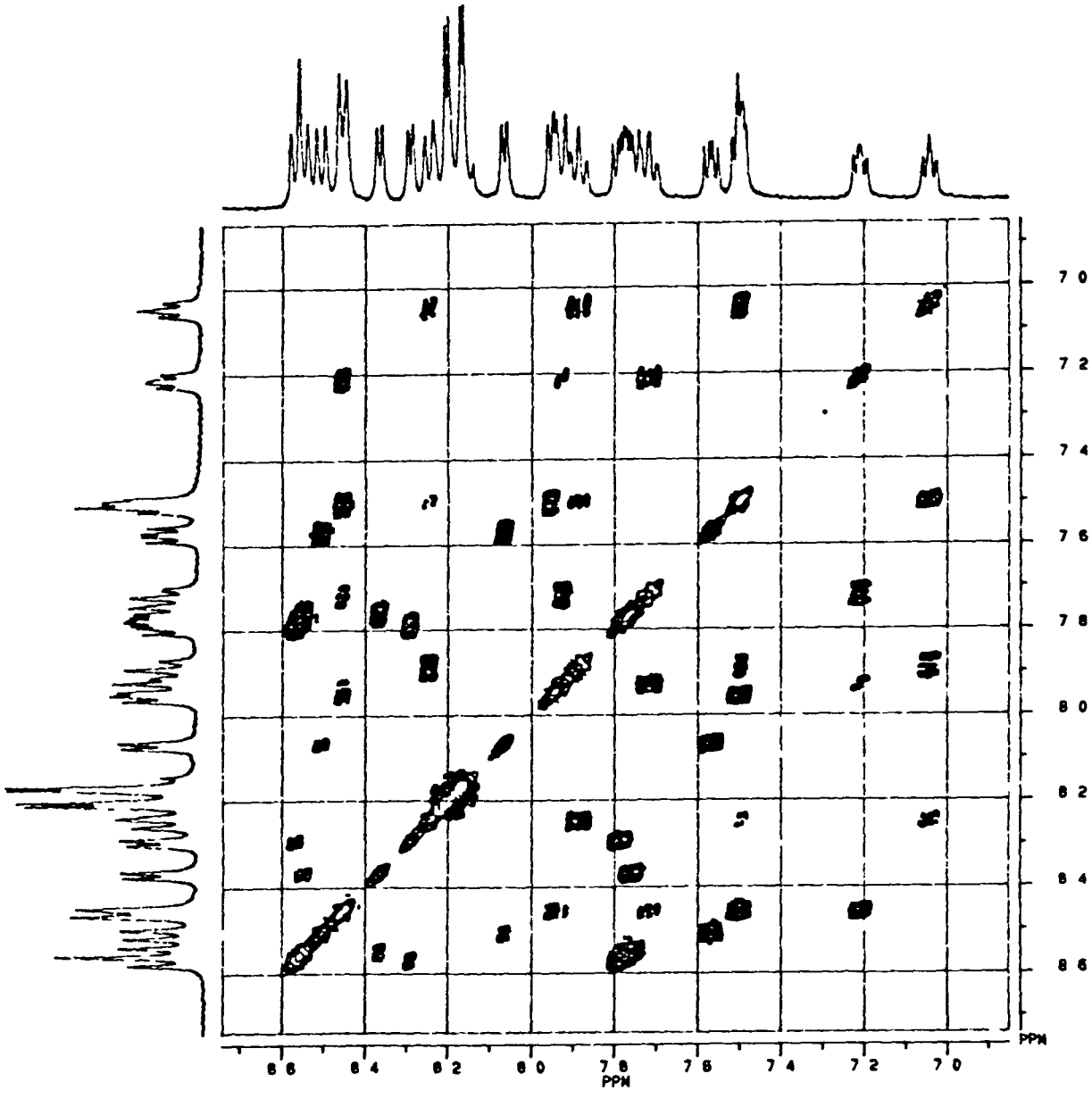

Figure 4 3 1

^1H and COSY NMR spectrum of the mononuclear $[Ru(phen)_2(bpt)]^+$ complex

Dinuclear compounds

Only one isomer was evident in the ^1H NMR spectrum of $[(Ru(bpy)_2)_2(bpt)]^{3+}$ complex The doublet at 6 69 ppm was assigned to the H^3 proton of ring A of the bpt^- ligand, since there is only a short distance between the H^3 proton of ring A and one of the bipyridine rings This should result in a large diamagnetic anisotrophic interaction occurring This results in a shift of the resonance of the H^3 proton to a higher field, as seen in the monomeric complex with the H^6 proton This coupled with the larger j-splitting of this doublet compared with a H^6 proton confirms its assignment as H^3 [47-48]

This doublet is again present in the NMR spectrum of the dinuclear phenanthroline complex, (**4**), implying that this doublet occurs irrespective of the nature of the $Ru(L\text{-}L')_2$ moiety co-ordinated to the bpt^- ligand, where L-L' is phen or bpy or dpphen By using COSY techniques, the H^4, H^5 and H^6 protons of the same ring were readily assigned

The doublet at 7 11 ppm has been assigned to the H^6 proton, shifted 0 85 ppm upfield due to its proximity to an adjacent bpy (or phen) ligand The upfield shift of the H^5 proton, compared to that of the free ligand, is similar to the mononuclear complexes and can be explained by the presence of the negatively charged bpt^- ligand It is interesting to note that again replacement of a bpy ligand by a phen ligand shifts all the protons of the bpt^- ligand considerably upfield Two geometrical isomers formed in a 1 1 ratio and are evident in the NMR spectrum of the dinuclear $[(Ru(phen)_2)_2(bpt)]^{3+}$ complex, as evident from the presence of two H^3 doublets observed at 6 22 and 6 32 ppm No attempts have been made to separate these isomers, as it has been shown previously that the physical properties of the two geometrical isomers of $[(Ru(bpy)_2)_2(bpt)]^{3+}$ are the same[39].

All future measurements on this complex are carried out with this mixture of the two isomers

The chemical shifts of the second pyridine ring are very different, H^3 of ring B is now observed at a much lower field (8 73 ppm for $[(Ru(bpy)_2)_2(bpt)]^{3+}$) This proton is not affected by an adjacent bpy (or phen) ligand By using COSY techniques, it was then possible to assign all other protons in this pyridine ring The H^6 proton for ring B is shifted more upfield than in ring A, occurring at 7 11 ppm, possibly due to the negatively charged bpt^- ligand and an adjacent bpy (or phen for compound (**4**)) ligand Figure 4 3 2 shows the proton NMR spectrum of the $[(Ru(phen)_2)_2(bpt)]^{3+}$ complex

The two related mixed-ligand dimeric species, compounds (**5**) and (**6**) show differences in their ^1H NMR spectra due to differences in their co-ordination at the triazole ring Figure 4 3 3 shows the proton NMR spectra obtained for both species The H^6 proton for ring B in complex (**5**) is shifted considerably more upfield than in complex (**6**) This is again due to the effect of the adjacent phen ligand causing a more dramatic upfield shift than an adjacent bpy ligand In compound (**6**), the H^6 proton for ring A is not as significantly shifted upfield as for compound (**5**) This is presumably due to the stronger σ-donor properties of the N1 position of the triazole ring It has been shown previously[49] for imidazole ligands that an increase of electron density on the ligand (with a consequent reduction in the σ-donor properties) causes an upfield shift of the imidazole protons The NMR data, therefore, suggest that bpy is a stronger σ-donor than phen For $[Ru(bpy)_2(bpt)Ru(dpphen)_2]^{3+}$, we see an increase in the upfield shift of the H^6 proton of ring B by 0 16 ppm when bpy is replaced by dpphen This would suggest that the larger π-system of the dpphen ligand may have stronger ring currents, thus causing an upfield shift of the bpt^- protons Compared with compound (**5**), a downfield shift of 0 09 ppm for the H^6 proton of this compound is observed

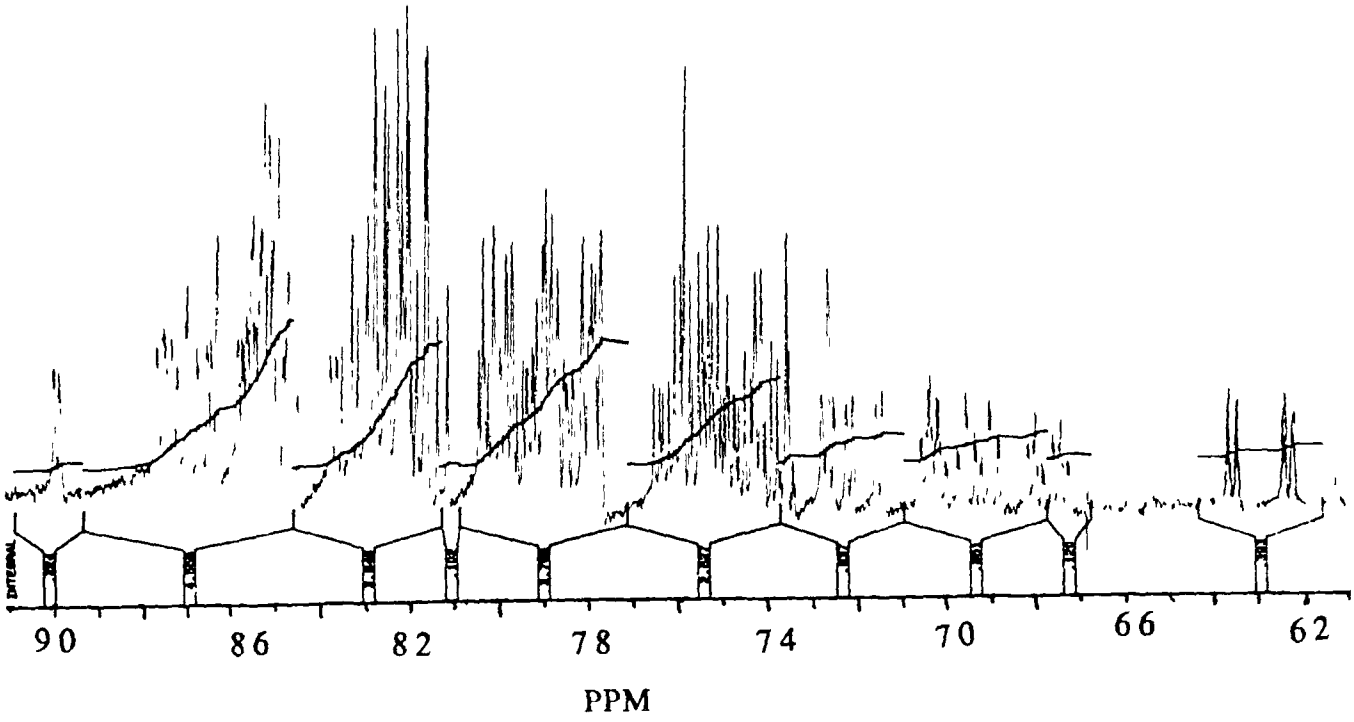

Figure 4 3 2

^1H NMR spectra obtained for the dinuclear $[(Ru(phen)_2)_2(bpt)]^{3+}$ compound in acetone-d^6

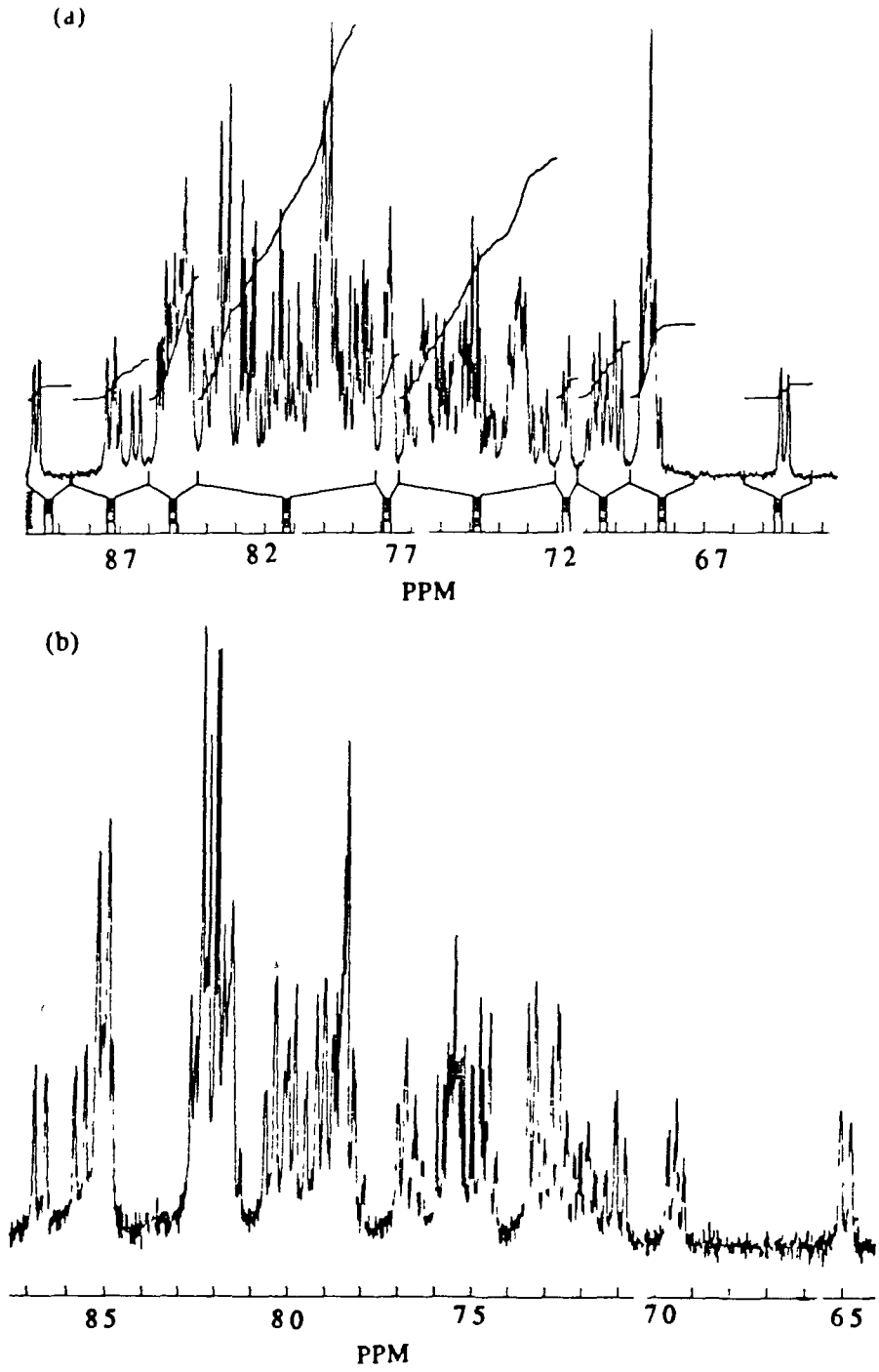

Figure 4 3 3

^{1}H NMR spectra of (a) $[Ru(bpy)_2(bpt)Ru(phen)_2]^{3+}$ and (b) $[Ru(phen)_2(bpt)Ru(bpy)_2]^{3+}$ obtained in acetone-d^6

4 3 2 *Absorption and emission properties*

The ligands 2,2'-bipyridine and 1,10-phenanthroline have very similar properties and there appears to be significant confusion in the literature with regards to quantitative differences between their σ-donor and π-acceptor properties[50-53] It is hoped to clarify these differences in the following sections of this chapter

All compounds isolated exhibit intense absorption bands in the visible region of the spectrum, which have been assigned as metal-to-ligand charge transfer (MLCT) bands in nature[54-56] Table 4 2 lists the absorption maxima of the mononuclear and dinuclear complexes in the visible region and the emission maxima at 300 K and at 77K The lifetime of the luminescent excited state and the quantum yield of emission (ϕ_{em}) of these compounds are also given

Mononuclear compounds

Replacement of a bpy ligand of $[Ru(bpy)_3]^{2+}$ by bpt^-, to give $[Ru(bpy)_2(bpt)]^+$ causes an increase in the electron density at the metal (therefore, an increase in the energy of the HOMO), with a consequent red shift of the metal-to-ligand ($d\pi$ - π^*(bpy)) charge-transfer absorption and emission bands An absorption maximum of 452 nm is observed for $[Ru(bpy)_3]^{2+}$ [18], whereas that of the $[Ru(bpy)_2(bpt)]^+$ monomer is at 475 nm The position of the MLCT band is governed by both the σ-donor and the π-acceptor properties of the ligand For $[Ru(phen)_2(bpt)]^+$, replacement of the 2,2'-bipyridine ligands with 1,10-phenanthroline ligands causes a blue shift of the MLCT absorption band Figure 4 3 4 shows the absorption spectra obtained for both mononuclear compounds As seen, a substantial difference exists between the peak shape of the bpy and phen

COMPOUND	[a]Absorption (logε)	[a]Emission τ/μs (300 K)	[b]Emission τ/μs (77 K)	[a]ϕ_{em}
$[Ru(bpy)_2(bpt)]^+$	475 (4 05)	650 (0 354)	624 (5 43)	$2\,4 \times 10^{-3}$
$[Ru(bpy)_2(Hbpt)]^{2+}$	429	640 (0 099)	612 (4 28)	$2\,2 \times 10^{-4}$
$[Ru(phen)_2(bpt)]^+$	430 (4 26)	652 (0 592)	599 (9 43)	$1\,2 \times 10^{-3}$
$[Ru(phen)_2(Hbpt)]^{2+}$	414	640 (0 161)	583 (8 88)	$1\,1 \times 10^{-3}$
$[(Ru(bpy)_2)_2(bpt)]^{3+}$	452 (4 30)	642 (0 085)	603 (4 16)	$2\,4 \times 10^{-3}$
$[(Ru(phen)_2)_2(bpt)]^{3+}$	421 (4 55)	627 (0 033)	597 (9 69)	$9\,9 \times 10^{-4}$
$[(Ru(bpy)_2(bpt)Ru(phen)_2]^{3+}$	440 (4 37)	640 (0 066)	606 (4 79)	$1\,8 \times 10^{-3}$
$[(Ru(phen)_2(bpt)Ru(bpy)_2]^{3+}$	450 (4 31)	636 (0 051)	603 (5 15)	$1\,7 \times 10^{-3}$
$[(Ru(bpy)_2(bpt)Ru(dpphen)_2]^{3+}$	437 (4 45)	642 (0 275)	608 (10 53)	$4\,1 \times 10^{-3}$

Table 4 2

Absorption and emission properties of the mononuclear and dinuclear complexes [a]Measured in acetonitrile [b]Measured in ethanol All lifetime measurements reported are carried out under argon (error ± 0 02μs) ϕ_{em} error = 10%

mononuclear species This becomes important for elucidation of the photochemical processes for the dinuclear complexes

Luminescence in these complexes originate from triplet MLCT excited states, which corresponds to a spin-forbidden Ru ----> bpy (or Ru ----> phen) transition[18,36,57] Again, upon replacement of a bpy ligand by bpt$^-$, a red-shift of the emission maxima is observed due to the stronger σ-donor ability of the bpt$^-$ ligand The emitting state is localised on the bpy ligand in both of these complexes[16] This is confirmed by the electrochemical measurements A direct

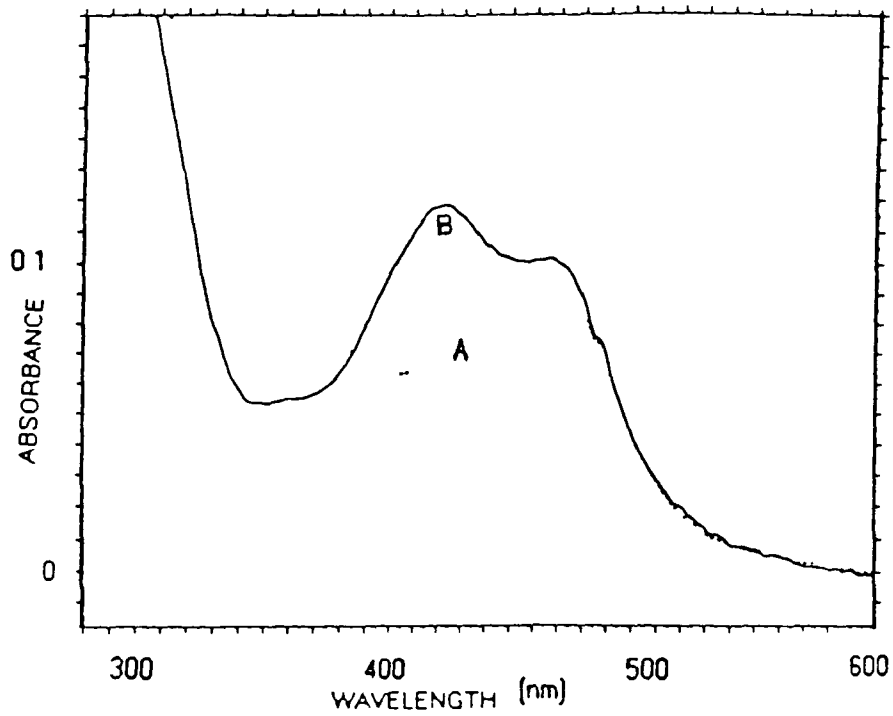

Figure 4 3 4

Absorption spectra for (A) $[Ru(bpy)_2(bpt)]^+$ and (B) $[Ru(phen)_2(bpt)]^+$ obtained in acetonitrile

correlation exists between the electrochemical potentials and the absorption and emission maxima[18] In a MLCT absorption process, an electron is removed from the filled dπ orbital on the metal and transferred to the lowest unoccupied molecular orbital (LUMO) located on the π^* level of the ligand Oxidation is metal-based and involved removal of an electron from the dπ-orbital, whereas reduction is ligand-based and involves placement of an electron in the LUMO or lowest π^* level of the complex[58-59]

The nature of the LUMO is very important in these complexes, as it is directly involved in the photochemical and photophysical properties of these compounds

Dinuclear compounds

The absorption bands of the dinuclear complexes have shifted to higher energy compared with the analogous mononuclear complexes (see Table 4 2) The negative charge on the triazolate anion has to be shared between two metal centres upon co-ordination of the second $Ru(bpy)_2$ (or $Ru(phen)_2$) unit to the bpt^- ligand This causes a decrease in the electron density on the metal centres and a corresponding blue-shift of the MLCT band A similar observation has been reported before for mononuclear and dinuclear complexes containing bisbenzimidazolate[34] Values for both the mixed-ligand complexes are very similar The different σ-donor abilities of the phen and bpy auxiliary ligands may be counteracted by the different σ-donor properties of the N1 and N4 sites of the triazole ring, thus causing both complexes to exhibit very similar properties The emission spectra obtained for $[Ru(phen)_2(bpt)Ru(bpy)_2]^{3+}$ at 300 K and at 77 K are given in Figure 4 3 5

The emission energies of the dinuclear complexes again show a shift to higher energy upon co-ordination of the second metal centre, due to the weaker σ-donor capability of the dinucleating bpt^- ligand The mixed-ligand complexes (**5**) and (**6**) again exhibit very similar excited state properties in all situations i e irrespective of whether bpy or phen is co-ordinated to the N4 site of the triazole ring, no shift in the emission maxima is observed either at room temperature or at 77 K

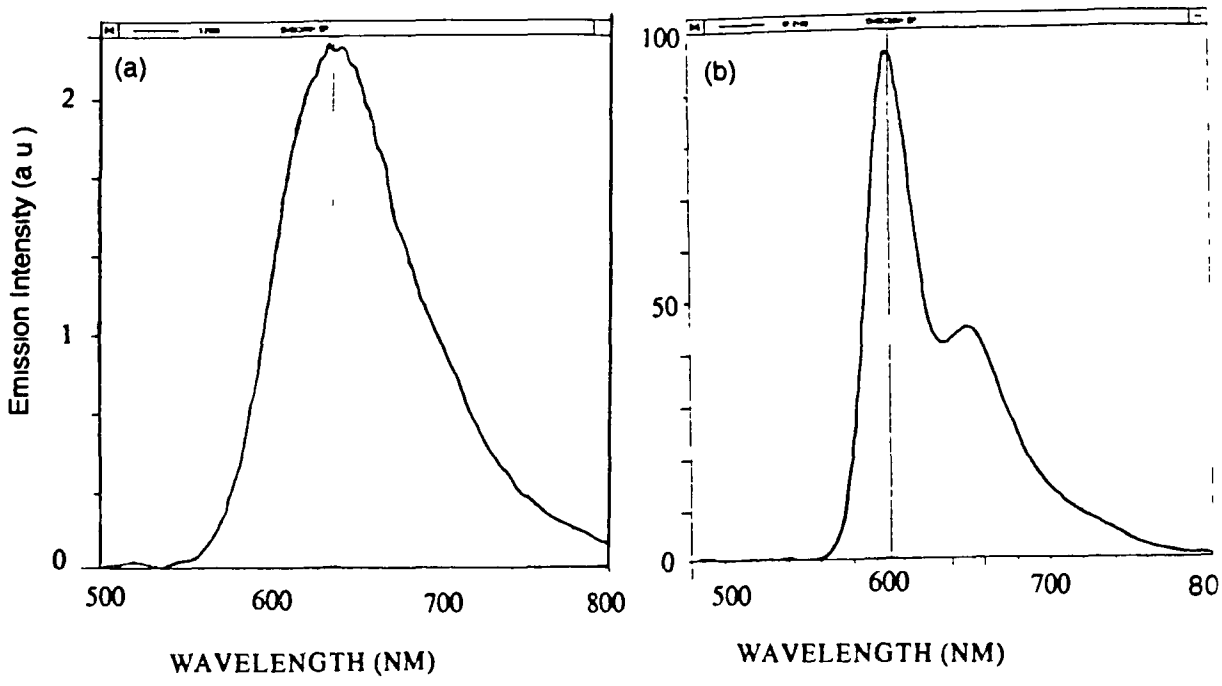

Figure 4 3 5

Emission spectra obtained for $[Ru(phen)_2(bpt)Ru(bpy)_2]^{3+}$ at (a) 300 K in acetonitrile and (b) 77 K in ethanol

4 3 3 *Ground-state and excited-state pK_a measurements*

The change in the absorption spectrum of $[Ru(phen)_2(bpt)]^+$ upon lowering the pH is shown in Figure 4 3 6 A similar behaviour has been observed for other complexes, including those containing pyrazole[60], 1,2,4-triazole ligands[61-62] and

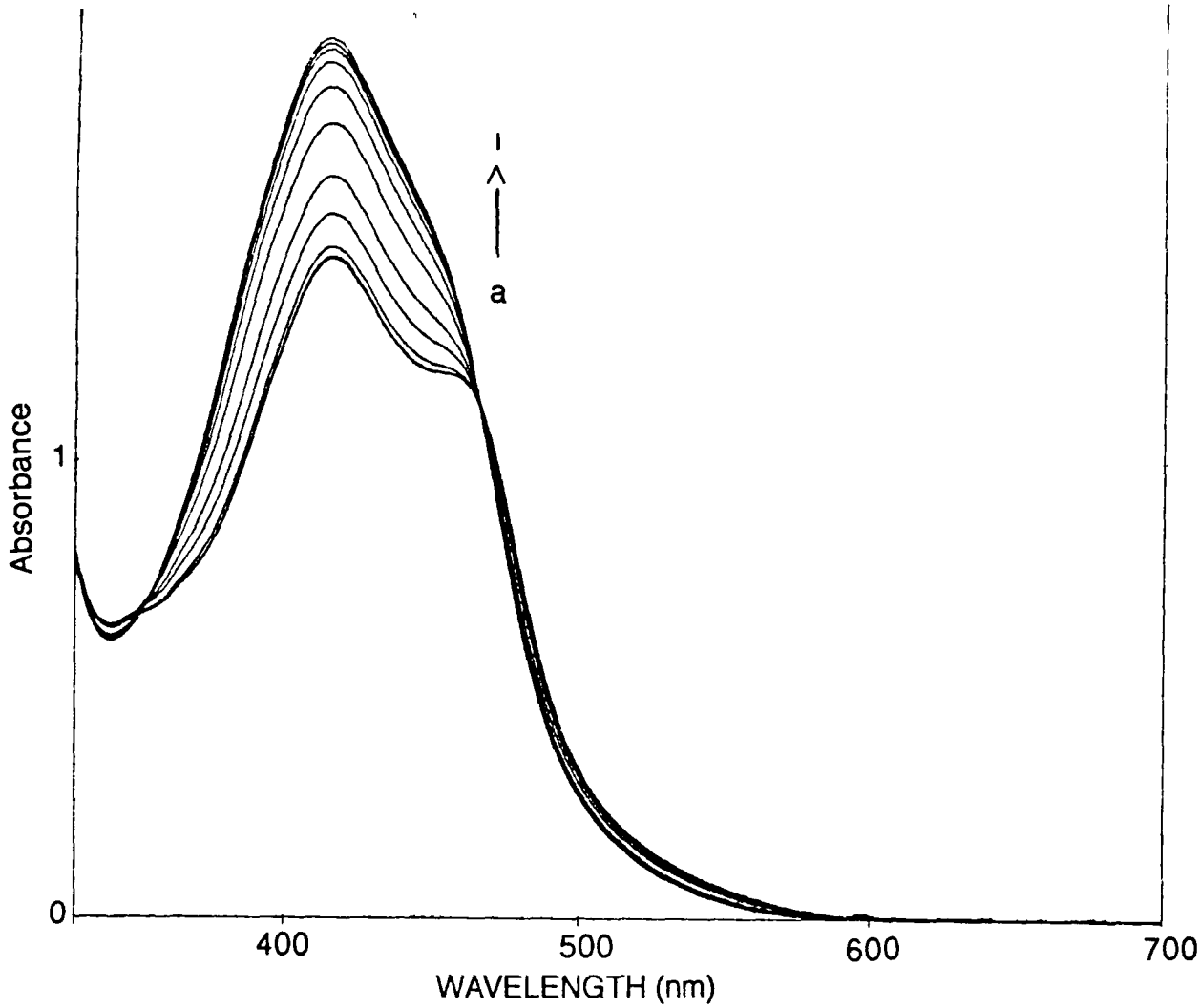

Figure 4 3 6

Changes in the absorption spectrum of $[Ru(phen)_2(bpt)]^+$ upon changing the pH Experiment carried out in Britton-Robinson buffer at pH (a) 1 88, (b) 3 09, (c) 3 54, (d) 3 81, (e) 4 33, (f) 4 72, (g) 5 11, (h) 5 71, and (i) 7 85

imidazole ligands[63-64] The shift to higher energy (λ_{max} = 422 nm) upon protonation of $[Ru(phen)_2(bpt)]^+$ can be explained by a decrease in the σ-donor strength of the protonated ligand compared with the deprotonated one There is therefore a reduction in the electron density at the metal centre and the absorption maximum shifts to a lower wavelength[32]

A pK_a of 4 3 ± 0 1 was obtained for the co-ordinated Hbpt ligand for this complex It was found to be significantly lower than the value of 8 4 ± 0 1 obtained

for the free Hbpt ligand This lowering in the pK_a value upon co-ordination can be explained by strong σ-donation effects from the ligand to the metal centre This causes the acidity of the triazole ligand in the ground state to increase considerably Similarly, a pK_a value of 4 2 ± 0 1 was obtained for $[Ru(bpy)_2(bpt)]^+$ in its ground state (A value of 4 0 ± 0 1 was found by Hage et al[39])

The excited state acidity has been investigated by a study of the pH dependence of the emitting properties of the compound The excited state acid-base properties of compounds can differ significantly from those in the ground state These changes in acidity can be explained by the differences in electron distribution between the ground state and the excited state[65] The changes in the emission spectrum of $[Ru(bpy)_2(bpt)]^+$ upon lowering the pH are presented in Figure 4 3 7 The emission titrations were carried out by excitation into the appropriate isosbestic point taken from the absorption pK_a titration An increase in the emission intensity was observed with increasing pH, until a maximum intensity was reached at a pH value of 5 2 A shift in the emission maximum from 678 nm to 645 nm was observed upon going from pH 6 77 to pH 1 93 and the pK_a (or pH_i) value is taken as the point of inflection of the curve

The point of inflection in the luminescence titration curves do not represent real excited-state pK_a values, or pK_a^*, because they need to be corrected for the different lifetimes of the protonated and deprotonated species[66] Equation 4 1 demonstrates how these lifetimes are taken into account

$$pK_a^*(1) = pH_i + \log(\tau_a/\tau_b) \qquad \textbf{4.1}$$

where τ_a is the lifetime of the protonated species and τ_b is the lifetime of the deprotonated species

An estimate of the pK_a^* value can also be obtained from the ground-state

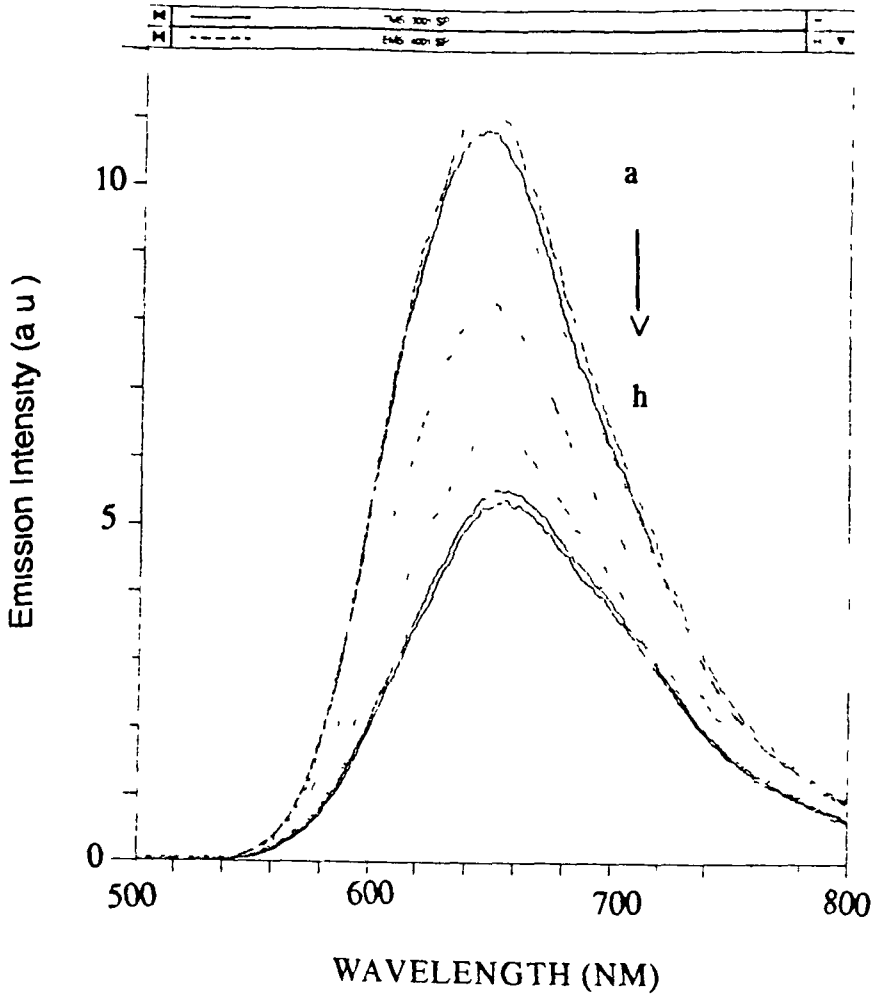

Figure 4 3 7

The emission spectrum of $[Ru(bpy)_2(bpt)]^+$ as a function of pH pH's are (a) 6 77, (b) 5 13, (c) 4 72, (d) 4 13, (e) 3 27, (f) 2 95, (g) 2 36, and (h) 1 93

pK_a values from the absorption titration and the emission energies of the protonated and deprotonated species, using the Forster equation as given in equation 4 2 [67-70]

$$pK_a^*(2) = pK_a + 0\,625(\nu_a - \nu_b) / T \qquad \textbf{4.2}$$

where ν_a and ν_b are the emission maxima of the deprotonated and protonated species respectively and T = temperature at which the experiments were carried out

Table 4 3 lists the ground state pK_a values, the excited-state pH_i values obtained from the point of inflection of the titration curves and the corrected pK_a^* values for the mononuclear complexes

Compound	pK_a	pH_i	pK_a^* (1)	pK_a^* (2)
$[Ru(bpy)_2(bpt)]^+$	4 2	3 9	3 3	3 7
$[Ru(phen)_2(bpt)]^+$	4 3	3 9	3 3	3 7

Table 4 3

Ground-state and excited-state pK_a values for the mononuclear Hbpt complexes

Although a small discrepancy is present for the calculated excited-state pK_a values of the compounds using equation (4 **1**) and (**4.2**), a general trend appears to be that the co-ordinated pyridyltriazole ligand is more acidic in the excited-state than in the ground-state This suggests that the bpt^- ligand acts as a spectator ligand and does not actively participate in the emission processes After excitation of the ruthenium polypyridyl complex, an electron is promoted from the metal to the bpy ligand This results in the creation of a ruthenium centre with a formal valence of 3+, with a consequent increase in σ-donation from the triazole ligand to the metal ion This causes a higher acidity for the ligand when the complex is excited

The discrepancy in the results obtained for both equations may be due to the fact that when using the Forster equation, the energy of the 0-0 transition has

to be estimated accurately Small errors in the energy of a transition results in large errors in the pK_a values obtained At 300 nm an error of 4 nm in the energy results in an error of 1 pK unit Determination of this energy is often difficult due to the presence of strong solvation effects or extensive vibrational fine structure Therefore, the Forster cycle can only be considered as a guide line with limited quantitative applicability[65]

4 3 4 *Electrochemical properties*

Table 4 4 lists the oxidation and reduction potentials observed for the mononuclear and dinuclear complexes containing the Hbpt ligand All values given are in volts versus SCE

Mononuclear compounds

The metal-based oxidation potential of $[Ru(bpy)_2(bpt)]^+$ is significantly lower than that of $[Ru(bpy)_3]^{2+}$, which has an oxidation potential of 1 26 V versus SCE[58] This is due to the increased σ-donor ability of the deprotonated triazole ligand compared with that of bpy An increase in oxidation potential is observed when the triazole ligand is protonated This is due to the decreased σ-donor abilities of the protonated ligand, with a consequent decrease in the electron density at the metal centre This means that the metal centre is more difficult to oxidise than in the deprotonated case The oxidation potentials for the protonated and deprotonated phen complexes are slightly higher than with bpy (a shift of 100 mV to a higher potential is observed for the protonated complexes)

The first two reduction waves observed at -1 44 and -1 68 V for

Compound	Oxidation pot. (V)	Reduction pot. (V)
$[Ru(bpy)_2(bpt)]^+$	0 85	-1 44 -1 68
$^a[Ru(bpy)_2(Hbpt)]^{2+}$	1 06	----
$[Ru(phen)_2(bpt)]^+$	0 86	-1 47 -1 79
$^a[Ru(phen)_2(Hbpt)]^{2+}$	1 16	----
$[(Ru(bpy)_2)_2(bpt)]^{3+}$	1 06 1 38	-1 42 -1 67
$[(Ru(phen)_2)_2(bpt)]^{3+}$	1 04 1 34	-1 48 -1 71
$[Ru(bpy)_2(bpt)Ru(phen)_2]^{3+}$	1 07 1 38	-1 35 -1 71
$[Ru(phen)_2(bpt)Ru(bpy)_2]^{3+}$	1 06 1 37	-1 33 -1 71
$[Ru(bpy)_2(bpt)Ru(dpphen)_2]^{3+}$	1 05 1 32	-1 42 -1 64

Table 4 4

Electrochemical potential (DPP) of the mononuclear and dinuclear complexes containing 3,5-bis-(pyridin-2-yl)-1,2,4-triazole All measurements carried out in acetonitrile with 0 1 M TEAP [a]The complexes were protonated by the addition of one drop of conc H_2SO_4

$[Ru(bpy)_2(bpt)]^+$ are most likely bpy-based Similarly, those observed at -1 47 and -1 79 V for $[Ru(phen)_2(bpt)]^+$ are most likely phen-based Pyridyltriazole ligands are known to be weaker π-acceptors than bpy and are consequently more difficult to reduce[32] Potentials for the pyridyltriazole ligands were therefore not observed in the reduction range measured Due to the difficulty observed in obtaining satisfactory reduction potentials in acidic solutions, such as adsorption on the electrode surface, no clear reduction waves could be produced

Dinuclear complexes

The oxidation potentials obtained for all five dinuclear complexes are listed in Table 4 4 A quite large difference in oxidation potentials of 300 mV is observed between the oxidation potentials of both metal centres This is illustrated in Figure 4 3 8, which shows the oxidation and reduction processes of $[(Ru(phen)_2)_2(bpt)]^{3+}$ obtained in acetonitrile and 0 1 M TEAP This difference may be due to many different effects

(a) Oxidation of the first metal centre causes an increase in the charge of the complex and subsequently a higher oxidation potential of the second metal ion will result (or electrostatic effects)

(b) The "Ru(II)" electron of the mixed-valence species may be delocalised into the Ru(III) centre, causing a shift of the second oxidation potential to a higher value than that observed for a totally oxidised system

(c) Statistical reasons, as the M(II) - M(II) complex can either be oxidised to M(II) - M(III) or M(III) - M(II), and

(d) The chemical environments of the two $Ru(bpy)_2$ (or $Ru(phen)_2$) moieties are different due to the difference in their co-ordination modes (N1 and N4) at the triazole ring, causing differences in their oxidation potentials[39]

The last possibility may prove to be important As mentioned in the introduction, the N1 atom is thought to have stronger σ-donor properties than the N4 atom of the triazole ring Therefore, one would expect that the $Ru(bpy)_2$ (or $Ru(phen)_2$) moiety bound at the N1 site will be oxidised easier than the N4 bonded group This will be discussed in more detail in the section on the mixed-valence species

It should also be noted that the first oxidation potential of the dinuclear complexes is nearly 200 mV higher than the oxidation potential of the

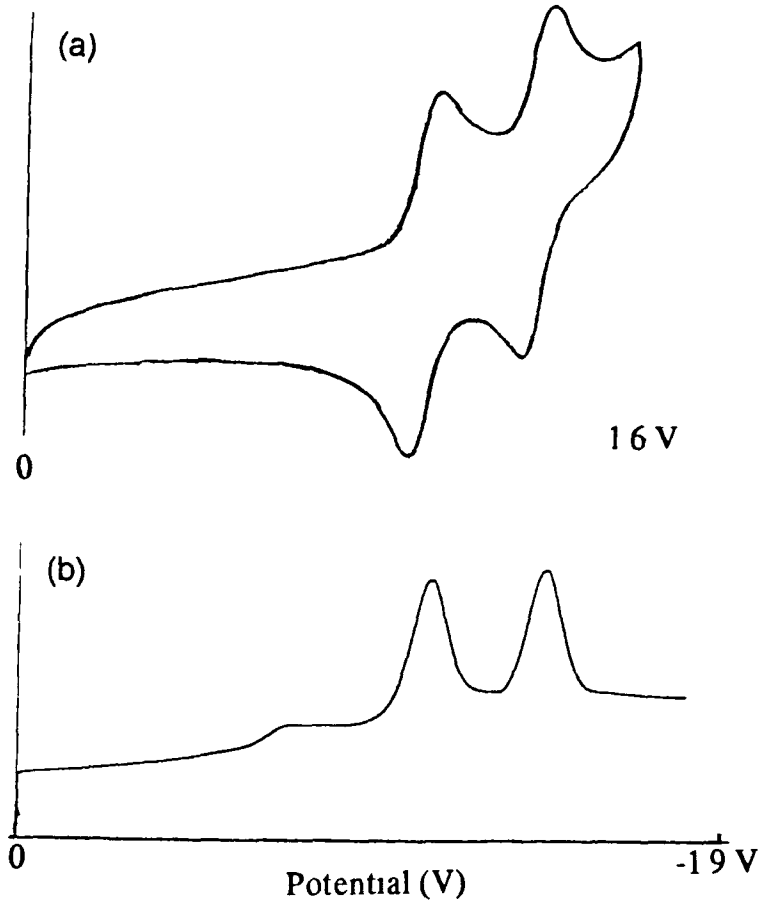

Figure 4 3 8

(a) Cyclic voltammogram of the oxidation (Scanrate 100 mV / sec) and (b) differential pulse polarogram of the reduction (Scanrate 10 mV / sec) processes of $[(Ru(phen)_2)_2(bpt)]^{3+}$ in MeCN and 0 1 M TEAP Measured in volts versus SCE

mononuclear complexes This is due to the fact that upon co-ordination of the second $Ru(bpy)_2$ (or $Ru(phen)_2$) moiety, the negative charge of the bpt^- ligand has to be shared between two metal centres Therefore, due to the decreased electron density on the metal centre, it is more difficult to oxidise

For the mixed ligand complexes, very similar values were obtained for the oxidation potentials, and particular redox processes cannot be identified with respect to specific $Ru(L)_2$ groupings

The reduction waves obtained again clearly correspond to addition of an electron into the π^* orbitals of either bpy or phen This indicates that the emitting excited-state (or LUMO) is located on the polypyridyl ligands in these complexes and that the bridging bpt$^-$ ligand acts solely as a spectator ligand[18] In the mixed-ligand complexes, it is not clear which polypyridyl ligand is the LUMO Compared with $[Ru(bpy)_2(bpt)]^+$, the first reduction wave of the dinuclear $[(Ru(bpy)_2)_2(bpt)]^{3+}$ complex is at a slightly less negative value This is again due to the decreased electron density to the metal centre, making the ligand easier to reduce, as the negative charge on the bridging ligand now has to be shared between two $Ru(bpy)_2$ units The same phenonomen is observed for the phen species

An interesting observation is that in the mixed-ligand complexes (**5**) and (**6**), a large difference of 350 mV exists between the first two reduction waves, compared with a 200 mV difference in the case where the ligands are not mixed This would suggest that the increased asymmetry causes the first reduction potential to be located at less negative values and the second reduction potential to occur at higher negative values This effect is not encountered for the oxidation potentials, possibly as the metal centres are in all cases co-ordinated to the same sites at the triazole ring

4 3 5 *Luminescent lifetime measurements*

Lifetime measurements at room temperature and at 77 K are presented in Table 4 2 for the mononuclear and dinuclear species These indicate that in the mononuclear complexes, the phen compound is considerably longer lived than the bpy complex, as expected[71] However, in the dinuclear complexes, the bis-phen species is shorter lived than the bis-bpy complex, its lifetime decreasing by a factor

of 20 compared to a decrease by a factor of four for the bpy complexes The low lifetime of the phen dinuclear complex is somewhat surprising The decrease in the luminescent lifetimes on going from the mononuclear to the dinuclear complexes is accounted for by the fact that the negative charge on the bpt$^-$ ligand is now shared between the two Ru units for the dinuclear system and therefore the σ-donor properties of the bridging ligand have decreased with the result that the deactivating ^{3}MC level is significantly lowered The decrease in the case of the phen dinuclear complex is, however, significantly larger than for normal bpy-based complexes Figure 4 3 9 shows a typical luminescence decay for $[Ru(phen)_2(bpt)]^{3+}$ in acetonitrile at room temperature

The mixed-ligand complexes (**5**) and (**6**) have very similar lifetimes, so no additional information about the nature of the emitting state is obtained from these measurements Replacement of phen ligands by dpphen ligands in complex (**7**) results in a significant increase in the lifetime of the dinuclear complex (see Table 4 2)

We already know that the luminescent excited state is located on the auxiliary ligands in these complexes, but we do not know whether it is phen or bpy-based in the mixed ligand dinuclear complexes (**5**) and (**6**), or whether it is dpphen or bpy-based in the mixed ligand complex (**7**) For this reason, temperature dependent luminescence lifetime studies were carried out on all complexes in order to investigate the thermally activated surface crossing to a ^{3}MC excited state at high temperatures (see Section 3 3 3) Table 4 5 lists the preexponential factors and activation energies obtained for both the mononuclear and dinuclear species

COMPOUND	E_a (cm^{-1})	A (s^{-1})
$[Ru(bpy)_2(bpt)]^+$	1127	3.8×10^8
$[Ru(phen)_2(bpt)]^+$	1328	4.9×10^8
$[Ru(bpy)_2)_2(bpt)]^{3+}$	4061	5.3×10^{15}
$[Ru(phen)_2)_2(bpt)]^{3+}$	2747	2.3×10^{13}
$[Ru(bpy)_2(bpt)Ru(phen)_2]^{3+}$	3470	3.6×10^{14}
$[Ru(phen)_2(bpt)Ru(bpy)_2]^{3+}$	3442	2.9×10^{14}
$[Ru(bpy)_2(bpt)Ru(dpphen)_2]^{3+}$	5230	1.1×10^{17}
$[Ru(bpy)_3]^{2+}$	3960	1.3×10^{14}
$[Ru(phen)_3]^{2+}$	3157	7.6×10^{12}

Table 4.5
Activation energies and prefactors obtained for the bpt^- complexes. All measurements were carried out in ethanol:methanol (4:1) at temperatures greater than 250 K. Errors ± 10 %.

Mononuclear complexes

Plots of $\ln(1/\tau)$ versus 1/T in the range 150 K to 300 K are presented in Figure 4.3.10 for the mononuclear species. Both complexes had low prefactors and low activation energies at temperatures greater than 250 K suggesting that these complexes are unreactive towards ligand photosubsitution. Population of the deactivating ^{3}MC state does not occur. The low prefactors suggest that the process involves the population of a state only weakly coupled to the ^{3}MLCT state[72-73]. The plot shows a second step occurring for $[Ru(bpy)_2(bpt)]^+$ at approximately 160 ^{o}K. This has already been discussed in Chapter 3, and has

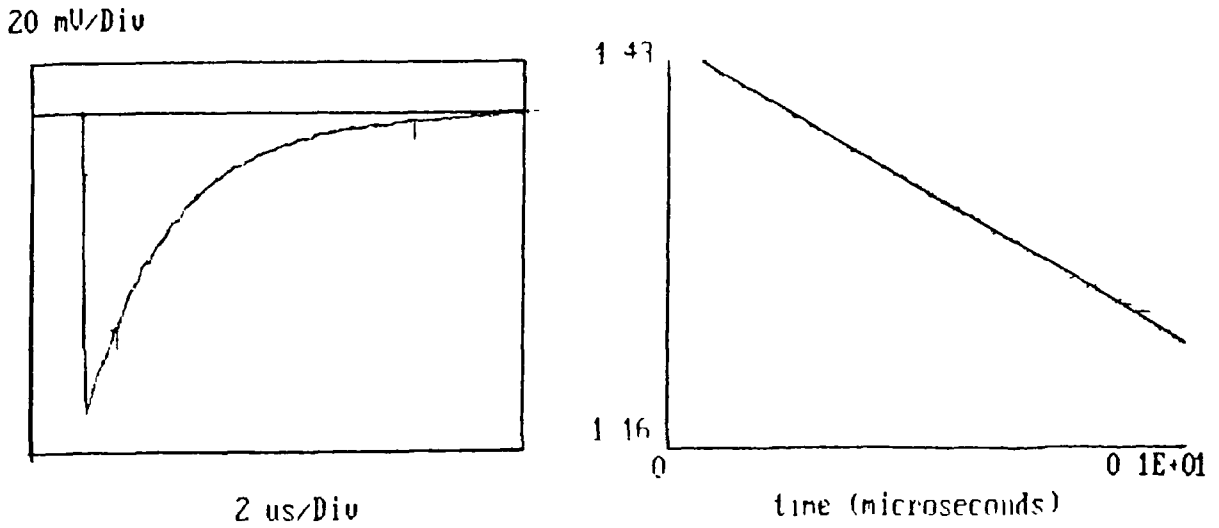

Figure 4 3 9

Luminescent decay of $[Ru(phen)_2(bpt)]^+$ under argon in acetonitrile at 298 K

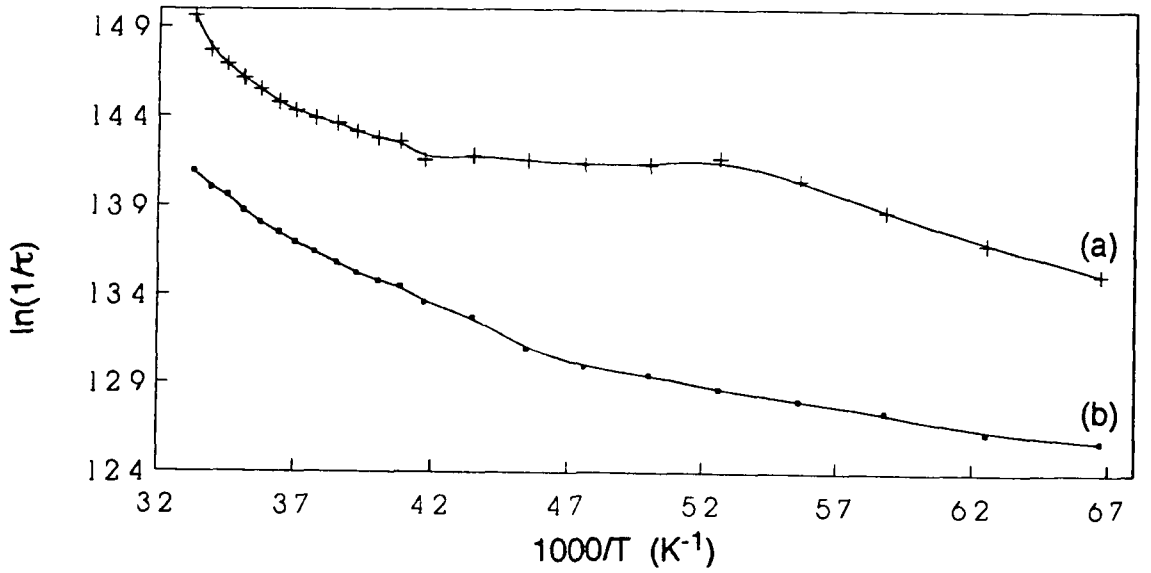

Figure 4 3 10

Plots of $\ln(1/\tau)$ versus 1/T for (a) $[Ru(bpy)_2(bpt)]^+$ and (b) $[Ru(phen)_2(bpt)]^+$ in etanol methanol (4 1) at temperatures > 150 K

been attributed to reorientation of the solvent molecules due to strong changes in the dipole moment caused by the Ru ---> bpy CT[74] Interestingly, a much smaller step is observed for $[Ru(phen)_2(bpt)]^+$ It is possible that the Ru ---> phen CT causes less changes in the dipole moment

We already know that the energy difference between the ^{3}MLCT and ^{3}MC levels is large for the bis-bpy complex Three MLCT states are normally observed for ruthenium(II) complexes below 200 K, but it has been suggested that a fourth MLCT state exists at higher energy [18] The presence of the deactivating ^{3}MC state usually masks the fourth MLCT state Perhaps for the mononuclear complexes, this state is now visible

Table 4 6 list the kinetic parameters obtained for these complexes (see Chapter 3) The "energy gap law" has been useful in rationalising the variations in the emission properties[72, 75-76], lowering of the energy of the emitting MLCT excited state is accompanied by enhanced non-radiative decay With respect to radiative properties of the charge transfer excited state, this translates to decreased emission quantum yields and radiative lifetimes As can be seen from Table 4 2, considerably lower quantum yield of emission (ϕ_{em}) is observed for both mononuclear complexes, in agreement with a large lowering of the energy of the MLCT excited state compared with $[Ru(bpy)_3]^{2+}$

Dinuclear complexes

Plots of $\ln(1/\tau)$ versus $1/T$ in the range 150 K to 300 K are presented in Figure 4 3 11 for all five dinuclear complexes Unfortunately, the luminescent lifetime measurements do not provide unequivocal evidence about the nature of the emitting state In these measurements there appears to be a trend in substituting phen for bpy A plot of number of phen ligands versus activation

Compound	k_r (s^{-1})	k_{nr} (s^{-1})	k_0 (s^{-1})	η_{ic}
$[Ru(bpy)_2(bpt)]^+$	6 69 x 10^3	2 34 x 10^5	2 41 x 10^5	---
$[Ru(phen)_2(bpt)]^+$	2 01 x 10^3	1 04 x 10^5	1 06 x 10^5	---
$[Ru(bpy)_2)_2(bpt)]^{3+}$	2 84 x 10^4	2 12 x 10^5	2 40 x 10^5	0 99
$[Ru(phen)_2)_2(bpt)]^{3+}$	2 99 x 10^4	7 33 x 10^5	1 03 x 10^5	0 99
$[Ru(bpy)_2(bpt)Ru(phen)_2]^{3+}$	2 77 x 10^4	1 81 x 10^5	2 09 x 10^5	0 99
$[Ru(phen)_2(bpt)Ru(bpy)_2]^{3+}$	3 24 x 10^4	1 62 x 10^5	1 94 x 10^5	0 99
$[Ru(bpy)_2(bpt)Ru(dpphen)_2]^{3+}$	1 50 x 10^4	8 02 x 10^4	9 52 x 10^5	---
$[Ru(bpy)_3]^{2+}$	8 00 x 10^4	1 30 x 10^4	2 10 x 10^4	1[18]
$[Ru(phen)_3]^{2+}$	x 10^4	x 10^5	x 10^5	

Table 4 6

Kinetic parameters obtained for the bpt^- complexes Rate constant error ± 5 %

energy is shown in Figure 4 3 12 As can be seen, the plot results in a perfect straight line The emission energies and lifetimes suggest that in the mixed-ligand dinuclear complexes (**5**) and (**6**), the lowest ^{3}MLCT state is bpy-based The bpy-containing complexes have higher prefactors and higher activation energies than phen-containing complexes, which again suggest that the emission is bpy-based The high frequency factors (A) and large activation energies (ΔE) suggest that at higher temperatures an activated surface crossing to a ^{3}MC excited state is occurring for these complexes Population of the ^{3}MC excited state leads to a fast deactivation to the ground state and/or decomposition of the complex[43,77] Indeed these complexes are photolabile

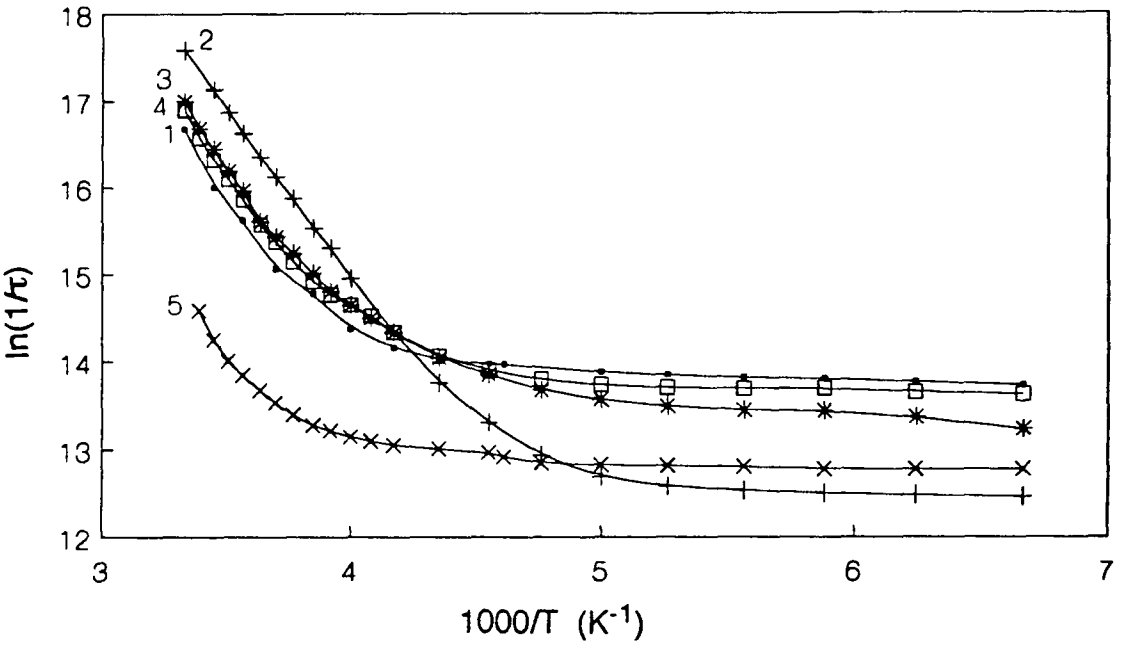

Figure 4 3 11

Plots of ln(1/τ) versus 1/T for (1) $[(Ru(bpy)_2)_2(bpt)]^{3+}$, (2) $[(Ru(phen)_2)_2(bpt)]^{3+}$, (3) $[Ru(bpy)_2(bpt)Ru(phen)_2]^{3+}$, (4) $[Ru(phen)_2(bpt)Ru(bpy)_2]^{3+}$, and (5) $[Ru(bpy)_2(bpt)Ru(dpphen)_2]^{3+}$ in ethanol methanol (4 1)

Further information can be obtained from examining the kinetic parameters obtained for these complexes As can be seen in Table 4 6, k_r is almost the same for $[Ru(bpy)_3]^{2+}$ as for all the dinuclear species If the values of k_{nr} are expected

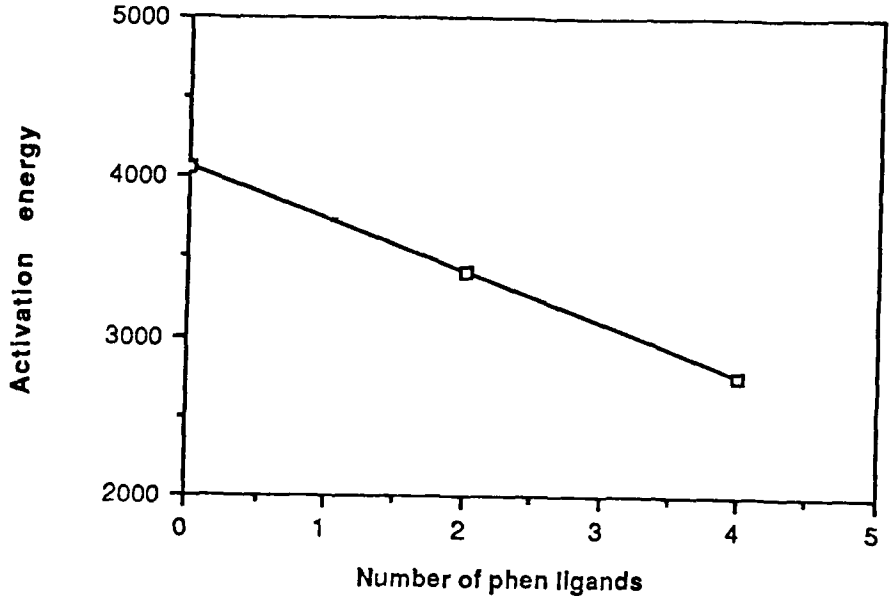

Figure 4 3 12

A plot of the number of phen ligands versus activation energies for the dinuclear complexes

to increase with decreasing energy of the luminescent level, these results would indicate that the bis-phen complex (**4**) has luminescent levels which lie at higher energy than for $[Ru(bpy)_3]^{2+}$, in agreement with its emission maximum The three dinuclear complexes (**3**), (**5**) and (**6**) are of the same order of magnitude as the k_{nr} calculated for $[Ru(bpy)_3]^{2+}$, within experimental error This suggests that in these compounds the lowest luminescent level is bpy-based The LUMO is of course located on phen for the bis-phen complex (**4**)

For $[Ru(bpy)_2(bpt)Ru(dpphen)_2]^{3+}$, the situation is less clear, as its λ_{max} of emission is similar to those of (**3**), (**5**) and (**6**), although its k_{nr} value is lower The presence of the two diphenyl groups on the phenanthroline ligand may alter the position of the LUMO The activation energy and pre-exponential factor for this complex are very large The long lifetime of this complex (4 times larger than that obtained for $[Ru(bpy)_2(bpt)Ru(phen)_2]^{3+}$) may suggest that the efficiency of internal conversion from the ^{3}MLCT to the ^{3}MC excited state is lower and that the emission may be dpphen based for this complex A long luminescent lifetime is, of course, a requirement of a photosensitizer and therefore this complex may have some useful light-induced functions compared with the bpy or phen species

The efficiency of internal conversion, η_{ic}, was calculated for these complexes The values represent the efficiency of population of the ^{3}MC state[78] It was found to be close to one for all dinuclear species indicating that no other deactivating process other than population of this ^{3}MC excited state is occurring here

4 3 6 *Resonance Raman Measurements*

Ground state resonance Raman measurements have been carried out for complexes (**3**), (**4**), (**5**) and (**6**) at excitation wavelengths of a series of wavelenghts within the MLCT band and 364 nm The 364 nm is close to the wavelength 354 7 nm employed for the single colour pulsed excitation transient resonance Raman studies Resonance Raman spectroscopy has been extensively used in order to assign the nature of the electronic transition occurring in ruthenium polypyridyl complexes[79-82] Enhancement is observed for the symmetrical stretching modes of the ligand which is involved in the Ru ---> π^*(L) transition The presence of

different electronic transitions underneath one absorbance band can therefore be detected and identified by studying the wavelength dependence of the resonance Raman spectra[83-85] We already know that the LUMO is located on the auxiliary ligands , but we do not know whether it is located on bpy or phen in the mixed ligand complexes

The ground-state spectra recorded at 457 nm for compounds (**3**) and (**4**) display features attributable to modes of bpy and phen respectively, while those of the mixed-ligand species (**5**) and (**6**) show features due to modes of both bpy and phen The other excitation wavelength used for CW studies, 364 nm, is not in resonance with MLCT transitions, but the spectra display bands which can largely be correlated with those attributed to bpy and phen modes in the 458 nm excited spectra Figure 4 3 13 contains the ground-state spectra for these complexes at 364 nm No trend in the ratio of bpy to phen resonances is observed as a function of the excitation energy

The points of more immediate significance in the context of the present investigation relate to the 354 7 nm pulse-excited Raman spectra of the complexes, as shown in Figure 4 3 14 The trace in Figure 4 3 14 (a) shows prominent bands at 1210, 1287, 1427, 1497, and 1552 cm^{-1} with other weaker features at 1177, 1321, and 1243 cm^{-1} This spectrum corresponds to excitation of the bis-bpy complex Apart from the band at 1243 cm^{-1}, all other features listed for compound (**3**) correlate closely in both position and relative band intensities with the spectrum of $[Ru(bpy)_3]^{2+*}$ originally reported by Woodruff and Dallinger[86] (using pulsed excitation at the same wavelength, 354 7 nm, as used in the present study) and assigned to the localised MLCT excited state $[(bpy)_2Ru^{III}(bpy^{-})]^{2+}$ We therefore formulate the above MLCT excited state for compound (**3**) as

$$[(bpy)Ru^{III}(bpy^{-})(bpt)Ru^{II}(bpy)_2]^{3+}$$

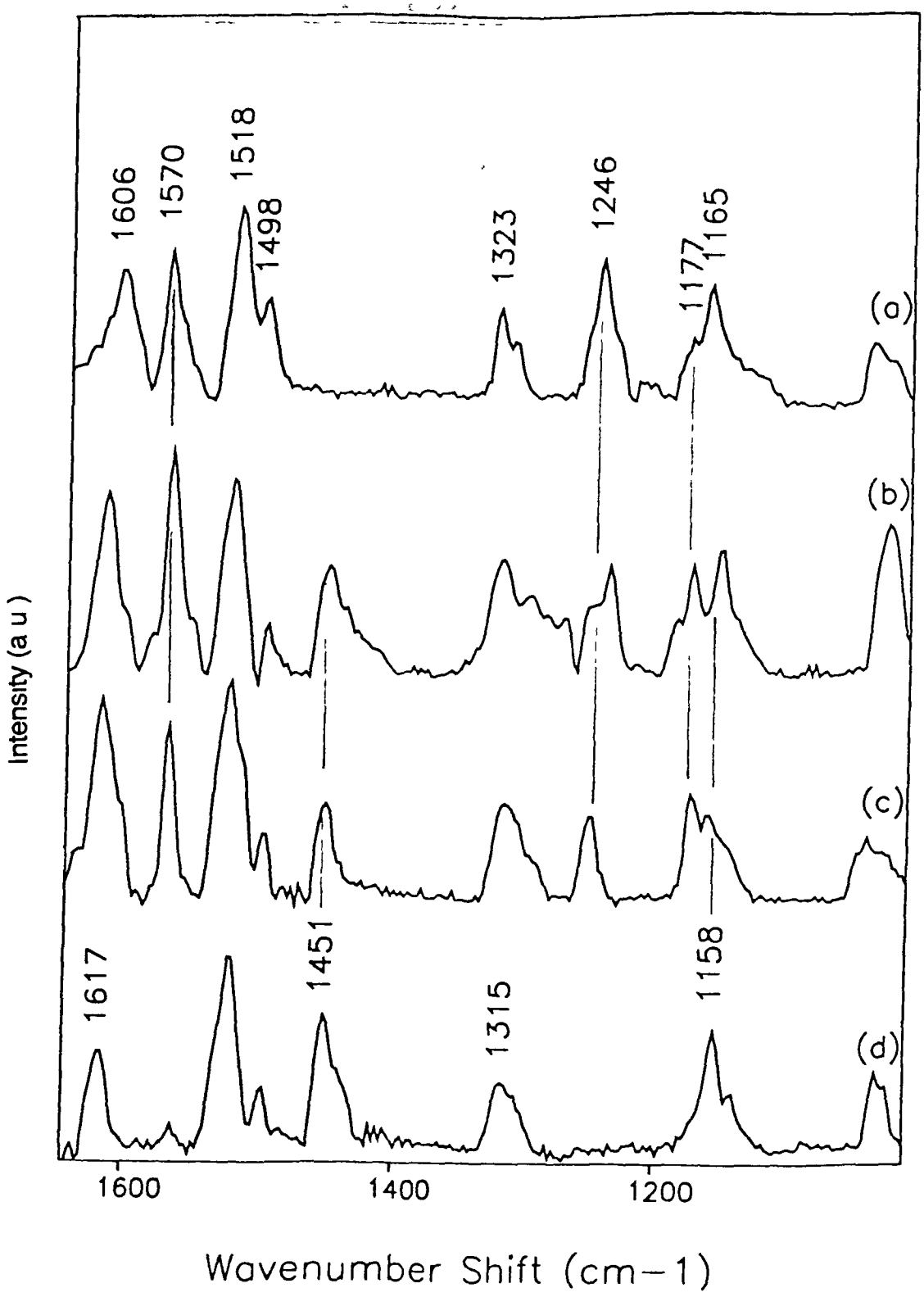

Figure 4 3 13

Resonance Raman spectra of the ground-state spectra of (a) $[(Ru(bpy)_2)_2(bpt)]^{3+}$, (b) $[Ru(bpy)_2(bpt)Ru(phen)_2]^{3+}$, (c) $[Ru(bpy)_2(bpt)Ru(phen)_2]^{3+}$, and (d) $[(Ru(phen)_2)_2(bpt)]^{3+}$ at 364 nm in acetone water (1 4)

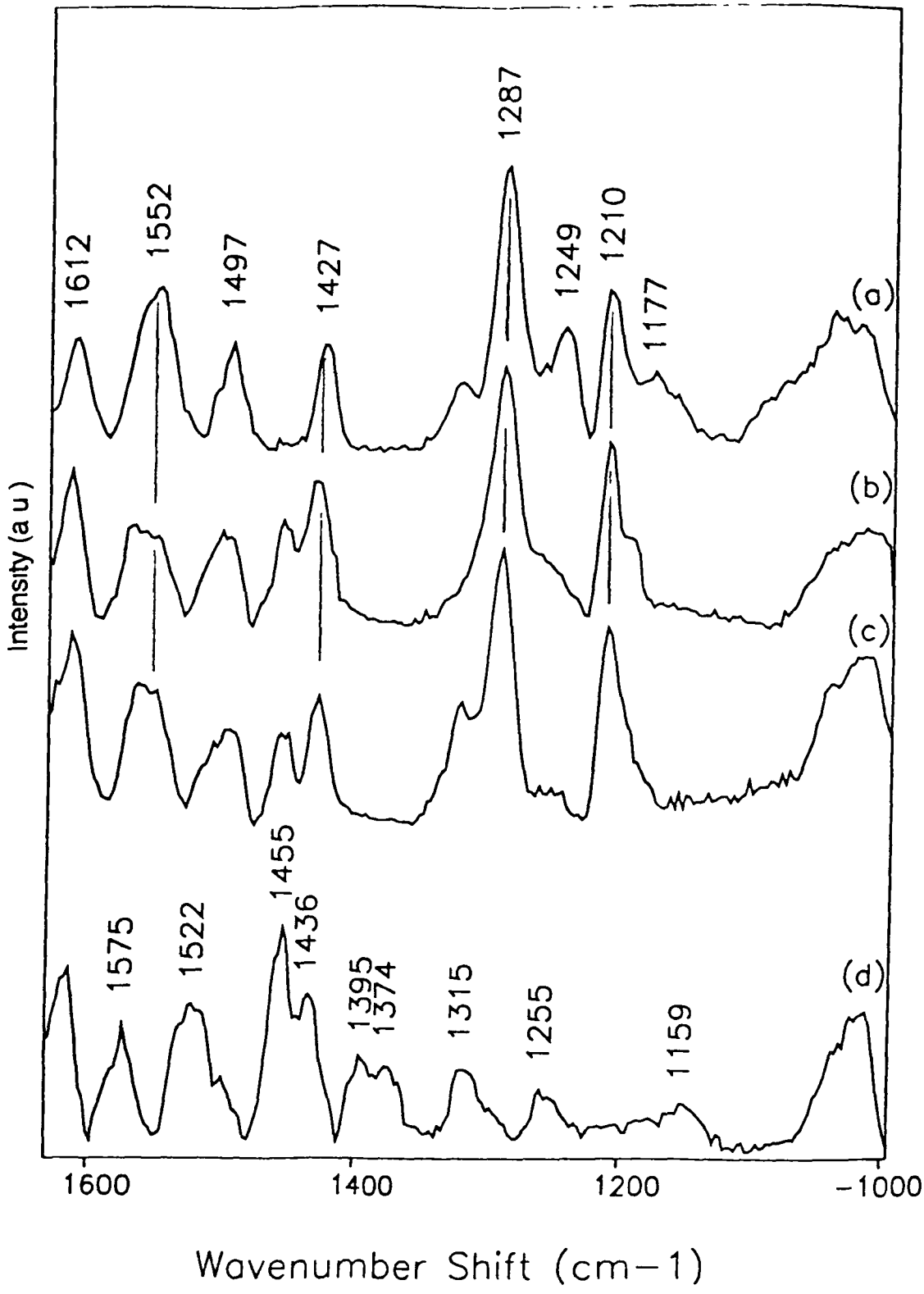

Figure 4 3 14

Excited-state resonance Raman spectra of (a) $[(Ru(bpy)_2)_2(bpt)]^{3+}$, (b) $[Ru(bpy)_2(bpt)Ru(phen)_2]^{3+}$, (c) $[Ru(bpy)_2(bpt)Ru(phen)_2]^{3+}$, and (d) $[(Ru(phen)_2)_2(bpt)]^{3+}$ at 354 7 nm in acetone water (1 4)

in which the Raman scattering arises predominantly from the $(bpy)Ru^{III}(bpy^{\cdot -})$ region of the complex

Similarly, for complexes (**5**) and (**6**), the Raman spectra again very closely resemble those of the ^{3}MLCT state of $[Ru(bpy)_3]^{2+*}$ and can therefore be attributed to excited states which contain the $(bpy)Ru^{III}(bpy^{\cdot -})$ chromophoric moiety These states may be characterised as follows

$$[(bpy)Ru^{III}(bpy^{-})(bpt)Ru^{II}(phen)_2]^{3+},$$

in which the bipyridyl co-ordinated ruthenium centre is attached to the N1 or N4 positions of the bpt^- ligand in complexes (**5**) and (**6**) respectively i e the excitation is localised on the bpy-co-ordinated Ru centre irrespective of the co-ordination position at the bpt^- ligand Neither (**5**) nor (**6**) exhibit any of the Raman marker bands for an excited $Ru(phen)_2$ centre [87] The spectrum of the bis-phen dinuclear species is given in Figure 4 3 14 (d) and the differences between the Raman spectra can be clearly seen there

Indeed, the only differences between the spectra of excited (**3**), (**5**) and (**6**) and those of the excited mononuclear $[Ru(bpy)_3]^{2+}$ complex are the appearance of one extra band at 1243 cm^{-1} in (**3**) and at 1458 cm^{-1} in (**5**) and (**6**) These extra bands in the dinuclear complexes may arise from the unexcited metal/ligand region which would be expected to continue to give "ground-state" spectra (i e neutral ligand modes) even in the ^{3}MLCT complexes The band at 1243 cm^{-1} found in (**3**) is also found in the ground-state spectrum of the same complex, while in complexes (**5**) and (**6**) the 1458 cm^{-1} band is close to a band at 1451 cm^{-1} found in the ground-state Raman spectrum of the bis-phen complex This phenonomen has been noticed before Previous work carried out by Turro et al[85] on the mixed ligand $[Ru(bpy)_2(phen)]^{2+}$ and $[Ru(bpy)(phen)_2]^{2+}$ complexes found

that if there was a bpy ligand present in the molecule, only bpy excited-state bands are observed and disagreed with previous suggestions by Crosby and Elfring[57] that the bands observed were due to a statistical average of the parent tris-chelates.

From the transient resonance Raman spectroscopy data direct evidence is obtained concerning the nature of the ^{3}MLCT band These indicate that in compounds containing bpy i e compounds (**3**), (**5**) and (**6**), the lowest excited state is bpy-based and are not influenced to a great extent by the asymmetric properties of the bridging triazole ligand The only case in which phen-based emission is evident is for the dinuclear $[(Ru(phen)_2)_2(bpt)]^{3+}$ complex This indicates that the ^{3}MLCT excited state for bpy is indeed lower than for phen, and correlates well with the temperature dependent lifetime measurement

4 3 7 *Excited state absorption*

Excited state absorption studies (ESA) were also carried out on complexes (**3**), (**4**), (**5**) and (**6**) and are presented in Figure 4 3 15 Those for the mixed-ligand species (**5**) and (**6**) are essentially identical, suggesting that the lowest MLCT state of these two complexes are likewise identical[88]

4 3 8 *Mixed Valence compounds*

Mixed-valence dinuclear systems often exhibit intervalence-transition (IT) bands A strong IT band points to significant communication between the metal centres[89] For the dinuclear complexes, spectroelectrochemistry has been carried

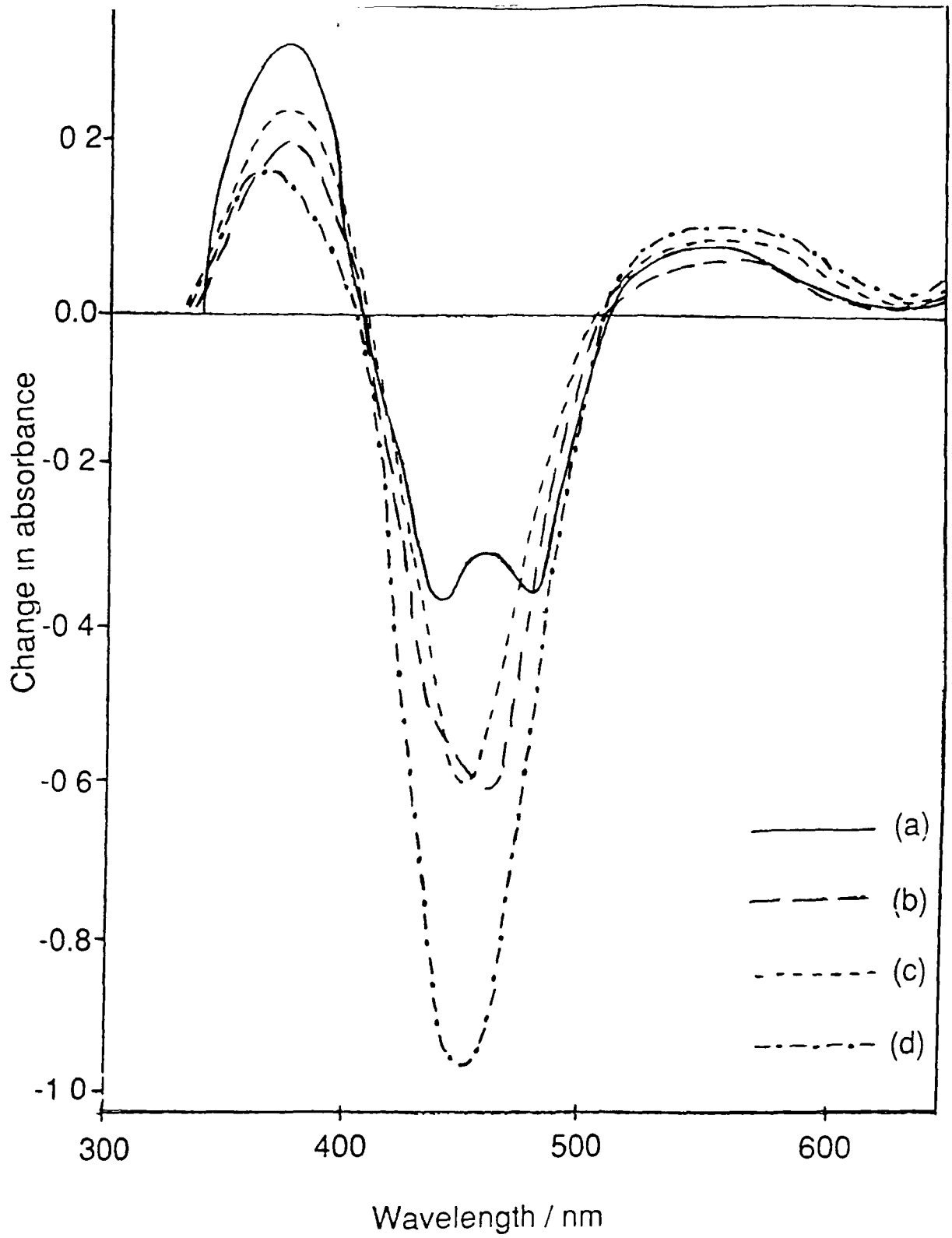

Figure 4 3 15

Excited state absorption spectra of (a) $[(Ru(bpy)_2)_2(bpt)]^{3+}$ (b) $[(Ru(bpy)_2(bpt)Ru(phen)_2]^{3+}$ (c) $[(Ru(phen)_2(bpt)Ru(bpy)_2]^{3+}$ and (d) $[(Ru(phen)_2)_2(bpt)]^{3+}$

out in the UV, visible and near IR region of the spectrum Only the experiments carried out in the near IR region give specific information regarding the IT bands The other two sets of data will be dealt with separately

Intervalence transition bands originate from a light induced electron transfer (e g $Ru^{III}Ru^{II}$ ---> $Ru^{II}Ru^{III}$) In a dinuclear system M_1-L-M_2 bridged via an appropriate bridging ligand L, different degrees of electronic coupling may occur, depending on the properties of the components Robin and Day[90] classified the situations that can arise as follows

CLASS 1 The electronic coupling between metal centres is very small Therefore, no interaction between the metal centres is present and the chance of light-induced electron transfer is negligible

CLASS 2 One of the energy transfer states is at relatively low energy Although most of the properties of the metallic centres are still consistent with their original oxidation states, the electronic coupling between the metallic centres is appreciable and a number of new properties characteristic of the ensemble (e g IT bands) also appear

CLASS 3 In this class of compounds, the properties of the isolated components are absent and the electronic coupling between the metallic centres is strong Only new properties characteristic of the ensemble are observed The new absorption bands do not involve new metal to metal charge transfer transitions and are better described in terms of a delocalised molecular orbital picture

The energy of the intervalence transition band can be considered to consist of an inner-sphere and an outer-sphere part The inner-sphere part has been attributed to changes in the metal-ligand bond lengths and force constants for M(II) and M(III) centres The outer-sphere part arises because solvent molecules have to reorganise themselves when the oxidation state of the metal ion is changed By

measuring the energy of the IT bands in different solvents, the inner-sphere and outer-sphere energies of the IT band can be estimated

The extent of delocalisation of the exchanging electron in mixed-valence ions can also be estimated from the properties of their IT bands according to the Hush model presented in equation 4 3[91-92]

$$\alpha^2 = \frac{(4.2 \times 10^{-4})\, \varepsilon_{max}\, \Delta\upsilon^{1/2}}{E_{op}\, d^2} \qquad \textbf{4.3}$$

where α^2 = the extent of electron delocalisation, ε_{max} = the extinction coefficient of the IT band ($M^{-1}cm^{-1}$), $\Delta\upsilon^{1/2}$ = the peak width at half height of the IT band (cm^{-1}), d = distance between the metal centres (A), and E_{op} = the energy of the IT band (cm^{-1}) The experimental α^2 value is the average of the α^2 values for the ground and mixed-valence (vertical) excited states If delocalisation is small, the electronic wave functions used for overlap are relatively unperturbed and α^2 is a direct measure of delocalisation in the ground-state[93]

Hush also showed[91-92] that the bandwidth at half height, $\Delta\upsilon^{1/2}$, of the intervalence band can be calculated according to equation 4 4

$$\Delta\upsilon^{1/2} = [2310\, (E_{op} - \delta E)\,]^{1/2} \qquad \textbf{4.4}$$

where E_{op} is the energy of the IT band and δE is the energy difference induced by the asymmetric co-ordination environment This asymmetry may be caused by either the presence of two different metal centres, by two different co-ordination sites present on the bridging ligand, or by different auxiliary ligands $\Delta\upsilon^{1/2}$ gives an indication about the type of mixed-valence species that has been obtained If the measured band width fits the calculated bandwidth, then the system is most likely

valence trapped (localised) If the observed band is too narrow, the species belongs to the class of delocalised systems[94]

The degree of electronic coupling between the metal centres, H_{AB}, can be evaluated from the position, bandwidth and intensity of the IT band through the following equation[91,94]

$$H_{AB} = \frac{[4.2 \times 10^{-4} \varepsilon_{max} \Delta\upsilon^{1/2} E_{op}]^{1/2}}{d^2} \qquad \textbf{4.5}$$

This can be simplified to read

$$H_{AB} = [\alpha^2 E_{op}^2]^{1/2} \qquad \textbf{4.6}$$

Another feature of the mixed-valence complexes, is the thermally-induced electron transfer from the M^{II} centre to the M^{III} centre[91-92] Hush has shown that the activation barrier of this electron transfer (E_{th}) is related to the energy of the IT band according to the equation

$$E_{th} = [(E_{op})^2 / 4(E_{op} - \delta E)] \qquad \textbf{4.7}$$

The rate constant of the thermally-induced electron transfer from the M^{II} centre to the M^{III} centre can then be calculated according to the following equation

$$k_{th} = \upsilon_n \exp(-E_{th} / kT) \qquad \textbf{4.8}$$

where k_{th} = the rate constant for the electron transfer (s^{-1}), k = the Boltzmann constant, and υ_n = the frequency factor (normally taken as 5×10^{12} s^{-1})[94] It

should be pointed out at this stage that even small errors in E_{th} can lead to quite large errors in the rate constants, k_{th}

Electrochemical oxidation of the dinuclear ruthenium compounds leads to the generation of a mixed-valence species Two new bands appear in the absorption spectrum at 735 nm and 1800 nm for $[(Ru(bpy)_2)_2(bpt)]^{3+}$ Similar spectral features were obtained for the complexes containing phen ligands Further oxidation to the $Ru^{III}Ru^{III}$ species leads to a disappearance of the band at 1800 nm with a small shift in the band at 735 nm to 725 nm As the band at 735 nm is still present after full oxidation, it cannot be caused by an intervalence transition from the Ru^{II} to the Ru^{III} centre Comparison with a similar band found for a Ru(II) polypyridyl complex containing benzimidazolate suggests that this band is a ligand-to-metal charge-transfer (LMCT) band[34] The disappearance of the band at 1800 nm when the complex is fully oxidised shows that this band must be an IT band A light-induced electron hopping from the Ru^{II} centre to the Ru^{III} centre takes place and therefore an IT band can only be observed for the mixed-valence species Figure 4 3 16 shows the near infrared spectrum of $[(Ru(bpy)_2)_2(bpt)]^{3+}$ upon oxidation in acetonitrile at 1 2 V, and illustrates the grow in of the IT band upon preparation of the mixed-valence species

Table 4 7 lists the extent of electron delocalisation (α^2), the bandwidth at half height of the IT band ($\Delta\upsilon^{1/2}$), electronic coupling (H_{AB}), the activation barrier for thermal-induced electron transfer (E_{th}) and the rate constant for the electron transfer (k_{th}) for the dinuclear species in acetonitrile This is quite a large value in comparison with most mixed-valence ruthenium species[11] It has been observed before for complexes containing bisbenzimidazolate[34] In this situation, it was thought that the negative charge of the imidazolate bridge enhanced the extent of electron delocalisation The presence of a negative charge on the bpt^- ligand in

Compound	$\Delta\upsilon^{1/2}$ (calc)	$\Delta\upsilon^{1/2}$ (expt)	$1/D_{OD} - 1/D_S$	α^2 $M^{-1}cm^{-1}$	H_{AB} (cm^{-1})	E_{th} ($J \times 10^{-20}$)	k_{th} ($s^{-1} \times 10^{11}$)
$[(Ru(bpy)_2)_2(bpt)]^{3+}$	3259	4020	0 528	0 025	854	1 5	1 3
$[(Ru(phen)_2)_2(bpt)]^{3+}$	3224	4000	0 528	0 026	855	1 6	1 0

Table 4 7

Properties of the IT bands at 298 K in MeCN Estimated errors are 10% for α^2, $\Delta\upsilon^{1/2}$, E_{th} and 50% for k_{th}

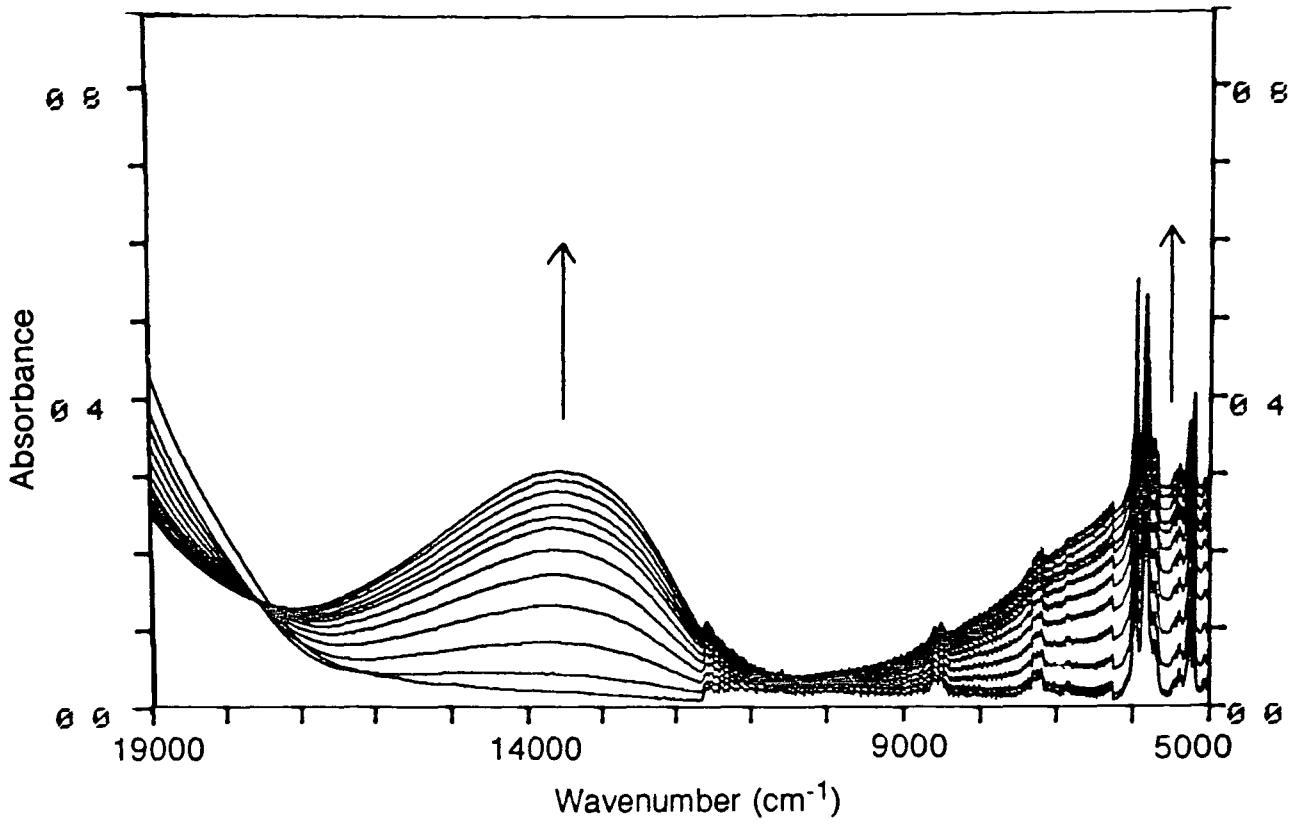

Figure 4 3 16

Near infrared spectrum of $[(Ru(bpy)_2)_2(bpt)]^{3+}$ in MeCN featuring the IT band taken at different time intervals Applied potential is 1 2 V

our case, suggests that this may also be having a similar effect here

The bandwidth at half height, $\Delta\upsilon^{1/2}$, has been measured for these complexes, by doubling width of half the band on the high energy side, as it was not possible to measure the entire bandwidth in the range of the instrument used. This value may also be calculated by using equation 4 4 It was found that the observed intervalence transition bandwidth and the calculated bandwidth agree reasonably well with each other, within experimental error This is further proof that the band at 1800 nm is indeed an IT band

The degree of electronic coupling, H_{AB}, was found to be rather large for the dinuclear species, which is in agreement with the high extent of electron delocalisation already found for these dinuclear systems Similar values (700 - 800 cm^{-1}) were reported for the benzimidazolate dinuclear complexes[34]

The values obtained for E_{th}, the activation barrier for thermally-induced electron transfer from the Ru^{II} centre to the Ru^{III} centre are all pretty similar δE has been estimated at 100 mV for the dinuclear complexes[95]

The rate constant for the thermally-induced electron transfer has also been calculated These values are quite large As mentioned previously, the negatively charged triazolate bridge probably facilitates electron transfer, thereby accounting for the large rate constant observed

As you can see from the data, the values of the IT parameters obtained for both dinuclear species are very similar This suggests that no differentiation is possible between these two ligands on this basis of their spectroelectrochemical data in the NIR region The IT parameters of the mixed-ligand complexes were not studied in detail, but it is suggested that the values obtained for these species would be similar to those found for the $[(Ru(bpy)_2)_2(bpt)]^{3+}$ and $[(Ru(phen)_2)_2(bpt)]^{3+}$ complexes and would not provide any insight into the location of the first metal based oxidation in these systems

4 3 9 *Localisation of metal based oxidation*

Spectroelectrochemistry has been highly successful in detecting redox orbital localisation in d^6 metal tris-(diimines)[96-98] For this reason it has been carried out in both the visible and ultra-violet regions In the mixed-valence species the absorption spectrum in the 300 - 500 nm region is dominated by the Ru^{II} centre It should therefore be possible to elucidate which metal centre is been oxidised first i e the N1 or the N4 centre A fully oxidised $Ru^{III}Ru^{III}$ species has no absorbance in the visible region (i e the MLCT band collapses under oxidation at 1 6 V) Figure 4 3 17 represents the absorbance spectra obtained for the mixed-valence dimers (**3**), (**4**), (**5**), and (**6**) in the 350 - 850 nm range The absorption spectra of the phen-based complex (Figure 4 3 17 (b)) has broader UV/vis spectra than the bpy-based complex (Figure 4 3 17 (a)) The maximum wavelength of absorption for $[(Ru(bpy)_2)_2(bpt)]^{3+}$ is found at 425 nm, whereas the maximum wavelength of absorption for $[(Ru(phen)_2)_2(bpt)]^{3+}$ is found at 405 nm Complex (**5**) has an absorbance spectrum similar to that observed for $[(Ru(phen)_2)_2(bpt)]^{3+}$, indicating that the $Ru(bpy)_2$ site is being oxidised first Complex (**6**) exhibits a spectrum similar to that obtained for $[(Ru(bpy)_2)_2(bpt)]^{3+}$ after its oxidation to the mixed-valence state, suggesting that $Ru(phen)_2$ is oxidised first in this situation These results indicate that in the mixed-ligand complexes (**5**) and (**6**), the centre attached to the N1 position of the triazole ring is oxidised first, irrespective of which Ru-containing unit is attached there This confirms earlier suggestions based on the acid-base properties of pyridyltriazole ligands, that the N1 position of the triazole ring is a better σ-donor than the N4 position This further suggests that the energy of the anti-bonding ^3MC state will be lower for the N4 position Since population of this level is responsible for the photodecomposition of ruthenium polypyridyl complexes, this observation is of importance for the analysis of the

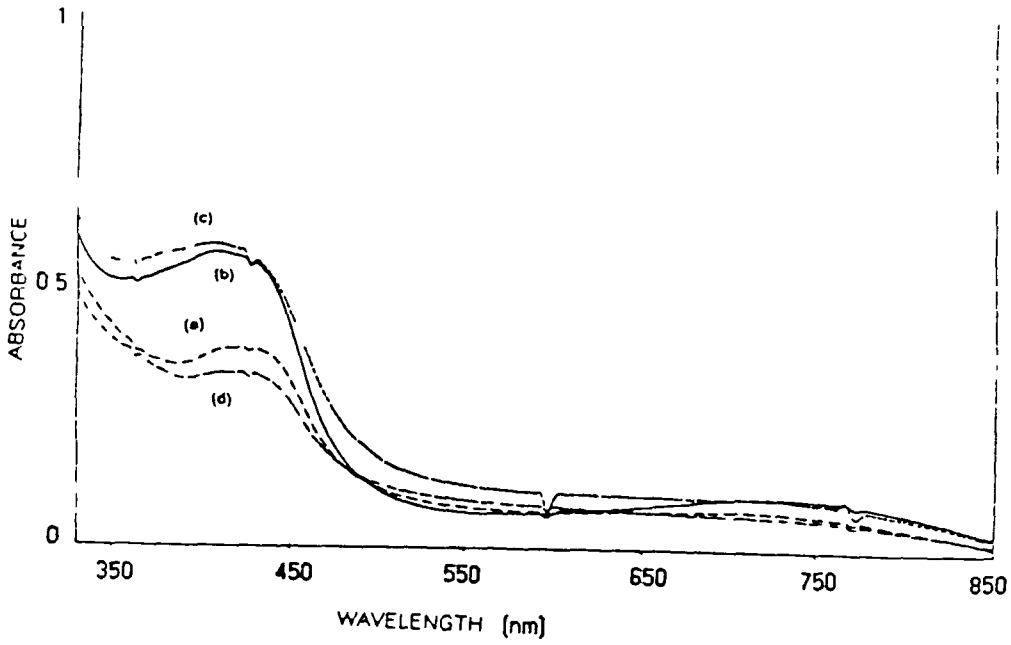

Figure 4 3 17

The absorbance spectra obtained for the mixed-valence dimers (a) $[(Ru(bpy)_2)_2(bpt)]^{3+}$, (b)$[(Ru(phen)_2)_2(bpt)]^{3+}$, (c) $[(Ru(bpy)_2(bpt)Ru(phen)_2]^{3+}$ and (d) $[(Ru(phen)_2(bpt)Ru(bpy)_2]^{3+}$

photochemical properties (vide infra)

More direct evidence about the localisation of the first metal-based oxidation comes from a study of the spectroelectrochemistry of these complexes in the UV region Figure 4 3 18 shows the spectra obtained for $[(Ru(bpy)_2)_2(bpt)]^{3+}$ before oxidation (1), in its mixed-valence state (2) and after full oxidation (3) The

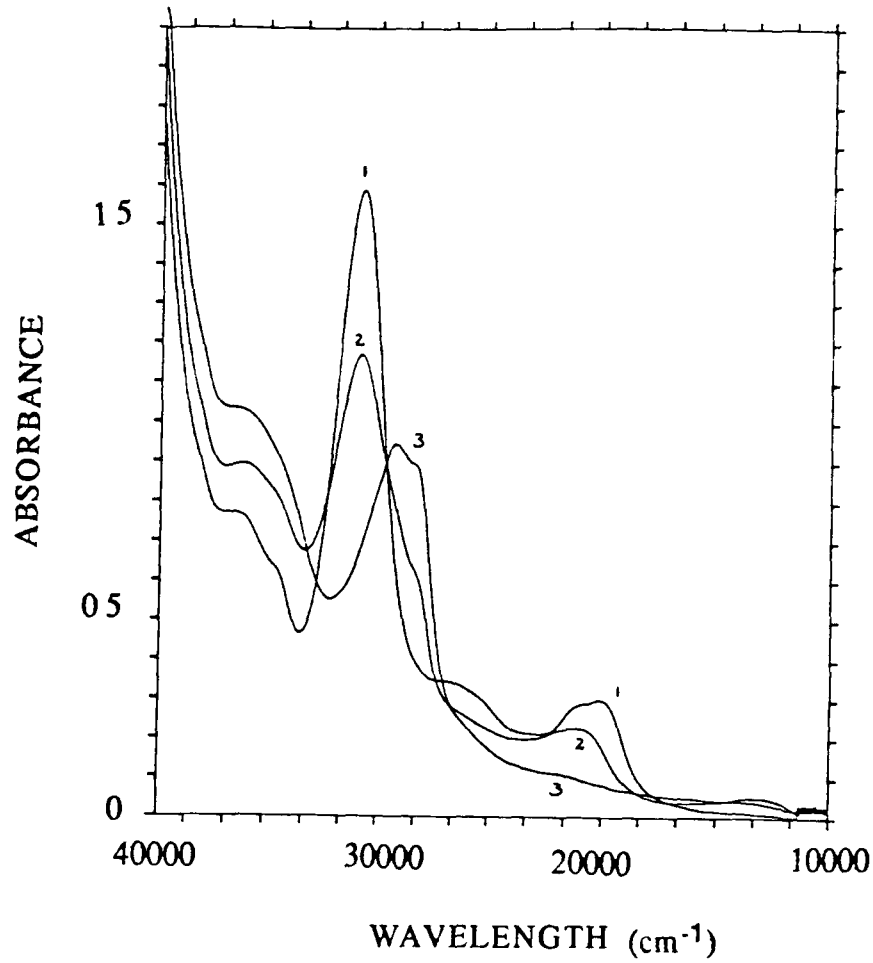

Figure 4 3 18

UV spectrum of $[(Ru(bpy)_2)_2(bpt)]^{3+}$ (1) before oxidation ($Ru^{II}Ru^{II}$), (2) in its mixed valence state ($Ru^{III}Ru^{II}$) and (3) in its fully oxidised state ($Ru^{III}Ru^{III}$)

UV/vis absorption spectrum depends on the oxidation state of the ruthenium ion Both "oxidised" and "reduced" Ru centres are observed simultaneously If the excited electron was delocalised, one would expect that the spectra of the mixed-

valence species would be intermediate between the spectra of the unoxidised and fully oxidised species[98] However, this is not the case In the mixed-valence species, no shift of the maximum wavelength of absorption is observed between this spectrum and the one of the unoxidised species However, when the complex is fully oxidised, a shift from 286 nm to 303 nm is observed The spectrum of the mixed valence species occurring at 286 nm can be attributed to that of the bpy mononuclear complex (**1**) A clear isosbestic point is maintained throughout the titration at 298 nm For all the dinuclear complexes, similar results are obtained Furthermore, for the $[(Ru(phen)_2)_2(bpt)]^{3+}$ complex, a shift in the λ_{max} from 263 nm to 272 nm is observed between that of the $Ru^{III}Ru^{II}$ and $Ru^{III}Ru^{III}$ species The spectrum obtained for the mixed-valence complex with a λ_{max} at 263 nm can be attributed to that of the phen mononuclear species (**2**) Similarly, the mixed valence spectrum obtained for $[(Ru(bpy)_2(bpt)Ru(phen)_2]^{3+}$ has a λ_{max} at 265 nm (corresponding to that of the phen monuclear complex), whereas that of $[(Ru(phen)_2(bpt)Ru(bpy)_2]^{3+}$ has a λ_{max} at 281 nm (attributable to that of the bpy monuclear species)

4 3 10 *Photochemical properties*

Photochemistry in CH_2Cl_2 containing 0 005 M Cl^-

During the photolysis of the mixed ligand species, compound (**5**) and compound (**6**) in CH_2Cl_2 containing 0 005 M Cl^-, UV/vis spectra taken at specified intervals show a decrease in the absorbance as the reaction proceeds Figure 4 3 19 shows the UV/vis spectra taken at different time intervals of compound (**5**) A clear isosbestic point is obtained with a shift in the absorbance maximum from

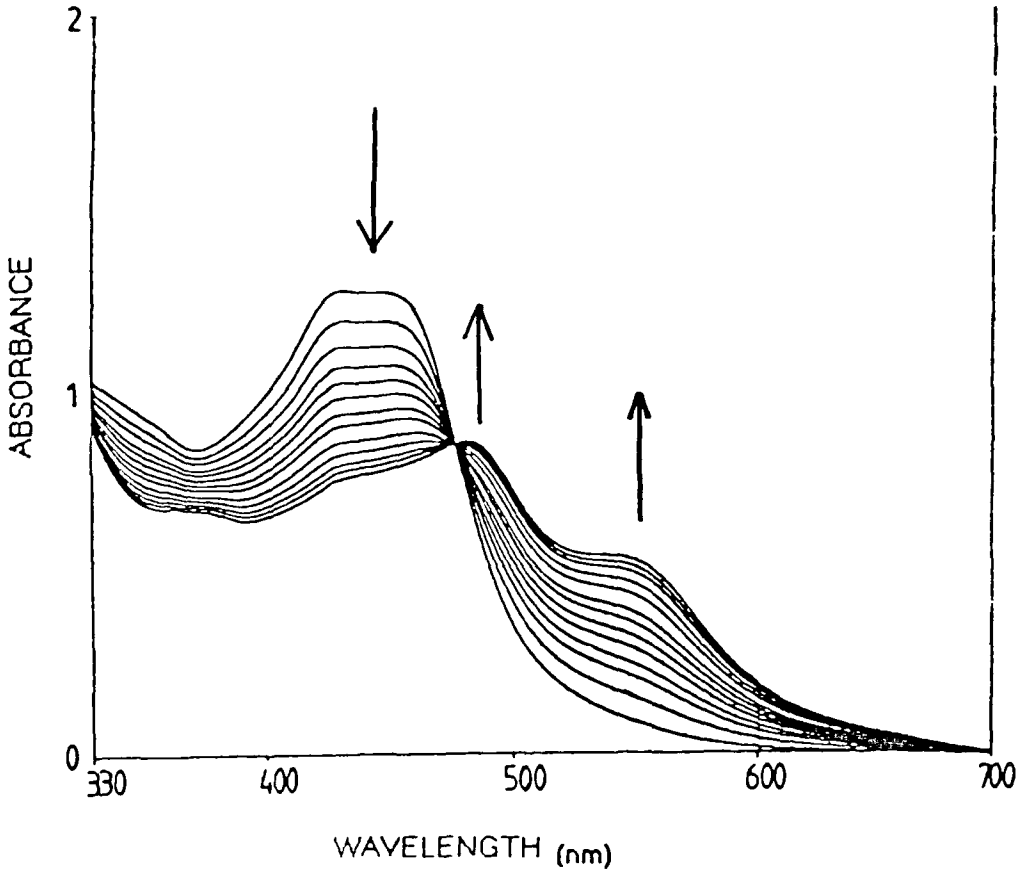

Figure 4 3 19

UV/vis spectra taken at different time intervals during the photolysis of $[Ru(bpy)_2(bpt)Ru(phen)_2]^{3+}$ in CH_2Cl_2 containing 0 005 M Cl^-

440 nm to 490 nm, with a subsequent growth in a new peak at 550 nm This confirms the results obtained be Barigelletti et al for $[(Ru(bpy)_2)_2(bpt)]^{3+}$ [16]

In order to investigate the photochemical process further, HPLC analysis was carried out at specified intervals throughout the photolysis A typical set of

traces obtained for the photolysis of compound (**5**) is given in Figure 4 3 20 From these traces it can be seen that, contrary to expectation, at least five main photoproducts were obtained The products are identified as follows Peak 1, retention time 2 12 mins, with an absorbance maximum of 520 nm, was identified as $[Ru(phen)_2Cl_2]$ Peak 2, retention time 2 30 mins, absorbance maximum at 365 and 520 nm was found to be $[Ru(bpy)_2Cl_2]$ Taking into account the extinction coefficients of these two products at the monitoring wavelength of 280 nm, their ratios were approximately 1 1 Peak 3, retention time 4 44 mins, absorbance maximum at 330 and 470 nm was identified as $[Ru(bpy)_2(MeCN)Cl]^{2+}$, presumably formed by interaction with the acetonitrile in the mobile phase Peaks 4 and 5, which are present in almost identical proportions, have been identified as two bpt^- containing mononuclear complexes Peak 4, with a retention time of 5 64 min and an absorption maximum at 430 nm, was identified as $[Ru(phen)_2(bpt)]^+$, the N4 isomer of compound (**2**), since it has a similar absorbance spectra to the N1 isomer, but a different retention time according to HPLC Attempts have been made to isolate this N4-bound isomer using a large scale photolysis experiment [99] However, sufficient amounts could not be isolated by semi-preparative HPLC, as the maximum amount formed during photolysis is less than 20% No evidence for the formation of an N4 isomer for either of the mononuclear complexes was evident during synthesis Finally, peak 5, with a retention time of 9 18 mins and a maximum absorbance of 475 nm, has been identified as the N1 isomer of the $[Ru(bpy)_2(bpt)]^+$ complex The UV/vis spectra absorption maxima were located using the HPLC photodiode array detector and the solvent is therefore mobile phase

Similar results to those obtained for compound (**5**), were also observed during the photolysis of compounds (**3**), (**4**) and (**6**) The presence of both $[Ru(bpy)_2Cl_2]$ and $[Ru(phen)_2Cl_2]$ and the presence of the two mononuclear bpt^-

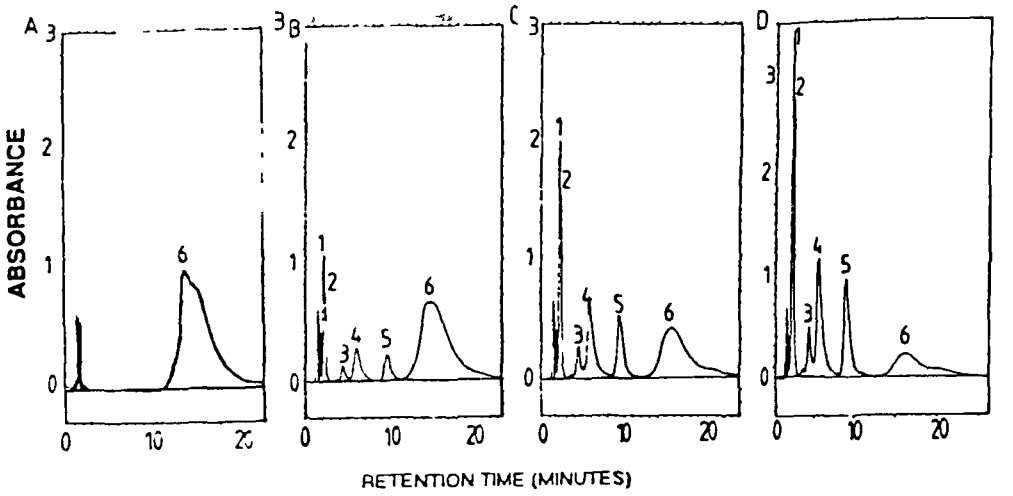

Figure 4 3 20

HPLC traces taken during the photolysis of $[Ru(bpy)_2(bpt)Ru(phen)_2]^{3+}$ in CH_2Cl_2 containing 0 005 M Cl^- Photolysis times are (a) 0 min, (b) 10 min, (c) 29 min, and (d) 74 min Mobile phase MeCN H_2O (80 20) containing 0 08 M $LiClO_4$ Flowrate 2 0 cm^3/min

complexes in the photolysis of these complexes, confirms the results obtained for compound (**5**) For compound (**3**), both the N1 and the N4 isomers of $[Ru(bpy)_2(bpt)]^+$ were present and for compound (**4**), both the N1 and the N4 isomers of $[Ru(phen)_2(bpt)]^+$ were obtained Finally for compound (**6**), the N1 isomer of $[Ru(phen)_2(bpt)]^+$ and the N4 isomer of $[Ru(bpy)_2(bpt)]^+$ were present upon irradiation

Photolysis of $[Ru(bpy)_2(bpt)Ru(dpphen)_2]^{3+}$ in CH_2Cl_2 containing 0 005 M Cl^- gave rise to the presence of both $[Ru(bpy)_2Cl_2]$ (ret time 5 35 min, λ_{max} 370

and 530 nm) and $[Ru(dpphen)_2Cl_2]$ (ret time 3 50 min, λ_{max} 540 nm) and the two mononuclear species $[Ru(bpy)_2(bpt)]^+$ (ret time 4 03 min, λ_{max} 475 nm) and the N4 isomer of $[Ru(dpphen)_2(bpt)]^+$ (ret time 4 26 min, λ_{max} 435 nm) Clearly, the same photolysis processes are occurring for this complex, as occurring for the other three complexes

Photochemistry in MeCN containing 0 01 M Cl^-

UV/vis spectra taken during the photolysis of $[Ru(bpy)_2(bpt)Ru(phen)_2]^{3+}$ in MeCN containing 0 01 M Cl^- show a single isosbestic point at 467 nm , with a shift in the absorbance maximum from 428 to 465 nm (see Figure 4 3 21) However, the HPLC traces again indicate the formation of at least four main photoproducts The photoproducts were identified by retention times, by UV/vis spectra taken from the HPLC photodiode array traces and by comparison with authentic samples Again, both the N1 and the N4 positions of the triazole ring are apparently photolabile in the presence of Cl^- ions Photolysis of the other three dinuclear complexes (**3**), (**4**) and (**6**) gave similar results In all four cases $[Ru(bpy)_2(MeCN)Cl]^{2+}$ and $[Ru(phen)_2(MeCN)Cl]^{2+}$ and two monomeric bpt^- containing complexes are formed during irradiation For compound (**3**), both the N1 and N4 isomers of $[Ru(bpy)_2(bpt)]^+$ were present, along with $[Ru(bpy)_2(MeCN)Cl]^{2+}$ as the sole photoproducts For compound (**4**), the N1 and N4 isomers of $[Ru(phen)_2(bpt)]^+$ formed with $[Ru(phen)_2(MeCN)Cl]^{2+}$ Figure 4 3 22 contains HPLC traces taken at specified intervals during this photolysis Compound (**5**) had the following photoproducts, the N1 isomer of $[Ru(bpy)_2(bpt)]^+$ and the N4 isomer of $[Ru(phen)_2(bpt)]^+$ formed in conjunction with both acetonitrile-chloride containing species Finally, for compound (**6**), the N1 isomer of $[Ru(phen)_2(bpt)]^+$ and the N4 isomer of $[Ru(bpy)_2(bpt)]^+$ formed again with the

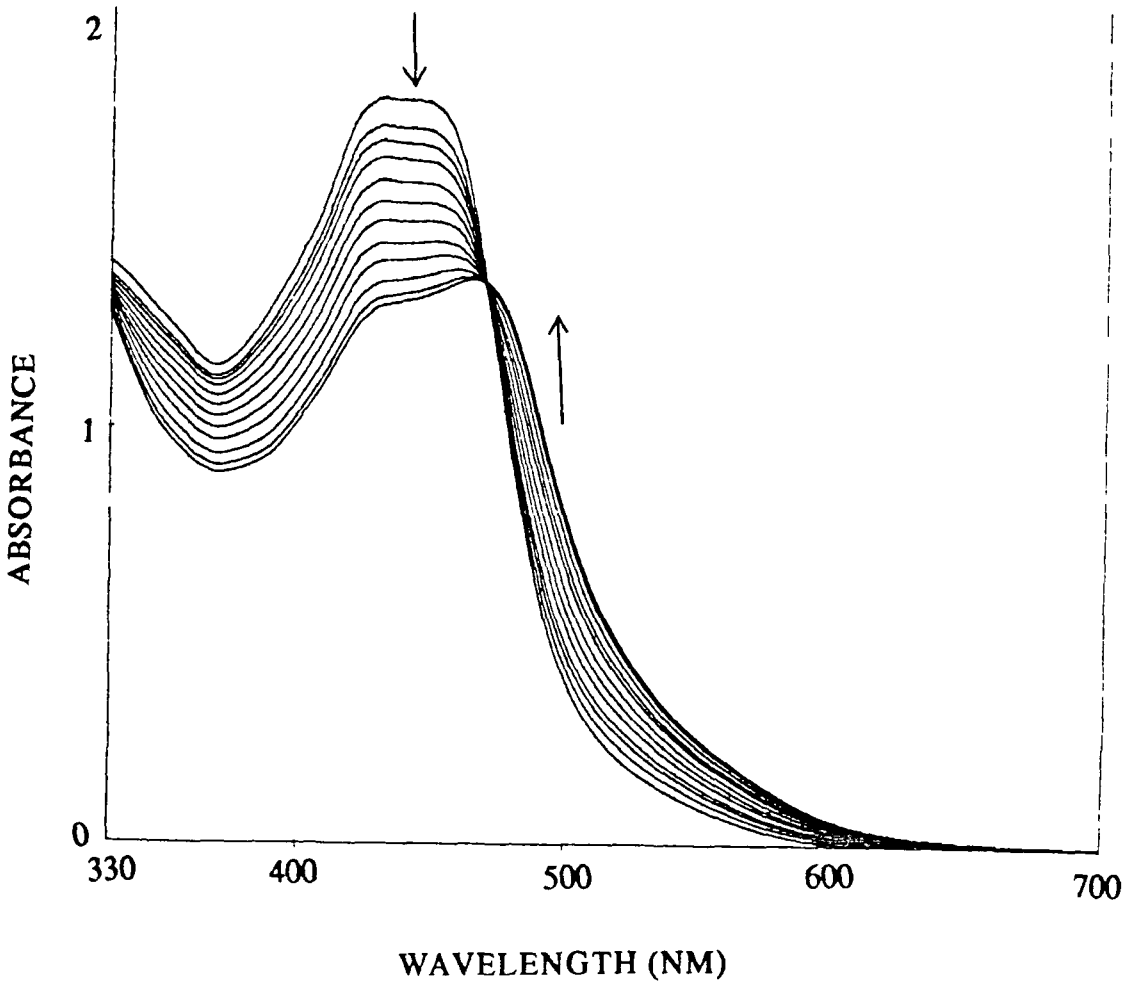

Figure 4 3 21

UV/vis spectra taken during the photolysis of $[Ru(bpy)_2(bpt)Ru(phen)_2]^{3+}$ in MeCN containing 0 01 M Cl^-

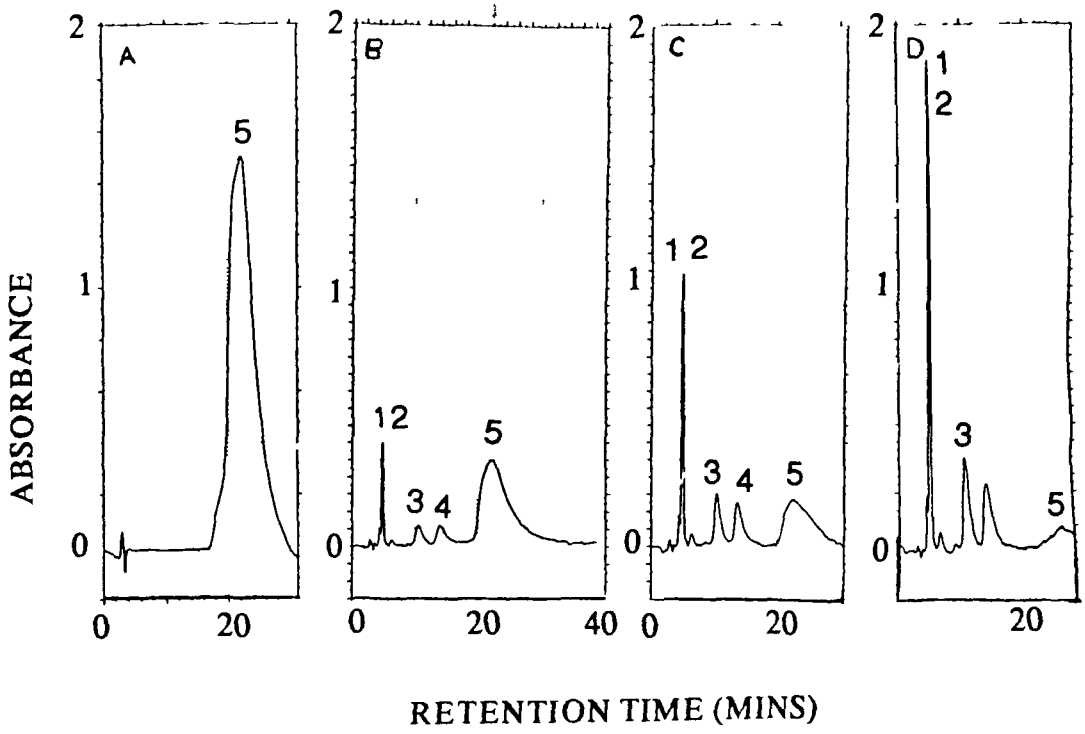

Figure 4 3 22

HPLC traces taken during the photolysis of $[Ru(phen)_2)_2(bpt)]^{3+}$ in MeCN containing 0 01 M Cl^- Photolysis times are (a) 0 min, (b) 10 min, (c) 30 min, and (d) 60 min HPLC conditions as for Figure 4 3 20

two acetonitrile-chloride containing species A graph of the decay of the starting material and the growth of the photolysis products for $[Ru(bpy)_2(bpt)Ru(phen)_2]^{3+}$ is presented in Figure 4 3 23 In this graph, both mononuclear species grow at the same rate and are superimposed They are therefore represented as photolysis product 3 Product 1 is $[Ru(bpy)_2Cl_2]$, product 2 is $[Ru(bpy)_2(MeCN)Cl]^{2+}$.

Photolysis of $[Ru(bpy)_2(bpt)Ru(dpphen)_2]^{3+}$ in MeCN containing 0 01 M Cl^- gave similar results to those obtained for the other four dinuclear complexes Again, both the N1 and the N4 sites of the triazole ring were photolabile

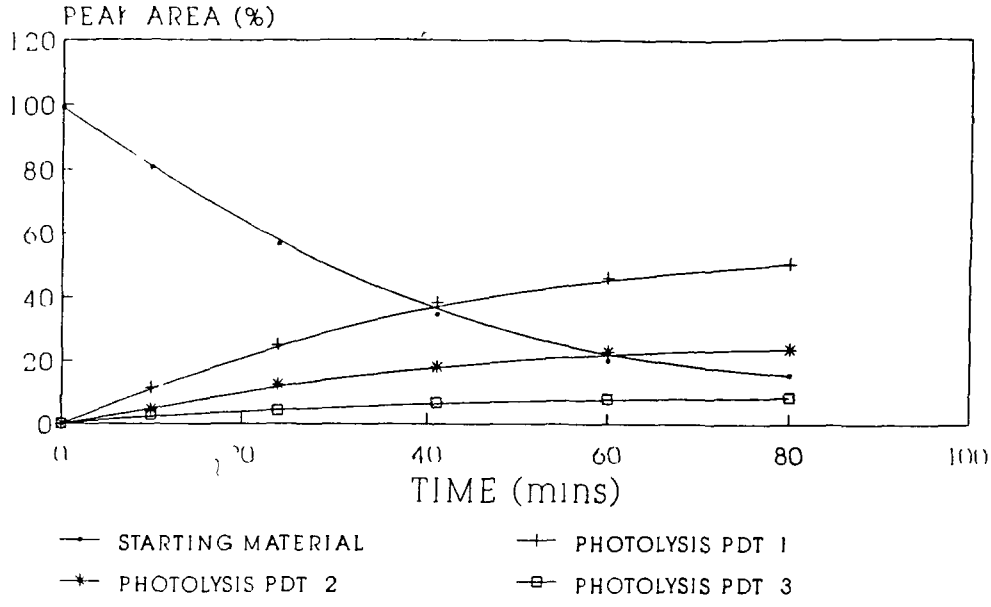

Figure 4 3 23

Graph of the decay of the starting material and growth of photolysis products versus irradiation time for $[Ru(bpy)_2(bpt)Ru(phen)_2]^{3+}$ in MeCN containing 0 01 M Cl^- For peak numbering see text

Photochemistry in MeCN

As can be seen in Figure 4 3 24, photolysis of $[Ru(phen)_2)_2(bpt)]^{3+}$ in MeCN gave rise to only 2 main photoproducts, which were identified as follows: Peak1, retention time 10 10 mins, λ_{max} 430 nm was found to be the N1 isomer of $[Ru(phen)_2(bpt)]^+$ complex and peak 2, retention time 15 05 mins, λ_{max} 425 nm was identified as the $[Ru(phen)_2(MeCN)_2]^{2+}$ complex No evidence for the formation of any other mononuclear complex was present All other complexes show similar results Upon irradiation of compound (**3**), only the N1 isomer of $[Ru(bpy)_2(bpt)]^+$ and $[Ru(bpy)_2(MeCN)_2]^{2+}$ are formed, for compound (**5**), $[Ru(bpy)_2(bpt)]^+$ and $[Ru(phen)_2(MeCN)_2]^{2+}$ are found, and for compound (**6**),

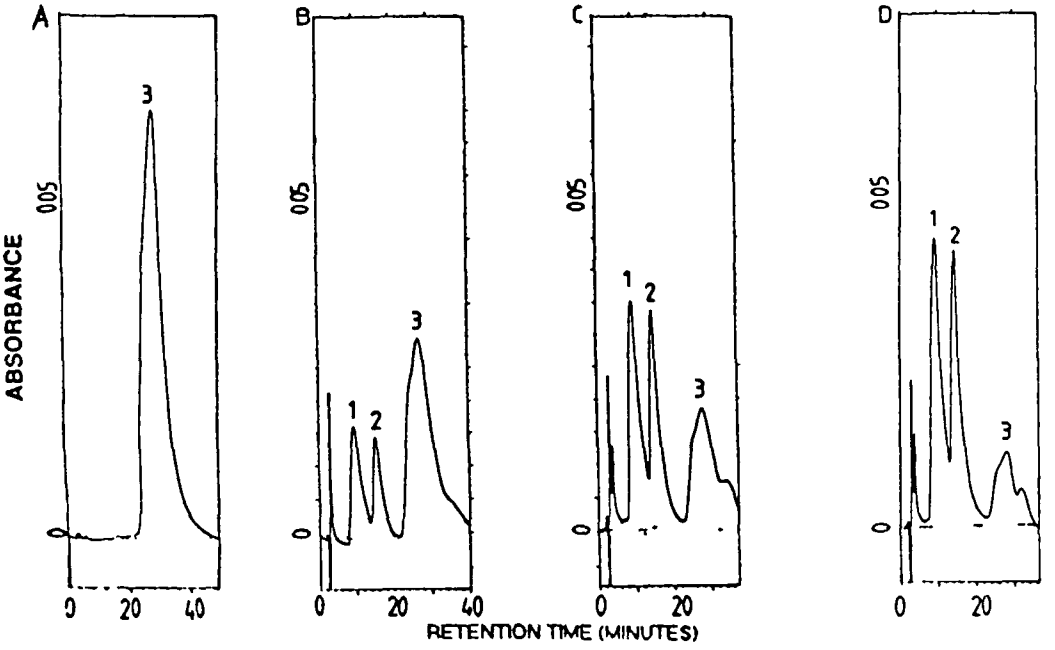

Figure 4 3 24

HPLC traces taken during the photolysis of $[Ru(phen)_2)_2(bpt)]^{3+}$ in MeCN Photolysis times are (a) 0 min, (b) 120 min, (c) 300 min, and (d) 420 min HPLC conditions as for Figure 4 3 20

$[Ru(phen)_2(bpt)]^+$ and $[Ru(bpy)_2(MeCN)_2]^{2+}$ results

Photolysis of $[Ru(bpy)_2(bpt)Ru(dpphen)_2]^{3+}$ in MeCN again showed similar results with the formation of $[Ru(bpy)_2(bpt)]^+$ (ret time 3 3 min, λ_{max} 475 nm) and $[Ru(dpphen)_2(MeCN)_2]^{2+}$ (ret time 4 05 min, λ_{max} 435 nm) as the sole photoproducts

All the photochemical data presented here lead to a number of conclusions The presence of Cl^- ions considerably speeds up the photochemical process and this may account for the fact that selective photodecomposition is not encountered

when these ions are present in solution during the reaction As we have seen the efficiency of population of the ^{3}MC state from the ^{3}MLCT level (η_{ic}) was found to be approximately one for all dinuclear complexes, indicating that no other deactivation process other than population of this ^{3}MC state is occurring here.

The photochemical results suggest that when Cl^- is present in solution photodissociation occurs at both the N1 and the N4 positions of the triazole ring, and therefore there is no localised photodissociation occurring from the N4 position Photoreaction appears to take place via population of ^{3}MC levels on both ruthenium units Although differences do exist (due to the non-equivalence of the co-ordinating nitrogens of the bridging ligand), between the positions of the lowest MLCT levels at each co-ordination site as confirmed by the spectroelectrochemical results, they appear not to be large enough to cause a large energy gap between the two ^{3}MC states[18,72,96] This energy gap was expected to be enhanced by the different polypyridyl ligands However, the different properties of the polypyridyl ligands do not appear to be large enough to make a significant difference under these conditions

In pure MeCN, however, a considerably slower reaction takes place, which most likely allows the different properties of the two nitrogen donor atoms (N1 versus N4) of the asymmetric ligand to become important in the photodecomposition of the complex The results show that population of the ^{3}MC state can occur either from the same Ru-containing unit if bpy is attached to the N4 position of the triazole ring or from different Ru-containing units if bpy is attached to the N1 position It appears that the energy of the reactive excited state (the ^{3}MC state) depends on the asymmetric σ-donor ability of the bridging triazole ligand, whereas the energy of the luminescent excited state (the ^{3}MLCT state) is mainly controlled by the properties of the auxiliary polypyridyl ligands attached to the Ru-containing unit

4.4 CONCLUSION

The data obtained suggest that the emitting state in mixed bpy/phen compounds is bpy-based This is an important result, since neither the ligand-based reductions nor the ground-state resonance Raman spectra could discriminate between the ^{1}MLCT levels of the two polypyridyl ligands The nature of the emitting state is most likely dpphen-based in the mixed ligand $[Ru(bpy)_2(bpt)Ru(dpphen)_2]^{3+}$ complex

The linear relationship between the number of bis(phen) units in the dinuclear complexes and the activation energy for the population of the ^{3}MC level, with the energy decreasing as the number of bis(phen) groups increase is quite an interesting phenonomen The results indicate that the nature of the emitting charge transfer states is solely determined by the nature of the polypyridyl ligand, but that on the other hand, the location of the first metal-based oxidation is controlled by the asymmetry of the bpt$^-$ ligand Photochemical experiments in MeCN strongly suggest that the ^{3}MC level of the ruthenium unit at the N4 triazole atom is lowest in energy However, in the presence of chloride ions, both the N1 and the N4 sites are labilised The efficiency of population of the ^{3}MC levels in all compounds is close to one The differences observed between the photochemical experiments carried out in pure MeCN and in the presence of chloride are, therefore, most likely explained by a large increase in the rate of the photodecomposition pathway with respect to radiationless decay as mechanisms for the deactivation of this metal-centred excited state

4.5 REFERENCES

1 F Scandola, C A Bignozzi, C Chiorboli, M T Indelli, and M A Rampi, *Coord Chem Rev*, **1990**, *97*, 299

2 V Balzani, L Moggi, and F Scandola, *Supramolecular photochemistry*, **1987**, 1-28

3 V Balzani, *Pure & Appl Chem*, **1990**, *62*, 6, 1099

4 S Bobmann, M Seiler, and H Durr, *J Phys Org Chem*, **1992**, *5*, 63

5 V Balzani and F Scandola, *Supramolecular photochemistry*, **1991**, Ellis Horwood Ltd (Ed)

6 J M Martin, D A Ryan, and T V O'Halloran, *J Am Chem Soc*, **1978**, *100*, 7, 2097

7 G Denti, S Serroni, L Sabatino, M Ciano, V Ricevuto, and S Campagna, *Gazz Chim Ital*, **1991**, *121*, 37

8 K Kalyanasundaram, M Gratzel, and M K Nazeeruddin, *J Chem Soc, Dalton Trans*, **1991**, 343

9 S Campagna, G Denti, S Serroni, M Ciano, and V Balzani, *Inorg Chem*, **1991**, *30*, 3728

10 M M Richter and K J Brewer, *Inorg Chem*, **1992**, *31*, 1594

11 G Denti, S Campagna, S Serroni, M Ciano, and V Balzani, *J Am Chem Soc*, **1992**, *114*, 2944

12 L De Cola, F Barigelletti, V Balzani, P Belser, A von Zelewsky, C Seel, M Frank, and F Vogtle, *Coord Chem Rev*, **1991**, *111*, 255

13 J D Petersen, L W Morgan, I Hsu, M A Billadeau, and S E Ronco, *Coord Chem Rev*, **1991**, *111*, 319

14 G Denti, S Serroni, S Campagna, V Ricevuto, and V Balzani, *Inorg Chim Acta*, **1991**, *182*, 127

15 C Y Ryu, R Wang, R H Schmehl, S Ferrere, M Ludwikow, J W Merkert, C E L Headford, and C M Elliot, *J Am Chem Soc*, **1992**, *114*, 430.

16 F Barigelletti, L De Cola, V Balzani, R Hage, J G Haasnoot, J Reedijk, and J G Vos, *Inorg Chem*, **1989**, *28*, 4344

17 D E Richardson and H Taube, *J Am Chem Soc*, **1983**, *105*, 40

18 A Juris, V Balzani, F Barigelletti, S Campagna, P Belser, and A von Zelewsky, *Coord Chem Rev*, **1988**, *84*, 85

19 P Belser, A von Zelewsky, A Juris, F Barigelletti, and V Balzani, *Gazz Chim Ital*, **1983**, *113*, 731

20 B P Sullivan, D J Salmon, T J Meyer, and J Peedin, *Inorg Chem*, **1979**, *18*, 12, 3369

21 M J Powers and T J Meyer, *Inorg Chem*, **1978**, *17*, 7, 1785

22 J E Sutton and H Taube, *Inorg Chem*, **1981**, *20*, 10, 3126

23 J T Hupp and T J Meyer, *Inorg Chem*, **1987**, *26*, 2332

24 M Haga, *Inorg Chim Acta*, **1980**, *45*, L183

25 E H Cutin and N E Katz, *Polyhedron*, **1991**, *10*, 7, 653

26 T S Akasheh and Z M Al-AhmaNd, *Dirstat, Ser B*, **1990**, *17B*, 2, 98

27 W Kaim and S Kohlmann, *Inorg Chem*, **1987**, *26*, 68

28 S Ernst, V Kasack, and W Kaim, *Inorg Chem*, **1988**, *27* 1146

29 W Kaim, S Ernst, S Kohlman, and P Welkerling, *Chem Phys Letts*, **1985**, *118*, 431

30 R Sahai, D A Baucom, and D P Rillema, *Inorg Chem*, **1986**, *25*, 3843

31 D P Rillema and K B Mack, *Inorg Chem*, **1982**, *21*, 3849

32 R Hage, R Prins, J G Haasnoot, J Reedijk, and J G Vos, *J Chem Soc, Dalton Trans*, **1987**, 1389

33 M Haga, T Ano, K Kano, and S Yamabe, *Inorg Chem*, **1991**, *30*, 3843

34 M Haga, T Matsumura-Inoue, and S Yamabe, *Inorg Chem*, **1987**, *26* 4148

35 F Barigelletti, L De Cola, V Balzani, R Hage, J G Haasnoot, J Reedijk, and J G Vos, *Inorg Chem*, **1991**, *30*, 641

36 L De Cola, F Barigelletti, V Balzani, R Hage, J G Haasnoot, J Reedijk, and J G Vos, *Chem Phys Letts*, **1991**, *178*, 5-6, 491

37 C A Bignozzi, S Roffia, and F Scandola, *J Am Chem Soc*, **1985**, *107*, 1644

38 R Hage, J G Haasnoot, H A Nieuwenhuis, J Reedijk, D J A De Ridder, and J G Vos, *J Am Chem Soc*, **1990**, *112*, 9245

39 R Hage, A J H Dijkhuis, J G Haasnoot, R Prins, J Reedijk, B E Buchanan, and J G Vos, *Inorg Chem*, **1988**, *27*, 2185

40 J E Baggot, G K Gregory, M J Pilling, S Anderson, K R Seddon, and J E Turp, *J Chem Soc, Faraday Trans 2*, **1983**, *79*, 195

41 B P Sullivan, D J Salmon, and T J Meyer, *Inorg Chem*, **1978**, *17*, 12, 3334

42 P J Steel, F Lahouse, D Lerner, and C Marzin, *Inorg Chem*, **1983**, *22*, 1488

43 G M Bryant and J E Fergusson, *Aust J Chem*, **1971**, *24*, 441

44 R Hage, A H J Dijkhuis, J G Haasnoot, R Prins, J Reedijk, B E Buchanan, and J G Vos, *Inorg Chem*, **1988**, *27*, 2185

45 R Hage, R A G de Graaff, J G Haasnoot, J Reedijk, and J G Vos, *Acta Cryst (C)*, **1988**, *44*, 56

46 B E Buchanan, R Wang, J G Vos, R Hage, J G Haasnoot, and J Reedijk, *Inorg Chem*, **1990**, *29*, 3263

47 E C Constable and J Lewis, *Inorg Chim Acta*, **1983**, *70*, 251

48 R Hage, J G Haasnoot, J Reedijk, R Wang, E M Ryan, J G Vos, A L. Spek, and A J M Duisenberg, *Inorg Chim Acta*, **1990**, *174*, 77

49 W Tang, D Chen, Z Liu, and A Dai, *Sci CHINA, Ser B*, **1991**, *34*, 8, 897

50 B Mayoh and P Day, *Theoret Chim Acta (Berl)*, **1978**, *49*, 259

51 F Barigelletti, A Juris, V Balzani, P Belser, and A von Zelewsky, *Inorg. Chem*, **1987**, *26*, 4115

52 C Creutz, M Chou, T L Netzel, M Okumura, and N Sutin, *J Am Chem Soc*, **1980**, *102*, 4, 1309

53 A H A Tinnemans, K Timmer, M Reinten, J G Kraaijkamp, A H Alberts, J G M van der Linden, J E J Schmitz, and A A Saaman, *Inorg Chem*, **1981**, *20*, 3698

54 C H Braunstein, A D Baker, T C Strekas, and H D Gafney, *Inorg. Chem*, **1984**, *23*, 857

55 M L Myrick and M K De Armond, *J Phys Chem*, 1989, *93*, 7099

56 A J Downard, G E Honey, and P J Steel, *Inorg Chem*, **1991**, *30*, 3733

57 G A Crosby and W H Elfring Jr, *J Phys Chem*, **1976**, *80*, 2206

58 N E Tokel-Takvoryan, R E Hemingway, and A J Bard, *J Am Chem Soc*, **1973**, *95*, 6582

59 M K DeArmond and C M Carlin, *Coord Chem Rev*, **1981**, *36*, 325

60 C R Johnson, W W Henderson, and R E Shepherd, *Inorg Chem*, **1984**, *23*, 18, 2754

61 B E Buchanan, J G Vos, M Kaneko, W J M van der Putten, J M Kelly, R Hage, R A G de Graaff, R Prins, J G Haasnoot, and J Reedijk, *J Chem Soc, Dalton Trans*, **1990**, 2425

62 B D J R Fennema, R Hage, J G Haasnoot, J Reedijk, and J G Vos, *Inorg Chim Acta*, **1990**, *171*, 223

63 C R Johnson, R E Shepherd, B Marr, S O'Donnell, and W Dressick, *J Am Chem Soc*, **1980**, *102*, 6227

64 H A Nieuwenhuis, J G Haasnoot, R Hage, J Reedijk, and J G Vos, *Inorg Chim Acta*, **1990**, *171*, 223

65 J G Vos, *Polyhedron*, **1992**, *11*, 18, 2285

66 Md K Nazeeruddin, K Kalyanasundaram, *Inorg Chem*, **1989**, *28*, 4251

67 T Forster, *Naturwiss*, **1989**, *36*, 186

68 J F Ireland and P A H Whyatt, *Adv Phys Org Chem*, **1976**, *12*, 131

69 N Lasser and J Feitelson, *J Phys Chem*, **1973**, *77*, 8, 1011

70 J J Aaron and J D Winefordner, *Photochem and Photobiol*, **1973**, *18*, 97

71 A T Cocks, R D Wright, and K R Seddon, *Chem Phys Letts*, **1982**, *85*, 3, 369

72 T J Meyer, *Pure and Appl Chem*, **1986**, *58*, 9, 1193

73 G H Allen, R P White, D P Rillema, and T J Meyer, *J Am Chem Soc*, **1984**, *106*, 2613

74 F Barigelletti, A Juris, V Balzani, P Belser, and A von Zelewsky, *J Phys Chem*, **1987**, *91*, 1095

75 K Kalyanasundaram and Md K Nazerruddin, *Chem Phys Letts*, **1992**, *193*, 4, 292

76 J V Caspar and T J Meyer, *J Am Chem Soc*, **1983**, *105*, 5583

77 V Balzani, A Juris, F Barigelletti, P Belser, and A von Zelewsky, *Sci Papers I P C R*, **1984**, *78*, 4

78 W F Wacholtz, R A Auerbach, and R H Schmehl, *Inorg Chem*, **1987**, *26*, 2989

79 J R Schoonover, C J Timpson, T J Meyer and C A Bignozzi, *Inorg Chem*, **1992**, *31*, 3185

80 S F McClamaham, R F Dallinger, F J Holler and J R Kincaid, *J Am. Chem Soc*, **1985**, *107*, 4853

81 D J Stufkens, T L Snoeck, and A B P Lever, *Inorg Chem*, **1988**, *27*, 953

82 P A Mabrouk and M S Wrighton, *Inorg Chem*, **1986**, *25*, 526

83 H E Toma, P S Santos, and A B P Lever, *Inorg Chem*, **1988**, *27*, 3850

84 K Maruszewski, D P Strommen, K Handrich, and J R Kincaid, *Inorg Chem*, **1991**, *30*, 4579

85 C V Kumar, J K Barton, I R Gould, N J Turro, and J van Houten, *Inorg Chem*, **1988**, *27*, 648

86 P G Bradley, N Kress, B A Hornberger, R F Dallinger, and W H Woodruff, *J Am Chem Soc*, **1981**, *103*, 7441

87 Y J Chang, X Xu, T Yabe, S Yu, D R Anderson, L K Orman, and B J Hopkins, *J Phys Chem*, **1990**, *94*, 729

88 S J Midler, J S Gold, and D S Klinger, *J Phys Chem*, **1986**, *90*, 548

89 R Hage, J G Haasnoot, J Reedijk, and J G Vos, *Chemtracts - Inorg Chem*, **1992**, *4*, 75

90 M B Robin and P Day, *Adv Inorg Chem Radiochem*, **1967**, *10*, 247

91 N S Hush, Prog *Inorg Chem*, **1967**, *8*, 391

92 N S Hush, *Electrochim Acta*, **1968**, *13*, 1005

93 R W Callahan, F R Keene, T J Meyer, and D J Salmon, *J Am Chem Soc*, **1977**, *99*, 4, 1064

94 C Creutz, Prog *Inorg Chem*, **1983**, *30*, 1

95 R Hage, Ph D Thesis, **1991**, Leiden University, The Netherlands

96 G A Heath, L J Yellowlees, and P S Braterman, *J Chem Soc, Chem. Commun*, **1981**, 287

97 G A Heath, L J Yellowlees, and P S Braterman, *Chem Phys Letts*, **1982**, *92*, 6, 646

98 P S Baterman, J Song, and R D Peacock, *Spectrochim Acta*, *48A*, 6, 899

99 B E Buchanan, P Degn, J M P Velasco, H Hughes, B S Creaven, C Long, J G Vos, R A Howie, R Hage, J H van Diemen, J G Haasnoot, and J Reedijk, *J Chem Soc, Dalton Trans*, **1992**, 7, 1177

CHAPTER 5

RUTHENIUM AND OSMIUM COMPLEXES WITH BIS(PYRAZYL)TRIAZOLE: EFFECT OF REPLACING A PYRIDINE RING BY A PYRAZINE RING ON THE PHOTOCHEMICAL AND PHOTOPHYSICAL PROPERTIES

5.1 INTRODUCTION

The design of polynuclear complexes capable of performing photoinduced energy migration or charge separation requires the assembly, in an appropriate spatial sequence, of building blocks that exhibit different excited-state energies or redox potentials[1] Hence, by changing one of the co-ordinating ligands, i e by replacing 2,2'-bipyridine by other similar ligands with slightly modified properties, it may be possible to design an interesting building block, thus, forming a polynuclear complex which is capable of performing useful light induced functions

For example, it has been shown that by replacing pyridine in a ligand by pyrazine, the LUMO of the resulting Ru(II) polypyridyl complex is lowered considerably This is caused by the stronger π-acceptor properties of pyrazine[2-6] The complex $[Ru(bpz)_3]^{2+}$ (where bpz = 2,2'-bipyrazine) has been shown to be an excellent photocatalyst, similar in many ways to $[Ru(bpy)_3]^{2+}$ [7-8] An important feature of the former is that the lifetime of the excited state is longer than that of the latter[9] Also, the standard redox potentials for $[Ru(bpz)_3]^{2+}$ are shifted by ca 0 5 V more positive than those of the corresponding couples for $[Ru(bpy)_3]^{2+}$ [10] An interesting feature of the $[Ru(bpz)_3]^{2+}$ complex, is the existence of two peripheral uncoordinated nitrogen atoms for each bpz available for protonation or for coupling substrates in energy-transfer or electron-transfer processes[11-15]

Another method of tailoring the properties of these complexes, is to change the metal attached to the polypyridine ligands Os(II)-polypyridine complexes also exhibit quite interesting photochemical, photophysical and redox properties[16-21] They have similar properties to Ru(II)-polypyridine complexes, in that their oxidation processes are metal-centred, their reduction processes are ligand-centred and the lowest (luminescent and long-lived) excited state is a triplet metal-to-ligand charge-transfer (^{3}MLCT) level[22-24] They also exhibit excellent

absorption properties in the visible region, stability in their oxidised and reduced forms and relatively long-lived luminescent excited states[15,25-27]

Os(II) complexes have certain advantages over Ru(II) complexes They can be oxidised at less positive potentials than the Ru(II) analogues, which also implies that the luminescent ^{3}MLCT level of an Os(II) complex lies lower in energy than that of an analogous Ru(II) complex The excited-state chemistry of ruthenium is strongly effected by low-lying dd-states, which tend to complicate the interpretation of the photophysical and photochemical properties and have been known to lead to photodecomposition[28-29] The dd states in osmium are much higher in energy than in ruthenium For these two reasons, osmium complexes are expected to be more stable towards photodissociation[1,28] and many of the problems associated with ruthenium can be avoided

As for Ru(II)-polypyridine complexes, oxidation processes are known to be metal-centred, thus the potential values mainly depend on the electronic density that the co-ordinated ligands leave on the metal[30-31] Also the energies of the MLCT transitions depend on the π^* level of the involved ligand and on the electron density on the Os(II) (which in turn results from a balance of the σ-donor and π-acceptor properties of all the co-ordinated ligands)[32-33] Therefore, the combination of the stronger π-accepting properties of the bridging ligand coupled with the increased energy gap between the ^{3}MLCT and ^{3}MC excited states for osmium complexes should lead to some interesting results

However, osmium(II) polypyridine complexes do have some major disadvantages for their application as potential photosensitizers

(a) The low energy of the ^{3}MLCT emission and their low absorption in the visible region of the spectrum means that they are unable to harvest sufficient light energy for solar energy conversion Also, the "energy-gap law" [25,34-35] states that as the energy gap between the ^{3}MLCT and ground-

state decreases, the rate of non-radiative decay increases This results in very short lifetimes for ^{3}MLCT emission in Os(II) complexes[36]

(b) An extensive background synthetic chemistry exists for Ru(II) and the preparative conditions involved are less demanding[37-38]

(c) The background synthetic chemistry to ligand-bridged dimers and oligomers and to intramolecular quenching is known and the potential clearly exists for designing complex systems where the Ru-bpy chromophore is attached to potential catalytic sites[5]

For these reasons, it is unlikely that Os(II) polypyridine complexes will supersede Ru(II) polypyridine complexes as superior sources of photosensitizers

Key components in polynuclear complexes are the bridging ligands, since the interaction between the bridged units and, thereby, the properties of the polynuclear complex, are critically dependent on the size, shape and electronic nature of the bridge[39] Therefore, even small changes in the bridging ligand can lead to large changes in the photophysical properties of these polypyridine Ru(II) complexes

In this chapter, the synthesis, characterisation, photochemical and photophysical properties of a series of mononuclear and dinuclear ruthenium and osmium complexes containing the asymmetric bridging ligand 3,5-bis-(pyrazin-2-yl)-1,2,4-triazole (Hbpzt) are reported Figure 5 1 1 contains the structure of the Hbpzt ligand The acid-based chemistry of the ruthenium mononuclear complex, the effect of the bpzt$^-$ ligand on the metal-metal communication in the ruthenium dinuclear system, and the nature of the emitting excited state in the ruthenium systems has been investigated by Hage et al[40] Results of electrochemical, resonance Raman data, absorption and emission experiments for the ruthenium complexes reveal that complexes with bpzt$^-$ are very unusual, as $[Ru(bpy)_2(bpzt)]^+$ shows a bpy-based emission / reduction, while $[(Ru(bpy)_2)_2(bpzt)]^{3+}$ exhibits a

bpzt⁻-based emission / reduction This switch-over in location of the LUMO causes minor changes in the absorption and emission MLCT energies in going from mononuclear to dinuclear compounds This is due to a combination of a lowering of the π^* level and the weaker σ-donor capabilities of the bridged bpzt⁻ ligand Considerable metal-metal interaction exists for the mixed-valence species containing this ligand

In this chapter, results for the Os(II) systems will be compared to those obtained by Hage[40] for the Ru(II) complexes The photochemical and photophysical properties of the complexes studied will be investigated in detail and the results compared to those obtained for complexes containing the bpt⁻ ligand, as already discussed in Chapter 4 The effect of replacing a pyridine ring by a pyrazine ring in a bridging ligand is closely examined

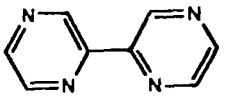

bpz

2,2'-bipyrazine

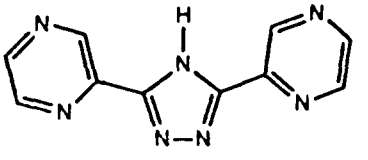

Hbpzt

3,5 bis(pyrazin 2 yl) 1,2,4-triazole

5 1 1 Structure of the 2,2'-bipyrazine (bpz) and 3,5-bis-(pyrazin-2-yl)-1,2,4-triazole (Hbpzt) ligands

5.2 EXPERIMENTAL

5 2 1 *Preparation of the ligand*

The ligand 3,5-bis-(pyrazin-2-yl)-1,2,4-triazole (Hbpzt) was prepared according to literature methods[41] $[Ru(bpy)_2Cl_2]\ 2H_2O$ was prepared as described in Chapter 3

5 2 2 *Preparation of the complexes*

$[Os(bpy)_2Cl_2]\ 2H_2O$

Potassium hexachloroosmate (IV) (1 9 g, 3 95 mmol) and 2,2'-bipyridine (1 3 g, 8 3 mmol) are suspended in 40 cm^3 DMF and heated at reflux in an oil bath for 1 hour while the solution is stirred magnetically The crystals of KCl are removed by filtration and the solution cooled to 0 °C in an ice-bath The complex cis-bis(2,2'-bipyridine-N,N')dichloroosmium (III) chloride dihydrate is precipitated by the slow addition of 250 cm^3 diethyl ether while the solution is stirred rapidly After the oily precipitate crystallises, it is collected on a medium-porosity sintered-glass funnel and air-dried The precipitate (1 0 g, 1 55 mmol) is dissolved in a mixture of DMF (20 cm^3) and MeOH (10 cm^3) contained in a 500 cm^3 beaker A dilute solution of sodium dithionite (2 0 g, 1 1 mmol in 200 cm^3) is added slowly with stirring over 0 5 hr The solution is cooled in an ice-bath and the dark purple oily suspension is filtered and washed with water and diethyl ether Yield 0 87 g (98%)[42]

$[Ru(bpy)_2(bpzt)]PF_6\ 2H_2O$ **(1)**

This compound was prepared as described in the literature[41] Hbpzt (2 mmol, 440 mg) was dissolved in 50 cm^3 of hot ethanol water (1 1 v/v) Cis-$[Ru(bpy)_2Cl_2]\ 2H_2O$ (520 mg, 1 mmol) was added in small portions to the

dissolved mixture and further heated at reflux for six hours The hot solution was filtered and evaporated to dryness 10 cm^3 of water and one drop of concentrated ammonia was added to the dark red residue The compound was precipitated by addition of an excess of aqueous NH_4PF_6 to the solution The compound was purified by semi-preparative HPLC using a mobile phase of 80 20 acetonitrile water containing 0 1 M KNO_3 at a flowrate of 2 5 cm^3/min Further purification took place by recrystallisation from acetone water (1 1 v/v) Yield 0 49 g (62%) Found C, 44 30, H, 2 96, N, 19 10% Anal Calcd for $C_{30}H_{26}F_6N_{11}O_2PRu$ C, 44 01, H, 3 18, N, 18 83%

$[(Ru(bpy)_2)_2(bpzt)](PF_6)_3\ 3H_2O$ (**2**)

This compound was prepared as for (**1**), except that 1 mmol cis-$[Ru(bpy)_2Cl_2]\ 2H_2O$ (520 mg) and 0 4 mmol Hbpzt (90 mg) were heated at reflux for 8 hr in 50 cm^3 ethanol water (2 1 v/v) The PF_6^- salt was isolated and purification took place by semi-preparative HPLC and by recrystallisation from acetone water (1 1 v/v) Yield 0 66 g (44%) Found C, 38 91, H, 2 72, N, 13 60% Anal Calcd for $C_{50}H_{44}F_{18}N_{15}O_3P_3Ru_2$ C, 38 98, H, 2 85, N, 13 64%

$[Os(bpy)_2(bpzt)](PF_6)_2\ H_2O$ (**3**)

This complex was prepared as for (**1**), except that 2 mmol Hbpzt (440 mg) was heated at reflux with 1 mmol cis-$[Os(bpy)_2Cl_2]$ (575 mg) for two days in 50 cm^3 ethanol water (1 1 v/v) Purification took place by semi-preparative HPLC and by recrystallisation from acetone water (1 1 v/v) Yield 0 47 mg (42%) Found C, 35 60, H, 2 34, N, 14 93% Anal Calcd for $C_{30}H_{24}F_{12}N_{11}OOsP_2$ C, 34 82, H, 2 32, N, 14 89%

$[(Os(bpy)_2)_2(bpzt)](PF_6)_3\ 3H_2O$ (**4**)

This complex was prepared as for (**2**) using 1 mmol cis-$[Os(bpy)_2Cl_2]$ (575 mg) and 0 4 mmol Hbpzt (90 mg) in 50 cm^3 ethanol water (2 1 v/v) and heated at reflux for three days Purification took place by semi-preparative HPLC using the conditions described for compound (**1**) and by from acetone water (1 1 v/v) Yield 0 68 mg (40%) Found C, 35 19, H, 2 43, N, 12 42% Anal Calcd for $C_{50}H_{42}F_{18}N_{15}O_2Os_2P_3$ C, 35 31, H, 2 47, N, 12 36%

5.3 RESULTS AND DISCUSSION

5 3 1 *^{1}H NMR spectroscopy*

A list of the ^{1}H NMR resonances for the mononuclear and dinuclear Hbpzt complexes is given in Table 5 1 We know from the X-ray structure analysis of $[Ru(bpy)_2(bpt)]^+$ that the Ru-containing unit is bound to the bpt^- ligand via N1 of the triazole ring[43] The similarities in the spectra observed for this complex and the mononuclear $[Ru(bpy)_2(bpzt)]^+$ complex, suggest that co-ordination is taking place via the same site in both complexes In addition, it is expected that binding via N4 causes significant steric interaction between the free pyrazine ring and an adjacent bulky $Ru(bpy)_2$ group and will, therefore, not be favoured Only the N1 isomer was found for the analogous compound containing 3-methyl-5-(pyrazin-2-yl)-1,2,4-triazole[2] The changes in the chemical shifts of the protons of the non co-ordinating ring B of the complex are small compared to those of ring A (or the co-ordinating ring) Replacement of a pyridine ring by a pyrazine ring considerably alters the positions of the H^5 and H^6 protons of the bridging ligand (see Figure 5 1 1) The H^6 proton does not appear to feel the effect of the adjacent bpy ring to such a large extent and, hence, is not shifted so far upfield, but the H^5 proton is considerably shifted upfield It is unclear why a different behaviour is observed for these complexes compared with their pyridine analogues The $[Os(bpy)_2(bpzt)]^+$ complex is also co-ordinated via the N1 site at the triazole ring The resonances of the osmium complex are found at slightly higher field than those of the ruthenium complex, which is in agreement with previous observations on either Ru(II) and Os(II) polypyridine complexes[44-45] Figure 5 3 1 shows the ^{1}H NMR spectrum obtained for $[Os(bpy)_2(bpzt)]^+$ in deuterated acetonitrile

The ^{1}H NMR spectra of the dinuclear complexes are very complicated and

Compound	H^3	H^4	H^5	H^6
$[Ru(bpy)_2(bpzt)]^+$				
Ring A	9 32 (-0 02) s	----	7 62 (-1 16) d	8 24 (-0 54) d
Ring B	9 22 (-0 12) s	----	8 48 (-0 30) d	8 48 (-0 30) d
$[(Ru(bpy)_2)_2(bpzt)]^{3+}$				
Ring A	7 68 (-1 66) s	----	7 44 (-1 34) d	8 29 (-0 49) d
Ring B	9 13 (-0 21) s	----	7 46 (-1 32) d	8 43 (-0 33) d
$[Os(bpy)_2(bpzt)]^+$				
Ring A	9 23 (-0 11) s	----	7 57 (-1 21) d	8 06 (-0 72) d
Ring B	9 20 (-0 14) s	----	8 46 (-0 32) d	8 46 (-0 32) d
$[(Os(bpy)_2)_2(bpzt)]^{3+}$				
Ring A	7 94 (-1 80) s	----	7 36 (-1 52) d	8 11 (-0 67) d
Ring B	9 24 (-0 10) s	----	7 59 (-1 19) d	8 36 (-0 42) d
Hbpzt	9 34 s	----	8 78 d	8 78 d

Table 5 1

Chemical shifts (ppm) of the protons of the $bpzt^-$ complexes in CD_3CN The free ligand is measured in $(CD_3)_2SO$ Values in parenthesis represent the shifts in the protons of the co-ordinated ligand compared with the free ligand (s = singlet, d = doublet)

no complete assignment could be made However, by using COSY techniques and by comparison with the $[(Ru(bpy)_2)_2(bpt)]^{3+}$ dimer[46], the protons of the $bpzt^-$ ligand could be identified Only one geometrical isomer was present in the ^1H NMR spectra of both dinuclear complexes, although it is expected that two optical isomers exist, which do not show up in the ^1H and COSY NMR spectrum of the

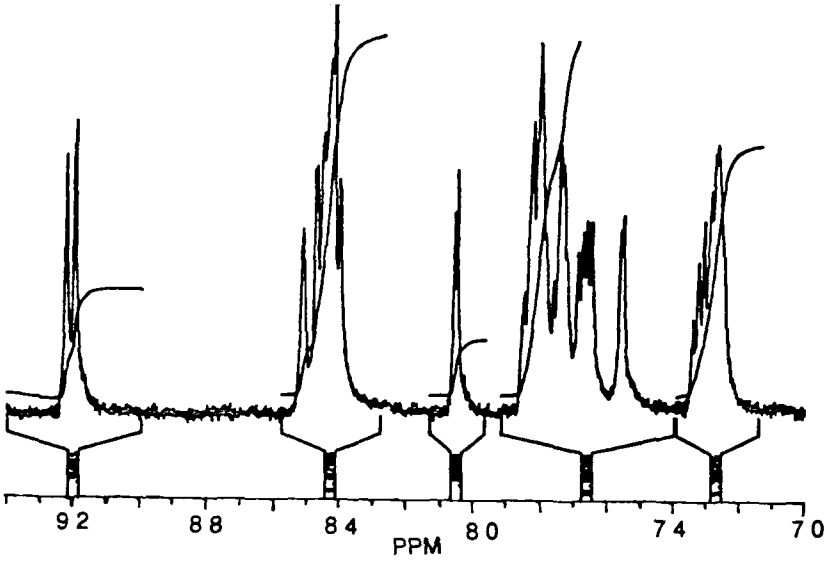

Figure 5 3 1

400 MHz ^{1}H NMR spectrum obtained for $[Os(bpy)_2(bpzt)]^+$ in CD_3CN

$[(Ru(bpy)_2)_2(bpzt)]^{3+}$ dimer (see Figure 5 3 2) In the dinuclear compounds, a very short distance between H^3 of ring A and one of the neighbouring bpy ligands is present, leading to a large shift towards a higher field of this proton The H^3 proton of ring B is not influenced by any neighbouring bpy ligands and is therefore not shifted upfield Co-ordination takes place via the N1 and N4 sites of the triazole ring Similar chemical shifts for the osmium dimer are found

5 3 2 *Absorption and Emission properties*

The UV/vis absorption and emission properties of the complexes are presented in Table 5 2 An intense band is observed for all complexes in the visible region, which has been assigned as metal-to-ligand charge-transfer (MLCT) in nature[47-49] Comparison with the values obtained for the Hbpt complex (see Table 4 2), shows a shift to higher energy of the maximum wavelength of absorption and the emission maxima at both room temperature and at 77 K This can be explained by the weaker σ-donor and stronger π-acceptor properties of the

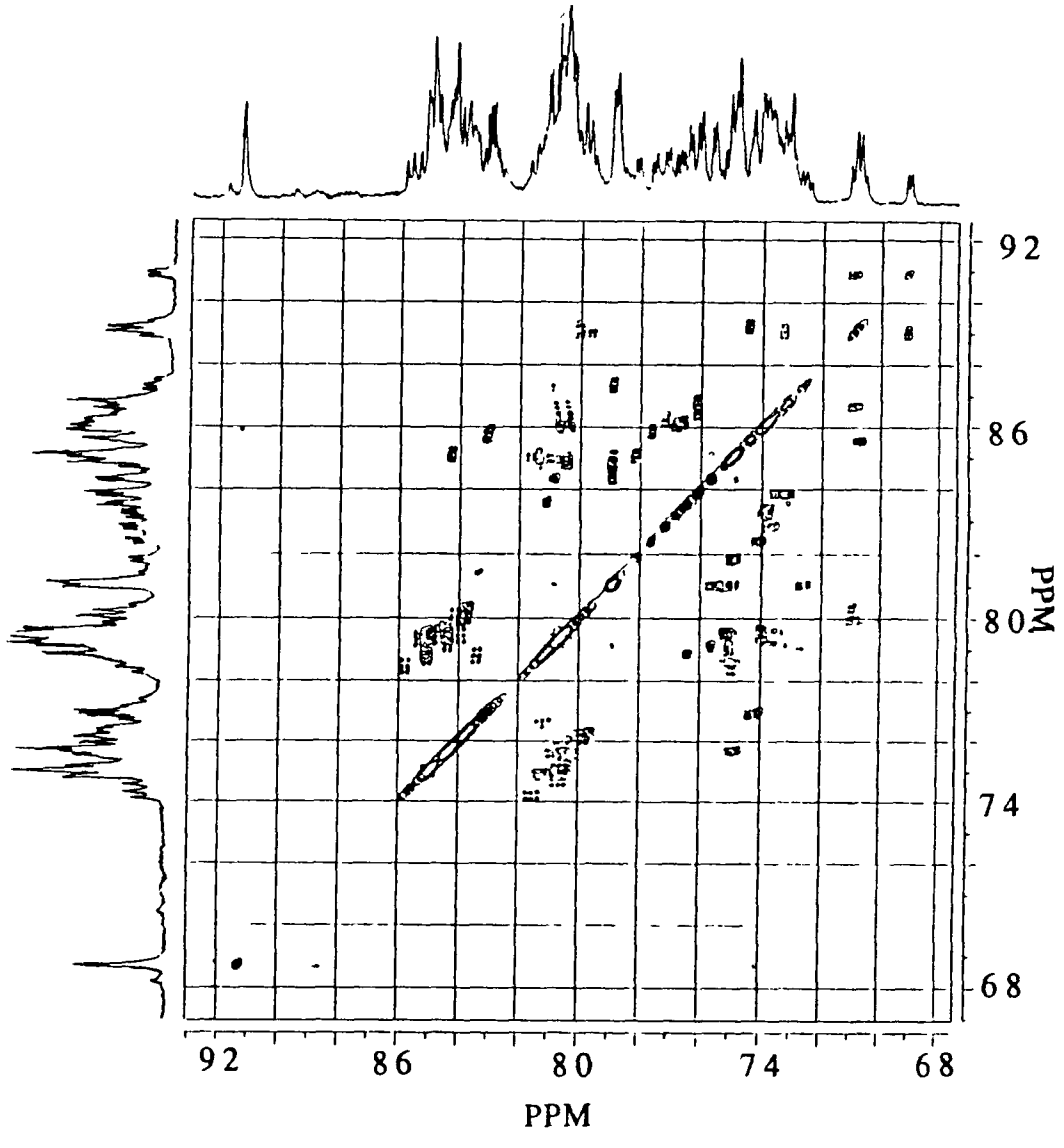

Figure 5 3 2

400 MHz ^1H and COSY NMR spectra of $[(Ru(bpy)_2)_2(bpzt)]^{3+}$ in CD_3CN

bpzt$^-$ ligand compared with the bpt$^-$ ligand, which causes less electron density to be present on the metal and consequently a shift to higher energy of the lowest unoccupied molecular orbital (LUMO)[49] The emission spectra at room temperature were broad and featureless, because interactions with the surrounding solvent molecules broaden the individual vibronic components resulting in Gaussian-shaped envelopes appearing[50] Protonation of the

Compound	Absorption (log ε)	Emission 298 K	Emission 77 K
$[Ru(bpy)_2(bpzt)]^+$	450 (4 09)	666	605
$[Ru(bpy)_2(Hbpzt)]^{2+}$	436 (4 07)	690	645
$[Os(bpy)_2(bpzt)]^+$	404 436 (3 66) 483 (3 70) 600	783	725
$[Os(bpy)_2(Hbpzt)]^{2+}$	416 452	791	717
$[(Ru(bpy)_2)_2(bpzt)]^{3+}$	452 (4 43)	671	617
$[(Os(bpy)_2)_2(bpzt)]^{3+}$	408 (3 78) 480 (3 79) 600	788	721

Table 5 2

Absorption maxima in MeCN at 298 K and emission maxima in MeCN at 298 K and in ethanol at 77 K for the bpzt$^-$ compounds

complexes does not lead to large changes in their absorption and emission properties This will be discussed in more detail in Section 5 3 3 The room temperature emission maxima of both the osmium monomer and the osmium dimer are shifted to shorter wavelengths compared with the bpt$^-$ complexes[41]

For Os(II)-polypyridyl complexes, at room temperature excited-state properties are determined by a series of three low-energy Boltzmann populated MLCT states which have considerable triplet character and which behave kinetically as a single state[35], while the fourth state is predominantly singlet in nature[17] It was found that the "triplet" states of osmium have 2-5 times as much singlet character as the Ru analogues[17] For osmium complexes, additional absorbance bands are observed at 600 - 660 nm, which can be assigned to a

formally forbidden triplet $d\pi$ - π^* (bpy) MLCT transitions[22,51] The intense absorption bands in the UV region observed for all complexes are due to the usual ligand-centred (π - π^*) transitions typical of these metal(II) polypyridyl complexes[51]

The absorption and emission energies are very similar for the mononuclear and corresponding dinuclear complexes This is quite unusual behaviour, as normally for ligands with low π^* levels such as pyrazine, upon going from a mononuclear to a dinuclear compound, the empty π^* level is stabilised, with the result that the absorption maxima are shifted to lower energy[52-54] For bridging ligands with a strong σ-donor ability, the formation of the dinuclear system leads to a shift of the maximum wavelength of absorption to higher energy[55-56] It has been suggested[40] that in $bpzt^-$ complexes, both effects are important with the result that no shift in the λ_{max} is observed This will be discussed in more detail in the next section

5 3 3 *Acid-base properties*

For pyrazyltriazole complexes, two (de)protonation steps are expected[2] For $[Ru(bpy)_2(bpzt)]^+$, these steps can be represented as follows

$$[Ru(bpy)_2(H_2bpzt)]^{3+} \overset{pK_a(1)}{\rightleftharpoons} [Ru(bpy)_2(Hbpzt)]^{2+} \overset{pK_a(2)}{\rightleftharpoons} [Ru(bpy)_2(bpzt)]^{+}$$

The first step involves the (de)protonation of the Ru-based pyrazine ring ($pK_a(1)$), whilst the second step ($pK_a(2)$) is related to (de)protonation of the triazole proton The same applies for the osmium mononuclear complex

Following from the work of Hage[41], who found a $pK_a(2)$ of 2 0 ± 0 2 for the ruthenium monomer, we measured the analogous osmium compound The changes observed in the absorption spectrum of $[Os(bpy)_2(Hbpzt)]^{2+}$ as a function of pH are presented in Figure 5 3 3 for determination of the $pK_a(2)$ value A $pK_a(2)$ value of 1 2 ± 0 2 is found for $[Os(bpy)_2(bpzt)]^+$ $[Ru(bpy)_2(bpzt)]^+$ had a $pK_a(2)$ of 2 0 ± 0 2 in agreement with earlier observations[40] The pK_a of the free ligand, Hbpzt, was found to be 7 1 ± 0 2

This lowering of the pK_a upon co-ordination can be explained by a strong σ-donation from the ligand to the metal centre, which reduces the electron density on the ligand and hence it is more acidic The similarity in the pK_a's of both complexes, indicates that the protonation step is the same for both complexes Only a very small shift in the absorbance maximum from 449 nm to 443 nm is observed in the absorbance spectra upon lowering the pH A similar small shift is found for the osmium complex A pK_a value of 4 1 ± 0 1 was found for $[Ru(bpy)_2(bpt)]^+$, and that of the free ligand Hbpt was found to be 8 4 ± 0 1 As the pK_a of the free ligand is related to the σ-donor capacities of the ligand[57], this confirms the assumption that the Hbpt ligand is a stronger σ-donor ligand than Hbpzt If stronger σ-donor ligands have weaker π-acceptor properties[58], then $bpzt^-$ is a stronger π-acceptor than bpt^-, but weaker than bpy (pK_a Hbpy = 4 4)

The excited-state acid-based properties were also evaluated Figure 5 3 4 shows the changes in the emission spectra upon changing the pH for $[Ru(bpy)_2(bpzt)]^+$ Again a very small shift in the emission maximum from 692 nm to 705 nm is observed Similar small shifts were observed for the osmium complex A pH_i value of 4 9 ± 0 1 was found for $[Ru(bpy)_2(bpzt)]^+$, and a pH_i value of 2 3 was found for $[Os(bpy)_2(bpzt)]^+$ As discussed previously in Chapter 4, these values do not represent real excited-state pK_a^* values Using equations 4 1 and 4 2 , excited-state pK_a^* values are calculated and are tabulated in Table 5 3

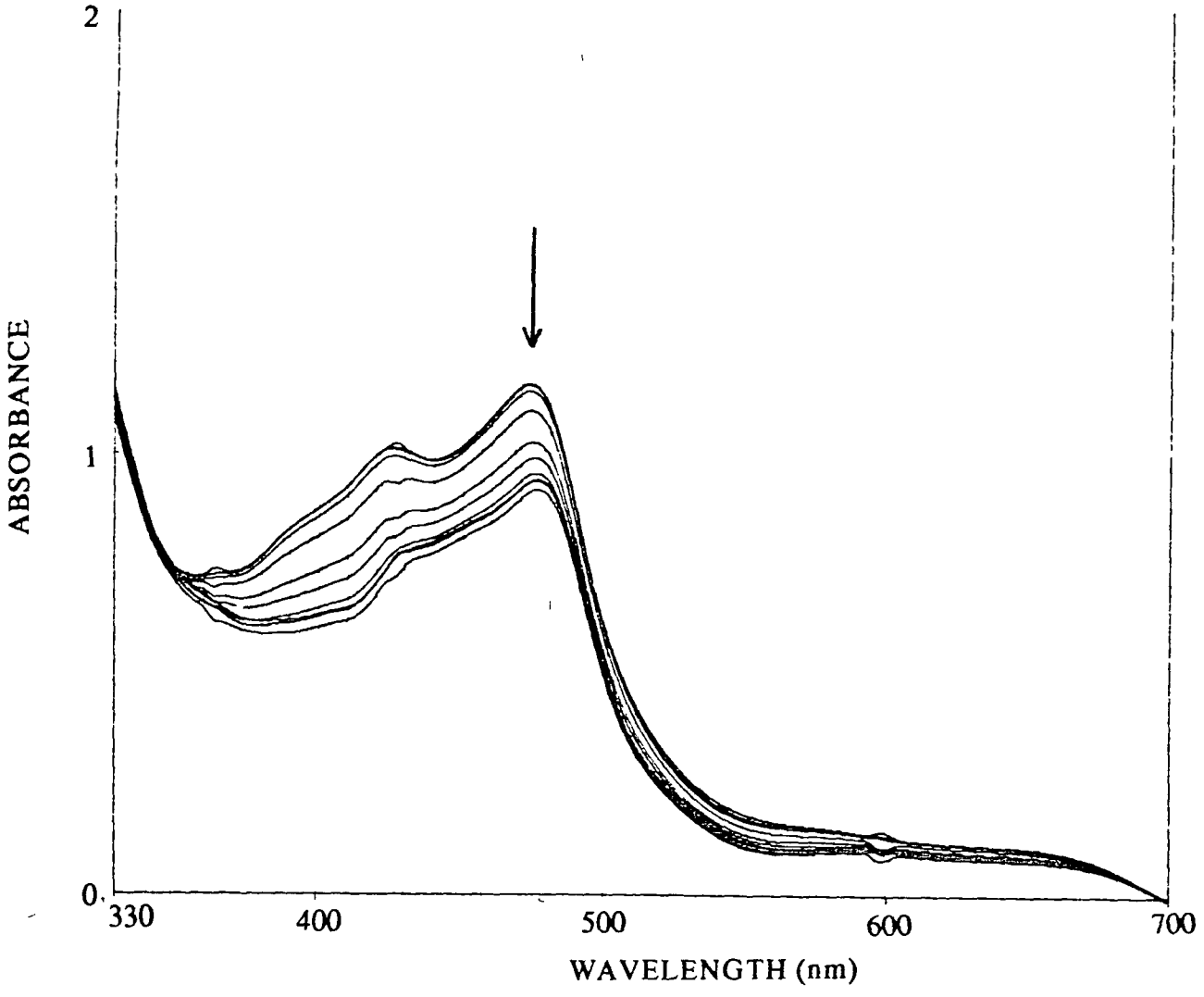

Figure 5 3 3

Changes in the absorption spectrum upon lowering the pH for $[Os(bpy)_2(bpzt)]^+$ in Britton-Robinson buffer (a) pH 4 48, (b) 3 85, (c) 2 93, (d) 2 70, (e) 2 44, (f) 2 31, (g) 1 93, (h) 1 50, (i) 1 06, (j) 0 80, (k) 0 60, (l) 0 33, and (m) 0 10

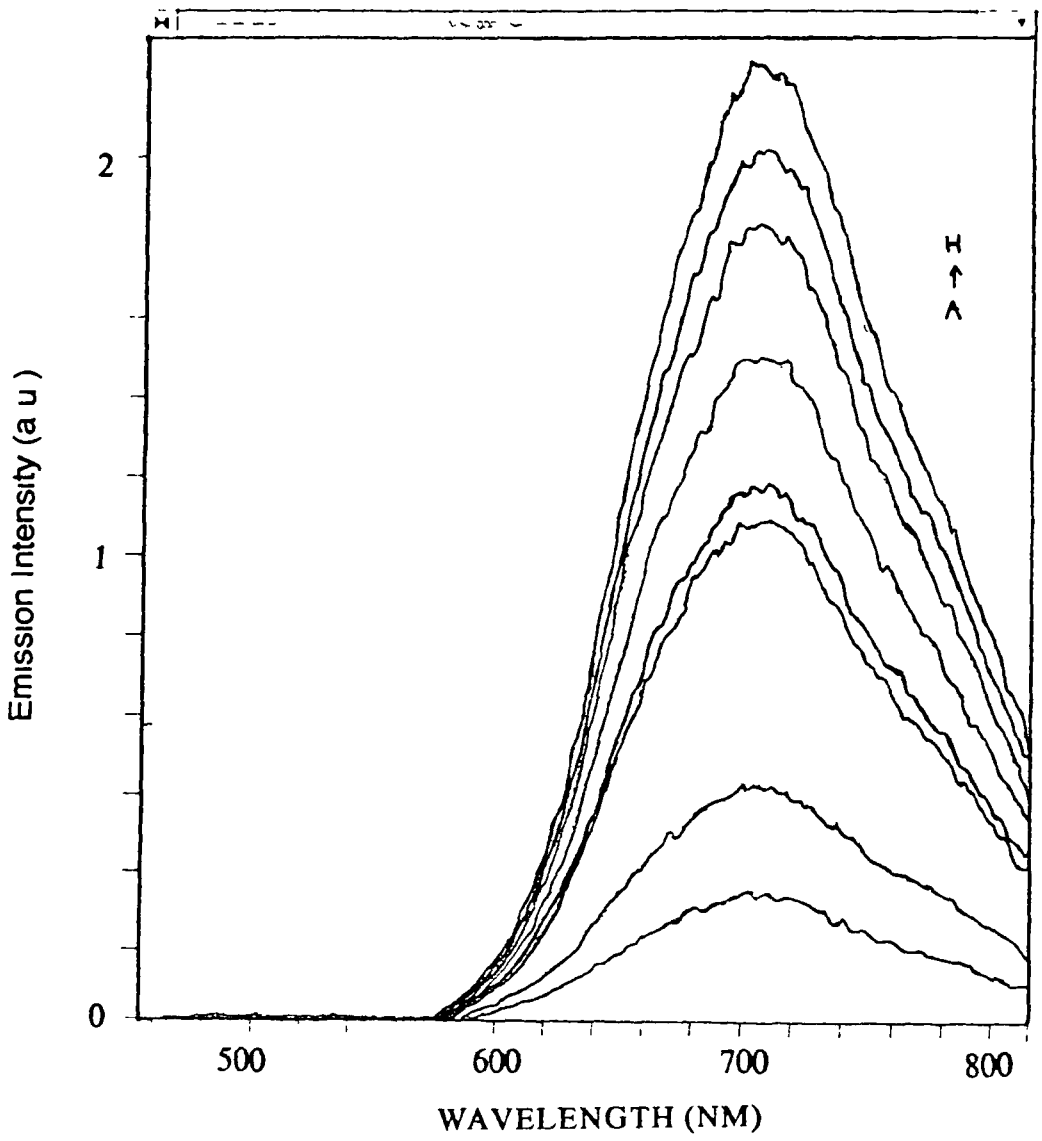

Figure 5 3 4

Changes in the emission spectrum as a function of pH for $[Ru(bpy)_2(bpzt)]^+$ in Britton-Robinson buffer (a) pH 2 55, (b) 2 95, (c) 3 60, (d) 4 95, (e) 5 95, (f) 6 95, (g) 7 83, and (h) 8 85

Compound	pK_a	pH_i	$pK_a^*(1)$	$pK_a^*(2)$
$[Ru(bpy)_2(bpzt)]^+$	2 0 ±0 2 -1 5 ± 0 2	4 9 ± 0 1	3 8 ± 0 2	2 8 ± 0 2
$[Os(bpy)_2(bpzt)]^+$	1 2 ± 0 2 -1 4 ± 0 2	2 3 ± 0 1	1 6 ± 0 2	1 3 ± 0 2

Table 5 3

Ground-state pK_a, pH_i (inflection points of the emission titration curve), and excited-state pK_a^* values obtained using equations 4 1 and 4 2 respectively

Although the calculated $pK_a^*(1)$ (using equation 4 1) and $pK_a^*(2)$ (using equation 4 2) values do not exactly agree with each other, they nevertheless point to a definite trend between the ground-state and excited-state pK_a values It is generally assumed[58] that the acidity of the excited state is increased with respect to the ground state when the ligand involved in the acid-base reaction is not directly involved in the emission process If, however, the acidity is decreased, the excited state is thought to be localised on the ligand showing the acid-base chemistry These assumptions are based on the knowledge that upon excitation of a ruthenium polypyridyl complex, a metal-based electron is promoted to a ligand-based π^* orbital This results in the creation of a ruthenium centre with a formal valence of 3+ A decreased basicity is then explained by a reduced electron density on the spectator acid-base ligand as a result of electron donation to the metal centre The fact that the pK_a^* values are higher or equal to the pK_a values suggest that the electron is excited into the pyrazine ligand so that the ligand does not just act as a spectator ligand

The larger the value of ΔpK_a^* (the difference between the ground state and excited state pK_a's), the less the dπ metal orbital contributes to the ground state mixed metal-ligand wavefunction i e the less the metal acts as a π-donor[59-60] In our complexes, ΔpK_a^* is larger for ruthenium than for osmium and therefore osmium acts as a better π-donor Conversely, the larger the value of ΔpK_a^*, the less the ligand acts as a π-acceptor towards the metal and therefore bpzt⁻ is a better π-acceptor than bpt⁻

Apart from (de)protonation of the triazole ring, the pyrazine ring can also be protonated, as seen previously by Crutchley et al for $[Ru(bpz)_3]^{2+}$, where bpz = 2,2'-bipyrazine[61] They found a pK_a value of -2 2 in the ground state for the first protonation step Titrations were carried out using concentrated sulphuric acid solutions, and a $pK_a(1)$ of -1 5 ± 0 2 was found for $[Ru(bpy)_2(Hbpzt)]^{2+}$, and -1 4 ± 0 2 for $[Os(bpy)_2(Hbpzt)]^{2+}$ Figure 5 3 5 illustrates the changes in the absorption spectrum upon changing the pH for the $[Os(bpy)_2(Hbpzt)]^{2+}$ complex over the pH range -0 5 to -2 9 As can be seen, a shift in the absorbance maximum from 465 nm to 490 nm occurs, with a subsequent growth in a new band at 520 nm An isosbestic point is also maintained throughout the titration, indicating that only one (de)protonation step is occurring in this region

5 3 4 *Redox properties*

Table 5 4 lists the oxidation and reduction potentials of the bpzt⁻ mononuclear and dinuclear complexes in MeCN containing 0 1 M TEAP The oxidation potential of $[Ru(bpy)_2(bpzt)]^+$ occurs at a higher value than that of the analogous bpt⁻ complex We have already seen from the pK_a measurements that bpzt⁻ is a stronger π-acceptor ligand than bpt⁻, thus causing less electron density on the

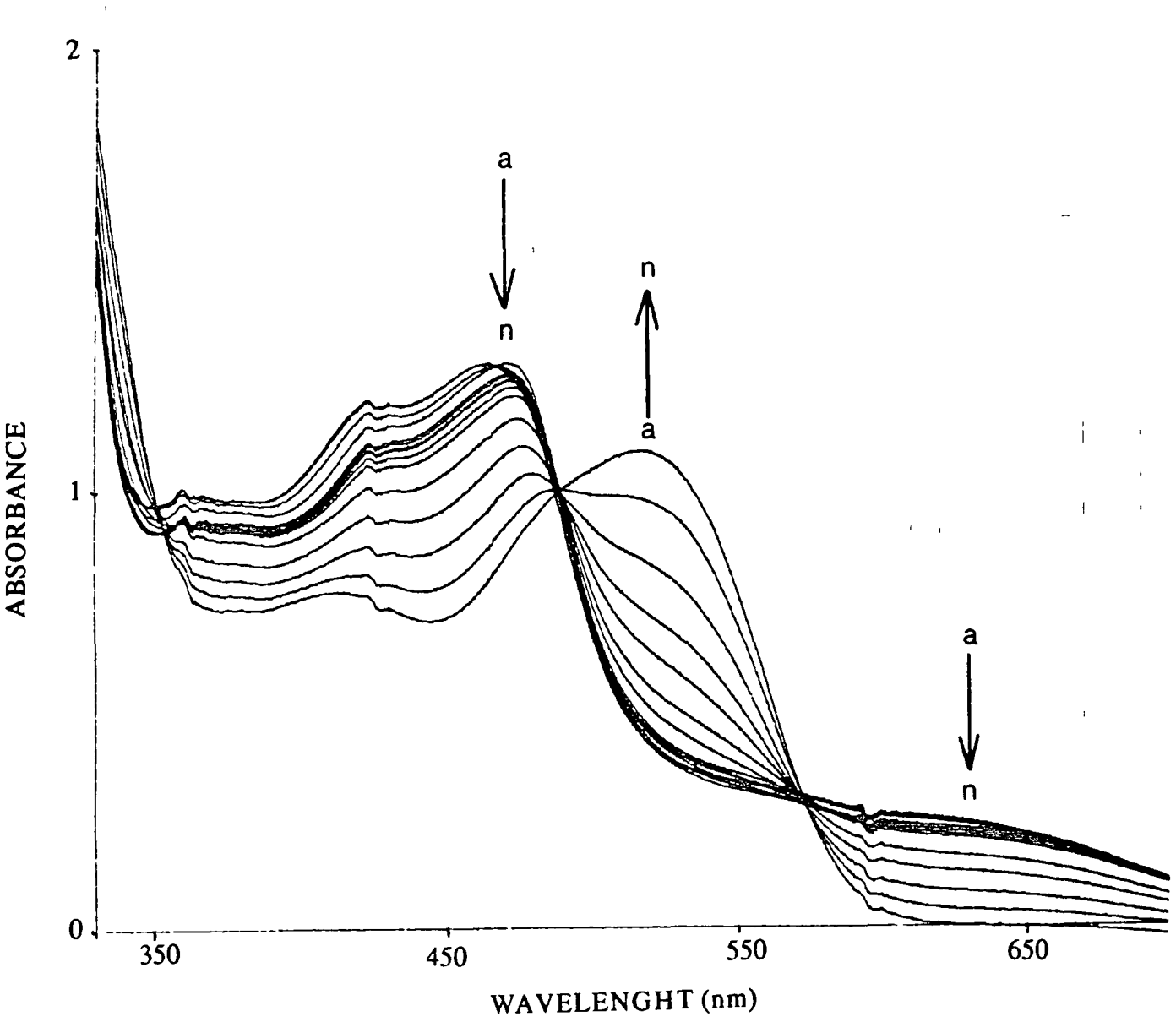

Figure 5 3 5

Changes in the absorption spectrum upon changing the pH for $[Os(bpy)_2(Hbpzt)]^{2+}$ using concentrated sulphuric acid (a) pH -0 56, (b) -0 86, (c) -1 04, (d) -1 16, (e) -1 26, (f) -1 41, (g) -1 52, (h) -1 67, (i) -1 82, (j) -1 96, (k) -2 10, (l) -2 21, (m) -2 43, and (n) -2 88

Compound	Oxidation (pot. V)	Reduction (pot. V)
$[Ru(bpy)_2(bpzt)]^+$	1 00	-1 41 -1 66
[a]$[Ru(bpy)_2(Hbpzt)]^{2+}$	1 29	
$[Os(bpy)_2(bpzt)]^+$	0 64	-1 41 -1 69
[a]$[Os(bpy)_2(Hbpzt)]^{2+}$	1 08	
$[Ru(bpy)_2)_2(bpzt)]^{3+}$	1 19 1 50	-1 27 -1 39 -1 59
$[Os(bpy)_2)_2(bpzt)]^{3+}$	0 47 0 71	-1 23 -1 42 -1 57 -1 68

Table 5 4

Electrochemical potentials (DPP) of the mononuclear and dinuclear $bpzt^-$ complexes in MeCN containing 0 1 M TEAP All potentials in volts versus SCE [a]Protonated measurements carried out by addition of 1 drop of concentrated H_2SO_4

metal, therefore, making it more difficult to oxidise The first reduction potential of both complexes is very similar, suggesting that a bpy-based reduction is occurring This observation is in agreement with the weaker π-acceptor properties of bpt^- and $bpzt^-$ in comparison with bpy, as inferred from the pK_a measurements An increase in the oxidation potential is observed when the complex becomes protonated This has been observed previously for Ru(II) and Os(II) polypyridyl complexes and occurs as a consequence of the weaker σ-donor ability of the protonated ligand[59]. No well defined reduction potentials are observed for $[Ru(bpy)_2(Hbpzt)]^{2+}$ due to adsorption on the electrode surface

The dinuclear complexes exhibit two oxidation waves, again occurring at slightly higher potentials than for the analogous bpt^- complexes, most likely due to

the weaker σ-donor and better π-acceptor capabilities of bpzt⁻ The first reduction wave is found at a less negative potential (-1 24 V) than for its bpt⁻ analogue This points to a bpzt⁻-based first reduction potential (vide supra) This has been confirmed by resonance Raman measurements carried out by Hage et al[40] They found that for $[Ru(bpy)_2(bpzt)]^+$ the lowest MLCT band is Ru ---> bpy based, whereas for $[Ru(bpy)_2(Hbpzt)]^{2+}$ and $[(Ru(bpy)_2)_2(bpzt)]^{3+}$ the LUMO is bpzt⁻ based The second reduction potential is comparable to that obtained for the first reduction potential of $[(Ru(bpy)_2)_2(bpzt)]^{3+}$ and therefore has been assigned as a bpy-based reduction As expected, the oxidation potential of the osmium moieties are about 0 4 V lower than those in the ruthenium analogues[62-65] ΔE, or the separation between the two monoelectronic reversible oxidations, reflects the amount of communication between the two metal centres[65-67] and is also related to the electronic and structural properties of the bridging ligand As the bridging ligand is bpzt⁻ in both the ruthenium and osmium dinuclear species, a comparison of the metal-metal communication is both systems is possible In the $[(Ru(bpy)_2)_2(bpzt)]^{3+}$ complex, the difference between the two oxidation potentials is 310 mV, indicating that noticeable electronic communication occurs between the two metals It is interesting to note that this difference is 240 mV for the analogous $[(Os(bpy)_2)_2(bpzt)]^{3+}$ complex and therefore the metal centres do not communicate as well in this complex as in the ruthenium case This can be accounted for by invoking interaction between the already oxidised trivalent metal ion and the electron-rich HOMO of the bridge This interaction reduces the electron density present on the other co-ordination centre for the second metal ion As Ru(III) is a better π-acceptor than Os(III), this effect is more pronounced for ruthenium than for osmium[68] The opposite effect is found for complexes containing dpp (where dpp = 2,3-bis(2-pyridyl)-pyrazine)[51,69], where back-donation of π electron density by the first metal centre to the LUMO of the bridge

increases the basicity of the free co-ordination centre with the result that the oxidation potential of the second metal ion will be higher Because of the stronger back-donation capabilities of osmium compared to ruthenium, this effect is expected to be more pronounced for osmium in the dpp system[68]

It is possible to correlate the redox properties and spectroscopic properties of these types of complex Redox potential measurements serve as a very good guide for the assignment of the excited-state luminescence Differences in the potential between the first oxidation potential and the first reduction potential, $\Delta E_{1/2}$, are of much interest[70] By plotting the energies of the MLCT absorption and emission bands (in eV) versus $\Delta E_{1/2}$, it is possible to examine if the same ligands are responsible for both the electrochemical and MLCT properties[71-73] Figure 5 3 6 contains these plots for the bpzt$^-$ complexes Some pyrazine-based complexes are included for comparison purposes As can be seen, the plot resulted in a straight line This is not an unexpected result, because as mentioned previously, oxidation involves removal of an electron from a d orbital, whereas reduction involves placing an electron in a ligand-based π^* orbital In an MLCT transition, an electron is removed from a metal-based $d\pi$ orbital and placed in a ligand-based π^* orbital[33] Therefore, a direct correlation between both electrochemical potentials and absorption / emission energies is not unusual

Variations in the MLCT excited-state energies, therefore, depend largely on two factors

(1) The relative energies of the π^* orbital of the luminophoric ligand, and

(2) The relative stabilisation of oxidation state Ru(II) (or Os(II)) compared to Ru(III) (or Os(III)) by a combination of σ and π effects as the ligand is varied[5]

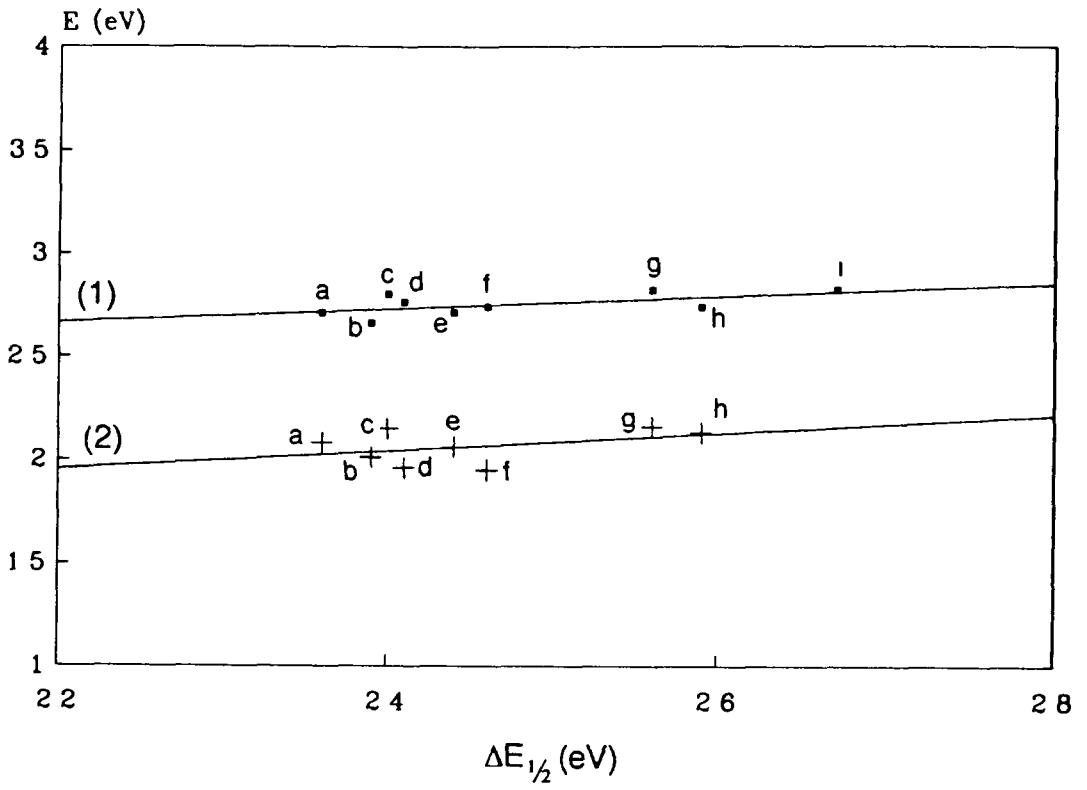

Figure 5 3 6

Plot of $\Delta E_{1/2}$ versus (1) absorption and (2) emission energies for the complexes (a) $[Ru(bpy)_2(3Mpztr)]^{2+}$, (b) $[Ru(bpy)_2(pztr)]^{+}$ isomer 2, (c) $[Ru(bpy)_2(1M5pztr)]^{2+}$, (d) $[Ru(bpy)_2(bpzt)]^{+}$, (e) $[Ru(bpy)_2(pztr)]^{+}$ isomer 1, (f) $[(Ru(bpy)_2)_2(bpzt)]^{3+}$, (g) $[Ru(bpy)_2(1M3pztr)]^{2+}$, (h) $[Ru(bpy)_3]^{2+}$, and (i) $[Ru(bpz)_3]^{2+}$

5 3 5 *Location of the emitting states*

As mentioned previously, nearly identical MLCT energies were found for the mononuclear and dinuclear complexes The switch-over from a bpy-based emission for $[Os(bpy)_2(bpzt)]^{+}$ to a bpzt-based emission for $[(Os(bpy)_2)_2(bpzt)]^{3+}$

and $[Os(bpy)_2(Hbpzt)]^{2+}$ could be responsible for the lack of a significant shift in the MLCT energies of the absorption and emission of these complexes This behaviour is similar to that obtained for the Ru(II) complexes and can be explained as follows[41]

Firstly, a lowering of the π^* level of the bridging ligand is observed on going from the mononuclear to the dinuclear complex As a result the $bpzt^-$-based π^* level is now located below the original emitting π^* bpy orbital This has been shown to be correct on the basis of resonance Raman spectroscopy[40]

Secondly, the higher oxidation potential observed for the $bpzt^-$ dinuclear compound compared to the analogous monomer shows that the filled d orbital is lowered This is caused by the fact that in the dinuclear compound, two $Os(bpy)_2$ units share the σ-donor capacity of the negatively-charged bridging ligand As the difference in first reduction potentials for $[Os(bpy)_2(bpzt)]^+$ and $[(Os(bpy)_2)_2(bpzt)]^{3+}$ (0 18 V) is nearly the same as the difference in their oxidation potentials (0 17 V), the two effects cancel out and very similar MLCT absorption and emission energies are observed for both compounds A similar effect was observed for the osmium complexes

This behaviour is very unusual for these type of M(II) polypyridyl complexes Thus, the position of the lowest unoccupied molecular orbital (LUMO), which is responsible for emission in these complexes, is an extremely important consideration for the design of supramolecular species, as it controls the energy of the MLCT bands and therefore the photochemical and photophysical properties of these complexes

5 3 6 *Mixed-Valence species*

Spectroelectrochemistry was carried out on $[(Ru(bpy)_2)_2(bpzt)]^{3+}$ in the NIR region A band was located around 1870 nm which was caused by an intervalence transition, i e , a light induced electron hopping from the Ru(II) centre to the Ru(III) centre Figure 5 3 7 shows the spectrum obtained upon generation of the intervalence transition Using the equations described in Chapter 4, the properties of the IT band of the mixed-valence species have been calculated and the results are presented in Table 5 5

The energy of an optical transition, E_{op}, is correlated according to the Hush model[74], to the energy gradient between the minima of the M(II)M(III) and M(III)M(II) curves, δE (the internal energy difference between the two oxidation-state isomers), and to the reorganisational energy Figure 5 3 8 contains a graphical representation of the nuclear configuration of the mixed valence states For symmetrical complexes $\delta E = 0$ In an asymmetric case, as for the ligands studied here, on the assumption that differences in entropy terms are negligible, δE can be estimated from standard redox potentials (see Chapter 4)

In mixed-valence species, the equilibrium nuclear configuration of a species changes when it looses or gains an electron In the case of a metal complex, this configuration change involves changes in the vibrations and rotations of the solvent dipoles (λ_o) and also changes in the metal-ligand and intra-ligand bond lengths and angles (λ_i) The changing nuclear configurations give rise to an activation barrier to electron transfer because nuclear motion occurs on a timescale of 10^{-11} - 10^{-13}, much longer than electronic motion (< 10^{-15} s) So λ_i is an intrinsic property of the binuclear complex, whereas λ_o depends on the reorganisation of the solvent environment[74]

The intervalence transition band energy is related to the Marcus-Hush

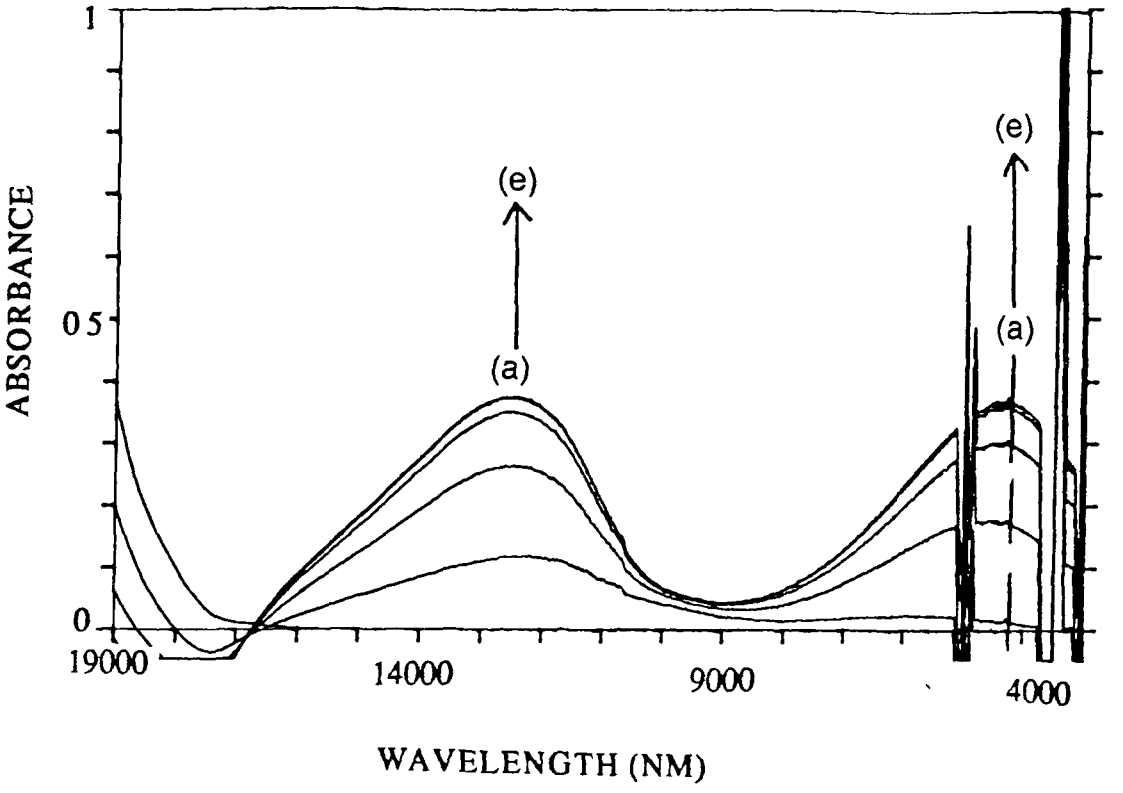

Figure 5 3 7

Near infrared spectra of $[(Ru(bpy)_2)_2(bpzt)]^{3+}$ on electrochemical oxidation in MeCN Applied potential is 1 3 V for (a) 10 min, (b) 20 min, (c) 30 min, (d) 40 min, and (e) 50 min

reorganisational energy term for thermal electron transfer by[75-76]

$$E_{op} = \lambda_i + \lambda_o \qquad \textbf{5.1}$$

where λ_i and λ_o are the inner and outer sphere reorganisational contributions to λ The energy of activation, E_{th}, is related to λ according to the following equation[77]

Solvent	E_{OD} (cm^{-1})	$\Delta\upsilon_{1/2}$ (exp)	$\Delta\upsilon_{1/2}$ (calc)	ε_{max} $M^{-1}cm^{-1}$	$1/D_{OD} - 1/D_S$	α^2	H_{AB}	k_{th} (s^{-1}) (x 10^{10})	E_{th} (J) (x 10^{-20})
[a]MeCN	5450	3800	3277	3149	0 528	0 024	844	13	1 5
[a]Acetone	5400	4600	3260	1734	0 495	0 016	683	6 3	1 8
[a]C_6H_5CN	5250	3800	3206	2063	0 391	0 016	664	6 3	1 8
[a]CH_2Cl_2	5200	3800	3188	1305	0 381	0 010	520	3 9	2 0
[b]MeCN	5450	4020	3259	3074	0 528	0 025	854	13	1 5
[b]Acetone	5370	4200	3249	4914	0 495	0 042	110 1	45	9 5
[b]C_6H_5CN	5280	4200	3217	3098	0 391	0 027	868	17	1 4
[b]CH_2Cl_2	5240	4100	3203	3094	0 381	0 027	861	17	1 4

Table 5 5

Properties of the IT band of (a) $[(Ru(bpy)_2)_2(bpzt)]^{3+}$ and (b) $[(Ru(bpy)_2)_2(bpt)]^{3+}$ in different solvents (see Chapter 4)

$$4E_{th} = \lambda \qquad \textbf{5 2}$$

Using a dielectric continuum model, the following equation has been derived for calculation of the outer sphere reorganisational energy[75-76]

$$\lambda_o = e^2 (1/2R_1 + 1/2R_2 - 1/d) (1/n^2 - 1/D_s) \qquad \textbf{5 3}$$

where R_1 and R_2 are the molecular radii at the redox centres, d is the internuclear separation between the metal centres, e is the unit electron charge, D_s is the static dielectric constant, and n^2 is the optical dielectric constant Since $E_{op} = \delta E$ and E_{op}

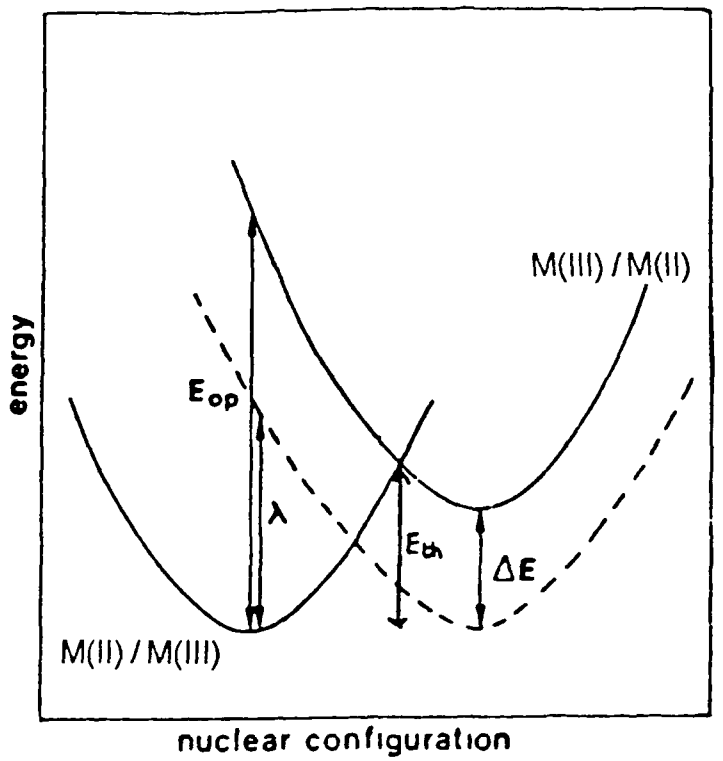

Figure 5 3 8

Nuclear configuration of the mixed-valence species

$= \lambda_o + \lambda_i$, in a series of solvents, the intervalence transition band energy should vary linearly with $1/n^2 - 1/D_s$ and the intercept of the plot should give a value for λ_i (the value at the intercept corresponds to the measurement of E_{op} in a solvent like CCl_4, where there is no permanent dipole moment[77]) The IT experiment thus allows the activation barrier to electron transfer to be partitioned between the inner and outer-sphere reorganisational contributions Table 5 5 contains the IT band parameters for $[(Ru(bpy)_2)_2(bpzt)]^{3+}$and the IT band parameters for $[(Ru(bpy)_2)_2(bpt)]^{3+}$ in four different solvents Figure 5 3 9 shows a plot of the solvent dependence of the Ru(II)Ru(III) complexes As can be seen a reasonable linear relationship was found for both complexes It was found that the energy of the intervalence transition band increased with increasing solvent polarity This

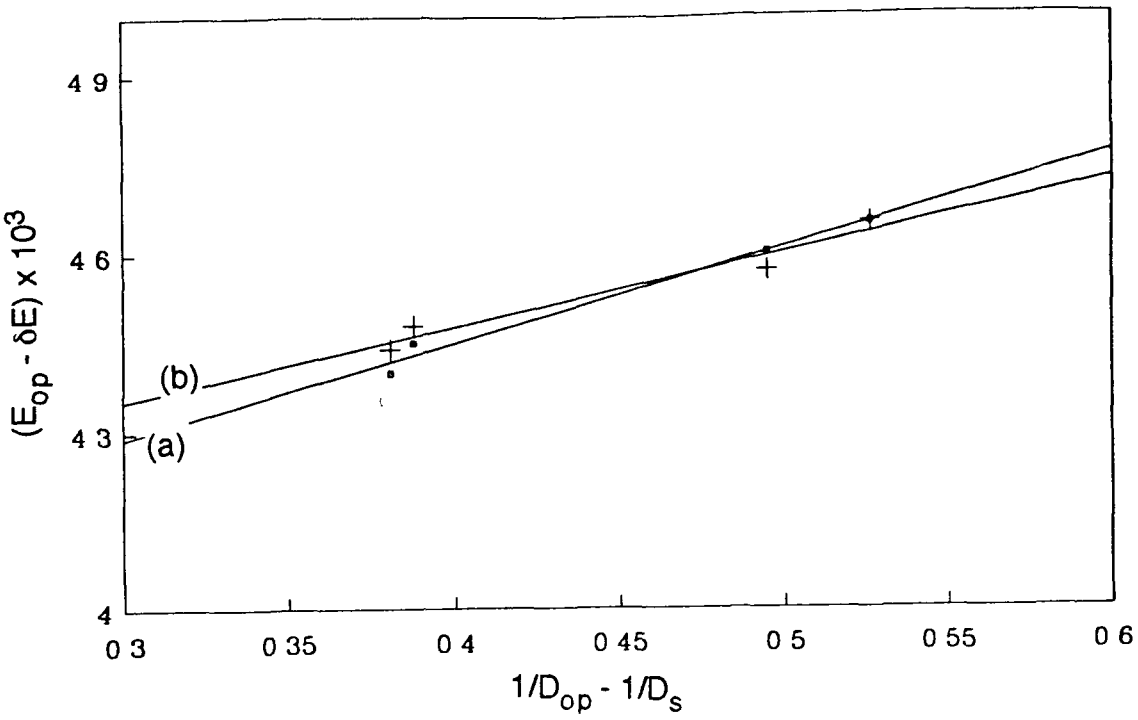

Figure 5 3 9

Plot of the solvent dependence of the mixed-valence species of (a) $[(Ru(bpy)_2)_2(bpt)]^{3+}$ and (b) $[(Ru(bpy)_2)_2(bpzt)]^{3+}$

would appear to be reasonable, because of the fact that more polar solvents have a greater dipole moment and therefore any change in the electronic state of a solvent complex will cause a greater activation barrier to the electron transfer taking place The values for the inner sphere reorganisational energy appear to be very similar for both complexes λ_i values of 3812 cm^{-1} for $[(Ru(bpy)_2)_2(bpzt)]^{3+}$ and 3977 $cm^{-1}$for $[(Ru(bpy)_2)_2(bpt)]^{3+}$ were calculated

An essential requirement for the stability of mixed-valence species is a sufficiently large comproportionation equilibrium constant, K_c [68], which can be formulated as follows

$$2[M\text{-}LL\text{-}M]^{n+} \rightleftharpoons [M\text{-}LL\text{-}M]^{(n+1)+} + [M\text{-}LL\text{-}M]^{(n-1)+}$$

K_c can be calculated from the following equation

$$\Delta E = 0\ 059\ log(K_c) \qquad \textbf{5.4}$$

where ΔE is the difference in oxidation potentials of the two metal centres The stability against redox dissociation for $[(Ru(bpy)_2)_2(bpt)]^{3+}$ ($1\ 2 \times 10^5$) and for $[(Ru(bpy)_2)_2(bpzt)]^{3+}$ ($1\ 8 \times 10^5$) are quite large, possibly due to effective mixing between the high-lying π-orbitals of the bridging ligand and the $d\pi$ metal(III)-based orbitals[55]

It has been suggested that hole transfer is an important pathway for intervalence transfer in mixed-valence species containing anionic bridges, such as those studied here[40,78] In other words, electron transfer occurs by holes transferring through the highest occupied molecular orbital (HOMO) If the HOMO of the triazolate bridge mediates the delocalisation, rather than the level of the LUMO, then similar values for α^2 should be observed for both complexes If, however, the level of the LUMO is mediating the extent of electron delocalisation, a much stronger metal-metal interaction for the bpzt$^-$ dinuclear compound compared with the bpt$^-$ complex would be expected, as the bpzt$^-$ system has a much lower π^* level than the bpt$^-$ system As can be seen from the results, very little difference exists in the extent of electron delocalisation for both complexes These results support the suggestion that hole transfer is playing an important role in intervalence transfer

As the extent of electron delocalisation was found to be quite large for $[(Ru(bpy)_2)_2(bpzt)]^{3+}$, this points to significant metal-metal communication The effective interaction between the π orbitals of the anionic bridging ligand and the $d\pi$ orbitals is most likely the reason for the relatively strong interaction[55]

The switch over of the LUMO from bpy-based to bpzt$^-$-based emission upon going from a mononuclear to a dinuclear species was previously only observed for complexes where no or very little communication between the metal centres was present for the bridging ligands[79-80] The high α^2 value for $[(Ru(bpy)_2)_2(bpzt)]^{3+}$ makes this system unique It was found previously that communication between the metal centres with pyrazine as a bridging group is far greater from osmium than for ruthenium[68], because the larger spin-orbital coupling constant for Os(III) in comparison with Ru(III), would tend to stabilise the ground-state of the Os(III) complexes to a greater extent We, therefore, have no reason to believe that the metal-metal interaction for $[(Os(bpy)_2)_2(bpzt)]^{3+}$ is as strong (if not stronger) as for the ruthenium dinuclear species This, however, has not been measured for this complex

The degree of electronic coupling H_{AB}, which dictates the intensity of the intervalence transition band, was found to vary with the solvent used as did the activation barrier to the thermally induced electron transfer from the M(II) centre to the M(III) centre, E_{th} The rate constant for the thermally induced electron transfer from the M(II) to the M(III) centre, k_{th}, was also measured and showed similar variations It should be noted that even small changes in E_{th} can lead to quite large errors in the rate constants However, it is possible to conclude that the compounds measured here show a definite solvent dependency If the measured bandwidth fits the calculated bandwidth, then the system is most likely valence trapped (localised) If the observed band is too narrow, the species belongs to the class of delocalised systems[81] Our calculated and experimentally obtained bandwidths agree reasonably well, suggesting a localised mixed-valence system in our dinuclear species

Spectroelectrochemistry was also carried out in the visible and UV regions Figure 5 3 10 shows the absorbance spectra obtained for the oxidation of $[(Ru(bpy)_2)_2(bpzt)]^{3+}$ in MeCN containing 0 1 M TEAP The absorbance maximum of the MLCT band at 450 nm shifts to 430 nm upon generation of the mixed-valence species and then disappears when the species is fully oxidised to its Ru(III)Ru(III) state The ligand-centred π - π^* transition occurring at 284 nm does not shift upon formation of the mixed valence species, but a considerable shift to 300 nm is observed upon generation of the fully oxidised Ru(III)Ru(III) species This has also been observed for the dinuclear complexes containing the bpt^- ligand, and suggests localisation of the excited electron on one Ru-containing site (see Chapter 4)

For this compound, it is also suggested that the N1 site of the triazole ring is a better σ-donor than the N4 site and therefore, the Ru-containing unit attached to the N1 position of the triazole ring is oxidised first

5 3 7 *Luminescent lifetime measurements*

Table 5 6 lists the luminescent lifetime measurements of the complexes at 298 K and at 77 K, including their quantum yield of emission values (ϕ_{em}) As can be seen from the data, protonation of the mononuclear complexes considerably decreases their luminescent lifetimes This is due to the weaker σ-donor capacity of the protonated ligand, leading to lower-lying metal-centred dd states which are easily populated, resulting in rapid radiationless deactivation to the ground-state of the complexes In general, it is notable that replacement of a Ru(II) centre by an Os(II) centre causes the luminescent lifetime to decrease by a factor of greater than 12 [36], due to the low energy of the MLCT emission for Os(II) complexes and

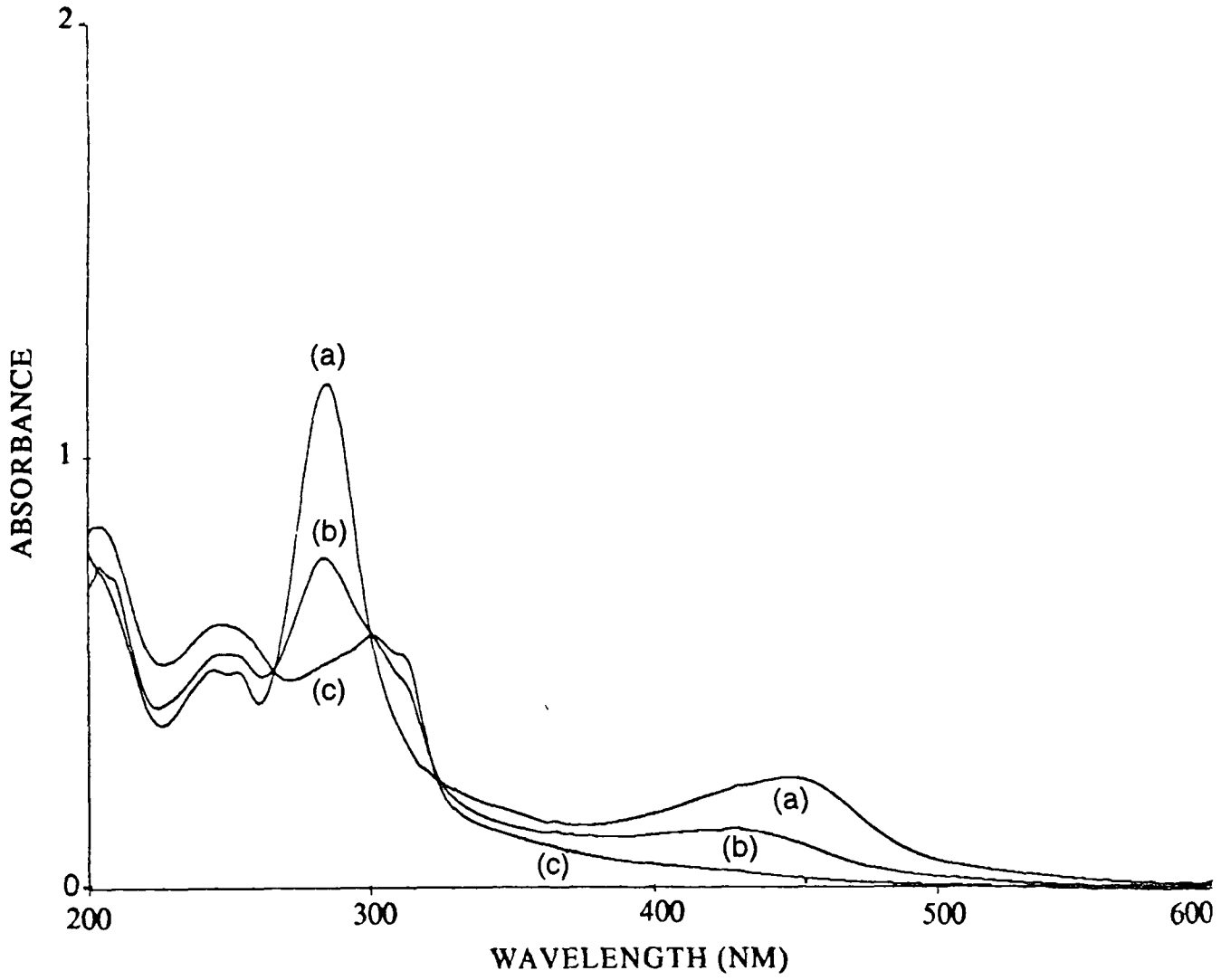

Figure 5 3 10

Absorbance spectra obtained for $[(Ru(bpy)_2)_2(bpzt)]^{3+}$ in MeCN containing 0 1 M TEAP Applied potentials are (a) 0 V, (b) 1 3 V, and (c) 1 7 V

the high percentage of singlet character of the MLCT excited states of Os(II) complexes, which increases the coupling with the ground state of the complex This is also observed for complexes containing the $bpzt^-$ ligand

Temperature dependent luminescent lifetime measurements have been carned out on both mononuclear complexes and on the dinuclear

Compound	[a]300K (μs)	[b]77K (μs)	[a]ϕ_{em}
$[Ru(bpy)_2(bpzt)]^+$	0 32	6 40	$2\,5 \times 10^{-3}$
$[Ru(bpy)_2(Hbpzt)]^{2+}$	0 23	4 97	$6\,8 \times 10^{-5}$
$[Os(bpy)_2(bpzt)]^+$	0 014	0 99	$5\,5 \times 10^{-4}$
$[Os(bpy)_2(Hbpzt)]^{2+}$	----	0 29	$1\,5 \times 10^{-5}$
$[(Ru(bpy)_2)_2(bpzt)]^{3+}$	0 20	7 03	$3\,0 \times 10^{-3}$
$[(Os(bpy)_2)_2(bpzt)]^{3+}$	0 008	0 97	$5\,2 \times 10^{-5}$

Table 5 6

Luminescent lifetimes (± 0 02 μs) and quantum yield of emission (error 10%) of the bpzt⁻ complexes [a]Measured under argon in MeCN [b]Measured in ethanol

$[(Ru(bpy)_2)_2(bpzt)]^{3+}$ complex No measurements were carried out on the dinuclear osmium complex, because its lifetime was below the rise-time available on our instrument The temperature dependence of the Ru(II) complexes is shown in Figure 5 3 11 over the temperature range 150 - 300 K As can be seen, $[Ru(bpy)_2(bpzt)]^+$ exhibits a steep increase in the $\ln(1/\tau)$ Vs 1/T plots in the temperature range 190 - 210 K This step has already been encountered for the $[Ru(bpy)_2(bpt)]^+$ complex (see Chapter 4) and was attributed to reorientation of the solvent molecules due to strong changes in the dipole moment caused by Ru ---> bpy charge transfer It was not observed for $[(Ru(bpy)_2)_2(bpt)]^{3+}$ [41] or in the case of the bpzt⁻ dinuclear system

The plot of the $\ln(1/\tau)$ versus 1/T for $[Os(bpy)_2(bpzt)]^+$ is shown in Figure 5 3 12 It does not contain this step at 190 - 210 K This is analogous to the result obtained for $[Os(bpy)_2(bpt)]^+$ by Barigelletti et al[1] The absence of this step was attributed to the more covalent character of the Os - N bonds (greater π-

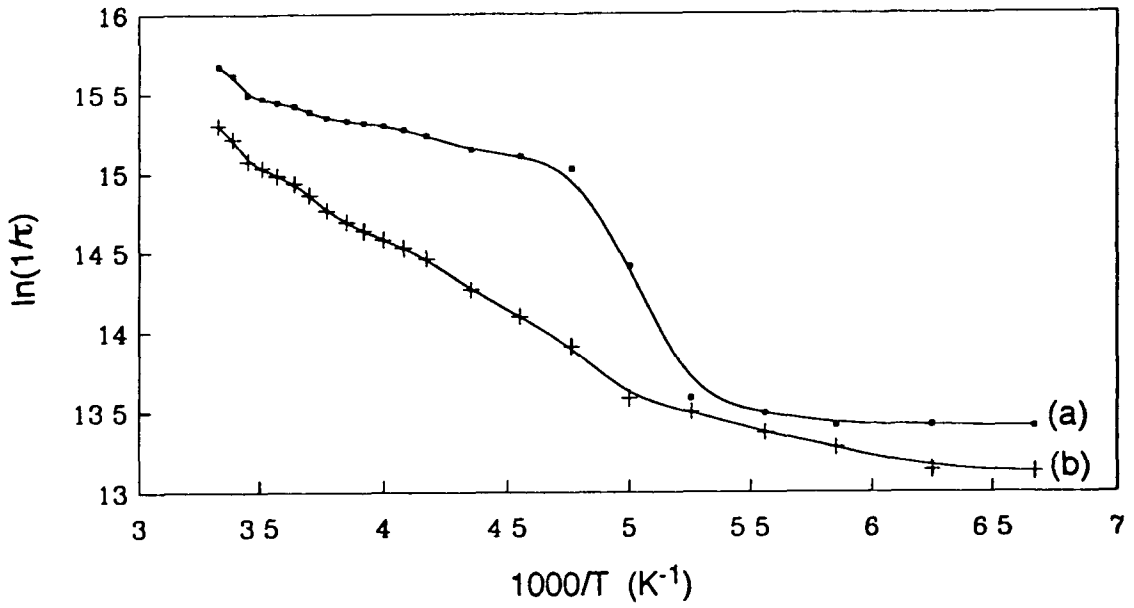

Figure 5 3 11

Plot of the ln(1/τ) Vs 1/T for (a) $[Ru(bpy)_2(bpzt)]^+$ and (b) $[(Ru(bpy)_2)_2(bpzt)]^{3+}$ in ethanol methanol (4 1)

backbonding for Os) and consequently the smaller amount of charge transferred in the ^{3}MLCT level most likely causes a smaller solvent interaction for the osmium compound

A very important observation is that for both mononuclear complexes, no steep rise in the temperature-dependent lifetime plots is observed at temperatures greater than 250 K However, a rise is observed for the dinuclear ruthenium complex Table 5 7 contains the activation energies and frequency factors obtained for these complexes The large E_a (3735 cm^{-1}) and large A (9 9 x 10^{13}) values obtained for the dinuclear Ru complex are indicative of a thermally activated surface crossing from the emitting ^{3}MLCT state to a ^{3}MC (deactivating) state[33] These values predict that this compound is photolabile Similarly, the low activation energies and frequency factors obtained for the mononuclear complexes

Compound	E_a (cm^{-1})	A (s^{-1})
$[Ru(bpy)_2(bpzt)]^+$	1370	2 1 x 10^9
$[Os(bpy)_2(bpzt)]^+$	128	2 5 x 10^8
$[(Ru(bpy)_2)_2(bpzt)]^{3+}$	3735	9 9 x 10^{13}

Table 5 7

Activation energies (E_a) and prefactors (A) (± 10%) obtained for the bpzt$^-$ complexes in ethanol methanol (4 1)

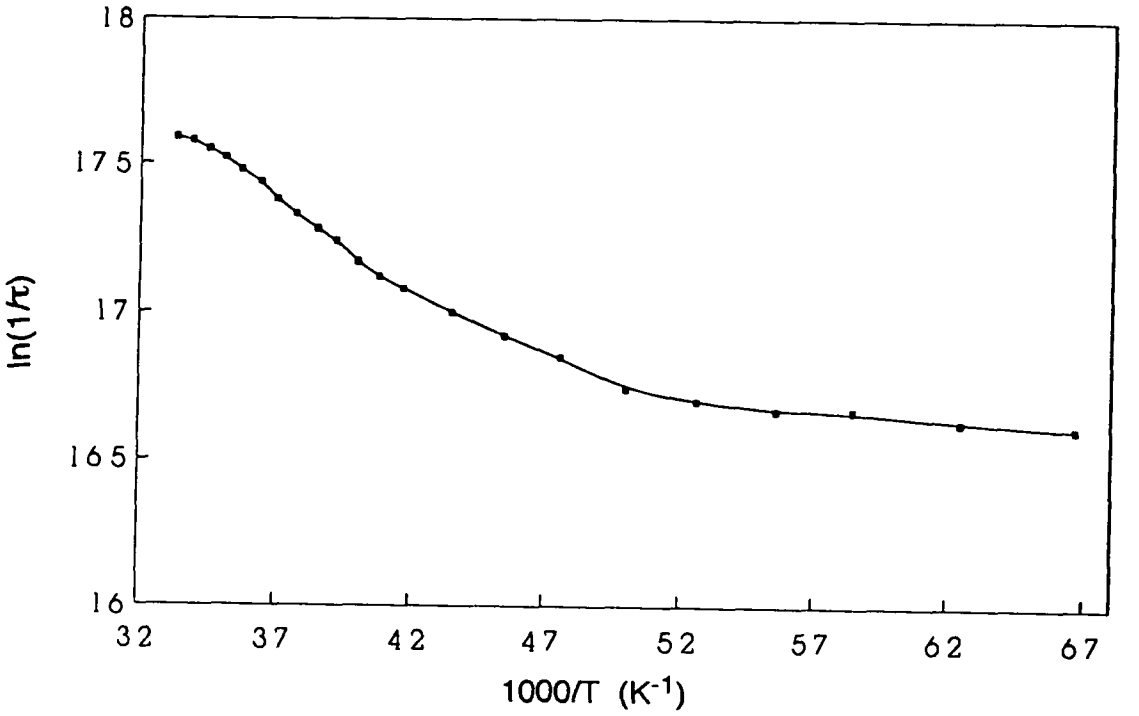

Figure 5 3 12

Plot of the ln(1/τ) versus 1/T for $[Os(bpy)_2(bpzt)]^+$ in ethanol methanol (4 1)

suggest that the ^{3}MC state cannot be populated in this temperature range, with the consequence that these complexes should be photostable In fact, irradiation of these complexes in CH_2Cl_2 containing Cl^- does not lead to any photodecomposition The ^{3}MLCT - ^{3}MC energy gap for the mononuclear complexes is expected to be larger than for the dinuclear complex, due to the stronger σ-donor ability of the mononucleating ligand

For $[Os(bpy)_3]^{2+}$, results of temperature dependent studies revealed that contributions to excited-state decay exist that occur from a series of low-lying Boltzmann-populated MLCT states[27] At the low end of the temperature range, population of a third state becomes important and plays an increasingly important role in determining excited-state properties as the temperature is increased At the high end of the temperature range, population of a fourth state probably accounts for the steady increase in the slope of $\ln(1/\tau)$ as the temperature increases[27] It was postulated that four low-lying MLCT states are needed to explain the temperature dependent properties of the excited state The three lowest lying states are quite close together in energy and are within 100 cm^{-1}, the fourth state for $[Os(bpy)_3]^{2+}$ lies approximately 600 cm^{-1} higher in energy[17] Usually, the ability to observe the fourth MLCT state for $[Ru(bpy)_3]^{2+}$ is masked by a surface-crossing process to low-lying dd (or ^{3}MC) states[82] In the osmium complexes, the presence of this state is evident from temperature dependent studies The slow rise in the $\ln(1/\tau)$ with increasing temperature above 200 K for $[Os(bpy)_2(bpzt)]^+$ suggests that some sort of deactivating process is occurring here, other than population of the ^{3}MC state Population of this fourth MLCT state, therefore, most likely accounts for the shortening of the lifetime of the complex at elevated temperatures The presence of a fourth MLCT state has also been suggested for Ru(II) polypyridine complexes and, therefore, this deactivating process could also

be occurring for $[Ru(bpy)_2(bpzt)]^{+}$ [83], since due to the absence of low-lying ^3MC excited states the presence of this MLCT state is not masked

The ϕ_{em} were found to decrease upon protonation of the mononuclear complexes and again when Ru(II) was replaced by Os(II) (see Table 5 6) The radiative (k_r) and non-radiative (k_{nr}) rate constants for these complexes are presented in Table 5 8, k_0 is the sum of the radiative and non-radiative rate constants

The non-radiative rate constant, k_{nr}, is a measure of the radiationless deactivation of the ^3MLCT states According to the energy gap law, k_{nr} decreases with increasing emission energy[34-35,84] This is clearly demonstrated by the osmium complexes which have the lowest emission energy of these species and an extremely short lifetime at room temperature The values of k_{nr} obtained for the ruthenium compounds are in close agreement with the value already obtained for $[Ru(bpy)_3]^{2+}$ [41]

A plot of $\ln(k_{nr})$ versus emission energy (E_{em}) is presented in Figure 5 3 13 Included in this plot are the values obtained for the bpt^- complexes A reasonable linear plot suggests that in these complexes, the energy-gap law is applicable[82-84] This implies that for a series of related excited states based on the same chromophoric unit, where variations in electronic coupling are not too large, radiationless decay rates are determined largely by the extent of vibrational overlap between the ground and excited states[34]

5 3 8 *Photochemical properties*

The photochemistry of the $bpzt^-$ complexes was investigated by irradiating the compounds in the following solvents, MeCN, MeCN containing 0 01 M Cl^- and

Compound	k_r (s^{-1})	k_{nr} (s^{-1})	k_0 (s^{-1})
$[Ru(bpy)_2(bpzt)]^+$	7 9 x 10^3	1 5 x 10^5	1 6 x 10^5
$[Ru(bpy)_2(Hbpzt)]^{2+}$	1 5 x 10^4	1 3 x 10^5	1 4 x 10^5
$[Os(bpy)_2(bpzt)]^+$	3 8 x 10^4	9 7 x 10^5	1 0 x 10^6
$[Ru(bpy)_2(Hbpzt)]^{2+}$	2 6 x 10^4	1 0 x 10^6	1 0 x 10^6
$[(Ru(bpy)_2)_2(bpzt)]^{3+}$	2 9 x 10^4	1 1 x 10^5	1 4 x 10^5
$[(Os(bpy)_2)_2(bpzt)]^{3+}$	7 6 x 10^3	3 5 x 10^6	x 10^3
$[Ru(bpy)_3]^{2+}$	8 0 x 10^4	1 3 x 10^5	2 1 x 10^4
$[Os(bpy)_3]^{2+}$	6 2 x 10^5	x 10^5	x 10^3

Table 5 8

Kinetic parameters (± 5%) obtained for the $bpzt^-$ complexes in ethanol methanol (4 1)

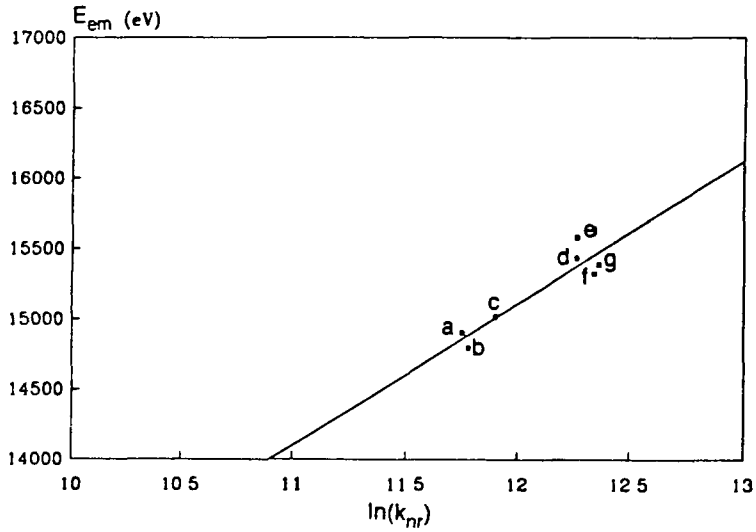

Figure 5 3 13

Plot of the $\ln(k_{nr})$ versus E_{em} for (a) $[(Ru(bpy)_2)_2(bpzt)]^{3+}$, (b) $[Ru(bpy)_2(Hbpzt)]^{2+}$, (c) $[Ru(bpy)_2(bpzt)]^+$, (d) $[(Ru(bpy)_2)_2(bpt)]^{3+}$, (e) $[Ru(bpy)_2(pztr)]^+$ isomer 1, (f) $[Ru(bpy)_2(pztr)]^+$ isomer 2, and (g) $[Ru(bpy)_2(bpt)]^+$

CH_2Cl_2 containing 0 005 M Cl^- The mononuclear complexes $[Ru(bpy)_2(bpzt)]^+$ and $[Os(bpy)_2(bpzt)]^+$ were found to be photostable, as expected from their temperature dependent luminescent lifetime measurements $[Ru(bpy)_2(Hbpzt)]^{2+}$ was found to be photolabile, and in chloride-containing solvents rupture of the Ru-N bond at the triazole ring occurs resulting in two main photoproducts which were identified as $[Ru(bpy)_2Cl_2]$ and free Hbpzt ligand The dinuclear $[(Os(bpy)_2)_2(bpzt)]^{3+}$ complex was also found to be photostable, as expected[17,85] The dinuclear $[(Ru(bpy)_2)_2(bpzt)]^{3+}$ species was photolabile This is the only compound which will be discussed in detail in this section The results obtained will be compared to those obtained for $[(Ru(bpy)_2)_2(bpt)]^{3+}$ in Chapter 6

Photochemistry in Acetonitrile

During the photolysis of $[(Ru(bpy)_2)_2(bpzt)]^{3+}$ in pure acetonitrile, UV/vis spectra taken at specified intervals show a decrease in the absorbance as the reaction proceeds (see Figure 5 3 14) The absorbance maximum shifts from 446 nm to 428 nm and a clear isosbestic point is maintained throughout the photolysis

In order to further investigate the photochemical process, HPLC analysis was carried out Figure 5 3 15 contains a typical set of traces obtained from the photolysis in MeCN From these traces, it can be seen that only two main photoproducts form These have been identified as follows Peak 1, retention time 5 28 min, λ_{max} 425 nm was identified as $[Ru(bpy)_2(MeCN)_2]^{2+}$ by comparison with an authentic sample Peak 2, retention time 10 88 min, λ_{max} 450 nm was identified as $[Ru(bpy)_2(bpzt)]^+$(the N1 isomer)

Taking into account the extinction coefficients of these two products at the monitoring wavelength of 280 nm, their ratios were approximately 1 1 These results are analogous to those obtained for the bpt^- dinuclear complexes, and it

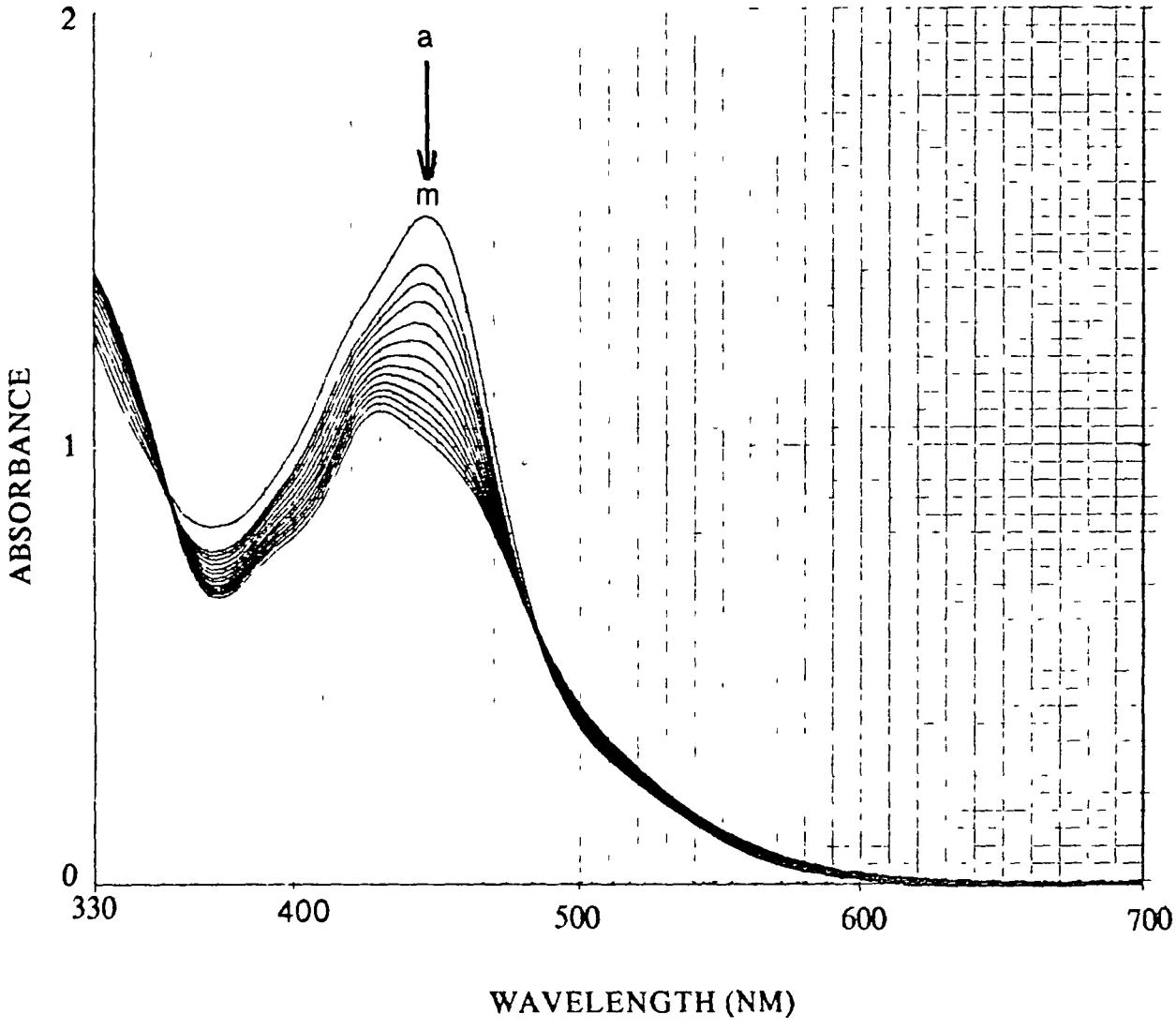

Figure 5 3 14

UV/vis spectra taken during the photolysis of $[(Ru(bpy)_2)_2(bpzt)]^{3+}$ in MeCN after (a) 0 min, (b) 10 min, (c) 15 min, (d) 22 min, (e) 29 min, (f) 36 min, (g) 43 min, (h) 50 min, (i) 59 min, (j) 68 min, (k) 80 min, (l) 95 min, and (m) 115 min

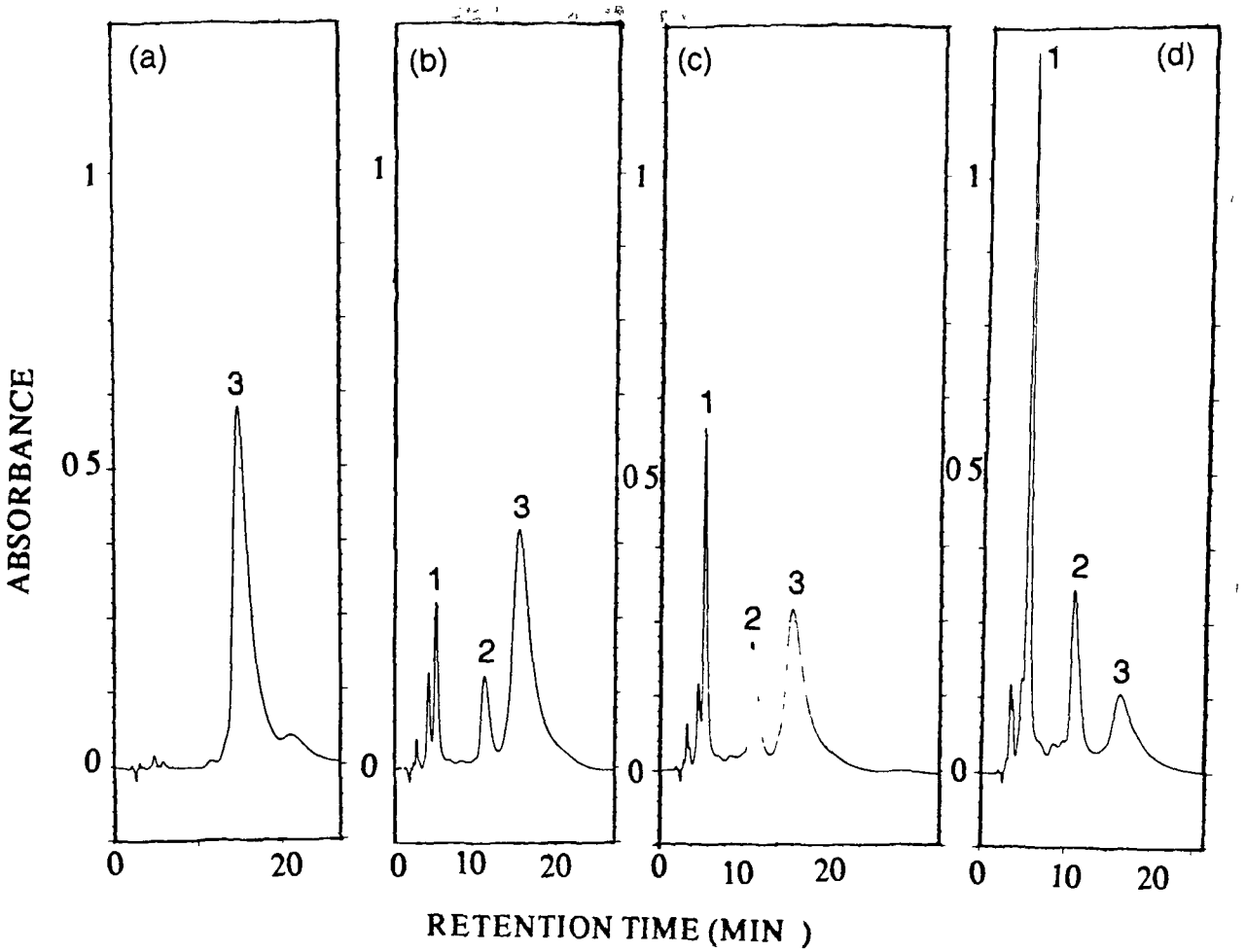

Figure 5 3 15

HPLC traces taken during the photolysis of $[(Ru(bpy)_2)_2(bpzt)]^{3+}$ in MeCN after (a) 0 min, (b) 80 min, (c) 145 min, and (d) 175 min Mobile phase 80 20 acetonitnle water containing 0 08 M LiCl Flowrate 1 5 cm^3 / min

was suggested that in this case, the different properties of the two nitrogen donor atoms (N1 versus N4) of the asymmetnc ligand govern the photochemical reactivity of these complexes Population of the ^3MC state occurs from the Ru-containing unit attached to the N4 position of the triazole ring for $[(Ru(bpy)_2)_2(bpt)]^{3+}$ (see Chapter 4 3 8) Similarly, irradiation of $[(Ru(bpy)_2)_2(bpzt)]^{3+}$ in MeCN results in population of a low-lying ^3MC state located on the N4 (or weaker σ-donor) site at the triazole nng, with subsequent photodecomposition of the complex occurring

Photochemistry in MeCN containing 0 01 M Cl^-

UV/vis spectra taken during the photolysis of $[(Ru(bpy)_2)_2(bpzt)]^{3+}$ in MeCN containing 0 01 M Cl^- (see Chapter 2) again resulted in a decrease in the absorbance at 447 nm, with a shift in the absorbance maximum to 452 nm Isosbestic points were maintained throughout the photolysis

HPLC traces were taken at specified intervals throughout the photolysis and are represented in Figure 5 3 16 Photolysis resulted in the simultaneous growth of four photoproducts which have been identified as follows Peak 1, retention time 2 3 min, λ_{max} 360 and 575 nm, was identified as $[Ru(bpy)_2Cl_2]$ Peak 2, retention time 5 2 min, λ_{max} 340 and 475 nm, was identified according to its UV/vis spectrum and by comparison with an authentic sample as $[Ru(bpy)_2(MeCN)Cl]^{2+}$ Peak 3, retention time 6 3 min, λ_{max} 425 nm was identified as $[Ru(bpy)_2(MeCN)_2]^{2+}$ and peak 4, retention time 8 64 min, λ_{max} 450 nm was identified as $[Ru(bpy)_2(bpzt)]^+$ (the N1 isomer) again by comparison with an authentic sample There was no evidence for the formation of any other isomer of the mononuclear species, as seen upon photolysis of $[(Ru(bpy)_2)_2(bpt)]^{3+}$ in MeCN containing 0 01 M Cl^-

Photochemistry in CH_2Cl_2 containing 0 005 M Cl^-

UV/vis spectra taken during the photolysis of $[(Ru(bpy)_2)_2(bpzt)]^{3+}$ in CH_2Cl_2 containing 0 005 M Cl^- (see Chapter 2) resulted in a decrease in the absorbance maximum at 450 nm, with a shift in the maximum to 452 nm A subsequent growth in two new peaks at 548 nm and 326 nm occurred Figure 5 3 17 shows the changes in the UV/vis spectra upon photolysis

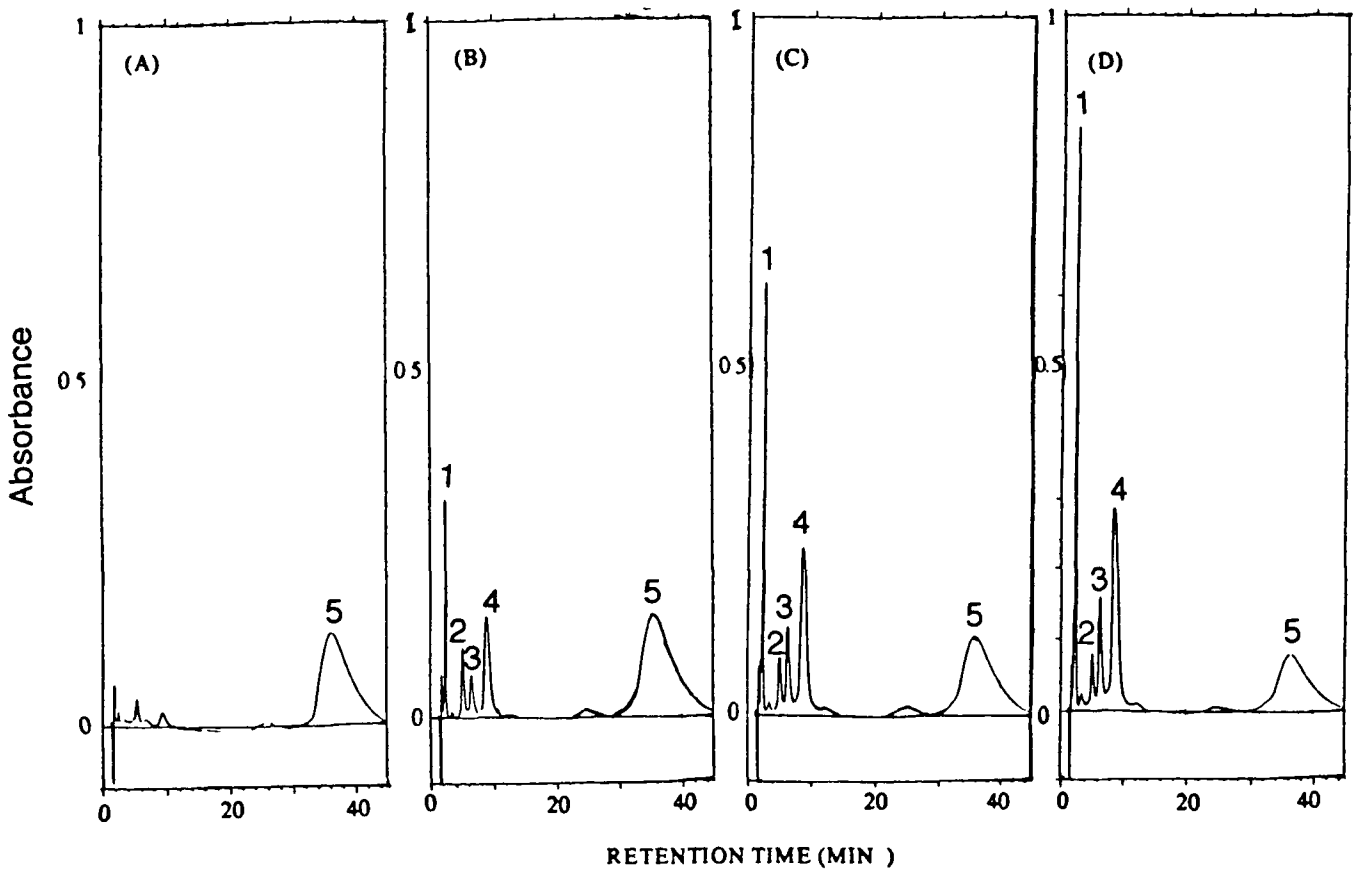

Figure 5 3 16

HPLC traces taken during the photolysis in MeCN containing 0 01 M Cl^- Photolysis times are (a) 0 min, (b) 30 min, (c) 90 min, and (d) 150 min Mobile phase 80 20 acetonitrile water containing 0 08 M LiCl Flowrate 1 0 cm^3/min

HPLC traces taken throughout the photolysis showed the formation of only two main photoproducts (see Figure 5 3 18) which have been identified as follows

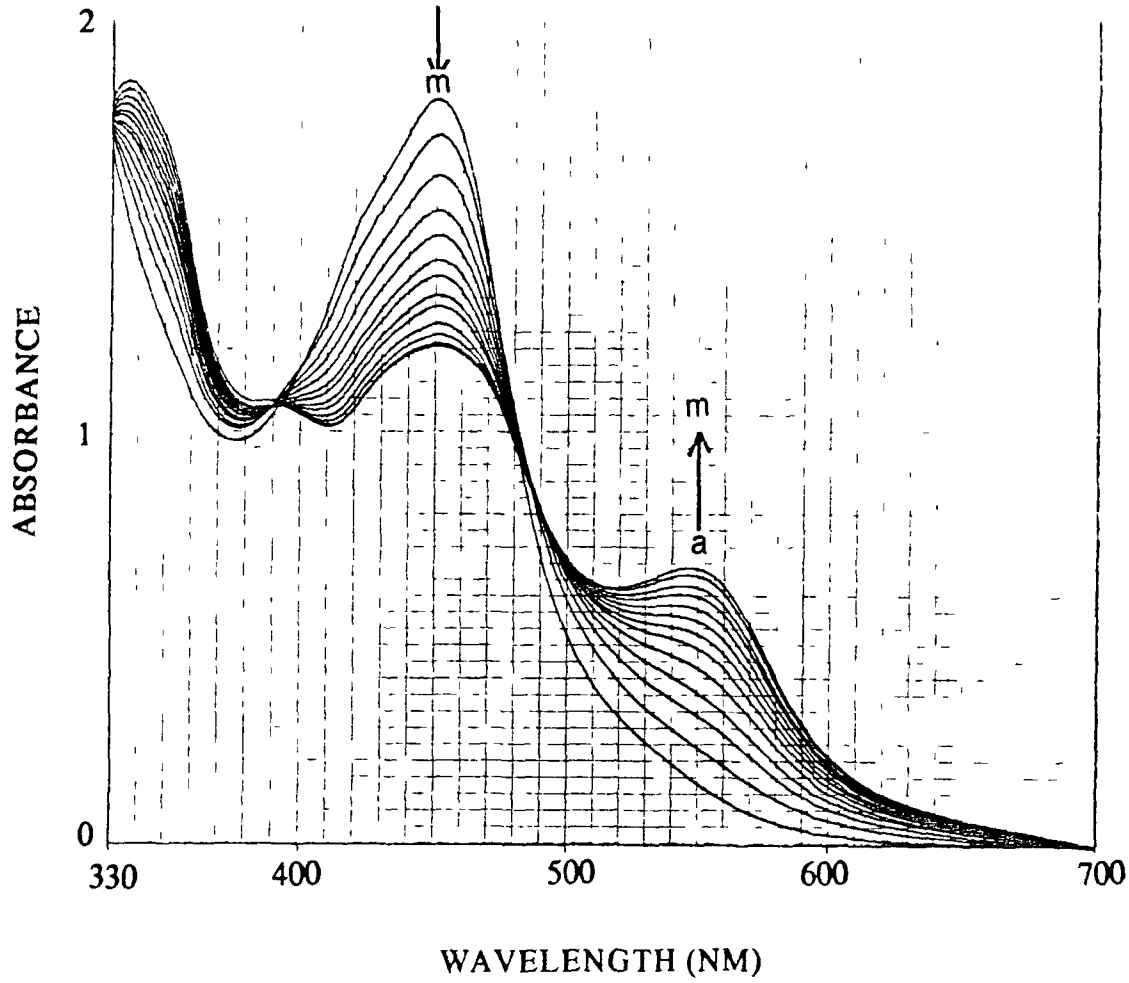

Figure 5 3 17

UV/vis spectra taken during the photolysis of $[(Ru(bpy)_2)_2(bpzt)]^{3+}$ in CH_2Cl_2 containing 0 005 M Cl^- Photolysis times are (a) 0 min, (b) 0 5 min, (c) 1 min, (d) 1 5 min, (e) 2 min, (f) 2 5 min, (g) 3 min, (h) 3 5 min, (i) 4 5 min, (j) 5 5 min, (k) 7 min, (l) 10 min, and (m) 15 min

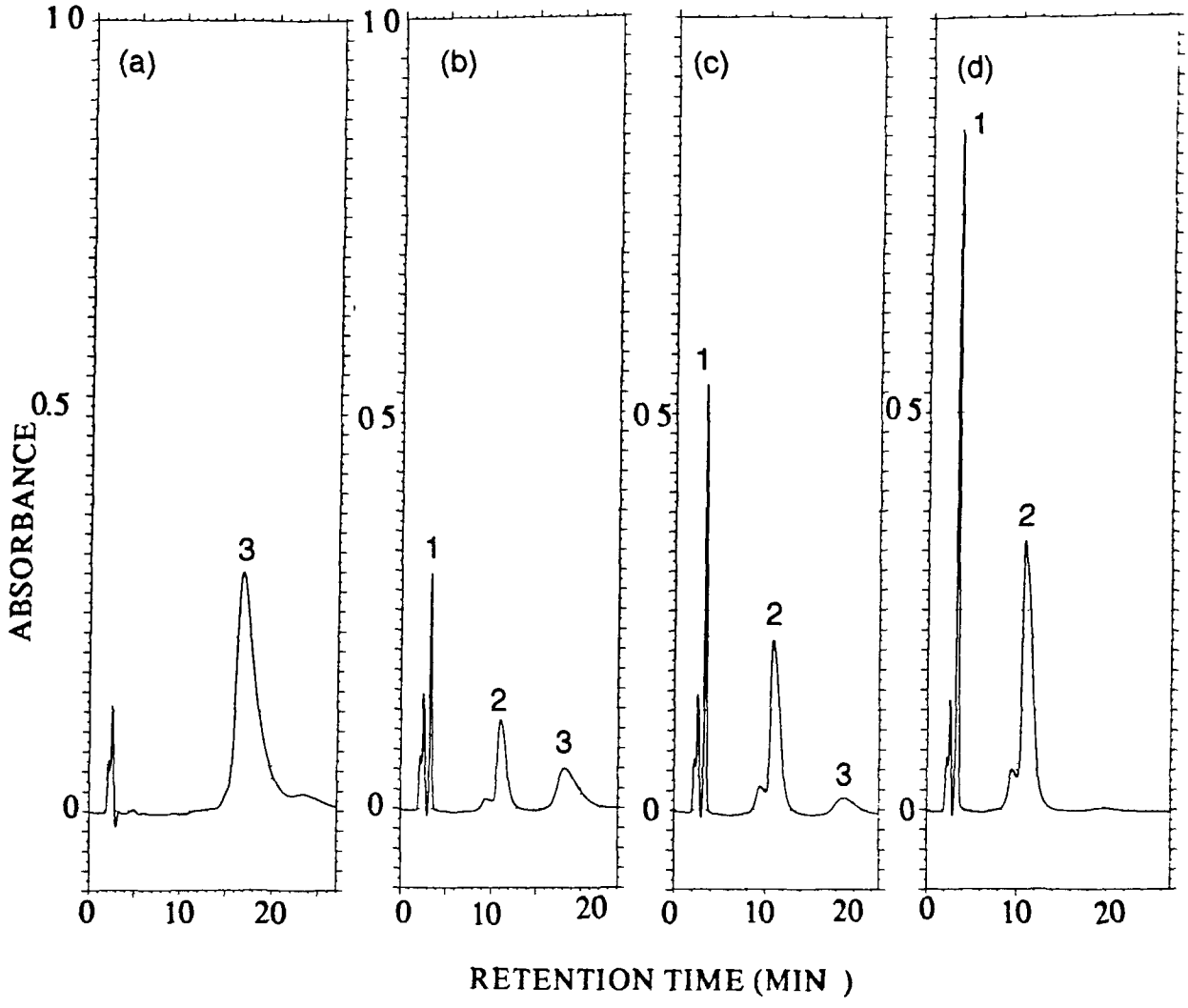

Figure 5 3 18

HPLC traces taken during the photolysis of $[(Ru(bpy)_2)_2(bpzt)]^{3+}$ in CH_2Cl_2 containing 0 005 M Cl^- Photolysis times are (a) 0 min, (b) 4 min, (c) 8 min, and (d) 17 min Mobile phase 60 40 acetonitrile water containing 0 06 M LiCl Flowrate 1 5 cm^3/min

Peak 1, retention time 3 4 min, λ_{max} 360 and 575 nm was identified as $[Ru(bpy)_2Cl_2]$ and peak 2, retention time 10 86 min, λ_{max} 450 nm was identified as $[Ru(bpy)_2(bpzt)]^+$ (the N1 isomer) Again, no evidence for the formation of the N4 isomer of $[Ru(bpy)_2(bpzt)]^+$ was present, unlike in the bpt^- dinuclear species

It appears that photolysis of $[(Ru(bpy)_2)_2(bpzt)]^{3+}$ in any of the solvents used results in preferential rupture of the Ru-N bond at the N4 site of the triazole ring. This supports the assumption that the N4 site is a weaker σ-donor than the N1 site[86]. It also suggests that the luminescent excited state (the lowest ^{3}MLCT excited state) and the photoactive excited state (the ^{3}MC excited state) are located on different Ru-containing units in the dinuclear $[(Ru(bpy)_2)_2(bpzt)]^{3+}$ species. Photodecomposition occurs exclusively from the ^{3}MC excited state located at the N4 site of the triazole ring.

An interesting observation is that photolysis of $[(Ru(bpy)_2)_2(bpt)]^{3+}$ in the presence of Cl^- ions results in photodecomposition occurring at both the N1 and N4 sites at the triazole ring. The results presented here suggest that the LUMO of the $[(Ru(bpy)_2)_2(bpzt)]^{3+}$ complex is lower than that of $[(Ru(bpy)_2)_2(bpt)]^{3+}$ (as expected from the electrochemical and emission measurements) resulting in a larger energy gap between the ^{3}MLCT and ^{3}MC excited states. Although this energy gap is not large enough to prevent photodecomposition occurring via the ^{3}MC deactivating pathway, it nevertheless causes an increase in the selectivity of this deactivation.

5.4 CONCLUSION

All of the performed measurements indicate that replacement of a pyridine by a pyrazine in a bridging ligand (i e upon going from Hbpt to Hbpzt) causes some interesting variations in the photochemical and photophysical properties of Ru(II) (and Os(II)) polypyridine complexes In agreement with the results obtained for $[Ru(bpy)_2(bpzt)]^+$, $[Os(bpy)_2(bpzt)]^+$ exhibits a Os ---> π^*(bpy) MLCT band for the absorbance and emission bands and the first reduction potential is therefore bpy-based However, upon protonation of the triazole ring or upon co-ordination of a second $Os(bpy)_2$ moiety, the level of the $\pi^*(bpzt^-)$ LUMO is lowered and now a $bpzt^-$-based first reduction potential is observed Also the lowest absorption and emission MLCT bands are now Os ----> π^*(bpzt) transitions This is very unusual for such complexes and to our knowledge is a unique property of the $bpzt^-$ system This ligand could be of interest for the design of tailor-made polynuclear complexes, in which the luminescent properties are conveniently located on either the bridge or on the auxiliary ligand

The photophysical properties of the $bpzt^-$ complexes are quite similar to those obtained for compounds containing the bpt^- bridging ligand Results of temperature dependent luminescent lifetime data, indicated that population of a ^3MC deactivating excited-state occurs for the $[(Ru(bpy)_2)_2(bpzt)]^{3+}$ dinuclear species, but not for the mononuclear ruthenium or osmium complexes In this system, replacement of a Ru(II) metal centre with an Os(II) metal centre leads to photostable products, but also to a significant reduction in the luminescent lifetime of the osmium species, in agreement with the energy-gap law and the results obtained for complexes containing the bridging bpt^- ligand

The photochemical properties indicate that as the dinuclear $[(Ru(bpy)_2)_2(bpzt)]^{3+}$ complex now has a $bpzt^-$-based LUMO, the energy gap

between the ^{3}MLCT and ^{3}MC excited states is larger than with bpt$^-$, with the result that due to the stronger σ-donor properties of the N1 site of the triazole ring, the ^{3}MC level of the Ru-containing unit at the N4 triazole atom is lowest in energy Therefore, photodecomposition occurs only from the N4 site The ^{3}MLCT and ^{3}MC excited states are localised on different Ru-containing units in the dinuclear system[87] Interestingly, for $[(Ru(bpy)_2)_2(bpt)]^{3+}$ photolysis in a chloride-containing solvent resulted in both the N1 and N4 sites being labilised This was not encountered for the bpzt$^-$ system The asymmetry of these ligands which contain two slightly different N-donor atoms allows the design of isomeric dinuclear species, each having different electrochemical and electronic properties

5.5 REFERENCES

1 F Barigelletti, L De Cola, V Balzani, R Hage, J G Haasnoot, J Reedijk, and J G Vos, *Inorg Chem*, **1991**, *30*, 641

2 R Hage, J G Haasnoot, H A Nieuwenhuis, J Reedijk, R Wang, and J G Vos, *J Chem Soc, Dalton Trans*, **1991**, 3271

3 C H Braunstein, A D Baker, T C Strekas, and H D Gafney, *Inorg Chem*, **1984**, *23*, 857

4 H E Toma, P S Santos, and A B P Lever, *Inorg Chem*, **1988**, *27*, 3850

5 G H Allen, R P White, D P Rillema, and T J Meyer, *J Am Chem Soc*, **1984**, *106*, 2613

6 G F Strousse, P A Anderson, J R Schoonover, T J Meyer, and F R Keene, *Inorg Chem*, **1992**, *31*, 3004

7 R J Crutchley and A B P Lever, *J Am Chem Soc*, **1980**, *102*, 7128

8 R J Crutchley and A B P Lever, *Inorg Chem*, **1982**, *21*, 2276

9 S Nishida, Y Harima, and K Yamashita, *Inorg Chem*, **1989**, *28*, 4073

10 N Kitamura, Y Kawanishi, and S Tazuke, *Chem Lett*, **1983**, 1185

11 K Shinozaki, Y Kaizu, H Hirai, and H Kobayashi, *Inorg Chem*, **1989**, *28*, 3675

12 H E Toma and A B P Lever, *Inorg Chem*, **1986**, *25*, 176.

13 H E Toma, P A Auburn, E S Dodsworth, M N Golovin, and A B P Lever, *Inorg Chem*, **1987**, *26*, 4257

14 R J Crutchley, A B P Lever, and A Poggi, *Inorg Chem*, **1983**, *22*, 2647

15 G Neshvad and M Z Hoffman, *J Phys Chem*, **1989**, *93*, 2445

16 E M Kober, J V Caspar, B P Sullivan, and T J Meyer, *Inorg Chem*, **1988**, *27*, 4587

17 E M Kober and T J Meyer, *Inorg Chem*, **1984**, *23*, 24, 3877

18 G M Bryant and J E Fergusson, *Aust J Chem*, **1971**, *24*, 441

19 M G Richmond, *J Organomet Chem*, **1991**, *404*, 213

20 J P Collin, S Guillerez, J P Sauvage, F Barigelletti, L DeCola, L Flamigni, and V Balzani, *Inorg Chem*, **1992**, *31*, 4112

21 O Monsted and G Nord, *Adv Inorg Chem*, **1991**, *37*, 381

22 M Haga, T Matsumura-Inoue, and S Yamabe, *Inorg Chem*, **1987**, *26*, 25, 4148

23 P A Lay, R H Magnuson, and H Taube, *Inorg Chem*, **1989**, *28*, 3001

24 G Denti, S Serroni, L Sabatino, M Ciano, V Ricevuto, and S Campagna, *Gazz Chim Ital*, **1991**, *121*, 37

25 T J Meyer, *Pure & Appl Chem*, **1986**, *58*, 9, 1193

26 T A Perkins, D B Pourreau, T L Netzel, and K S Schanze, *J Phys Chem*, **1989**, *93*, 4511

27 R S Lumpkin and T J Meyer, *J Phys Chem*, **1986**, *90*, 5307

28 M M Richter and K J Brewer, *Inorg Chem*, **1992**, *31*, 1594

29 D Pinnick and B Durham, *Inorg Chem*, **1984**, *23*, 1440

30 S Campagna, G Denti, L Sabatino, S Serroni, M Ciano, and V Balzani, *J Chem Soc, Chem Commun*, **1989**, 1500

31 A M Bond and M Haga, *Inorg Chem*, **1986**, *25*, 4507

32 T S Akasheh and Z M El-Ahmad, *Chem Phys Letts*, **1988**, *152*, 414

33 A Juris, V Balzani, F Barigelletti, S Campagna, P Belser, and A von Zelewsky, *Coord Chem Rev*, **1988**, *84*, 85

34 J V Caspar, B P Sullivan, E M Kober, and T J Meyer, *Chem Phys Letts*, **1982**, *91*, 2, 91

35 W J Vining, J V Caspar, and T J Meyer, *J Phys Chem*, **1985**, *89*, 1095

36 J V Caspar, E M Kober, B P Sullivan, and T J Meyer, *J Am Chem Soc*, **1982**, *104*, 630

37 E M Kober, B P Sullivan, W J Dressick, J V Caspar, and T J Meyer, *Inorg Chem*, **1980**, *102*, 7383

38 D A Buckingham, F P Dwyer, H A Goodwin, and A M Sargeson, *Aust J. Chem*, **1964**, *17*, 325

39 D E Richardson and H Taube, *J Am Chem Soc*, **1983**, *105*, 40

40 R Hage, J G Haasnoot, J Reedijk, R Wang, and J G Vos, *Inorg Chem*, **1991**, *30*, 3263

41 R Hage, Ph D Thesis, **1991**, Leiden University, The Netherlands

42 P A Lay, A M Sargeson, H Taube, M H Chou, and C Creutz, *Inorg Synth*, **1986**, *24*, John Wiley and Sons (Publishers)

43 R Hage, R A G de Graaff, J G Haasnoot, J P Turkenberg, J Reedijk, and J G Vos, *Acta Crystallogr, Sect C*, **1989**, *C45* 381

44 Y Ohsawa, M K DeArmond, K W Hanck, and C G Moreland, *J Am Chem Soc*, **1985**, *107*, 5383

45 J M de Wolf, R Hage, J G Haasnoot, J Reedijk, and J G Vos, *New J Chem*, **1991**, *15*, 501

46 R Hage, A H J Dijkhuis, J G Haasnoot, R Prins, J Reedijk, B E Buchanan, and J G Vos, *Inorg Chem*, **1988**, *27*, 2185

47 G A Crosby and W H Elfring, Jr, *J Phys Chem*, **1976**, *80*, 20, 2206

48 K R Barqawi, T S Akasheh, P C Beaumont, B J Parsons, and G O Phillips, *J Phys Chem*, **1988**, *92*, 291

49 D B MacQueen and J D Peterson, *Coord Chem Rev*, **1990**, *97*, 249

50 S Ernst and W Kaim, *J Am Chem Soc*, **1986**, *108*, 3578

51 L DeCola, F Barigelletti, V Balzani, R Hage, J G Haasnoot, J Reedijk, and J G Vos, *Chem Phys Letts*, **1991**, *178*, 5-6, 491

52 M Haga, T Ano, K Kano, and S Yamabe, *Inorg Chem*, **1991**, *30*, 3843

53 K Kalyanasundaram and Md K Nazeeruddin, *Chem Phys Letts*, **1989**, *158*, 45

54 D P Rillema and K B Mack, *Inorg Chem*, **1982**, *21*, 3849

55 R Hage, J G Haasnoot, J Reedijk, and J G Vos, *Chemtracts - Inorg. Chem*, **1992**, *4*, 75

56 M Haga, *Inorg Chim Acta*, **1983**, *75*, 29

57 J G Vos, *Polyhedron*, **1992**, *11*, 18, 2285

58 S D Ernst and W Kaim, *Inorg Chem*, **1989**, *28*, 1520

59 S Zhang and R E Shepherd, *Trans Met Chem*, **1992**, *17*, 199

60 C R Johnson and R E Shepherd, *Inorg Chem*, **1983**, *22*, 1117

61 R J Crutchley, N Kress, and A B P Lever, *J Am Chem Soc*, **1983**, *105*, 1170

62 C Creutz and M J Chou, *Inorg Chem*, **1987**, *26*, 2995

63 D W Pipes and T J Meyer, *Inorg Chem*, **1984**, *23*, 2466

64 K S Schanze, G A Neyhart, and T J Meyer, *J Phys Chem*, **1986**, *90*, 2182

65 G A Neyhart and T J Meyer, *Inorg Chem*, **1986**, *25*, 4807

66 L De Cola, M Ciano, F Barigelletti, M P Garcia, and L A Oro, *Inorg Chim Acta*, **1990**, *172*, 181

67 F Barigelletti, A Juris, V Balzani, P Belser, and A von Zelewsky, *J Phys Chem*, **1987**, *91*, 1095

68 P A Lay, R H Magnuson, and H Taube, *Inorg Chem*, **1988**, *27*, 2364

69 G Denti, S Campagna, L Sabatino, S Serroni, M Ciano, and V Balzani, *Inorg Chem*, **1990**, *29*, 4750

70 K Kalyanasundaram and Md K Nazeeruddin, *Inorg Chem*, **1990**, *29*, 10, 1888

71 H A Nieuwenhuis, J G Haasnoot, R Hage, J Reedijk, T L Snoeck, D J Stufkens, and J G Vos, *Inorg Chem*, **1991**, *30*, 48

72 Y Kawanishi, N Kitamura, and S Tazuke, *Inorg Chem*, **1989**, *28*, 2968

73 Y Kawanishi, N Kitamura, Y Kim, and S Tazuke, *Sci Papers I P C R.*, **1984**, *78*, 4, 212

74 N S Hush, *Prog Inorg Chem*, **1967**, *8*, 391

75 R A Marcus, *J Phys Chem*, **1963**, *67*, 853

76 N S Hush, *Trans Faraday Soc*, **1961**, *57*, 557

77 R W Callahan, F R Keene, T J Meyer, and D J Salmon, *J Am Chem Soc*, **1977**, *99*, 4, 1064

78 J T Hupp, *J Am Chem Soc*, **1990**, *112*, 1563

79 W F Wacholtz, R A Auerbach, and R S Schmehl, *Inorg Chem*, **1987**, *26*, 2989

80 R H Schmehl, R A Auerbach, and W F Wacholtz, *J Phys Chem*, **1988**, *92*, 6202

81 C Creutz, Prog *Inorg Chem*, **1983**, *30*, 1

82 J van Houten and R J Watts, *Inorg Chem*, **1978**, *17*, 12, 3381

83 J N Demas and G A Crosby, *J Am Chem Soc*, **1971**, *93*, 12, 2841

84 P Chen, R Duesing, D K Graff, and T J Meyer, *J Phys Chem*, **1991**, *95*, 5850

85 J M de Wolf, R Hage, J G Haasnoot, J Reedijk, and J G Vos, *New J Chem*, **1991**, *15*, 501

86 F Barigelletti, L De Cola, V Balzani, R Hage, J G Haasnoot, J Reedijk, and J G Vos, *Inorg Chem*, **1989**, *28*, 4344

CHAPTER 6

RUTHENIUM AND OSMIUM COMPLEXES WITH 3-(PYRAZIN-2-YL)-5-(PYRIDIN-2-YL)-1,2,4-TRIAZOLE

6.1 INTRODUCTION

It is well known that in the photosynthetic reaction centres of photosynthetic bacteria, photon absorption by chlorophyll (photosensitizer) causes a charge separation and then an intramolecular electron-transfer process, which ends up with the reduction of ubiquinone (electron acceptor) coupled with protonation [1-2] (see Chapter 1) In Ru(II) complexes, excitation leads to an electron being transferred from the Ru(II) moiety to the ligand-based π^* orbital [3-4] This might also be considered to be an intramolecular electron-transfer process

Artificial photochemical molecular devices (PMD's) based on ruthenium compounds have, therefore, attracted much attention due to the possibility of mimicking the natural photosynthetic process [5-8] They can be designed on the basis of (1) metal-containing building blocks that exhibit suitable ground- and excited-state properties, and (2) bridging ligands capable of linking the building blocks to form appropriate supramolecular structures [9-12] Intramolecular energy- and electron-transfer processes in dinuclear and oligonuclear complexes have, therefore, attracted increased attention due to their importance in the design of PMD's

Mixed-metal complexes have not been studied to a very large extent, due to the lack of convenient synthetic methods for their preparation and isolation [13-14] With the recent developments by Balzani et al using the "complexes-as ligands" and "complexes-as metals" strategy [15-17], it is now possible to produce heteronuclear complexes relatively easily The design of effective synthetic procedures to prepare systems having particular compositions and topologies represent a major advance in Ru(II)polypyridyl chemistry

Part of the interest in studying mixed-metal systems arises from a possible use of these materials to control photochemical processes in which optical

excitation is followed by spatially directed energy or electron transfer [18-20] Energy transfer can take place via a dipole-dipole interaction between an electronically excited donor and an acceptor in the ground state Alternatively, energy transfer takes place via an electron-exchange mechanism in which a spatial overlap of the donor and acceptor orbitals is required

Efficient energy transfer has already been noted for a number of mixed-metal systems For example, in heteronuclear complexes containing the bridging ligand bpt$^-$, efficient energy transfer takes place from the $Ru(bpy)_2$ moiety to the $Os(bpy)_2$ group, even though the bpt$^-$ ligand is not directly involved in the emission process [21] For mixed-metal ruthenium / rhodium complexes containing the same ligand, a Ru-based emission and a Rh-based photochemistry is observed when exciting at high energy [22-23] Again, excitation-energy transfer from co-ordinated Ru centres to a central iron bipyridyl complex occurs for complexes bridged by covalently linked 2,2'-bipyridine derivatives [24] The intramolecular energy transfer in this system is analogous to that observed in organic donor-acceptor complexes linked by an alkyl chain and is a good example of intramolecular energy transfer in inorganic systems having no ground-state electronic interaction between the donor and acceptor orbitals

As already discussed in Section 4 1, a large problem associated with the use of Ru(II)polypyridyl complexes as PMD's is their limited photostability due to population of low-lying ^{3}MC excited states [25-27] In order to isolate the ^{3}MC state (or the deactivating state) from the ^{3}MLCT excited state (or the state responsible for luminescence), it is necessary to increase the energy-gap between these two states as much as is possible [28-31] It is hoped that by the combination of the stronger σ-donor pyridyltriazole ring and the stronger π-accepting pyrazine ring in this ligand, sufficient perturbation of the ^{3}MC excited state will occur that will prevent its population Strong σ-donating ligands tend to increase the ^{3}MC energy

level, but the t_{2g} - ^{3}MLCT energy gap may decrease because of destabilisation of the t_{2g} energy level [32-34] These ligands act as spectator ligands and are not directly involved in the emission process Good π-accepting ligands may also serve to enlarge the ^{3}MLCT - ^{3}MC energy gap, but again the t_{2g} - ^{3}MLCT energy gap will be decreased [35-37] These ligands are expected to be directly involved in the electrochemical and emission processes by lowering the energy of the ^{3}MLCT level

In this chapter, the synthesis, characterisation, photochemical and photophysical properties of a series of mononuclear and dinuclear Ru(II) and Os(II)polypyridyl complexes containing the ligand 3-(pyrazin-2-yl)-5-(pyridin-2-yl)-1,2,4-triazole (Hppt) are reported (for structure see Figure 6 1 1) In addition to the homonuclear complexes, mixed-metal complexes containing the aforementioned ligand are also studied

It is of interest to examine the effect of increasing the asymmetry in this ligand (one co-ordination site is pyridine-based and the other co-ordination site is pyrazine-based) on the photophysical and photochemical properties of these complexes

The effect of the increased asymmetry on the metal-metal interaction across the bridge is also examined by studying the properties of the intervalence transition bands Intramolecular energy transfer in mixed-metal RuOs complexes is also studied The origin of the luminescence in these complexes is compared with that obtained for compounds containing the more symmetric (although still inequivalent due to the weaker σ-donor properties of the N4 site compared with the N1 position of the triazole ring) Hbpt and Hbpzt ligands In particular the nature of the LUMO is or interest since both bpy and pyrazine based emissions can be expected

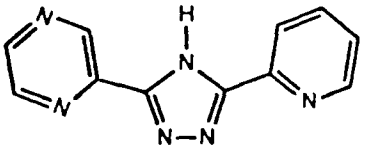

Hppt

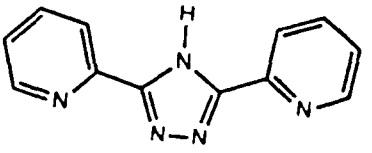

Hbpt

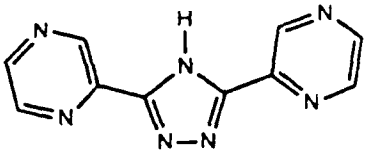

Hbpzt

Figure 6 1 1

Structure of the ligands 3-(pyrazin-2-yl)-5-(pyridin-2-yl)-1,2,4-triazole (Hppt), 3,5-bis-(pyridin-2-yl)-1,2,4-triazole (Hbpt) and 3,5-bis-(pyrazin-2-yl)-1,2,4-triazole (Hbpzt)

6 2 EXPERIMENTAL

Unless otherwise stated, all materials and solvents used were of commercial grade cis-$[Ru(bpy)_2Cl_2]$ $2H_2O$ was prepared as described in Section 3 2 cis-$[Os(bpy)_2Cl_2]$ $2H_2O$ was synthesised as described in Section 5 2

6 2 1 *Preparation of the ligand*

3-(pyridin-2-yl)-5-(pyrazin-2-yl)-1,2,4-triazole

15 g 2-pyrazylcarboxylic acid was dissolved in 50 cm^3 ethanol and 20 cm^3 concentrated H_2SO_4 and heated under reflux for 3 hours After neutralisation with sodium carbonate, an equimolar amount of hydrazine hydrate was added to the ester After leaving the reaction mixture at 0 °C for 3 hours, the hydrazide precipitated An equimolar amount of 5 g 2-cyanopyridine was dissolved in 20 cm^3 MeOH and was heated at reflux with 0 5 g Na for 3 hours to form the pyridylmethyl-imidate The isolated pyrazylhydrazide was added and the solution was heated for 15 minutes A yellow product appeared, which was heated to 250 °C and recrystallised from hot ethanol Yield 15 g (56%) M P 250 -252 °C ^1H NMR data $[(CD_3)_2(SO)]$ Pyrazine ring 9 35 (H^3, s), 8 72 (H^5 and H^6,m), Pyridine ring 8 20 (H^3,d), 8 03 (H^4,t), 7 56 (H^5,t), 8 79 (H^6, d)

6 2 2 *Preparation of the complexes*

$[Ru(bpy)_2(ppt)]PF_6$ $2H_2O$ **(1)**

This complex was prepared by adding 520 mg of cis-$[Ru(bpy)_2Cl_2]$ $2H_2O$ [38] (1 mmol) to 224 mg Hppt (1 mmol) in 50 cm^3 ethanol water (1 1 v/v), which was then heated under reflux for 6 hours The solution was evaporated to dryness and

the residue then dissolved in 10 cm^3 water and precipitated by addition of aqueous ammonium hexafluorophosphate The resulting complex was a mixture of two isomers, which were separated by semi-preparative HPLC Further purification took place by recrystallisation from acetone water (1 1 v/v) Isomer 1 was formed as a deprotonated species whereas isomer 2 was found in its protonated form Yield of combined fractions 0 84 g (90%) Found for $[Ru(bpy)_2(ppt)]PF_6\ 2H_2O$ (isomer 1) C, 45 7, H, 3 2 N, 17 0% Anal Calcd for $C_{31}H_{27}F_6N_{10}O_2PRu$ C, 45 5, H, 3 3, N, 17 1% Found for $[Ru(bpy)_2(Hppt)](PF_6)_2\ 2H_2O$ (isomer 2) C, 38 4, H, 2 7, N, 14 3% Anal Calcd for $C_{31}H_{27}F_{12}N_{10}O_2P_2Ru$ C, 38 7, H, 2 8, N, 14 6%

$[(Ru(bpy)_2)_2(ppt)](PF_6)_3\ 2H_2O$ (RuRu) Method A (**2**)

This compound was prepared as for (**1**), except that 0 57 g of $[Ru(bpy)_2Cl_2]\ 2H_2O$ (1 1 mmol) was added to a refluxing mixture of 0 11 g Hppt (0 5 mmol) in 50 cm^3 ethanol water (2 1 v/v) and heated for 8 hours After isolation as an PF_6 salt, the compound was purified by semi-preparative HPLC and by recrystallisation from acetone water (1 1 v/v) Yield after purification 0 6 g (82%) Found C, 40 3, H, 2 8, N, 12 6% Anal Calcd for $C_{51}H_{43}F_{18}N_{14}O_2P_3Ru_2$ C, 40 3, H, 2 8, N, 12 9%

$[(Ru(bpy)_2)_2(ppt)](PF_6)_3\ 2H_2O$ (RuRu) Method B

This complex was also prepared by an alternative method 220 mg of $[(Ru(bpy)_2(ppt)]PF_6\ 2H_2O$ (isomer 1 or isomer 2) (0 24 mmol) was heated under reflux with 140 mg (0 24 mmol) of $[Ru(bpy)_2Cl_2]\ 2H_2O$ in 50 cm^3 ethanol water (2 1 v/v) for 8 hr The complexes were isolated as PF_6 salts and purified by recrystallisation from acetone water (1 1 v/v) Yield after purification 360 mg (90 %) for isomer 1 and 320 mg (80 %) for isomer 2

$[Ru(bpy)_2(ppt)Os(bpy)_2](PF_6)_3\ H_2O\ 3C_3H_6O$ (isomer 1) (RuOs1) **(3)**

This complex was prepared as for (**1**), except that 110 mg of $[(Ru(bpy)_2(ppt)]PF_6\ 2H_2O$ (isomer 1) (0 12 mmol) was refluxed with 70 mg $[Os(bpy)_2Cl_2]\ 2H_2O$ [39] (0 12 mmol) for 8 hours in 50 cm^3 ethanol methanol (2 1 v/v) The complex was isolated by addition of aqueous NH_4PF_6 and purified by semi-preparative HPLC and by recrystallisation from acetone water (1 1 v/v) Yield after purification 60 mg (30%) Found C, 40 7, H, 3 1, N, 10 9% Anal Calcd for $C_{60}H_{59}F_{18}N_{14}O_4OsP_3Ru$ C, 40 8, H, 3 3, N, 11 1%

$[Ru(bpy)_2(ppt)Os(bpy)_2](PF_6)_3\ 2H_2O$ (isomer 2) (RuOs2) **(4)**

This compound was prepared as for (**3**), except that 110 mg of $[Ru(bpy)_2(ppt)](PF_6)_2\ 2H_2O$ (isomer 2) (0 12 mmol) was refluxed with 70 mg $[Os(bpy)_2Cl_2]\ 2H_2O$ (0 12 mmol) Similar purification procedures took place Yield after recrystallisation 60 mg (30%) Found C, 38 5, H, 2 6, N, 12 3% Anal Calcd for $C_{51}H_{43}F_{18}N_{14}OsO_2P_3Ru$ C, 38 0, H, 2 7, N, 12 2%

$[Os(bpy)_2(ppt)]PF_6\ 2H_2O$ **(5)**

This complex was prepared as for (**1**), except that 575 mg $[Os(bpy)_2Cl_2]\ 2H_2O$ (1 mmol) was added to a refluxing mixture of 223 mg Hppt (**1** mmol) for 2 days Again 2 isomers formed which were separated by semi-preparative HPLC and recrystallised from acetone water (1 1 v/v) Yield of combined fractions 0 82 g (78%) Found for $[Os(bpy)_2(ppt)]PF_6\ 2H_2O$ (isomer 1) C, 41 1, H, 2 8, N, 15 3% Anal Calcd for $C_{31}H_{27}F_6N_{10}O_2OsP$ C, 41 1, H, 3 0, N, 15 5% Found for $[Os(bpy)_2(Hppt)](PF_6)_2\ 2H_2O$ (isomer 2) C, 35 6, H, 2 6, N, 13 5% Anal Calcd for $C_{31}H_{27}F_{12}N_{10}O_2OsP_2$ C, 35 4, H, 2 6, N, 13 3%

$[(Os(bpy)_2)_2(ppt)](PF_6)_3\ 2H_2O\ 2C_3H_6O$ (OsOs) **(6)**

This complex was prepared as for compound (**2**) Method **A**, except that 1 mmol $[Os(bpy)_2Cl_2]\ 2H_2O$ (575 mg) was refluxed for 3 days with 0 5 mmol Hppt (112 mg) The complex was isolated and purified by semi-preparative HPLC Yield after purification 0 68 g (36%) Found C, 35 7, H, 3 1, N, 10 1% Anal Calcd for $C_{57}H_{55}F_{18}N_{14}O_4Os_2P_3$ C, 35 7, H, 3 1, N, 10 2%

6.3 RESULTS AND DISCUSSION

6 3 1 *^{1}H NMR spectroscopy*

Mononuclear compounds

The ^{1}H NMR resonances of the ppt$^-$ complexes and Hppt are presented in Table 6 1 For the mononuclear ruthenium and osmium complexes, two isomers are formed It is of utmost importance to verify the co-ordination mode of the ppt$^-$ ligands in these mononuclear species, as they are further used as starting materials to synthesise the mixed-metal complexes There are potentially four possible co-ordination modes for binding a $Ru(bpy)_2$ (or $Os(bpy)_2$) moiety to Hppt, i e via N1 of the triazole ring and the N of the pyrazine ring, via N4 of the triazole ring and the N of the pyrazine ring, via N2 of the triazole ring and the N of the pyridine ring and finally, via N4 of the triazole ring and the N of the pyridine ring

As seen previously and verified by X-ray structure analysis of $[Ru(bpy)_2(bpt)]^+$, in mononuclear compounds the bpt$^-$ ligand is bound via N1 of the triazole ring to the metal ion[40] Similarly, for $[Ru(bpy)_2(bpzt)]^+$ (see Chapter 5 3 1) the bpzt$^-$ ligand is bound via N1 of the triazole ring to the metal ion No evidence for binding via N4 of the triazole ring for any of the complexes is observed This is indeed expected from steric considerations It, therefore, seems reasonable to suggest that the two isomers produced using the ppt$^-$ ligand have the $Ru(bpy)_2$ (or $Os(bpy)_2$) unit co-ordinated via N1 of the triazole ring and the pyrazine ring and via N2 of the triazole ring and the pyridine ring This assumption has been verified using ^{1}H NMR spectroscopy Figure 6 3 1 contains the ^{1}H NMR spectra of the two isomers of $[Ru(bpy)_2(ppt)]^+$

For isomer 1, the H^6 proton of the pyridine ring, ring B, is considerably shifted upfield compared with the H^6 proton of the pyrazine ring, ring A This can

Compound		H^3	H^4	H^5	H^6
$[Ru(bpy)_2(ppt)]^+$ (1)	A	9 22 (-0 13) s	----	8 54 (-0 18) d	8 49 (-0 23) d
	Ring B	8 20 (0 00) d	7 95 (-0 08) m	7 20 (-0 36) m	7 94 (-0 85) d
$[Ru(bpy)_2(ppt)]^+$ (2)	A	9 32 (-0 03) s	----	7 68 (-1 04) d	8 34 (-0 38) d
	Ring B	8 18 (-0 02) d	7 59 (-0 44) m	8 06 (+0 50) m	8 49 (-0 30) d
$[Os(bpy)_2(ppt)]^+$ (1)	A	9 19 (-0 16) s	----	8 50 (-0 22) d	8 43 (-0 29) d
	Ring B	8 13 (-0 07) d	7 75 (-0 28) m	7 07 (-0 49) m	7 42 (-1 37) d
$[Os(bpy)_2(ppt)]^+$ (2)	A	9 25 (-0 10) s	----	7 64 (-1 08) d	8 13 (-0 59) d
	Ring B	8 46 (+0 26) d	7 31 (-0 72) m	7 75 (+0 19) m	8 53 (-0 26) d
RuRu	Ring A	9 11 (-0 24) d	----	7 40 (-1 32) d	8 28 (-0 44) d
	Ring B	6 69 (-1 51) d	7 08 (-0 95) m	7 97 (+0 41) m	8 38 (-0 41) d
OsOs	Ring A	8 97 (-0 38) d	----	7 73 (-0 99) d	8 29 (-0 43) d
	Ring B	6 53 (-1 67) d	7 03 (-1 00) m	6 89 (-0 67) m	8 32 (-0 47) d
RuOs1	Ring A	9 05 (-0 30) d	----	7 41 (-1 31) d	8 38 (-0 34) d
	Ring B	6 82 (-1 38) d	7 03 (-1 00) m	7 95 (+0 39) m	8 37 (-0 42) d
RuOs2	Ring A	9 10 (-0 25) d	----	7 39 (-1 33) d	8 04 (-0 68) d
	Ring B	6 85 (-1 35) d	7 08 (-0 95) m	7 97 (+0 41) m	8 37 (-0 42) d
Hppt	Ring A	9 35 (s)	----	8 72 (d)	8 72 (d)
	Ring B	8 20 (d)	8 03 (t)	7 56 (t)	8 79 (d)

Table 6 1

400 MHz ^1H NMR resonances observed for the complexes containing the ppt$^-$ ligand in CD_3CN Hppt was measured in deuterated DMSO Values in parenthesis are the chemical shifts compared with the free ligand (s = singlet, d = doublet, t = triplet and m = multiplet)

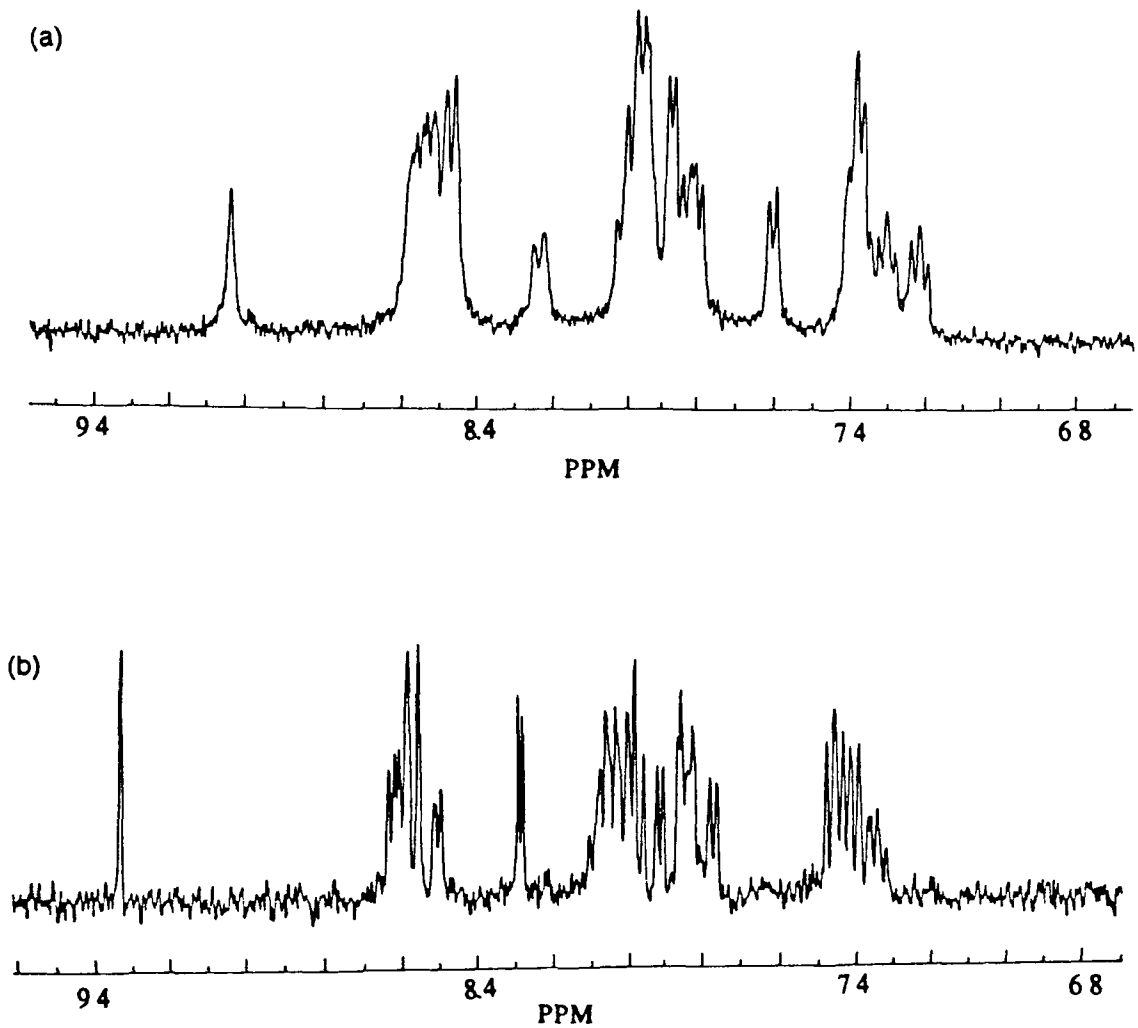

Figure 6 3 1

400 MHz ^1H NMR spectra of (a) isomer 1 and (b) isomer 2 of $[Ru(bpy)_2(ppt)]^+$ in CD_3CN

be explained by the fact that the H^6 proton feels the ring current of an adjacent bpy ligand when co-ordinated to $Ru(bpy)_2^{2+}$ (or $Os(bpy)_2$) A general upfield shift is observed for all the protons of the ppt$^-$ ligand, because of the proximity of the negatively charged triazole ring causing more electron density to be present at the pyridine and pyrazine rings compared with the free ligand Assignment of the H^5, H^4 and H^3 protons of these rings are now straightforward, using 2-dimensional COSY techniques The main conclusion for these observations is that the structure of isomer 1 of the ruthenium and osmium mononuclear complexes are similar and that in both cases co-ordination is taking place via N2 of the triazole ring and via the N of the pyridine ring The pyrazine ring is in this case uncoordinated

For isomer 2, it is suggested that co-ordination is taking place via N1 of the triazole ring and via the pyrazine ring Comparing the chemical shifts of the pyrazine ring, ring A, with those obtained for $[Ru(bpy)_2(bpzt)]^+$ (see Chapter 5 3 1), we see the same large upfield shift of the H^5 proton of the co-ordinated pyrazine ring This shielding must be caused by an adjacent bpy ring[41] Using 2-dimensional COSY techniques it is then possible to assign the other protons of the pyrazine ring The resonances for the free pyridine ring show a small shift upfield of the protons due to the influence of the deprotonated triazole ring The H^5 proton on this ring is slightly shifted downfield Again similarities in the ^1H NMR resonances for the second isomer of the ruthenium and osmium mononuclear complexes show that they are both co-ordinated in a similar manner

What is interesting to note is that the osmium mononuclear complexes are shifted more upfield that the corresponding ruthenium mononuclear complexes This has been noted before[42-44], and was attributed to the increasing L <---- M π-bonding as ruthenium is replaced by osmium The π-bond is considered to affect the ring protons in the same way as an electron donating substituent on the ring

Dinuclear compounds

The ^{1}H NMR resonances of the dinuclear ppt$^-$ complexes are also presented in Table 6 1 Figure 6 3 2 contains the ^{1}H and COSY NMR spectrum of the dinuclear $[(Ru(bpy)_2)_2(ppt)]^{3+}$ complex This compound can have three different isomers The $Ru(bpy)_2$ moieties can be co-ordinated via N1 of the triazole ring and the pyrazine ring and via N4 of the triazole ring and the pyridine ring, via N1 of the triazole ring and the pyrazine ring and via N2 of the triazole ring and the pyridine ring, and finally, via N4 of the triazole ring and the pyrazine ring and via N2 of the triazole ring and the pyridine ring

H^3 of the pyridine ring and H^5 of the pyrazine ring are both shifted considerably upfield due to the magnetic anisotrophic effect of adjacent bpy rings[45-47] Due to the complexity of the ^{1}H NMR spectra, however, unequivocal evidence as to which co-ordination isomer is present in this complex is not obtained In order to ascertain the binding sites at the triazole ring, two different synthetic procedures were carried out to make the dinuclear species (see Section 6 2) A comparison of the ^{1}H NMR resonances obtained for the dinuclear complexes prepared by using the mononuclear complexes as starting materials with those of the dinuclear species prepared by reacting Hppt with two Ru equivalents gave the following conclusions, when the pyrazine-bound monomer (isomer 2) was used as a starting material in the synthesis of the dinuclear species, a ^{1}H NMR spectrum was obtained that exactly matched that of the original dinuclear species However, when the pyridine bound monomer (isomer 1) was used as the starting material, the ^{1}H NMR spectrum which resulted showed considerably differences when compared to the ^{1}H NMR spectrum of the original dinuclear species (see Figures 6 3 2 and 6 3 3)

Examination of the ^{1}H NMR resonances and comparison with the resonances observed for $[(Ru(bpy)_2)_2(bpt)]^{3+}$, suggest that the co-ordination mode

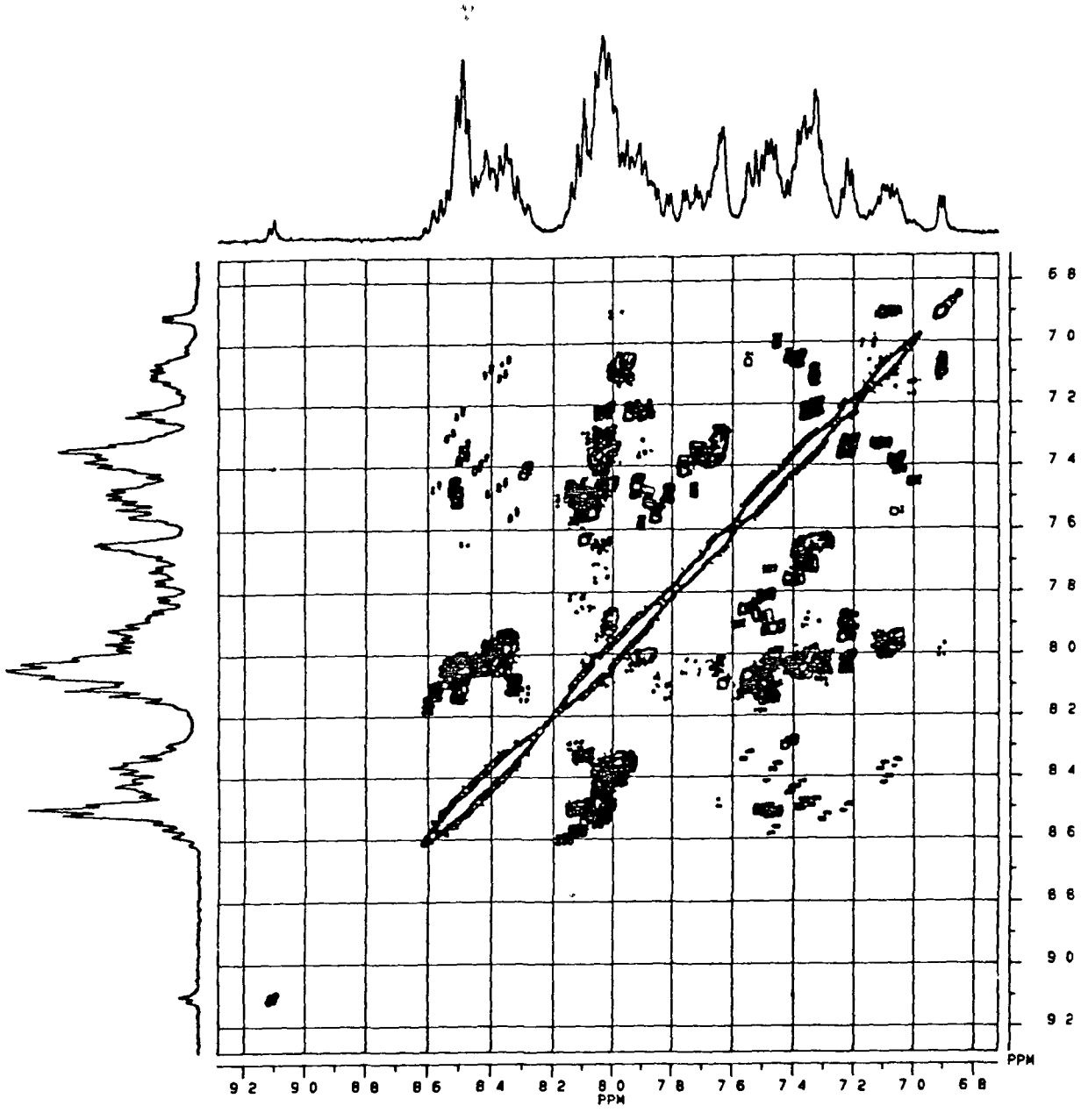

Figure 6 3 2

400 MHz ^1H and COSY NMR spectrum of $[(Ru(bpy)_2)_2(ppt)]^{3+}$ in CD_3CN as prepared from reacting Hppt with two equivalents of $[Ru(bpy)_2Cl_2]$

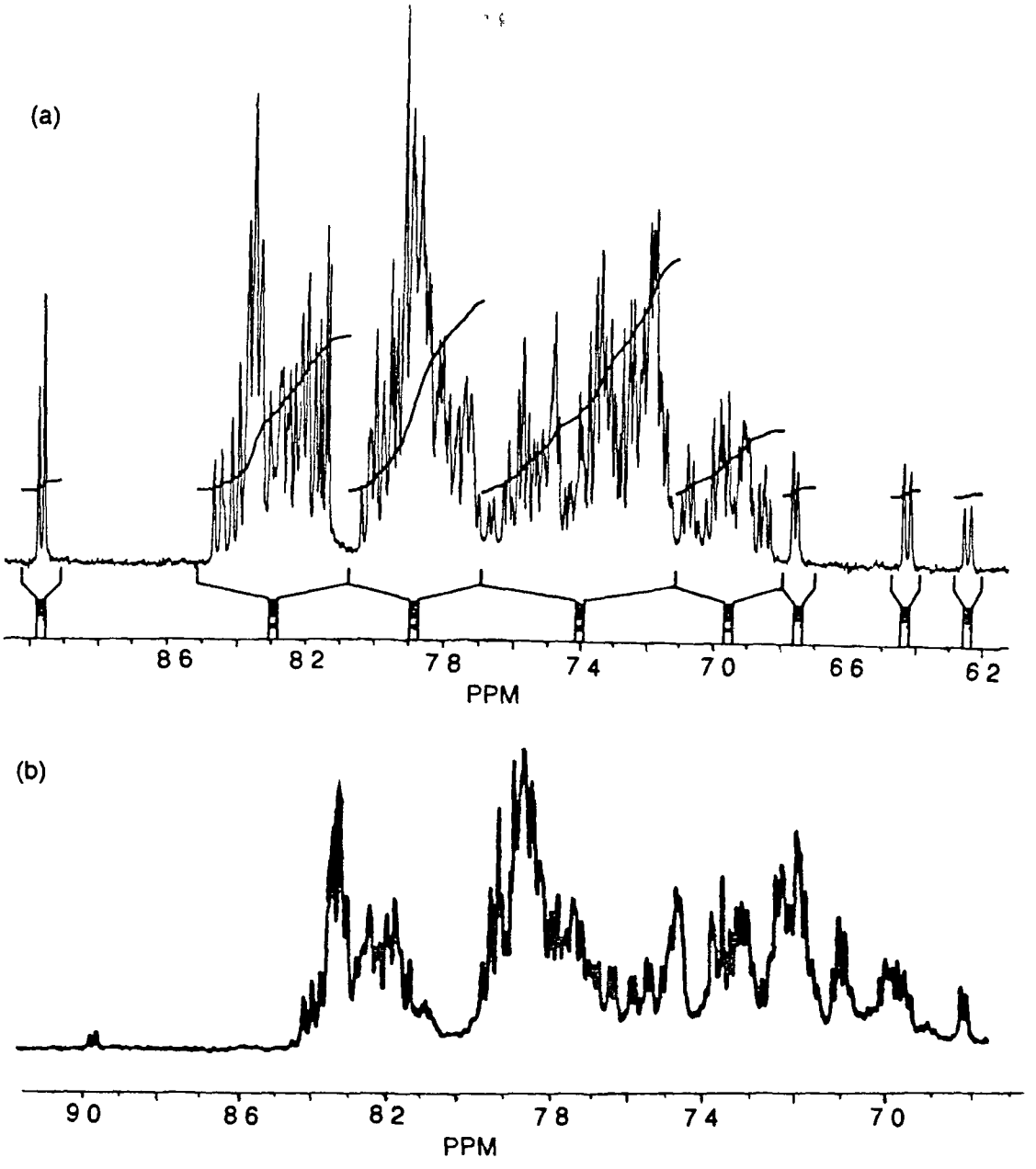

Figure 6 3 3

Comparison of the 400 MHz ^1H NMR spectra of $[(Ru(bpy)_2)_2(ppt)]^{3+}$ in CD_3CN prepared from (a) the pyridine-bound mononuclear complex, isomer 1 and (b) the pyrazine-bound mononuclear complex, isomer 2

of ring B is very similar in both cases, H^3 of ring B is now observed at much lower field This proton does not feel the ring current of an adjacent pyridine ring and is not effected by magnetic anisotropy from bpy ligands This proton is a doublet in the spectra of the dinuclear species, indicating that long range coupling with H^5 must be occurring for this proton The H^6 proton is shifted more upfield than that of ring A, due to the presence of the negatively charged ppt^- ligand and the short intramolecular distance between the H^6 proton and a bpy ligand Therefore, it can be concluded that co-ordination in the dinuclear complexes takes place via N1 of the triazole ring and the pyrazine ring and via N4 of the triazole ring and the pyridine ring

According to the similarities in both spectra, it is also reasonable to assume that the same sort of co-ordination is taking place for the dinuclear $[(Os(bpy)_2)_2(ppt)]^{3+}$ complex Again, larger upfield shifts are observed for the osmium dinuclear species compared with the ruthenium complex

The mixed-metal complexes were prepared according to Scheme 6 1 Differences exist in the chemical shifts observed for both complexes (see Figure 6 3 4) due to their different co-ordination modes at the triazole ring, albeit the differences are quite small In fact, comparing the ^1H NMR spectra of all four dinuclear species, only minor differences exist in the chemical shifts of all the complexes This has already been encountered for the mixed-metal complexes containing the bpt^- ligand[48] The resonances of the H^5 proton at 7 40 ppm is similar for RuRu and both RuOs complexes, but is replaced by a resonance at 7 73 ppm for the OsOs species This phenonomen was seen previously[49] for mixed-metal complexes It appears that this proton is particularly sensitive to the effect of an adjacent metal group Only one geometrical isomer was evident from the ^1H NMR spectra of all these dinuclear species According to the synthetic procedure, isomer 1 contains a $Ru(bpy)_2$ unit co-ordinated to the N2 site of the

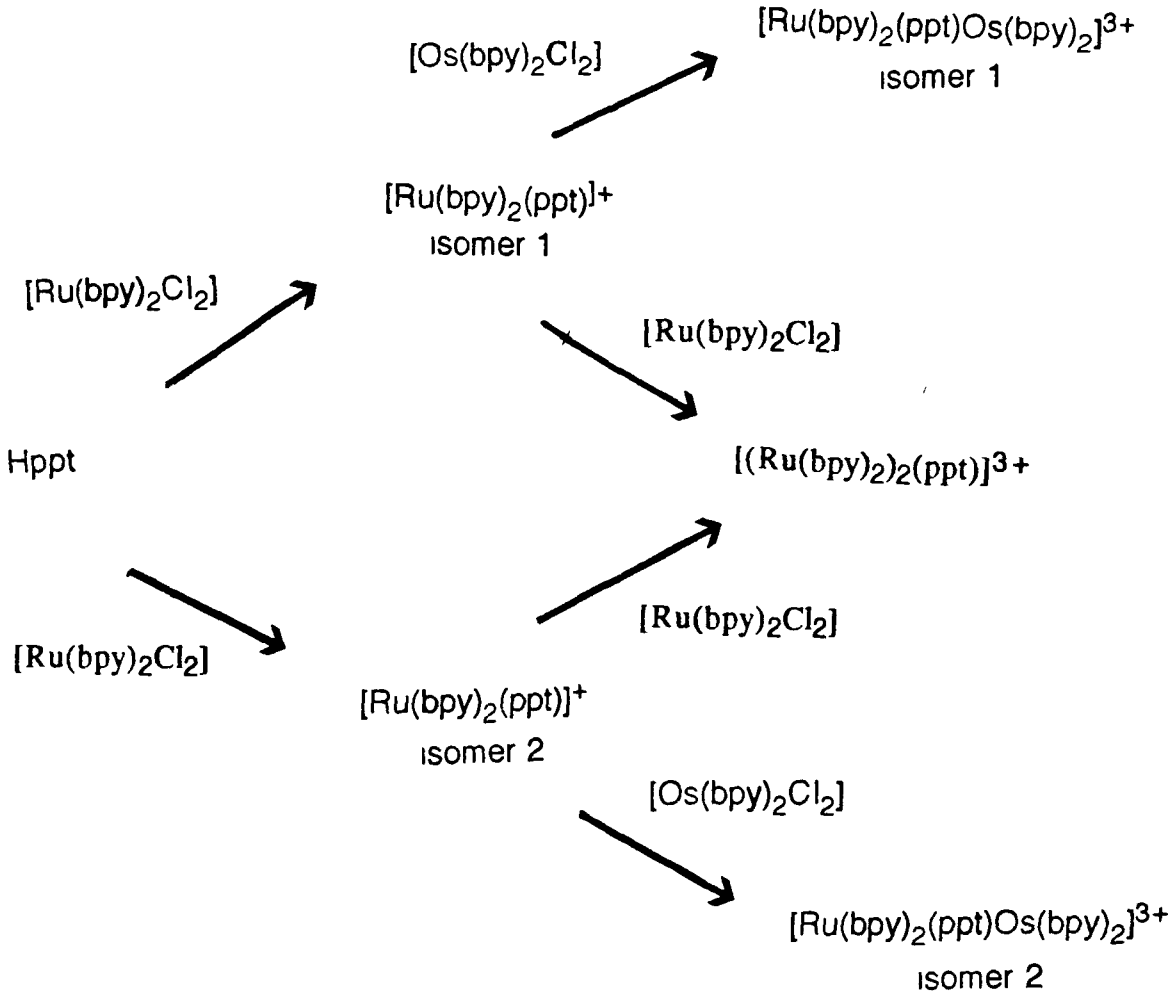

Scheme 6 1

Synthetic method for the preparation of the mixed-metal dinuclear complexes RuOs1 and RuOs2

tnazole ring and to the pyridine ring and an $Os(bpy)_2$ unit attached to the N4 site of the triazole ring and to the pyrazine ring Isomer 2, on the other hand, contains a $Ru(bpy)_2$ co-ordinated to the N1 site of the triazole ring and to the pyrazine ring, whereas the $Os(bpy)_2$ unit is attached to the N4 site of the triazole ring and the

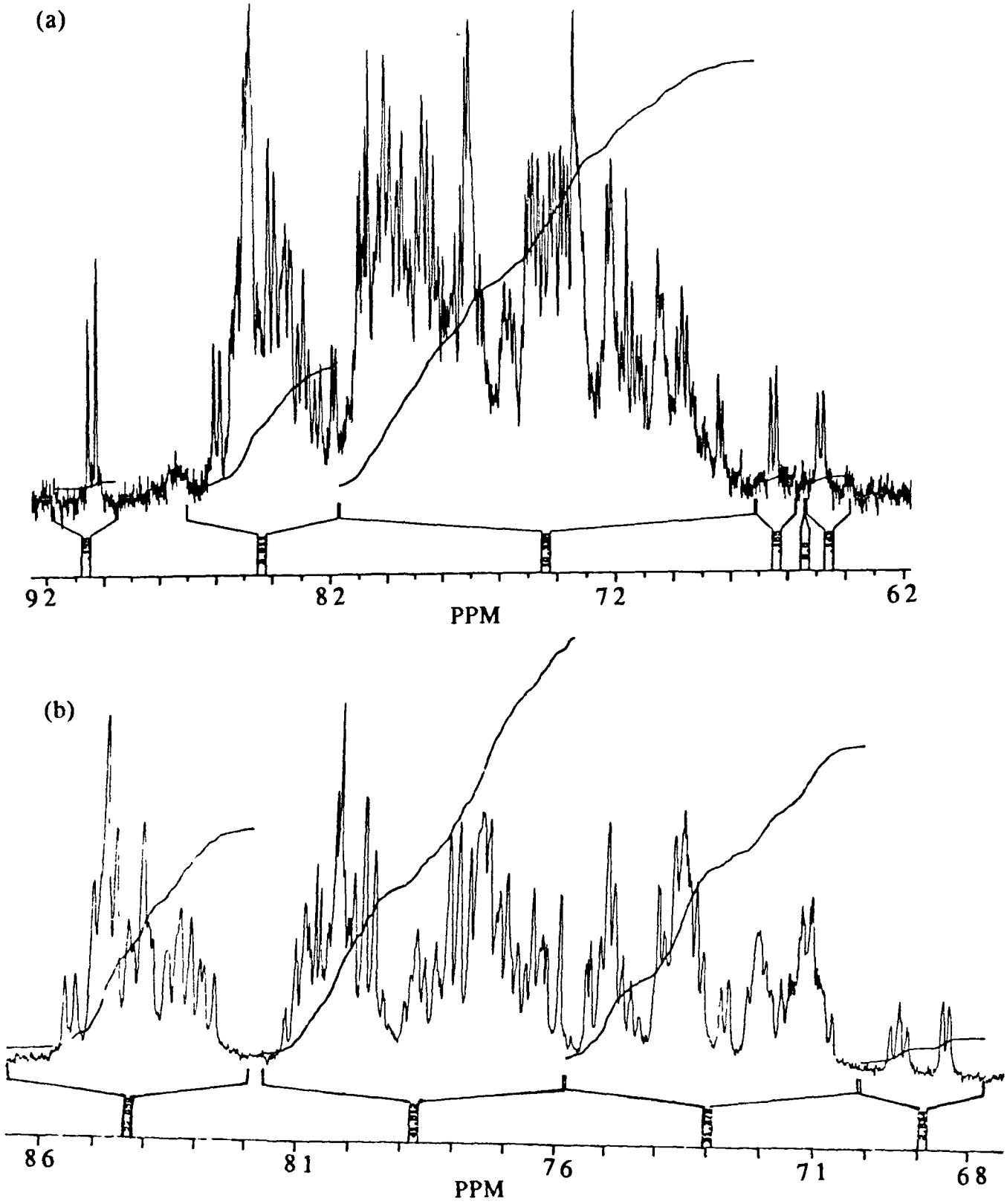

Figure 6 3 4

400 MHz ^{1}H NMR spectra of (a) isomer 1 (RuOs1) and (b) isomer 2 (RuOs2) of $[Ru(bpy)_2(ppt)Os(bpy)_2]^{3+}$ in CD_3CN

pyridine ring

6 3 2 *Absorption and Emission properties*

Table 6 2 contains the absorption and emission maxima of the ppt$^-$ complexes and their luminescent lifetimes at room temperature and at 77 K All the complexes exhibit the usual dπ-π^* (bpy) metal-to-ligand charge-transfer bands in the visible region between 350 and 500 nm characteristic of Ru(polypyridyl) complexes[49-52] Emission occurs from ^{3}MLCT excited states[53-54] Protonation of the complexes causes a shift to higher energy of the MLCT bands, because of the decreased σ-donor capacity of the protonated ligands resulting in a stabilisation of the d-orbitals[55-57] A shift to higher energy of the MLCT band is also evident on going from $[Ru(bpy)_2(ppt)]^+$ isomer 1 to isomer 2 (and again in the osmium mononuclear species) due to the better π-acceptor capabilities of the pyrazine ring compared with the pyridine ring (see Chapter 5 3 2) Very little difference exists between the absorption and emission maxima of the two mixed-metal species (except for the room temperature emission maximum) again agreeing with the small differences in the ^{1}H NMR data At lower energies, some additional bands are visible for the compounds containing osmium These bands have been observed before for other osmium complexes and have been assigned as forbidden transitions to triplet states[58] At higher energies, i e in the UV region, very intense bands are present for all complexes which have been assigned as π-π^* transitions[59-60]

A feature of these complexes is that replacement of a ruthenium-containing unit by an osmium-containing unit causes a shift to lower energy of the MLCT absorption and emission bands This has been observed for other osmium

Compound	Absorption (log ε) (nm)	Emission (τ) (nm) 298 K	Emission (τ) (nm) 77K
$[Ru(bpy)_2(ppt)]^+$ (1)	475 (4 04)	676 (0 22)	612 (6 33)
$[Ru(bpy)_2(Hppt)]^{2+}$ (1)	440	612 (0 007)	581 (3 72)
$[Ru(bpy)_2(ppt)]^+$ (2)	438 (4 35)	657 (0 14)	602 (6 60)
$[Ru(bpy)_2(Hppt)]^{2+}$ (2)	425	670 (0 014)	612 (6 18)
$[Os(bpy)_2(ppt)]^+$ (1)	385 (3 95) 446 (3 74) 498 (3 82) 620	730 (0 045)	743 (0 37)
$[Os(bpy)_2(Hppt)]^{2+}$ (1)	392 432 470 600	701 (0 025)	706 (0 26)
$[Os(bpy)_2(ppt)]^+$ (2)	408 (4 04) 432 (4 07) 474 (4 11) 610	759 (0 043)	723 (0 88)
$[Os(bpy)_2(Hppt)]^{2+}$ (2)	408 450 600	739 (0 027)	719 (0 31)
RuRu	453 (4 35)	675 (0 22)	607 (5 25)
OsOs	395 (4 30) 440 (4 34) 475 (4 36)	776 (0 047)	730 (0 73)
RuOs1	450 (4 51) 600	725 (0 075)	706 (0 89)
RuOs2	452 (4 43) 600	765 (0 10)	719 (0 76)

Table 6 2

Absorption, emission data and luminescent lifetime measurements for the ppt$^-$ complexes [a]Acetonitrile, [b]Ethanol Lifetimes values ± 0 01 μs

systems and is caused by the higher energy of the Os 5d orbitals compared with the Ru 4d orbitals[61-62] The dinuclear $[(Ru(bpy)_2)_2(ppt)]^{3+}$ complex exhibits a shift to higher energy compared with the mononuclear $[Ru(bpy)_2(ppt)]^+$ isomer 1 and a shift to lower energy compared with isomer 2 For $[(Ru(bpy)_2)_2(bpt)]^{3+}$, a shift to higher energy was observed which was explained by the fact that upon co-ordination of the second $Ru(bpy)_2$ unit to the bpt^- ligand, the negative charge on the triazolate anion is now shared between two metal centres This results in a decreased electron density on the metal centre causing a blue shift of the MLCT band

For $[(Ru(bpy)_2)_2(bpzt)]^{3+}$, very little shift in the absorbance or emission maxima at 77 K was observed upon going from a mononuclear to a dinuclear species, most likely because the blue shift caused by the sharing of the negative charge of the triazole ring is counteracted by a red shift of the MLCT band caused by a switch-over from a bpy-based LUMO to a $bpzt^-$-based LUMO[21] For $[(Ru(bpy)_2)_2(ppt)]^{3+}$, co-ordination of the second metal centre, causes a shift to higher energy of the MLCT band compared with isomer 1 consistent with the weaker σ-donor properties of the ligand due to the negative charge now being shared between two $Ru(bpy)_2$ units However, the π^* level of the ppt^- ligand must also be lowered as in the $bpzt^-$ case, as a shift to lower energy compared with isomer 2 is observed The nature of the emitting state in dinuclear complexes containing the ppt^- ligand will be investigated further by examination of its electrochemical properties and by using resonance Raman spectroscopy The mixed-metal complexes exhibit very similar absorption and emission properties Emission in these compounds appears to be osmium-based No evidence for any emission from the ruthenium-containing unit is found

6 3 3 *Acid-Base properties*

The changes in the absorption spectrum of $[Ru(bpy)_2(ppt)]^+$ isomer 1 and isomer 2 upon lowering the pH are presented in Figure 6 3 5 We know that isomer 1 is the pyridine-bound isomer and we therefore expect a pK_a of ca 4 0, by comparison with the similar $[Ru(bpy)_2(bpt)]^+$ species As isomer 2 is the pyrazine-bound isomer, it is reasonable to suggest a pK_a of ca 2 2 for this species by comparison with $[Ru(bpy)_2(bpzt)]^+$ A shift in the λ_{max} from 436 nm to 424 nm is observed for isomer 1, whereas a shift from 444 nm to 450 nm is observed for isomer 2 This small shift in the λ_{max} upon (de)protonation of the triazole ring for the latter species has already been observed for $[Ru(bpy)_2(bpzt)]^+$ $[Ru(bpy)_2(ppt)]^+$ isomer 2, therefore, exhibits similar behaviour to a mononuclear complex containing the $bpzt^-$ ligand, whereas isomer 1 exhibits behaviour similar to that of a complex containing the bpt^- ligand The resulting dinuclear complex contains contributions from both the pyridine and pyrazine rings and therefore an intermediate behaviour is observed in its MLCT energies

Table 6 3 lists the pK_a data As can be seen from the results presented here, $[Ru(bpy)_2(ppt)]^+$ isomer 1 exhibits a pK_a value of 2 7 Isomer 2, on the other hand, yields a pK_a value of 3 8 Again in the case of $[Os(bpy)_2(ppt)]^+$, isomer 1 has a pK_a of 2 1, whereas the pK_a of isomer 2 is 3 5 In fact, these results are exactly opposite to those expected for these complexes in comparison to the data obtained for the bpt^- and $bpzt^-$ mononuclear complexes

The excited-state pK_a^* values were also examined and are tabulated in Table 6 3 pH_i values represent the point of inflection of the emission titration curve As these values do not represent real pK_a^* values, pK_a^* has been calculated using equations 4 1 and 4 2 For isomer 1 of both monomeric species, the acidity of the excited state is increased with respect to the ground state

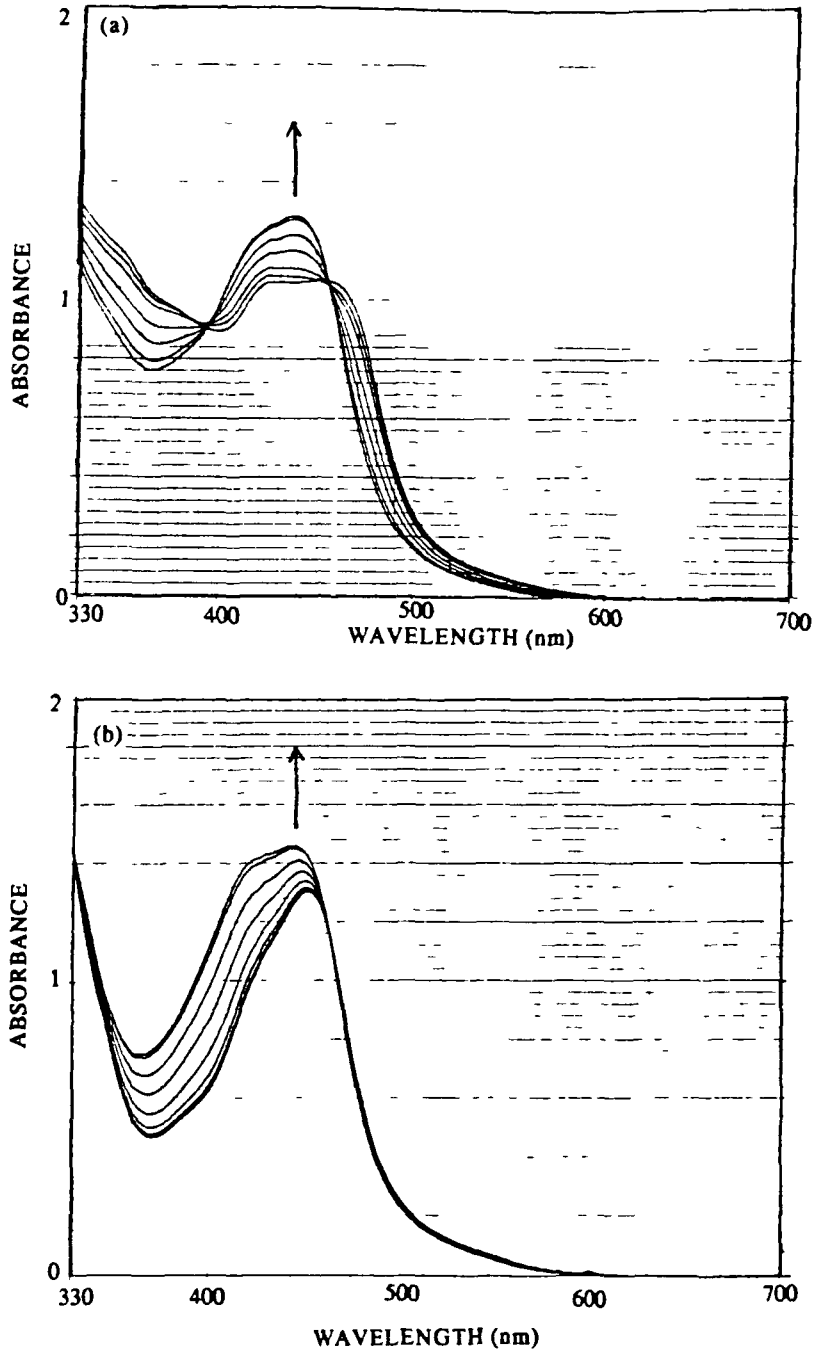

Figure 6 3 5

The absorption spectrum in Britton-Robinson buffer of (a) isomer 1 and (b) isomer 2 of $[Ru(bpy)_2(ppt)]^+$ as a function of pH The pH was varied from 1 62 to 5 88 by addition of 3 M NaOH

Compound	pK_a	pH_I	$pK_a^*(1)$	$pK_a^*(2)$
$[Ru(bpy)_2(ppt)]^+$ (1)	2 7	1 7	0 3	1 0
$[Ru(bpy)_2(ppt)]^+$ (2)	3 8	2 5	1 8	4 0
$[Os(bpy)_2(ppt)]^+$ (1)	2 1	1 3	1 1	1 5
$[Os(bpy)_2(ppt)]^+$ (2)	3 5	3 0	2 9	3 5
$[Ru(bpy)_2(bpt)]^+$	4 2	3 9	3 3	3 7
$[Os(bpy)_2(bpt)]^+$	4 0	----	----	----
$[Ru(bpy)_2(bpzt)]^+$	2 0	4 9	3 8	2 8
$[Os(bpy)_2(bpzt)]^+$	1 2	2 3	1 6	1 3

Table 6 3

Ground state pK_a and excited state pK_a^* values of the mononuclear ppt^- complexes and some related compounds $pK_a^*(1)$ and $pK_a^*(2)$ were calculated using equations 4 1 and 4 2 respectively All measurements are carried out in Britton-Robinson buffer All values ± 0 1

and therefore the ligand involved in the acid-base process is not directly involved in the emission process[63-65] This is a reasonable conclusion, as we already know that the complex $[Ru(bpy)_2(bpt)]^+$, in which the $Ru(bpy)_2$ unit is also bound to a pyridine ligand, the LUMO is situation on the bpy ligands and the bridging bpt^- ligand acts solely as a spectator ligand

For the second isomer of both complexes, the excited-state acidity is very similar (if not slightly increased for $[Ru(bpy)_2(ppt)]^+$ isomer 2) to the ground-state acidity The similarity of the ground state and excited state acidity in complexes containing the similar ligand Hpztr (where Hpztr = 3-(pyrazin-2-yl)-1,2,4-triazole) has been explained by a change in the nature of the emitting state upon

protonation[66] The lowest MLCT state is based on the pyrazine ligand when the triazole ring is protonated and based on the bpy when deprotonated[67] Therefore, for $[Ru(bpy)_2(ppt)]^+$ isomer 2, a switch-over from a bpy-based luminescence to a pyrazine-based luminescence may be observed upon protonation of the triazole ring Furthermore, the relatively small increase of the $pK_a^*(2)$ value compared with the ground-state value suggests that while the excited electron is clearly located on the ppt^- ligand when protonated, the major part of the electron density is present in the pyrazine ring

The ground-state pK_a values of 2 7 and 3 8 for $[Ru(bpy)_2(ppt)]^+$ isomer 1 and isomer 2 respectively, suggest that isomer 1 (or the pyridine bound isomer) is a weaker σ-donor than isomer 2 (or the pyrazine bound isomer)[68-70] In general, ligands with high pK_a values are strong σ-donor ligands and weak π-accepting ligands[71] However, it has already been shown that pyrazyltriazole ligands are weaker σ-donor ligands than their pyridyltriazole analogues[67] Therefore H-bonding between the triazole ring and the free pyrazine ring must be occurring for isomer 1, thus causing the pK_a to be influenced by the weaker σ-donor properties of the pyrazine ring and causing a drop of the pK_a to 2 7 Similarly, for isomer 2, H-bonding between the triazole ring and the free pyridine ring causes the pK_a to increase dramatically

A second pK_a value has been obtained for isomer 2 of both mononuclear species This is very direct evidence for the fact that isomer 2 is co-ordinated to the pyrazine ring, since free pyrazine is only protonated at much more acidic values No second pK_a was observed for isomer 1 in the pH range 2 0 to -1 5 A typical pK_a absorption titration at low pH's is presented in Figure 6 3 6 for $[Ru(bpy)_2(Hppt)]^{2+}$ isomer 2 This type of behaviour has been observed previously for $[Ru(bpy)_2(Hbpzt)]^{2+}$ and was attributed to (de)protonation of the pyrazine ring. Therefore the (de)protonation steps for this complex (and its osmium analogue)

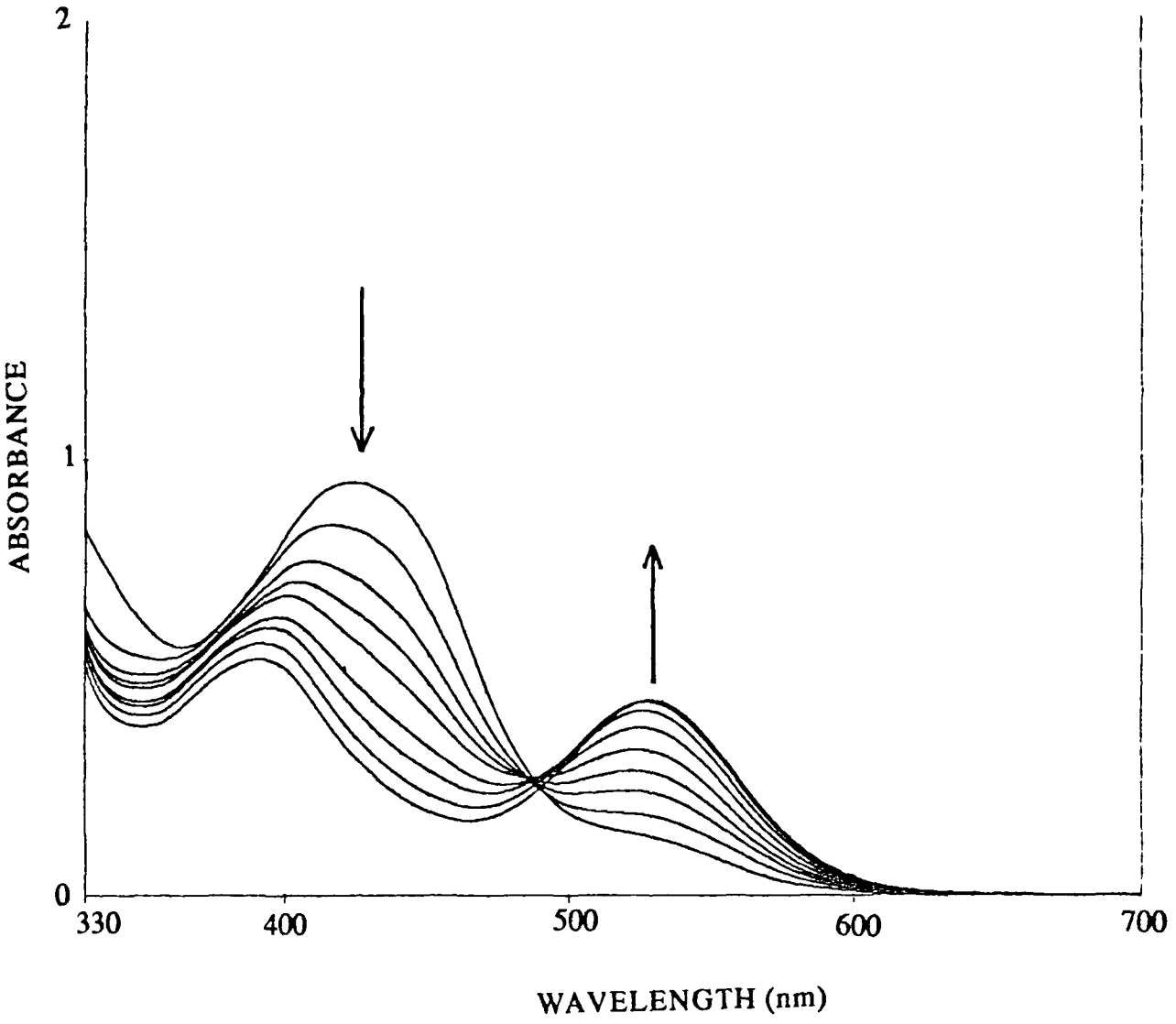

Figure 6 3 6

Changes in the absorption spectrum in acetonitrile upon changing the pH by addition of concentrated H_2SO_4 for $[Ru(bpy)_2(Hppt)]^{2+}$ isomer 2 in the pH range 2 0 to -1 5 pH units

are as follows

$$[Ru(bpy)_2(H_2ppt)]^{3+} \overset{pK_a(1)}{\rightleftharpoons} [Ru(bpy)_2(Hppt)]^{2+} \overset{pK_a(2)}{\rightleftharpoons} [Ru(bpy)_2(ppt)]^{+}$$

Values of -1 5 and -1 4 were calculated for isomer 2 of $[Ru(bpy)_2(Hppt)]^{2+}$ and $[Os(bpy)_2(Hppt)]^{2+}$ respectively

6 3 4 *Electrochemical properties*

Mononuclear compounds

Table 6 4 contains the electrochemical potentials obtained for all the ppt$^-$ complexes As can be seen from the data, isomers 2 of both mononuclear species have a metal-based oxidation at a higher potential than the analogous isomer 1 This is due to the weaker σ-donor properties of the pyrazine ligand, less electron density is present on the metal and therefore it is harder to oxidise[72-73]

The reduction potentials observed for the mononuclear deprotonated complexes are most likely bpy-based[74-75] Unfortunately, it was not possible to obtain satisfactory reduction potentials of the protonated complexes due to hydrogen formation in acidic solutions

The oxidation potentials of the osmium complexes are approximately 400 mV lower than those of the corresponding ruthenium complexes This is normal behaviour for these types of systems and is attributed to the higher energy of the 5d orbitals compared to the 4d orbitals[76-77]

Dinuclear compounds

Each dinuclear complex exhibits two reversible metal-based oxidation

Compound	Oxidation Pot (V)	Reduction Pot. (V)
$[Ru(bpy)_2(ppt)]^+$ (1)	0 94	-1 47 -1 71
$[Ru(bpy)_2(Hppt)]^{2+}$ (1)	1 27	(----)
$[Ru(bpy)_2(ppt)]^+$ (2)	1 03	-1 51 -1 74
$[Ru(bpy)_2(Hppt)]^{2+}$ (2)	1 18	(----)
$[Os(bpy)_2(ppt)]^+$ (1)	0 52	-1 42 -1 69
$[Os(bpy)_2(Hppt)]^{2+}$ (1)	0 80	(----)
$[Os(bpy)_2(ppt)]^+$ (2)	0 63	-1 44 -1 72
$[Os(bpy)_2(Hppt)]^{2+}$ (2)	0 77	(----)
RuRu	1 16 1 43	-1 22 -1 45 -1 66
OsOs	0 68 0 93	-1 21 -1 39 -1 62
RuOs1	0 83 1 21	-1 22 -1 43 -1 69
RuOs2	0 73 1 28	-1 25 -1 45 -1 60

Table 6 4

Electrochemical potential (DPP) of the mononuclear and dinuclear ppt⁻ ligands at a scanrate of 10 mV/sec All measurements carried out in acetonitrile containing 0 1 M TEAP Protonation by addition of concentrated H_2SO_4

processes A difference of 270 mV exists for the oxidation potentials of the RuRu species, whereas the difference is 250 mV for the OsOs system The similarities in the value obtained for the difference in oxidation potentials of both the RuRu and OsOs dinuclear species further substantiate the assumption that the co-ordination environment of these two species is the same

Part of the large difference in oxidation potentials observed for these complexes may be caused by the different co-ordination environments of the two metal centres The two mixed-metal species RuOs1 and RuOs2 may, therefore, yield information regarding the different co-ordination sites of the bridging triazole ligand and indeed differences are observed

In the RuOs1 dinuclear compound, the Os ion is bound to N4 of the triazole ring and pyrazine is oxidised first at 0 83 V, whilst the Ru ion bound via N2 of the triazole ring and pyridine is oxidised at 1 21 V In the RuOs2 complex, the Os ion bound via N4 of the triazole ring and pyridine is oxidised at a lower potential (0 73 V *versus* SCE), whilst that of the Ru ion bound via N1 of the triazole ring and pyrazine is oxidised at a higher potential (1 28 V) than for the RuOs1 complex This can be rationalised as follows In RuOs1, the $Ru(bpy)_2$ moiety is co-ordination via the stronger σ-donating pyridine ring, which causes a shift to lower potential of the oxidation, the $Os(bpy)_2$ moiety is co-ordinated via the weaker σ-donating and stronger π-accepting pyrazine ring, which reduces the electron density present on the metal centre, thus making it more difficult to oxidise and hence a higher oxidation potential results Similarly, for RuOs2, the $Ru(bpy)_2$ unit is co-ordinated via the stronger π-accepting pyrazine ring, causing a shift to higher oxidation potential compared with RuOs1, whereas the $Os(bpy)_2$ moiety is co-ordinated via the stronger σ-donating pyridine ring, causing more electron density to be present on the metal and making it easier to oxidise The result of the different properties of the co-ordination sites is that a difference of 550 mV exists between the oxidation potentials of the RuOs2 complex, compared with a difference of only 380 mV for the RuOs1 complex Figure 6 3 7 shows the cyclic voltammograms of these two complexes

The reduction potentials obtained for all four dinuclear species indicate that the first reduction must be ppt^- based, as it is found at a less negative potential

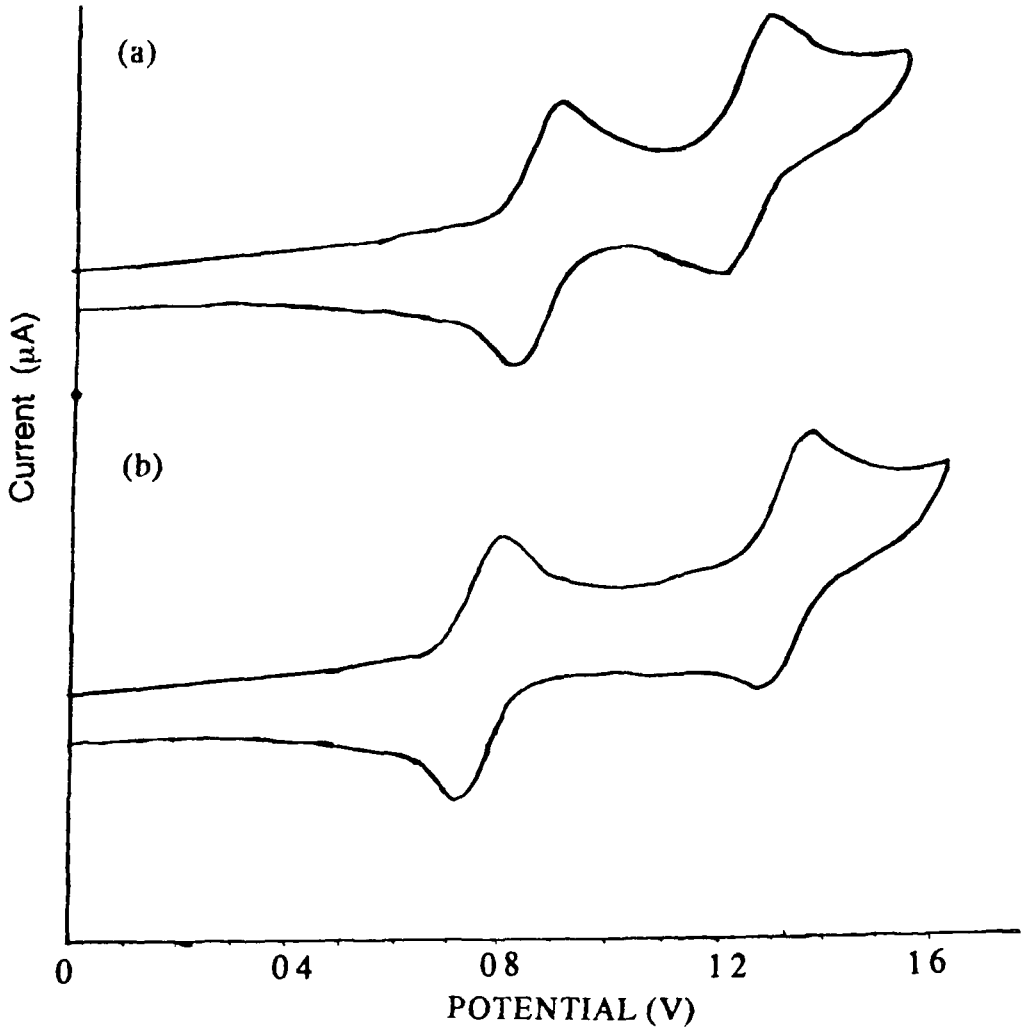

Figure 6 3 7

Cyclic voltammograms (scanrate 100 mV/sec) of the mixed-metal species (a) RuOs1 and (b) RuOs2 in CH_3CN containing 0 1 M TEAP

than that of the bpt$^-$ analogue The second two reduction waves are attributable to successive one electron reductions of the bpy ligands Therefore, similar behaviour occurs for the ppt$^-$ ligand as occurred for the bpzt$^-$ ligand, i e in the mononuclear species a bpy-based LUMO is observed (only bpy-based reductions) However, upon co-ordination of a second $Ru(bpy)_2$ (or $Os(bpy)_2$) moiety, the π^* level of the ppt$^-$ ligand is lowered The π^* level of the dinucleating ppt$^-$ ligand is now slightly lower than that of bpy, with a consequent less negative ppt$^-$-based reduction potential observed at ca -1 22 V

Again it is possible to correlate the electrochemical potentials (where $\Delta E_{1/2}$ is the difference between the first oxidation potential and first reduction potential of the species) and the MLCT (absorption / emission) energies of the ruthenium and osmium species[78-79] A plot of such data is presented in Figure 6 3 8 Included in the plot are a number of other mononuclear and dinuclear species containing bridging ligands as this is useful for good correlation The appearance of a relatively straight line for such data indicates that in these complexes containing the ppt$^-$ bridging ligand, the same type of orbitals play a role in the absorption, emission and electrochemical processes

6 3 5 *Luminescent lifetime measurements*

Luminescent lifetimes at room temperature and at 77 K of these complexes are presented in Table 6 2 A decrease in the lifetime of the ^{3}MLCT excited state is observed upon protonation of the mononuclear species and upon co-ordination of a second $Ru(bpy)_2$ (or $Os(bpy)_2$) moiety to generate the dinuclear species

In order to investigate further the photophysical processes occurring for these complexes, temperature dependent lifetime measurements were carried out on all compounds Exponential prefactors (A) and activation energies (E_a) were calculated according to the formula described in section 3 3, and are tabulated in Table 6 5

Mononuclear compounds

As seen from the data in Table 6 5, very low activation energies (E_a) and prefactors (A) result for all the mononuclear species, suggesting photostable complexes In fact, prolonged irradiation of any of these species in CH_2Cl_2

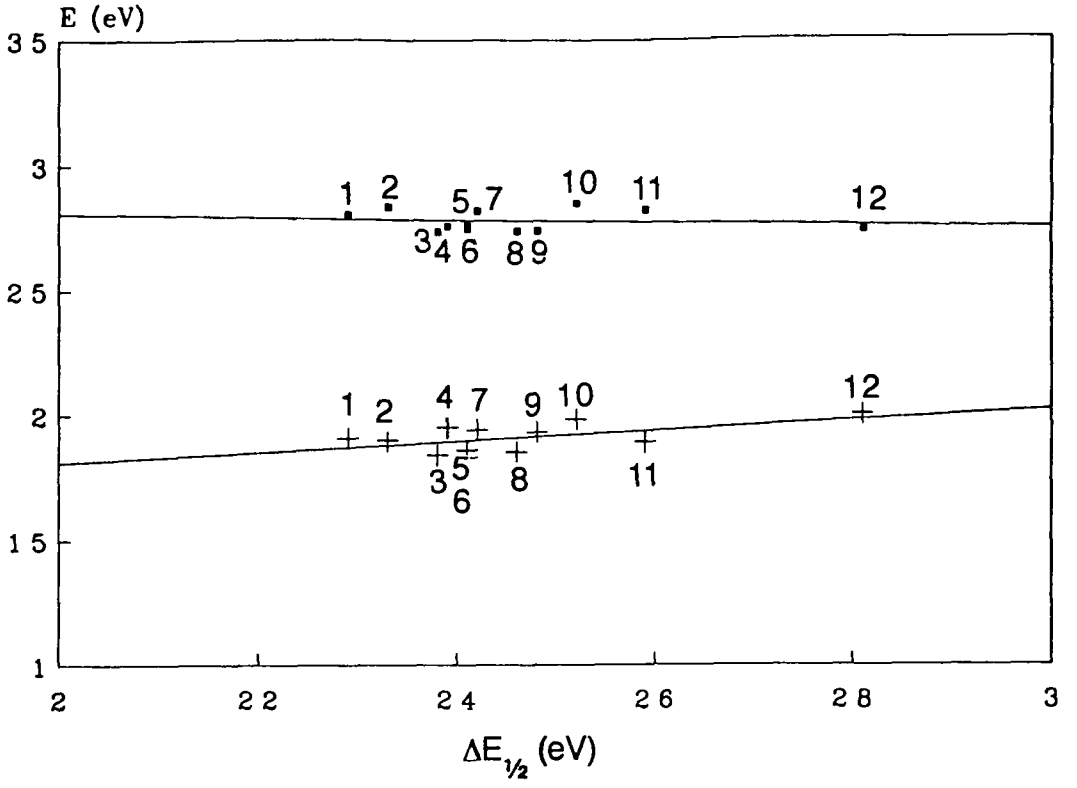

Figure 6 3 8

Correlation between the absorption / emission energies and $\Delta E_{1/2}$ for the complexes (1) $[Ru(bpy)_2(bpt)]^+$, (2) $[Ru(phen)_2(bpt)]^+$, (3) $[(Ru(bpy)_2)_2(ppt)]^{3+}$, (4) $[Ru(phen)_2(bpt)Ru(bpy)_2]^{3+}$, (5) $[Ru(bpy)_2(bpzt)]^+$, (6) $[Ru(bpy)_2(ppt)]^+$ isomer 1, (7) $[Ru(bpy)_2(bpt)Ru(phen)_2]^{3+}$, (8) $[(Ru(bpy)_2)_2(bpzt)]^{3+}$, (9) $[(Ru(bpy)_2)_2(bpt)]^{3+}$, (10) $[(Ru(phen)_2)_2(bpt)]^{3+}$, (11) $[Ru(bpy)_2(ppt)]^+$ isomer 2, and (12) $[Ru(bpy)_3]^{2+}$

containing Cl^- does not result in any appreciable photodecomposition occurring Thermal population of the dd states is insignificant at room temperature due to the large ^{3}MLCT - ^{3}MC energy gap for these complexes[80-81]

Plots of $\ln(1/\tau)$ versus $1/T$ for the mononuclear $[Ru(bpy)_2(ppt)]^+$ complexes are presented in Figure 6 3 9 and show a discontinuity around 120 - 130 K At this temperature, the solvent molecules around the cation and metal-ligand bonds can

Compound	E_a (cm^{-1})	A (s^{-1})
$[Ru(bpy)_2(ppt)]^+$ (1)	513	$5\,56 \times 10^7$
$[Ru(bpy)_2(ppt)]^+$ (2)	514	$1\,25 \times 10^8$
$[Os(bpy)_2(ppt)]^+$ (1)	1064	$3\,59 \times 10^9$
$[Os(bpy)_2(ppt)]^+$ (2)	834	$2\,77 \times 10^9$
RuRu	2844	$2\,27 \times 10^{13}$
OsOs	565	$4\,29 \times 10^8$
RuOs1	440	$2\,57 \times 10^8$
RuOs2	212	$2\,20 \times 10^8$

Table 6 5

Activation energies and prefactors for the ppt^- complexes at temperatures > 250 K in ethanol / methanol (4/1 v/v) (Values ± 10%)

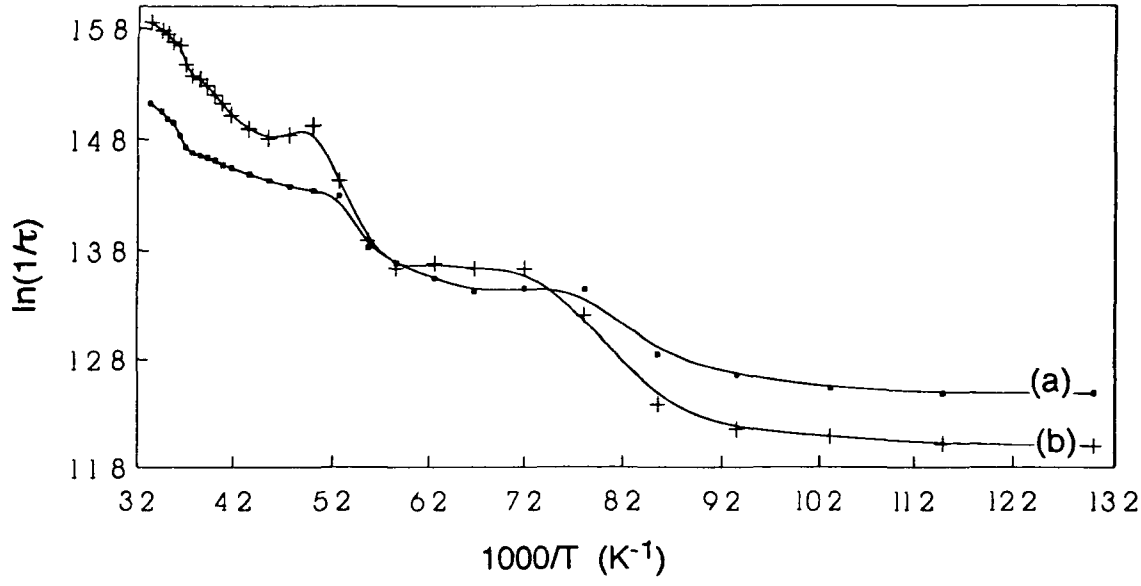

Figure 6 3 9

Plot of the $\ln(1/\tau)$ versus 1/T for $[Ru(bpy)_2(ppt)]^+$ (a) isomer 1 and (b) isomer 2. All measurements were carried out in ethanol methanol (4 1)

relax to their most favourable state after excitation of the complex and consequently the ^{3}MLCT energy is decreased In a rigid glass matrix, this relaxation process cannot occur as the solvent molecules cannot react to the change in elution distribution which occurs upon excitation, as they have not sufficient time to reorientate themselves in the excited state in response to the changing dipole This type of activated surface process can be dealt with by the empirical equation[82-84]

$$k_{nr} = B / [1 + \exp\{C(1/T - 1/T(B))\}] \qquad \textbf{6.1}$$

which describes a stepwise change of lifetime centred at a certain temperature T(B) In this equation C is a temperature related to the smoothness of the step and B is the increment for k_{nr} at T >> T(B) The values for the mononuclear complexes relating to the reorientation of the solvent molecules occurring above the glass transition temperature ($T(B_2)$) are presented in Table 6 6 There is also an increase in the non-radiative rate constant related to the melting of the solvent at T = $T(B_1)$ This was found to occur at 128 K for $[Ru(bpy)_2(ppt)]^+$ isomer 1 and at 127 K for $[Ru(bpy)_2(ppt)]^+$ isomer 2

A second step is encountered around 180 K in the $\ln(1/\tau)$ versus 1/T plots for both complexes A similar behaviour has been observed before for $[Ru(bpy)_2(bpt)]^+$ and $[Ru(bpy)_2(bpzt)]^+$ and has been attributed to reorientation of the solvent molecules due to a strong change in dipole moment caused by the Ru ---> bpy charge transfer, and the possibility of interacting with the solvent molecules via hydrogen bonds[85]

The $\ln(1/\tau)$ versus 1/T plot for the osmium mononuclear complexes is presented in Figure 6 3 10 For Os(II) polypyridyl complexes where 10 Dq is ca 30% larger than for the Ru(II) complexes, dd states are expected to be thermally

Compound	B (s^{-1})	C (K^{-1})	$T(B_2)$ (K)
$[Ru(bpy)_2(ppt)]^+$ (1)	9 29 x 10^5	8996	183
$[Ru(bpy)_2(ppt)]^+$ (2)	9 78 x 10^5	13411	187
$[Os(bpy)_2(ppt)]^+$ (1)	2 47 x 10^7	25325	179
$[Os(bpy)_2(ppt)]^+$ (2)	9 27 x 10^6	19039	226

Table 6 6

Kinetic parameters obtained for the ppt^- complexes The B values represent the increase of the nonradiative rate constant (s^{-1}) related to reorientation of the solvent molecules around $T = T(B_2)$ (see text) Errors ± 5 %

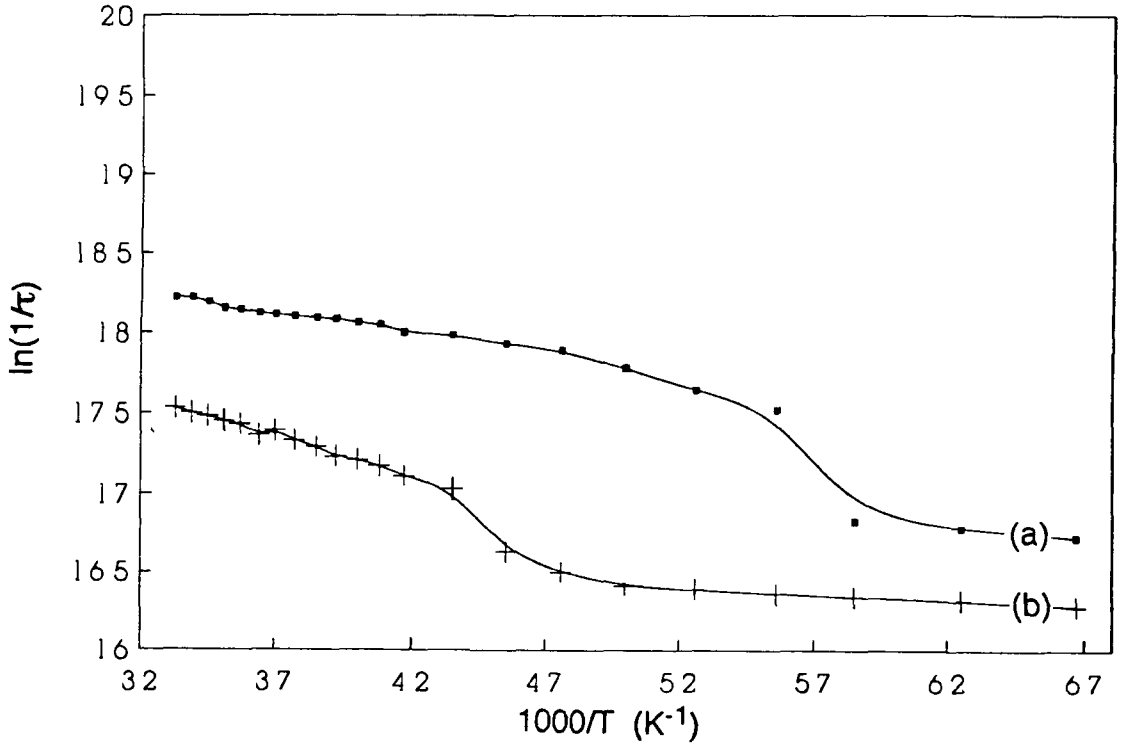

Figure 6 3 10

Plot of the $\ln(1/\tau)$ versus $1/T$ for $[Os(bpy)_2(ppt)]^+$ (a) isomer 1 and (b) isomer 2 in ethanol / methanol (4/1 v/v)

inaccessible[86] The small activation energies and prefactors obtained for these complexes support this conclusion As mentioned in the previous chapter, the slow rise in the $\ln(1/\tau)$ with increasing temperature above 150 K has been observed for all osmium complexes and suggests that some other sort of deactivating process must be occurring Meyer et al[87] have shown that a fourth MLCT state is populated at increasing temperatures This state has been shown to have increased singlet character compared with the other three low-lying MLCT states and therefore population of this state leads to a shortening of the lifetime of the complexes For $[Ru(bpy)_3]^{2+}$ the existence of a fourth state is obscured in the temperature dependent lifetime measurements in solution because of the intervention of a strongly temperature dependent transition to a low-lying dd state or states that become important above 200 K As we have good evidence to suggest a large energy gap between the ^{3}MLCT and ^{3}MC excited states for the ruthenium mononuclear complexes, population of this fourth MLCT excited state may also be occurring for these compounds, thereby accounting for the small rise in the $\ln(1/\tau)$ above 250 K

A small step is observed at 170 - 180 K for $[Os(bpy)_2(ppt)]^+$ isomer 1, due to the reorientation of the solvent molecules due to the Os ---> bpy charge transfer This step is encountered for isomer 2 at 220 K, but not for the mononuclear osmium complexes containing the ligands bpt^- and $bpzt^-$

The kinetic parameters calculated for all the ppt^- complexes are presented in Table 6 7 As can be seen from the data, the value of the radiative rate constant, k_r, is of the same order of magnitude for all the complexes studied, except for $[Ru(bpy)_2(ppt)]^+$ isomer 1 and $[Os(bpy)_2(ppt)]^+$ isomer 1, which have a considerably lower value k_r is expected to vary linearly with E_{em}^3 [59,88] The relatively slight variations in k_r strongly suggest that variations in the quantum yield of inter-system crossing from the ^{1}MLCT to the ^{3}MLCT excited states, ϕ_{isc},

Compound	k_r (s^{-1})	k_{nr} (s^{-1})	ϕ_{em}
$[Ru(bpy)_2(ppt)]^+$ (1)	6 68 x 10^3	2 62 x 10^5	1 53 x 10^{-3}
$[Ru(bpy)_2(Hppt)]^{2+}$ (1)	3 29 x 10^4	2 36 x 10^5	2 30 x 10^{-4}
$[Ru(bpy)_2(ppt)]^+$ (2)	1 84 x 10^4	1 44 x 10^5	2 52 x 10^{-3}
$[Ru(bpy)_2(Hppt)]^{2+}$ (2)	2 69 x 10^4	1 32 x 10^5	4 15 x 10^{-4}
$[Os(bpy)_2(ppt)]^+$ (1)	4 91 x 10^3	2 67 x 10^6	2 21 x 10^{-4}
$[Os(bpy)_2(Hppt)]^{2+}$ (1)	6 28 x 10^3	3 78 x 10^6	1 57 x 10^{-4}
$[Os(bpy)_2(ppt)]^+$ (2)	1 40 x 10^4	1 12 x 10^6	6 00 x 10^{-4}
$[Os(bpy)_2(Hppt)]^{2+}$ (2)	2 77 x 10^3	3 21 x 10^6	7 47 x 10^{-5}
RuRu	1 28 x 10^4	1 78 x 10^5	2 80 x 10^{-3}
OsOs	3 72 x 10^4	1 33 x 10^6	1 75 x 10^{-3}
RuOs1	2 41 x 10^4	9 95 x 10^5	1 81 x 10^{-3}
RuOs2	1 60 x 10^4	1 29 x 10^6	1 63 x 10^{-3}

Table 6 7

Kinetic parameters obtained for the ppt⁻ complexes ϕ_{em} values ± 10% Rate constant values ± 5%

throughout the series cannot be too significant[86]

The non-radiative rate constants, k_{nr}, are expected to increase with decreasing energy of the luminescent level, as predicted on the basis of the "energy-gap law"[88-91] The values of k_{nr} are higher for complexes containing osmium This has been noted previously for other osmium-containing complexes[86] An increase in k_{nr} by a factor of three for complexes of Os(II) compared to complexes of Ru(II) that have the same emission energy was

observed This was rationalised by taking into account the enhanced singlet character of the osmium excited states resulting from the larger magnitude of the spin-orbital coupling constant for osmium compared to that of ruthenium

Although the ^{3}MLCT excited state lifetimes can be increased by increasing the energy gap between the ^{3}MLCT and ^{3}MC excited states, this may not completely solve all the photodecomposition problems associated with Ru(II)polypyridyl complexes We have seen that as the energy of emission increases, k_{nr} decreases, but k_r increases, albeit at a slower rate Eventually, k_r will dictate the excited-state lifetimes especially for osmium complexes where there is no complication arising from decay through a dd channel

A comparison of the temperature dependence of the ruthenium mononuclear complexes containing the bpt$^-$, bpzt$^-$, and ppt$^-$ ligands are represented in Figure 6 3 11 As can be seen, the bpzt$^-$ complex and $[Ru(bpy)_2(ppt)]^+$ isomer 2 exhibit quite different behaviour from the other two complexes, a much larger step occurring at around 180 K The similarities of the temperature dependence of $[Ru(bpy)_2(bpt)]^+$ and $[Ru(bpy)_2(ppt)]^+$ isomer 1, suggest very similar emission processes for these complexes, whereas the similarities of the emission profile for the remaining two complexes indicates that the emission is similar for these compounds and, therefore, a pyrazine-based emission is occurring in isomer 2

Dinuclear compounds

Examination of the activation energies and prefactors obtained for the dinuclear complexes, suggest that only the dinuclear $[(Ru(bpy)_2)_2(ppt)]^{3+}$ species is photochemically active In fact irradiation of the other three dinuclear complexes does not lead to any photodecomposition A plot of the $\ln(1/\tau)$ versus $1/T$ for the

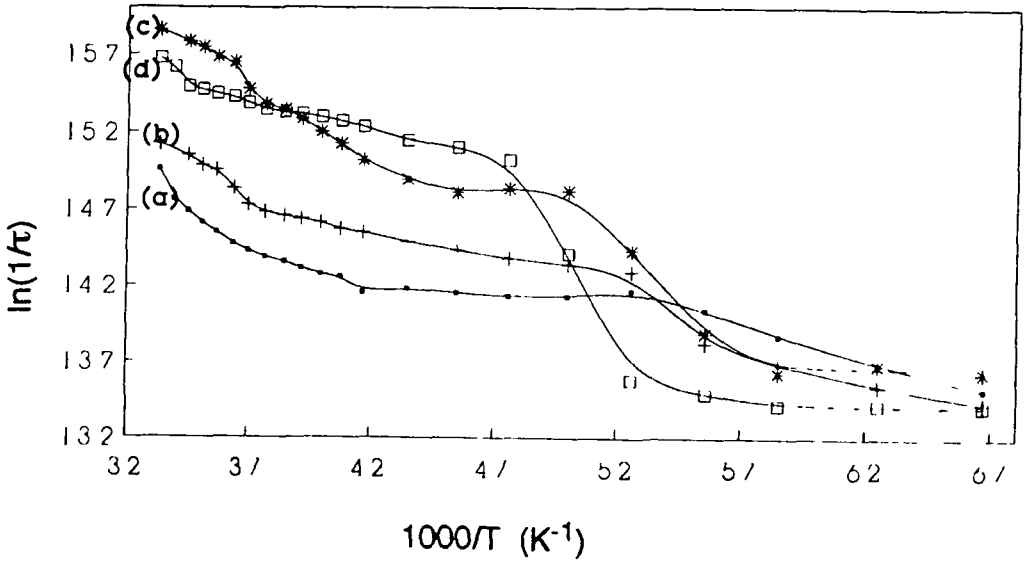

Figure 6 3 11

Plot of ln(1/τ) versus 1/T for the mononuclear ruthenium complexes (a) $[Ru(bpy)_2(bpt)]^+$, (b) $[Ru(bpy)_2(bpzt)]^+$, (c) $[Ru(bpy)_2(ppt)]^+$ isomer 1, and (d) $[Ru(bpy)_2(ppt)]^+$ isomer 2 in ethanol / methanol (4/1 v/v)

dinuclear complexes is presented in Figure 6 3 12 $[(Ru(bpy)_2)_2(ppt)]^{3+}$ shows a similar temperature dependence to that found for the bpt^- and $bpzt^-$ dimers A steep rise in the ln(1/τ) occurring at temperatures greater than 250 K, suggest that an activated surface crossing to a ^3MC excited state is occurring[92-93] Population of this state leads to fast radiationless deactivation to the ground state and/or to photodecomposition of the complex The second step observed for the mononuclear complexes is not seen here Most likely, the weaker σ-donating

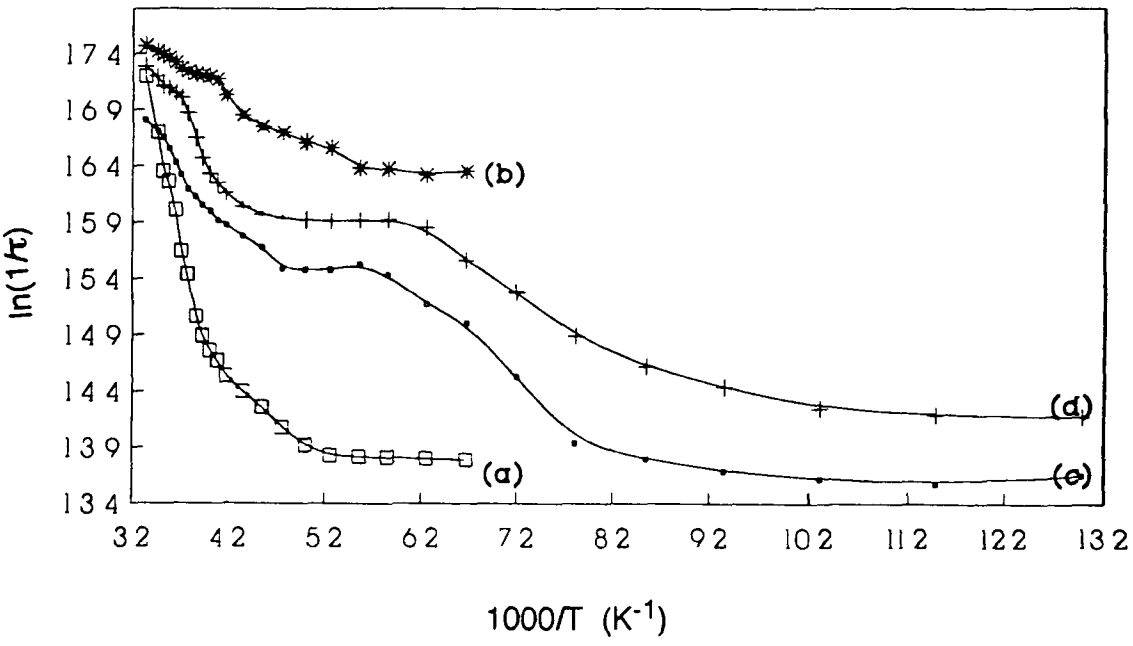

Figure 6 3 12

Plot of the ln(1/τ) versus 1/T for the dinuclear complexes (a) RuRu, (b) OsOs, (c) RuOs1, and (d) RuOs2 in ethanol / methanol (4/1 v/v)

ability of the dinucleating ppt⁻ ligand causes the ^{3}MLCT - ^{3}MC energy gap to decrease, thereby facilitating population of the ^{3}MC excited state

For the osmium dinuclear compound, a step is observed at around 180 K This has also been noted for the complexes containing the bpt⁻ and bpzt⁻ ligands and was explained by the possibility of having two closely lying excited states of MLCT origin involved in the emission processes[94] A very important observation is

the absence of the steep rise in the ln(1/τ) versus 1/T plot observed for the OsOs complex This is due to the greater ligand-field splitting of osmium compounds with respect to ruthenium complexes causing a larger energy gap between the ^{3}MLCT and ^{3}MC excited states Population of a higher ^{3}MLCT excited state must be occurring for this complex also, as the emission lifetime still continues to decrease slightly with increasing energies The increased singlet character of this fourth MLCT state leads to a shortening of the lifetime of the complex[87]

The ln(1/τ) versus 1/T plots for the mixed-metal dinuclear complexes show a discontinuity in the plot at the glass-fluid transition region, 120 K, as seen for the ruthenium mononuclear complexes in this region This is again caused by solvent reorientations as the glass melts The plot above 250 K is very similar to that observed for the osmium dinuclear species In fact, the activation energies and prefactors are very similar for these three compounds within experimental error, but differ significantly from the ruthenium dinuclear complex

The emission energies for these compounds indicate that emission occurs only from the osmium site The absence of a ruthenium-based emission for the two heteronuclear complexes is reflected in the temperature dependent profiles This indicates that either an efficient energy-transfer or electron-transfer process is taking place in these complexes Comparison with the work carried out for the mixed-metal complexes containing the bpt$^-$ ligand[95] suggest that for this system an efficient energy-transfer process from the $Ru(bpy)_2$ to the $Os(bpy)_2$ moiety is present A consequence of this behaviour is that the RuOs1 and RuOs2 complexes take on the properties of osmium complexes with resulting photostability

The quantum yield of internal conversion from the ^{3}MLCT to the ^{3}MC excited states, η_{ic}, was calculated for the $[(Ru(bpy)_2)_2(ppt)]^{3+}$ complex A value of close to one was observed for $[(Ru(bpy)_2)_2(ppt)]^{3+}$ indicating that no other

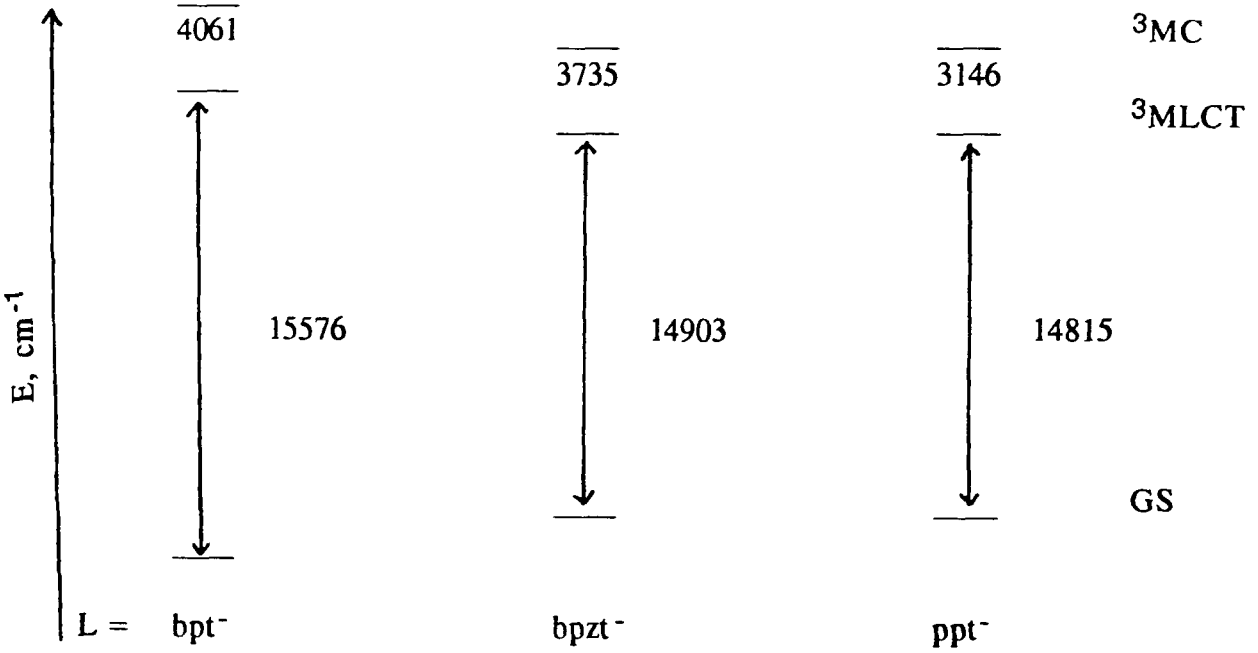

Figure 6 3 13

Energy level diagrams for (a) $[(Ru(bpy)_2)_2(bpt)]^{3+}$ (b) $[(Ru(bpy)_2)_2(bpzt)]^{3+}$ and (c) $[(Ru(bpy)_2)_2(ppt)]^{3+}$

deactivation processes are occurring for this complex

A comparison of the energy level diagrams of the ruthenium dinuclear species containing the bpt$^-$, bpzt$^-$, and ppt$^-$ ligands (see Figure 6 3 13) show that the complexes containing the bpzt$^-$ and ppt$^-$ ligands have very similar properties Population of the ^{3}MC state is more difficult for complexes containing bpt$^-$ than for those containing the other two ligands In fact the energy of the ^{3}MLCT - ^{3}MC gap increases in the following order ppt$^-$ < bpzt$^-$ < bpt$^-$ This energy-gap should affect

the photochemical properties of these complexes This will be discussed in more detail in Section 6 3 8

6 3 6 *Mixed-valence species*

In mixed valence compounds the interaction between the metal centres can be probed by studying the intervalence transition bands (IT)[96-98] Figure 6 3 14 shows the IT band of the $[(Ru(bpy)_2)_2(ppt)]^{4+}$ complex upon oxidation at 1 4 V at different time intervals Two absorption bands are visible, one centred at 13800 cm^{-1} and the other at 5300 cm^{-1} The former band has been assigned as a ligand-to-metal charge transfer (LMCT) band by comparison with literature data[99-100] Further oxidation to the $Ru^{III}Ru^{III}$ species leads to a complete disappearance of the band at 5300 cm^{-1}, which supports its assignment as an intervalence transition band[101-102]

The characteristics of the IT band have been studied in a number of solvents and the data are presented in Table 6 8 A plot of the solvent dependence of the IT band is shown in Figure 6 3 15 Included in this plot is the solvent dependence of the other two dinuclear species containing the bpt^- and $bpzt^-$ ligands An inner-sphere reorganisational energy, λ_i, of 3987 cm^{-1} was calculated from this plot for the ppt^- dimer, which was very similar to the values obtained for the other two dimers Therefore, changing the bridging ligand does not appear to have a very large effect on λ_i for this series of complexes

All three complexes exhibit a certain amount of solvent dependence Because of the large error involved in these measurements, it is difficult to accurately assess the effect of changing the bridging ligand However, it is noteworthy that the energy of the IT band increases with increasing polarity of the

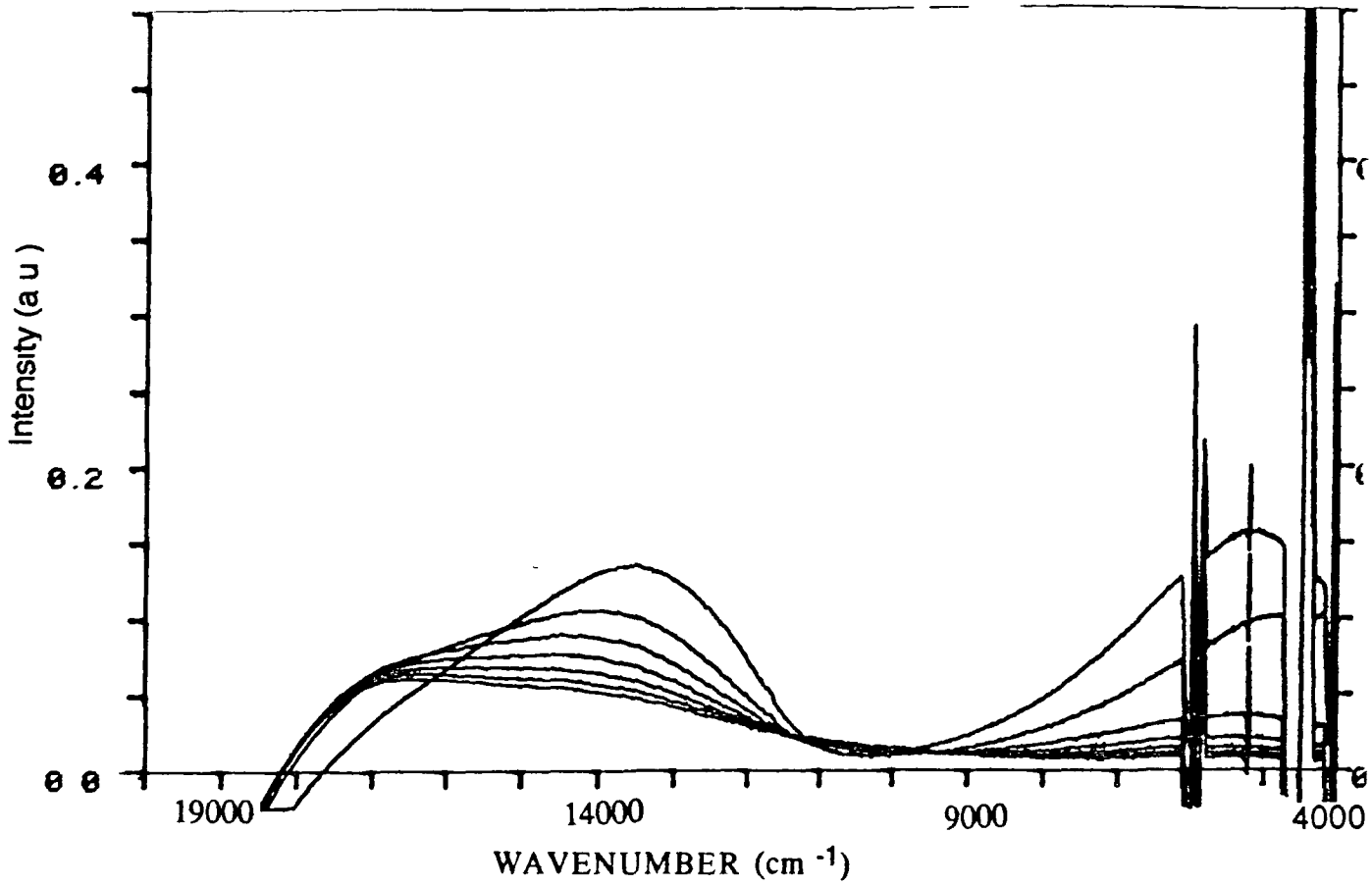

Figure 6 3 14

IT band of $[(Ru(bpy)_2)_2(ppt)]^{4+}$ in MeCN Applied potential is 1 4 V Spectra are taken as a function of time from 0 to 60 min

solvent, as expected due to the greater dipole moment of the more polar solvents Any change in the electronic state of a solvent complex will cause a greater activation barrier to electron transfer taking place

The value of α^2, the extent of electron delocalisation, is 0 025 for $[(Ru(bpy)_2)_2(ppt)]^{3+}$ and indicates a relatively large metal-metal interaction for the mixed-valence complex, in agreement with the measurements for the bpt^- and

Solvent	E_{OD} (cm^{-1})	$\Delta\upsilon_{1/2}$ (exp)	$\Delta\upsilon_{1/2}$ (calc)	ε_{max} $M^{-1}cm^{-1}$	$1/D_{OD} - 1/D_S$	α^2	H_{AB} (cm^{-1})	k_{th} (s^{-1}) (x 10^{11})	E_{th} (J) (x 10^{-20})
MeCN	5200	3800	3188	3102	0 528	0 025	822	1 7	1 4
Acetone	5180	3900	3180	2958	0 495	0 024	802	1 7	1 4
C_6H_6CN	5100	3800	3152	2825	0 391	0 023	773	1 3	1 5
CH_2Cl_2	5080	3800	3144	1891	0 381	0 016	643	3 3	1 7

Table 6 8

Properties of the IT band calculated for $[(Ru(bpy)_2)_2(ppt)]^{3+}$.

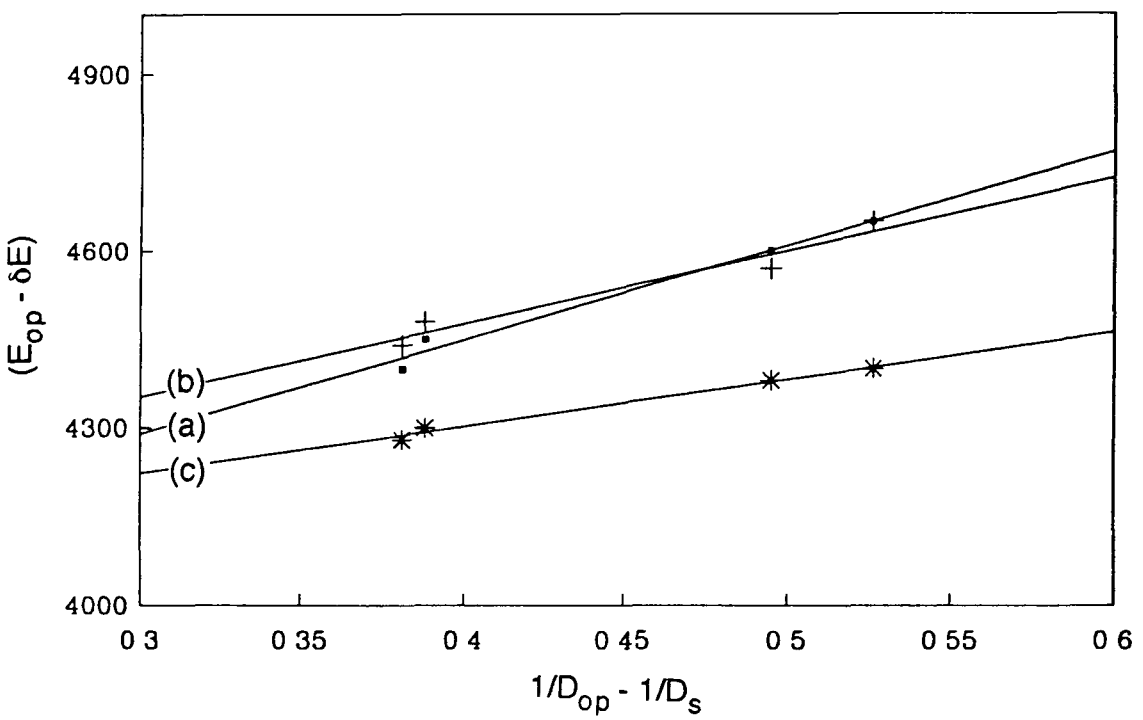

Figure 6 3 15

Plot of the solvent dependence of the IT parameters for (a) $[(Ru(bpy)_2)_2(bpt)]^{3+}$, (b) $[(Ru(bpy)_2)_2(bpzt)]^{3+}$ and (c) $[(Ru(bpy)_2)_2(ppt)]^{3+}$

bpzt$^-$ systems This further supports the hole-transfer mechanism proposed by Hupp and Taube[103-104] as mentioned in Section 5 3 6 It also indicates that the metal-metal interaction is to an extent independent of the π^* level of the bridging ligand for these complexes

6 3 7 *Localisation of the metal based oxidation*

Evidence of the localisation of the metal based oxidation for the dinuclear complexes was obtained from a study of the spectroelectrochemical properties in the visible and UV regions of the compounds Figure 6 3 16 contains the absorption spectrum of the $[(Ru(bpy)_2)_2(ppt)]^{3+}$ complex in the following oxidation states $Ru^{II}Ru^{II}$, $Ru^{III}Ru^{II}$, and $Ru^{III}Ru^{III}$ The MLCT band occurring at 452 nm shifts to 430 nm upon partial oxidation of the complex and completely disappears upon full oxidation Actually, the absorbance spectrum of the mixed-valence species closely resembles that of the mononuclear pyrazine-bound isomer (isomer 2) with a λ_{max} at 430 nm This would suggest that the Ru-containing unit co-ordinated via N4 of the triazole ring and the pyridine ring is oxidised first This is a reasonable assumption, as the pyridine ring is a stronger σ-donor than the pyrazine ring, causing the amount of electron density on the ruthenium metal attached to the pyridine ring to be greater, thus making it easier to oxidise

In the $Ru^{II}Ru^{II}$ species, a π - π^* band at 285 nm is observed In the mixed-valence $Ru^{III}Ru^{II}$ species, the intensity of this band decreases significantly However, no shift in the λ_{max} is observed In the fully oxidised $Ru^{III}Ru^{III}$ species, a shift in the λ_{max} to 302 nm occurs As seen for the bpt$^-$ and bpzt$^-$ dimers, if the metal based oxidation was delocalised, an intermediate shift in the λ_{max} between the unoxidised and fully oxidised complexes would be expected for the mixed-

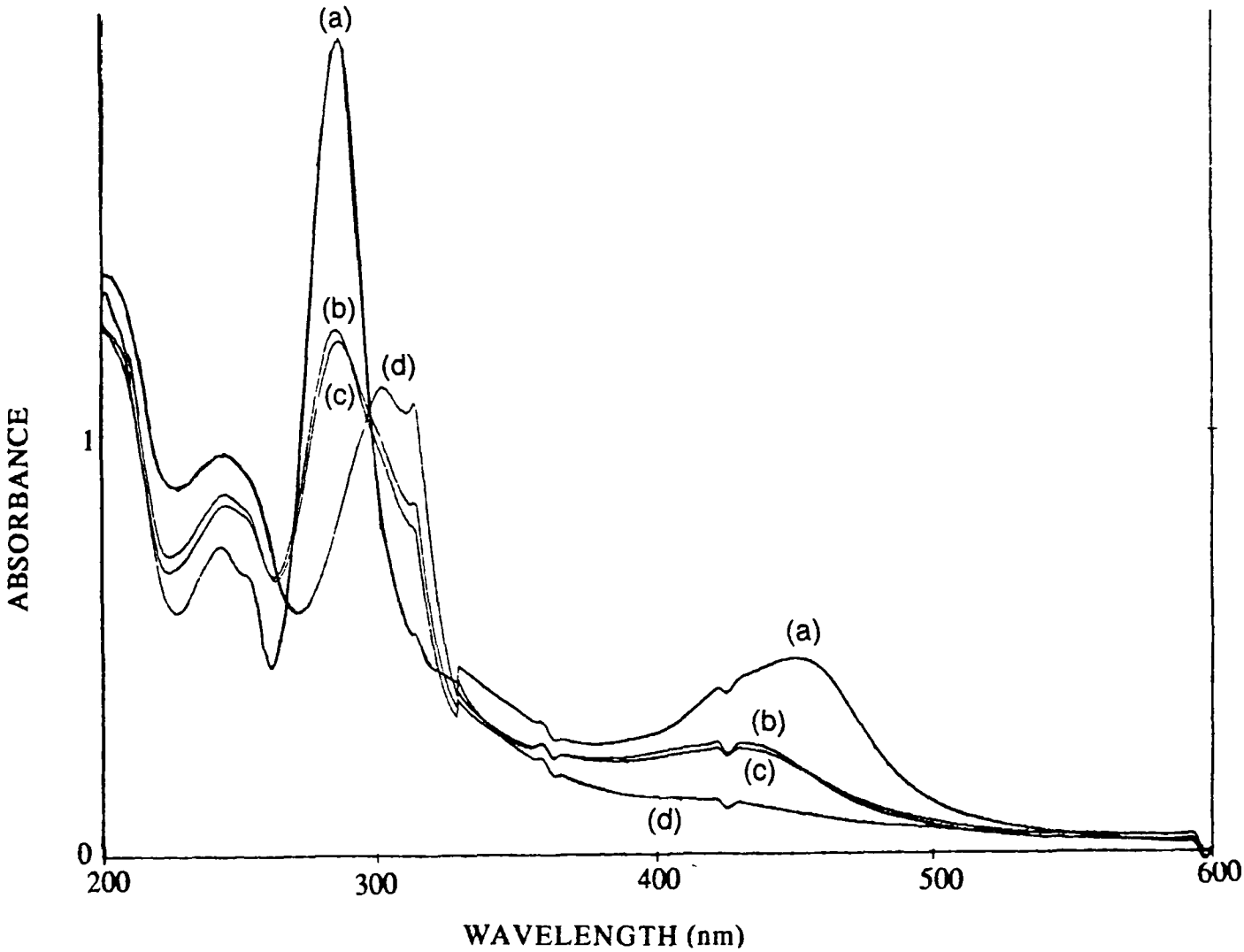

Figure 6 3 16

Absorbance spectrum of $[(Ru(bpy)_2)_2(ppt)]^{3+}$ at applied potentials of (a) 0 9 V ($Ru^{II}Ru^{II}$), (b) 1 2 V ($Ru^{III}Ru^{II}$), (c) 1 4 V ($Ru^{III}Ru^{II}$) and (d) 1 7 V ($Ru^{III}Ru^{III}$) in MeCN containing 0 1 M TEAP

valence species The absence of this shift suggests a localised model for the metal based oxidation is most appropriate in these systems

Again for the other three dinuclear complexes, OsOs, RuOs1 and RuOs2, evidence for the localisation of the metal based oxidation is obtained from their

absorbance spectra in the mixed-valence state Also for the OsOs dimer, there is evidence to suggest that the Os-containing unit attached to the N4 position of the triazole ring and to the pyridine ring is oxidised first, due to the better σ-donor properties of the pyridine ring compared with the pyrazine ring As expected, in the mixed-metal dimers, the osmium-containing unit is always oxidised first

6 3 8 *Resonance Raman Spectra*

Resonance Raman spectroscopy can be useful for the assignment of the nature and characterisation of electronic transitions[67] If excitation takes place into an allowed electronic transition, the resonance Raman spectrum is characterised by strong Raman effects for the vibrations of those bonds that are mostly affected by the electronic transition For this reason, resonance Raman spectra of the ppt$^-$ complexes were carried out

The ground-state Raman spectra for $[Ru(bpy)_2(ppt)]^+$ isomer 1 and $[Ru(bpy)_2(Hppt)]^{2+}$ isomer 2 are presented in Figure 6 3 17 Both spectra exhibit enhancements of the rR peaks at 1610, 1567, 1491, 1318, 1178, 1040, and 1023 cm^{-1} These features can be attributed to the ground-state features of bpy[105-107] The spectra also exhibit extra bands at 1528, 1449, 1412, 1282, 1246, 1162, and 1095 cm^{-1} which may be attributed to the ground-state features of the bridging ppt ligand The wavelength of 364 nm employed for these studies lies close to the wavelength of 354 7 nm employed for the single colour pulsed excitation transient rR studies Similarly, for the dinuclear $[(Ru(bpy)_2)_2(ppt)]^{3+}$ complex, ground-state features of both bpy and ppt$^-$ have been observed in the spectrum

Much more direct evidence concerning the nature of the emitting state can be obtained from the 354 7 nm pulsed-excited Raman spectra of the complexes

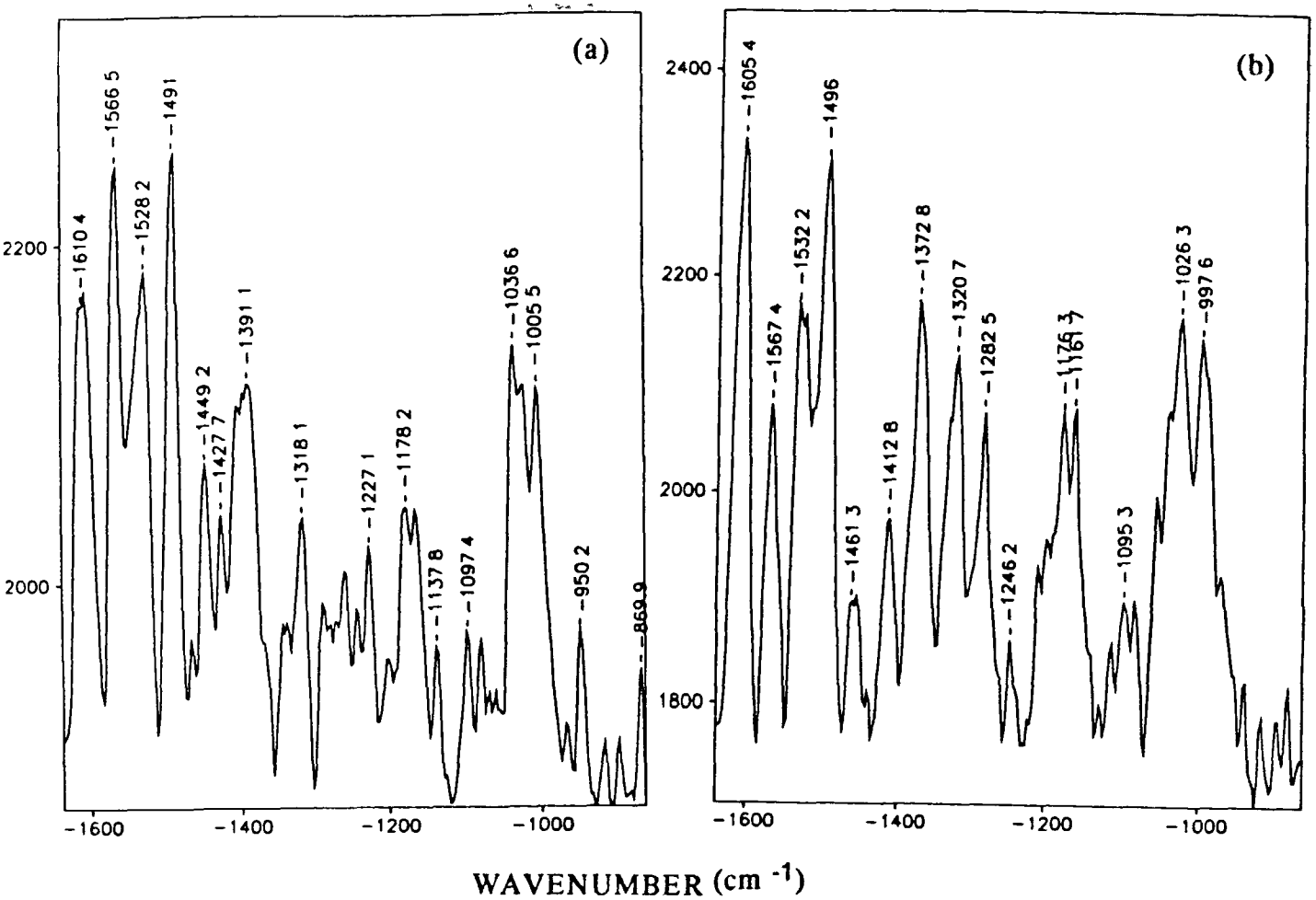

Figure 6 3 17

Resonance Raman spectrum obtained in the ground-state for (a) $[Ru(bpy)_2(ppt)]^+$ isomer 1 and (b) $[Ru(bpy)_2(Hppt)]^{2+}$ isomer 2 in acetone / water (5/1 v/v)

Figure 6 3 18 contains the excited-state rR spectra of $[Ru(bpy)_2(ppt)]^+$ isomer 1 and $[Ru(bpy)_2(Hppt)]^{2+}$ isomer 2 A considerably more simple spectrum is obtained for the pyridine-bound isomer (isomer 1) In fact, the excited-state resonances observed for this complex at 1547, 1502, 1424, 1287, and 1212 cm^{-1} correlate closely in both position and relative intensities with the spectrum of $[Ru(bpy)_3]^{2+*}$ using pulsed excitation at the same wavelength, 354 7 nm, as used

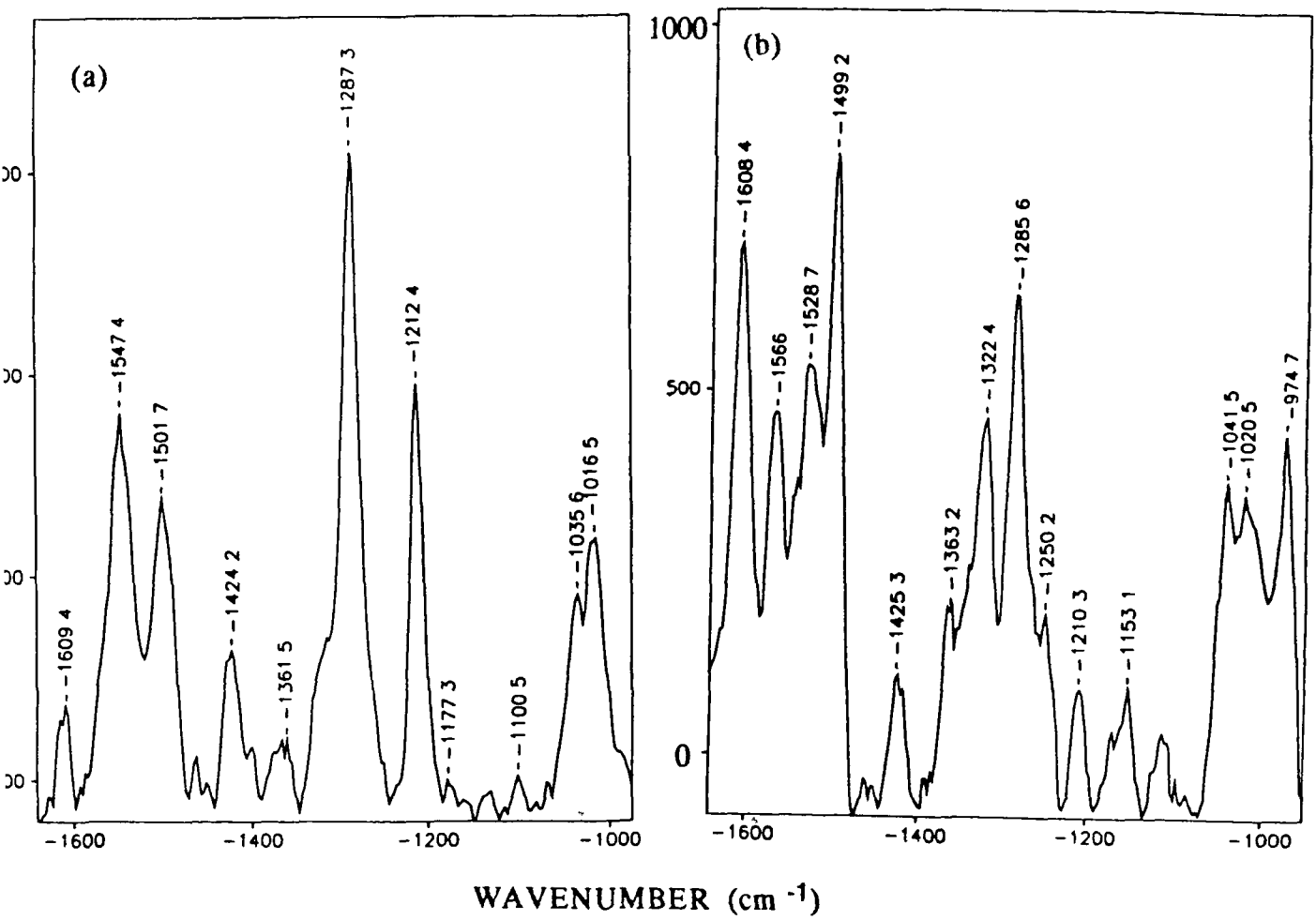

Figure 6 3 18

Excited-state Resonance Raman spectra of (a) $[Ru(bpy)_2(ppt)]^+$ isomer 1 and (b) $[Ru(bpy)_2(Hppt)]^{2+}$ isomer 2 in acetone / water (5/1 v/v)

in the present study[108] The localised excited state for $[Ru(bpy)_3]^{2+}$ was assigned as $[(bpy)Ru^{III}(bpy^{\cdot-})]^{2+}$ Therefore, it is possible to formulate isomer 1 as $[(bpy)Ru^{III}(bpy^{\cdot-})(ppt)]^+$, in which the Raman scattering rises predominantly from the $(bpy)Ru^{III}(bpy^{\cdot-})$ region of the complex

The excited-state spectra of $[Ru(bpy)_2(Hppt)]^{2+}$ isomer 2 and of the dinuclear $[(Ru(bpy)_2)_2(ppt)]^{3+}$ complex are considerably different than that

observed for the mononuclear pyridine-bound isomer (isomer 1) They contain common features at 1608, 1566, 1528, 1499, 1322, 1285, 1211, and 1041 cm^{-1} No evidence for any $bpy^{\cdot -}$ modes are present in the spectra Therefore, the excited-state spectra obtained must correspond to excitation of the bridging ligand and not of the auxiliary polypyridyl ligands, in agreement with the electrochemical data obtained for these complexes[106, 109-110] This would suggest that for these complexes, the lowest ^{3}MLCT band is a Ru ---> Hppt transition for $[Ru(bpy)_2(Hppt)]^{2+}$ isomer 2 and a Ru ---> ppt^- transition for the dinuclear complex This shows that upon protonation of the ppt^- ligand, or upon addition of a second $Ru(bpy)_2$ moiety, the π^* level is lowered significantly, as concluded before for the pyrazyltriazole containing complexes[67] The results given are only a preliminary investigation and the rR spectra of $[Ru(bpy)_2(Hppt)]^{2+}$ isomer 1 and $[Ru(bpy)_2(ppt)]^+$ isomer 2 would be necessary in order to confirm these results

6 3 9 *Photochemical properties*

As $[(Ru(bpy)_2)_2(ppt)]^{3+}$ was the only complex in this series which exhibited photolability, photochemical discussions will be restricted to this compound However, the photochemical stability of the RuOs1 and RuOs2 complexes is notable As seen before for mixed-metal complexes containing the bpt^- ligand, an efficient intramolecular energy-transfer is occurring from the $Ru(bpy)_2$ moiety to the lower energy $Os(bpy)_2$ moiety This causes emission to result totally from the $Os(bpy)_2$ site and eliminates population of the ^{3}MC state, which is an inherent property of ruthenium complexes and ultimately leads to photodecomposition This is an important observation, as it implies that these mixed-metal complexes are now photostable This coupled with the increased absorbance in the visible region

due to the presence of both the $Os(bpy)_2$ and the $Ru(bpy)_2$ moieties make these complexes candidates for solar-energy conversion systems However, the luminescent lifetimes of these complexes are very short which is a distinct disadvantage for their application

Photochemistry in CH_2Cl_2 containing Cl^-

UV/vis absorbance spectra taken during the photolysis of $[(Ru(bpy)_2)_2(ppt)]^{3+}$ in CH_2Cl_2 containing 0 005 M Cl^- shows a decrease in the λ_{max} occurring at 455 nm, with a subsequent growth of two new peaks with λ_{max} at 480 and 550 nm (see Figure 6 3 19) In order to investigate further the photochemical processes occurring for this complex, HPLC traces were taken at specified intervals during the photolysis Figure 6 3 20 contains a representative example of these traces As can be seen from the HPLC analysis, photolysis results in the simultaneous growth of three main photoproducts, which were identified according to their HPLC retention times, UV/vis absorbance spectra and by comparison with authentic samples as follows Peak 1, retention time 2 05 min, λ_{max} 370 and 530 nm was identified as $[Ru(bpy)_2Cl_2]$ Peak 2, retention time 4 05 min, λ_{max} 340 and 475 nm was found to be $[Ru(bpy)_2(MeCN)Cl]^{2+}$ Peak 3, retention time 5 65 minutes, λ_{max} 475 nm was identified as $[Ru(bpy)_2(ppt)]^+$ isomer 1 (or the pyridine-bound isomer) Peak 4, retention time 6 10 minutes, λ_{max} 475 nm, was identified as $[Ru(bpy)_2(ppt)]^+$, which may be co-ordinated via N4 of the triazole ring and via the pyridine ring This is similar to the N4 isomer of $[Ru(bpy)_2(bpt)]^+$ as described in Section 4 3 8 Peak 5, retention time 10 2 min, λ_{max} 450 nm did not correspond to any of the known isomers of the ppt^- mononuclear species It is, therefore, most likely that the photolysis product is another unknown isomer This photoisomerisation implies that the photolysis product can only be produced by photochemical means, as from synthesis

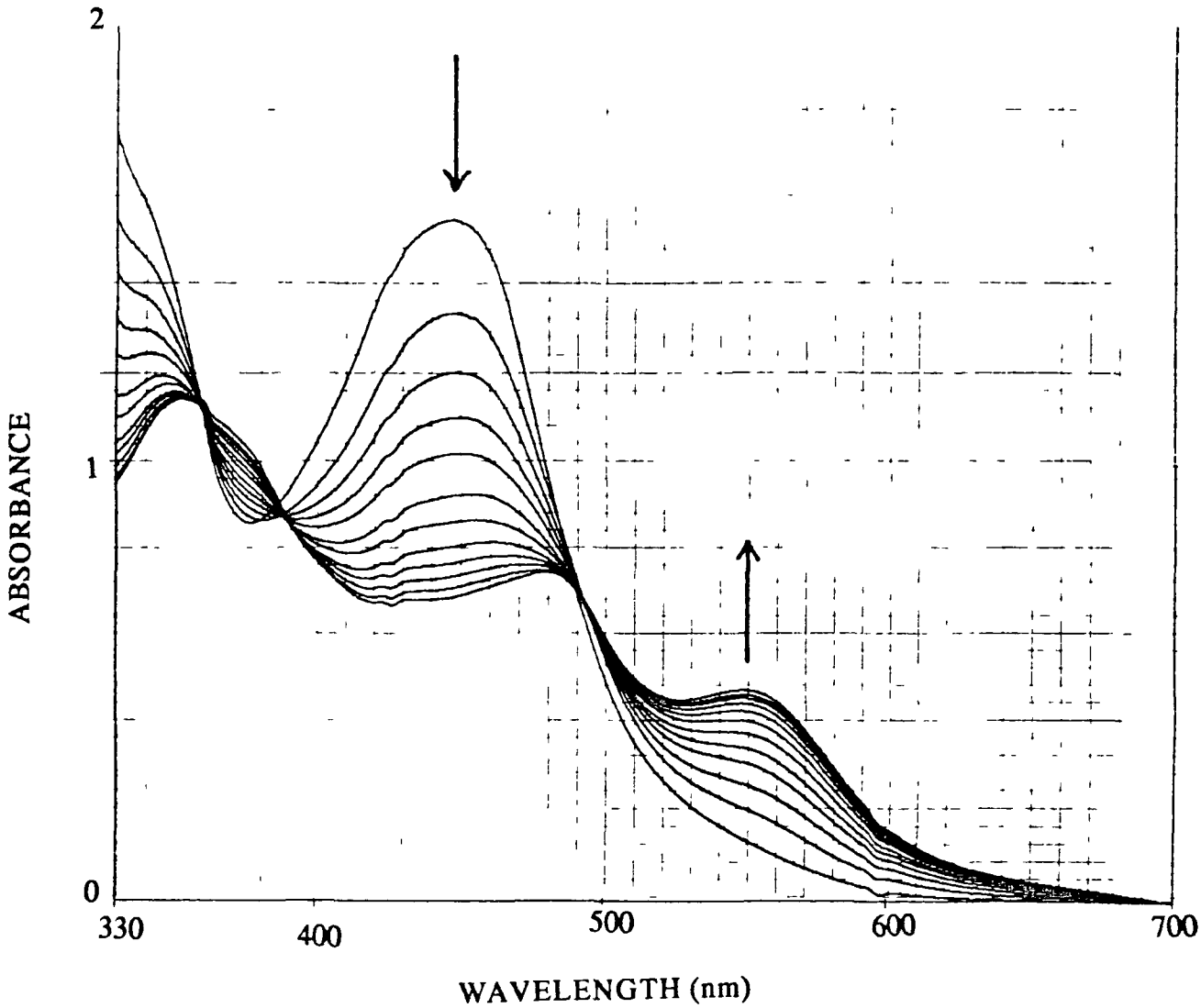

Figure 6 3 19

Changes in the absorbance spectrum upon photolysis in CH_2Cl_2 containing 0 005 M Cl^- for $[(Ru(bpy)_2)_2(ppt)]^{3+}$

(thermal reaction) there is no evidence for this isomer No evidence for any of the known pyrazine-bound isomers is apparent from the HPLC spectra.

These are very different results in comparison with the photochemical properties of the bpt^- and $bpzt^-$ dinuclear complexes It appears that photolysis of the ppt^- complex leads to a rupture of the Ru-N bond at the Ru-containing unit attached to N1 of the triazole ring and the pyrazine ring In the $bpzt^-$ dimer, rupture

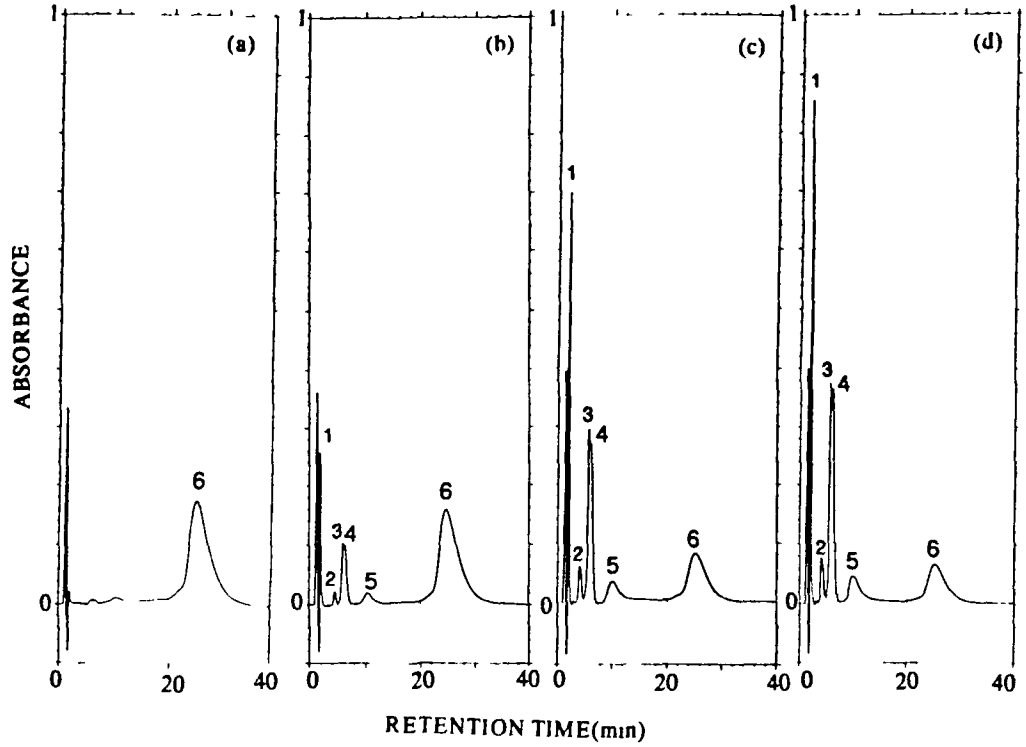

Figure 6 3 20

HPLC traces taken during the photolysis in CH_2Cl_2 containing 0 005 M Cl^- for $[(Ru(bpy)_2)_2(ppt)]^{3+}$ after (a) 0 min, (b) 10 min, (c) 50 min, and (d) 80 min Mobile phase 80 20 MeCN H_2O containing 0 08 M $LiClO_4$ Flowrate 2 0 cm^3/min Detector wavelength 280 nm

of the Ru-N bond occurs at the N4 (or the weaker σ-donor) position of the triazole ring Obviously, in this situation, the weaker σ-donor properties of the pyrazine ring causes the ^3MC (or metal-centred) excited state to be localised on this Ru-containing unit Population of this excited state leads to rapid photodecomposition of the complex The N2-bound pyridine isomer (isomer 1) is much more stable than the N4-bound isomer (as inferred from the absence of the N4-bound isomer in the synthetic process) and, therefore, conversion to the N2-bound pyridine isomer appears to occur during photolysis

Photochemistry in MeCN containing Cl^-

UV/vis absorbance spectra taken during the photolysis of $[(Ru(bpy)_2)_2(ppt)]^{3+}$ in MeCN containing 0 01 M Cl^-, again shows a decrease in the λ_{max} at 450 nm, with a subsequent increase in a new band at 460 nm HPLC traces taken during the photolysis show the simultaneous growth of four main photoproducts identified as follows (see Figure 3 6 21) Peak 1, retention time 2 1 minutes, λ_{max} 360 and 575 nm was identified as $[Ru(bpy)_2Cl_2]$, Peak 2, retention time 2 45 minutes, λ_{max} 340 and 475 nm was identified as $[Ru(bpy)_2(MeCN)Cl]^{2+}$, Peak 3, retention time 6 min, λ_{max} 470 nm was found to be $[Ru(bpy)_2(ppt)]^+$ isomer 1 (the pyridine-bound isomer) and Peak 4, retention time 7 minutes, λ_{max} 470 nm was identified as the N4-pyridine bound isomer of $[Ru(bpy)_2(ppt)]^+$

In this solvent, the lowest ^3MC state again resides on the Ru-containing unit attached to the weaker σ-donor pyrazine ligand

Photolychemistry in MeCN

UV/vis spectra taken during the photolysis of $[(Ru(bpy)_2)_2(ppt)]^{3+}$ in pure MeCN shows a decrease in the absorbance at 450 nm, with a simultaneous growth in a new peak at 425 nm HPLC traces taken during the photolysis (see Figure 6 3 22) shows the growth of two main photoproducts which were identified as follows Peak 1, retention time 7 25 minutes, λ_{max} 470 nm was identified as $[Ru(bpy)_2(ppt)]^+$ isomer 1 Peak 2, retention time 8 1 minutes, λ_{max} 425 nm was identified as $[Ru(bpy)_2(MeCN)_2]^{2+}$ The longer time necessary for this photolysis allows complete conversion to the N2-bound pyridine isomer (or the more stable isomer) No evidence for the formation of any pyrazine-bound isomer is again apparent from this analysis

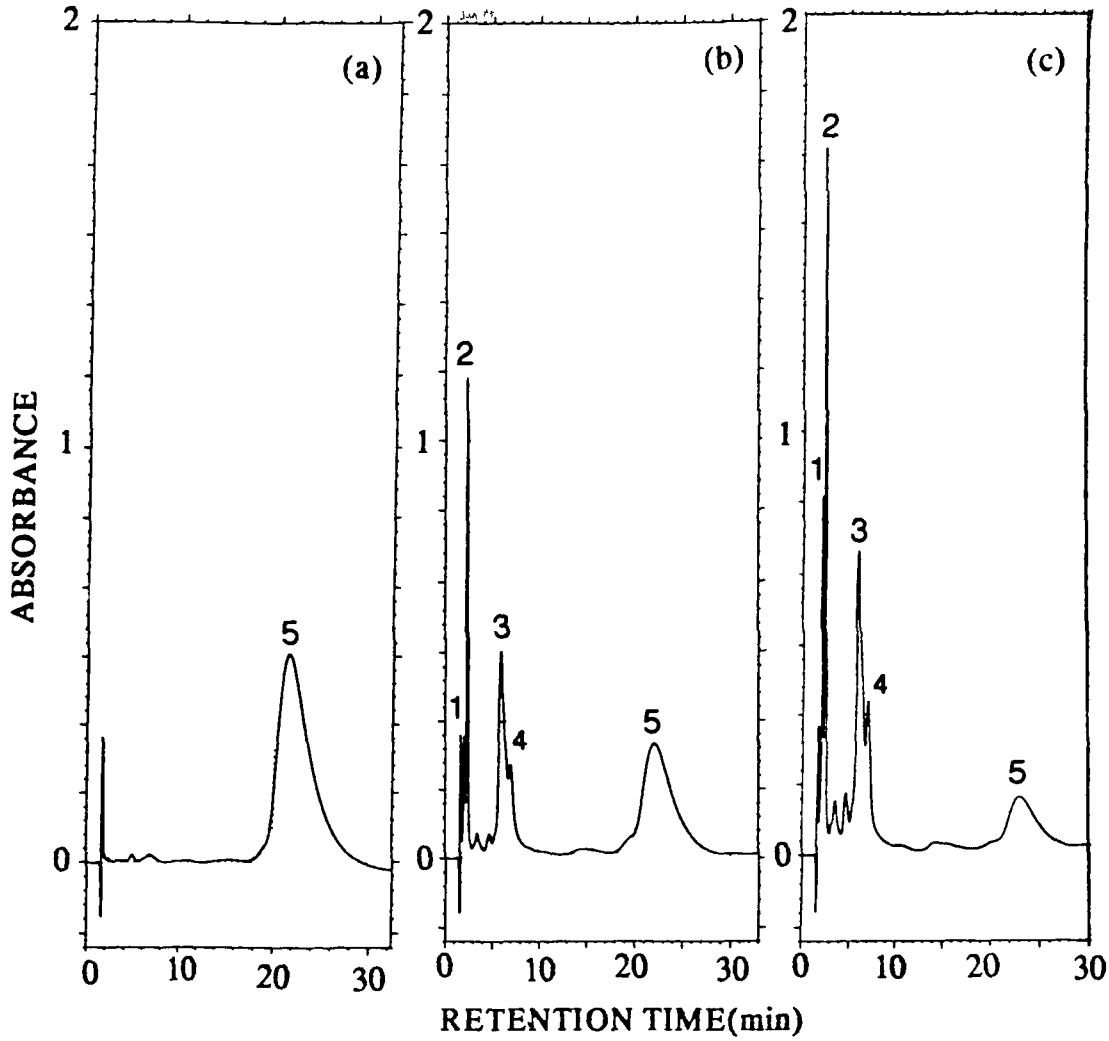

Figure 6 3 21

HPLC traces taken during the photolysis of $[(Ru(bpy)_2)_2(ppt)]^{3+}$ in MeCN containing 0 01 M Cl^- Photolysis times are (a) 0 min, (b) 120 min, and (c) 300 min For separation conditions see Figure 6 3 20

It, therefore, seems reasonable to assume that for $[(Ru(bpy)_2)_2(ppt)]^{3+}$, photolysis results in a cleavage of the Ru-N bond centred at the Ru-containing unit attached to the N1 position of the triazole ring and to the pyrazine ring Therefore, the ^3MC state responsible for this photolysis is localised at this site The ^3MLCT excited state responsible for emission is localised on this Ru-containing unit also (the LUMO is pyrazine-based)

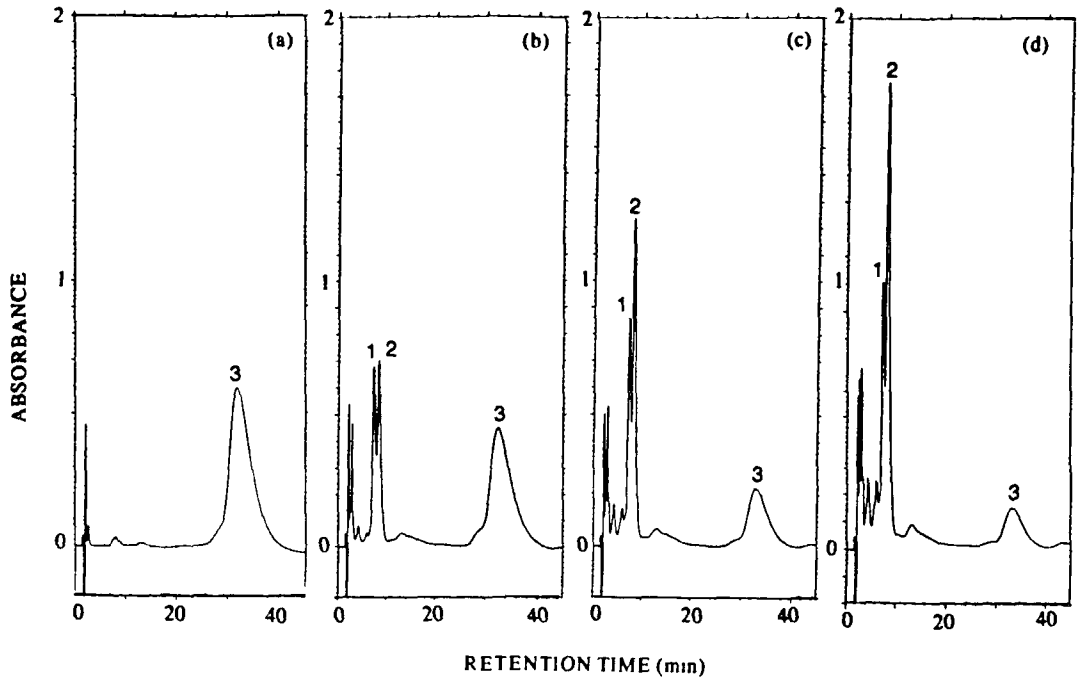

Figure 6 3 22

HPLC traces taken during the photolysis in MeCN of $[(Ru(bpy)_2)_2(ppt)]^{3+}$ Photolysis times are (a) 0 min, (b) For HPLC conditions see Figure 6 3 20.

The reason for the differences in photochemical properties for the dinuclear complexes containing the bpt^-, $bpzt^-$ and ppt^- bridging ligands is not that clear A tentative explanation is as follows

In the bpt^- dimer, the ^3MC excited states localised on both Ru-containing units are very close in energy, thus facilitating population of both sites in Cl^- containing solvents and leading to photodecomposition occurring from both Ru-containing units in the dinuclear complex Selective photodecomposition from the N4 site of the triazole ring is only encountered in pure MeCN

The ppt$^-$ dimer has greater asymmetric properties The weaker σ-donor properties of the pyrazine ring dominates the photochemical process, as the LUMO is now pyrazine-based Therefore, the ^{3}MLCT level may be lower in energy than for the bpt$^-$ complex However, the strong σ-donating properties of the pyridine ring leads to a much higher lying ^{3}MC state for this Ru-containing unit (perhaps even equivalent to the level at which the bpt$^-$ ^{3}MC state is found) This, therefore, leads to photodecomposition occurring only from the pyrazine-bound Ru-containing unit

For the bpzt$^-$ dimer, the situation is less clear In theory, the asymmetric properties of this ligand should be similar to those of the bpt$^-$ ligand and consequently their photochemical properties should be similar This, however, was not found to be the case The energy-gap between the ^{3}MLCT and ^{3}MC excited states is quite similar to that found for the bpt$^-$ dimer (3735 cm^{-1} for bpzt$^-$ versus 4061 cm^{-1} for bpt$^-$) The weaker σ-donor properties of the N4 site of the triazole ligand cause the lowest ^{3}MC excited state to be localised here, whereas the ^{3}MLCT excited state is localised on the Ru-containing unit attached to the N1 site of the triazole ring This latter state is much lower in energy (comparable to that of the ppt$^-$ dimer) than for bpt$^-$ The weaker σ-donor properties of pyrazine compared to pyridine must further attenuate the weaker σ-donor properties of the N4 site at the triazole ring This causes the ^{3}MC excited state of the Ru-containing unit attached to the N1 site of the triazole ring to be at a much higher energy than that of the N4 site and thus prevents its population, with the result that photodecomposition takes place solely from the Ru-containing unit attached to the N4 site of the triazole ring The behaviour observed is very much a combination of both the asymmetry of the triazole ligand and the differences between pyrazine and pyridine

6.4 CONCLUSION

In this chapter, the synthesis and properties of Ru(II)polypyridyl and Os(II)polypyridyl complexes containing the ppt$^-$ ligand have been illustrated and compared to the properties of analogous complexes containing the bpt$^-$ and bpzt$^-$ ligands It has been shown that even small changes in the bridging ligand can lead to quite large changes in the photochemical and photophysical properties of these compounds The Hppt ligand is a very interesting bridge as it has increased asymmetric properties compared with the other two ligands, thus making it's two co-ordination sites at the triazole ring very different The combination of both a pyridine and a pyrazine ring in the bridge results in Ru(II) (or Os(II)) mononuclear complexes which can have either properties related to either a weaker σ-donor (pyrazine) or a strong σ-donor (pyridine) ligand The uncoordinated ring can effect the properties as seen in the section on acid-base chemistry

In the dinuclear systems and for the protonated pyrazine-bound mononuclear complexes, the compounds take on properties very similar to those of the bpzt$^-$ dinuclear complex, with emission now becoming ppt$^-$-based Photochemistry becomes localised from the Ru-containing unit attached to the pyrazine ligand The influence of the asymmetric properties of the triazole ligand (i e N1 is a stronger σ-donor than N4 of the triazole ring) on the photochemical properties of complexes containing the Hppt ligand are negligible compared with the influence of the pyridine and pyrazine rings in the ligand

In the mixed-metal dimers, efficient energy-transfer takes place from the $Ru(bpy)_2$ to the $Os(bpy)_2$ moiety, resulting in emission that occurs exclusively from the latter site, with a consequent reduction in the luminescent lifetimes of the complexes The properties of the intervalence transition band point to strong metal-metal interaction for these complexes supporting this conclusion The

asymmetric properties of the bridging ligand is reflected in the differences in electrochemical potentials observed for these mixed-metal complexes Another result of this energy-transfer is that the dinuclear complexes are now photostable In fact, their temperature dependent luminescent lifetime profiles resemble closely those of the homonuclear osmium complex

Therefore, it is possible to alter the position of the ^{3}MLCT and ^{3}MC excited states by changing the bridging ligand or the metals in these systems Based on the knowledge gained in this study, it should be possible to predict the position of these excited states and thus the photochemical and photophysical properties of Ru(II)polypyridyl (or Os(II)polypyridyl) complexes relatively easily

6.5 REFERENCES

1 D Voet and J G Voet, *Biochemistry*, John Wiley and Sons, Inc , New York, **1990**, 586

2 J R Norris and M Schiffer, *Chem, & Chem Eng News*, **1990**, 23

3 P J Carroll and L E Brus, *J Am Chem Soc* , **1987**, *109*, 7613

4 D P Rillema and K B Mack, *Inorg Chem* , **1982**, *21*, 3849

5 V Balzani and F Scandola, *Supramolecular Photochemistry*, Ellis Horwood, **1991**

6 J R Norris and P Gast, *J Photochem* , **1985**, *29*, 185

7 V Balzani, *Pure & Appl Chem* , **1990**, *62*, 6, 1099

8 V Balzani, L Moggi, and F Scandola, *Supramolecular Photochemistry*, Reidel Publishing Company, **1987**, 1-28

9 S Bossmann and D Heinz, *EPA Newsl* , **1992**, *45*, 17

10 F Scandola, M T Indelli, C Chiroboli, and C A Bignozzi, *Top Curr Chem* , **1990**, *158*, 73

11 R H Morris, *Polyhedron*, **1987**, *6*, 793

12 R Ballardini, M T Gandolfi, M L Moya, L Prodi, and V Balzani, *Isr J Chem* , **1992**, *32*, 1, 47

13 J P Collman and J M Garner, *J Am Chem Soc* , **1990**, *112*, 166

14 L De Cola, F Barigelletti, V Balzani, P Belser, A von Zelewsky, C Seel, M Frank, and F Vogtle, *Coord Chem Rev* , **1991**, *111*, 255

15 S Serroni and G Denti, *Inorg Chem* , **1992**, *31*, 4251

16 G Denti, S Serroni, S Campagna, V Ricevuto, A Juris, M Ciano, and V Balzani, *Inorg Chim Acta*, **1992**, *198-200*, 507

17 S Campagna, G Denti, S Serroni, M Ciano, and V Balzani, *Inorg Chem* , **1991**, *30*, 3728

18 M Furue, T Yoshidzumi, S Kinoshita, T Kushida, S Nozakura, and M Kamachi, *Bull Chem Soc Jpn*, **1991**, *64*, 5, 1632

19 R Deusing, G Tapolsky, and T J Meyer, *J Am Chem Soc*, **1990**, *112*, 5378

20 K S Schanze and L Cabana, *J Phys Chem*, **1990**, *94*, 2740

21 R Hage, J G Haasnoot, J Reedijk, and J G Vos, *Chemtracts - Inorg Chem*, **1992**, *4*, 75

22 J H van Diemen, R Hage, J G Haasnoot, H E B Lempers, J Reedijk, J G Vos, L De Cola, F Barigelletti, and V Balzani, *Inorg Chem*, **1992**, *31*, 3518

23 D B McQueen and J D Peterson, *Coord Chem Rev*, **1990**, *97*, 249

24 R H Schmehl, R A Auerbach, W F Wacholtz, C M Elliot, R A Frietag, and J W Merkert, *Inorg Chem*, **1986**, *25*, 2440

25 T J Meyer, *Pure & Appl Chem*, **1986**, *58*, 9, 1193

26 J Van Houten and R J Watts, *J Am Chem Soc*, **1976**, *98*, 16, 4853

27 M A Ollino and A J Rest, *J Photochem Photobiol A Chem*, **1992**, 69, 73

28 Y Kawanishi, N Kitamura, and S Tazuke, *Inorg Chem*, **1989**, *28*, 2968

29 W F Wacholtz, R A Auerbach, and R H Schmehl, *Inorg Chem*, **1987**, *26*, 2989

30 J R Kirchhoff, D R McMillin, P A Marnot, and J P Sauvage, *J Am Chem Soc*, **1985**, *107*, 1138

31 F Barigelletti, A Juris, V Balzani, P Belser, and A von Zelewsky, *Inorg Chem*, **1987**, *26*, 4115

32 M Haga, *Inorg Chim Acta*, **1980**, *45*, L183

33 A M Bond and M Haga, *Inorg Chem*, **1986**, *25*, 4507

34 P Day and N Sanders, *J Chem Soc, A*, **1967**, 1536

35 J D Peterson, W R Murphy Jr , R Sahai, K J Brewer, and R R Ruminski, *Coord Chem Rev* , **1985**, *64*, 261

36 Y Fuchs, S Lofters, T Deiter, W Shi, R Morgan, T C Strekas, H D Gafney, and A D Baker, *J Am Chem Soc* , **1987**, *26*, 4148

37 S Ernst, V Kasack, and W Kaim, *Inorg Chem* , **1988**, *27*, 1146

38 B P Sullivan, D J Salmon, and T J Meyer, *Inorg Chem* , **1978**, *17*, 12, 3334

39 P A Lay, A M Sargeson, H Taube, M H Chou, and C Creutz, *Inorg Synth* , John Wiley and Sons, **1986**, 24

40 R Hage, R A G de Graaff, J G Haasnoot, J P Turkenberg, J Reedijk, and J G Vos, *Acta Crystallogr , Sect C* , **1989**, *C45*, 381

41 G Orellana, C A Ibarra, and J Santoro, *Inorg Chem* , **1988**, *27*, 1025

42 G M Bryant and J E Fergusson, *Aust J Chem* , **1971**, *24*, 441

43 Y Ohsawa, M K DeArmond, K W Hanck, and C G Moreland, *J Am Chem Soc* , **1985**, *107*, 5383

44 J M de Wolf, R Hage, J G Haasnoot, J Reedijk, and J G Vos, *New J Chem* , **1991**, *15*, 501

45 M N Ackermann and L V Interrante, *Inorg Chem* , **1984**, *23*, 3904

46 E C Constable and J Lewis, *Inorg Chim Acta*, **1983**, *70*, 251

47 M Haga, *Inorg Chim Acta*, **1983**, *77*, L39

48 R Hage, J G Haasnoot, H A Nieuwenhuis, J Reedijk, D J A De Ridder, and J G Vos, *J Am Chem Soc* , **1990**, *112*, 9245

49 K Kalyanasundaram, Md K Nazeeruddin, M Gratzel, G Viscardi, P Savarino, and E Barni, *Inorg Chim Acta*, **1992**, *198-200*, 831

50 R J Staniewicz and D G Hendricker, *J Am Chem Soc* , **1977**, *99*,20, 6581

51 R M Berger, *Inorg Chem* , **1990**, *29*, 1920

52 J M Kelly, C Long, C M O'Connell, J G Vos, and A H A Tinnemans, *Inorg Chem*, **1983**, *22*, 20, 2818

53 R W Harrigan and G A Crosby, *J Chem Phys*, **1973**, *59*, 7, 3468.

54 D Sandrini, M Maestri, V Balzani, U Maeder, and A von Zelewsky, *Inorg Chem*, **1988**, *27*, 2640

55 R Hage, A H J Dijkhuis, J G Haasnoot, R Prins, J Reedijk, B E Buchanan, and J G Vos, *Inorg Chem*, **1988**, *27*, 2185

56 M Haga, T Matsumura-Inoue, and S Yamabe, *Inorg Chem*, **1987**, *26*, 4148

57 R Hage, R Prins, J G Haasnoot, J Reedijk, and J G Vos, *J Chem Soc, Dalton Trans*, **1987**, 1389

58 G Denti, S Serroni, L Sabatino, M Ciano, V Ricevuto, and S Campagna, *Gazz Chem Ital*, **1991**, *121*, 37

59 L M Vogler, B Scott, and K J Brewer, *Inorg Chem*, **1993**, *32*, 898

60 M L Myrick and M K De Armond, *J Phys Chem*, **1989**, *93*, 7099

61 K A Goldsby and T J Meyer, *Inorg Chem*, **1984**, *23*, 3002

62 K Kalyanasundaram and Md K Nazeeruddin, *Chem Phys Letts*, **1989**, *158*, 45

63 J G Vos, *Polyhedron*, **1992**, *11*, 18, 2285

64 C Long and J G Vos, *Inorg Chim Acta*, **1984**, *89*, 125

65 J Davila, C A Bignozzi, and F Scandola, *J Phys Chem*, **1989**, *93*, 1373

66 R Hage, J G Haasnoot, H A Nieuwenhuis, J Reedijk, R Wang, and J G Vos, *J Chem Soc, Dalton Trans*, **1991**, 3271

67 H A Nieuwenhuis, J G Haasnoot, R Hage, J Reedijk, T L Snoeck, D J Stufkens, and J G Vos, *Inorg Chem*, **1991**, *30*, 48

68 B D J R Fennema, J G Haasnoot, R Hage, J Reedijk, and J G Vos, *Inorg Chim Acta*, **1990**, *171*, 223

69 B E Buchanan, R Wang, J G Vos, R Hage, J G Haasnoot, and J. Reedijk, *Inorg Chem*, **1990**, *29*, 3263

70 R Hage, J G Haasnoot, J Reedijk, R Wang, E M Ryan, J G Vos, A L. Spek, and A J M Duisenberg, *Inorg Chim Acta*, **1990**, *174*, 77.

71 S D Ernst and W Kaim, *Inorg Chem*, **1989**, *28*, 1520

72 E S Dodsworth and A B P Lever, *Chem Phys Letts*, **1986**, *124*, 2, 152

73 D P Rillema, G Allen, T J Meyer, and D Conrad, *Inorg Chem*, **1983**, *22*, 1617

74 C M Elliot and E J Hershenhart, *J Am Chem Soc*, **1982**, *104*, 7519

75 R Hage, J G Haasnoot, D J Stufkens, T L Snoeck, J G Vos, and J Reedijk, *Inorg Chem*, **1989**, *28*, 1413

76 K J Takeuchi, M S Thompson, D W Pipes, and T J Meyer, *Inorg Chem*, **1984**, *23*, 1845

77 K Kalyanasundaram and Md K Nazeeruddin, *Inorg Chim Acta*, **1990**, *171*, 213

78 E S Dodsworth and A B P Lever, *Chem Phys Letts*, **1984**, *112*, 6, 567.

79 E S Dodsworth and A B P Lever, *Chem Phys Letts*, **1985**, *119*, 1, 61

80 F Barigelletti, L De Cola, V Balzani, R Hage, J G Haasnoot, J Reedijk, and J G Vos, *Inorg Chem*, **1989**, *28*, 4344

81 A Juris, V Balzani, F Barigelletti, S Campagna, P Belser, and A von Zelewsky, *Coord Chem Rev*, **1988**, *84*, 85

82 F Barigelletti, L De Cola, V Balzani, P Belser, A von Zelewsky, F. Vogtle, F Ebmeyer, and S Grammenudi, *J Am Chem Soc*, **1989**, *111*, 4662

83 F Barigelletti, A Juris, V Balzani, P Belser, and A von Zelewsky, *Inorg. Chem*, **1983**, *22*, 3335

84 A Juris, F Barigelletti, V Balzani, P Belser, and A von Zelewsky, *J Chem Soc , Faraday Trans 2*, **1987**, *83*, 12, 2295

85 F Barigelletti, A Juris, V Balzani, P Belser, and A von Zelewsky, *J. Phys Chem* , **1987**, *91*, 1095

86 J V Caspar and T J Meyer, *Inorg Chem* , **1983**, *22*, 2444

87 E M Kober and T J Meyer, *Inorg Chem* , **1984**, *23*, 3877

88 G H Allen, R P White, D P Rillema, and T J Meyer, *J Am Chem Soc* , **1984**, *106*, 2613

89 K R Barqawi, A Llobet, and T J Meyer, *J Am Chem Soc* , **1988**, *110*, 7751

90 S F McClamaham, R F Dallinger, F J Holler, and J R Kincaid, *J Am Chem Soc* , **1985**, *107*, 4853

91 E M Kober, J V Caspar, R S Lumpkin, and T J Meyer, *J Phys Chem* , **1986**, *90*, 3722

92 J Van Houten and R J Watts, *Inorg Chem* , **1978**, *17*, 12, 3381

93 B Durham, J V Caspar, J K Nagle, and T J Meyer, *J Am Chem Soc* , **1982**, *104*, 4803

94 F Barigelletti, L De Cola, V Balzani, R Hage, J G Haasnoot, J Reedijk, and J G Vos, *Inorg Chem* , **1991**, *30*, 641

95 R Hage, *Coord Chem Rev* , **1991**, *111*, 161

96 G A Heath, L J Yellowlees, and P S Braterman, *Chem Phys Letts* , **1982**, *92*, 6, 646

97 A H A Tinnemans, K Timmer, M Reinten, J G Kraaijkamp, A H Alberts, J G M van der Linden, J E J Schmitz, and A A Saaman, *Inorg Chem.*, **1981**, *20*, 3698

98 J T Hupp and T J Meyer, *Inorg Chem* , **1987**, *26*, 2332

99 R Hage, J G Haasnoot, J Reedijk, R Wang, and J G Vos, *Inorg Chem*, *1991*, *30*, 3263

100 M Haga, *Inorg Chim Acta*, **1983**, *75*, 29

101 J E Sutton and H Taube, *Inorg Chem*, **1981**, *20*, 10, 3125

102 C Creutz, *Prog Inorg Chem*, **1983**, *30*, 1

103 D E Richardson and H Taube, *J Am Chem Soc*, **1983**, *105*, 40

104 J T Hupp, *J Am Chem Soc*, **1990**, *112*, 1563

105 Y J Chang, X Xu, T Yabe, S Yu, D R Anderson, L K Orman, and J B Hopkins, *J Phys Chem*, **1990**, *94*, 729

106 P A Mabrouk and M S Wrighton, *Inorg Chem*, **1986**, *25*, 526

107 C H Braunstein, A D Baker, T C Strekas, and H D Gafney, *Inorg. Chem*, **1984**, *23*, 857

108 P G Bradley, N Kress, B A Hornberger, R F Dallinger, and W H Woodruff, *J Am Chem Soc*, **1981**, *103*, 7441

109 J R Kincaid, *Energy Res Abstr*, **1990**, *15*, 17, 1

110 G D Danzer and J R Kincaid, *J Phys Chem*, **1990**, *94*, 3976

CHAPTER 7

RUTHENIUM COMPOUNDS WITH PYRIDYLTRIAZINE LIGANDS: FINE-TUNING OF THE ELECTROCHEMICAL AND PHOTOPHYSICAL PROPERTIES

7.1 INTRODUCTION

As we have already seen in Chapter 1, photosubstitution of Ru(II) polypyridyl complexes represent a major problem for their application in solar-energy conversion systems Strategies to eliminate the dd state from its role in the excited-state manifolds of these complexes have involved turning to Os(II), where 10 Dq is approximately 30% greater than for Ru(II)[1-2], and to mixed-ligand chelates of ruthenium(II), where the ^{3}MLCT - ^{3}MC energy gap can be increased by lowering the energy of the ^{3}MLCT level[3]

The properties of a series of Ru(II) polypyridyl complexes containing strong σ-donor ligands have already been examined in detail in the previous chapters 1,2,4-triazole ligands act as spectator ligands and are in most cases not directly involved in the emission processes[4-8] They can, however, control metal-metal interaction, influence the position of the lowest MLCT band and dictate the photostability (i e whether population of the ^{3}MC excited state can occur) of the compounds[9]

The properties of Ru(II) polypyridyl complexes containing weak σ-donor ligand with strong π-acceptor properties (compared with bpy) have also been examined in great detail Examples of such ligands are 2,3-bis(2-pyridyl)pyrazine (dpp)[10-13], pyrazine (pz)[14-15], 4,4'-di-(carboxy)-2,2'-bipyridine (dcbpy)[16-17], 2,2'-bipyrimidine (bpym)[18-22] and dipyrido[3,2-c 2',3'-e]pyridazine (taphen)[23-24] Analysis of these $[Ru(bpy)_2(LL')]^{n+}$ complexes reveal that these ligands are directly involved in the emission processes i e the lowest unoccupied molecular orbital (LUMO) is located on the LL' ligand and the bpy ligands merely act as spectator ligands Low first reduction potentials and high oxidation potentials result for the ruthenium compounds It was found that low lying π* levels in complexes that contain ligands such as those mentioned above, lead to significant changes in

ground- and excited-state redox potentials, but to relatively small changes in absorption and emission spectral properties[25-26] The compounds, therefore, retain their useful light absorption properties in the visible region of the spectrum, while at the same time, the photostability of the complexes may be increased

According to Lever[26], a ligand with a weaker σ-donor capacity compared to bpy gives rise to a greater effective nuclear charge on the ruthenium centre which results in stabilisation of the metal d orbitals The greater effective nuclear charge on the ruthenium could have the synergistic effect of lowering the energy of the ligand π^* level through charge interaction, thus destabilising the ligand π^* level[19] Further stabilisation of Ru(II) could then occur by back-bonding of the $d\pi$ orbitals with the π^* level of the co-ordinating ligands This would further suggest that the lower π^* levels in the ligand would result in more effective mixing with the metal $d\pi$ energy levels and result in stabilisation of the $(d\pi)^6$ configuration for Ru(II)

Furthermore, electron-withdrawing substituents should also stabilise the lowest lying MLCT states relative to the dd states resulting in a larger energy gap between the ^{3}MLCT and the ^{3}MC excited states[27] Hence, with sufficiently good electron-withdrawing substituents, thermally accessible dd states and ligand loss photochemistry can in principle be designed out of the complex In terms of synthetic design, chromophoric ligands having low-lying π^* levels offer the advantage of loss of complications arising from low-lying dd states without a significant lowering in the excited-state lifetimes There is evidence that photosubstitution follows a general pattern based on the energy-gap between the ^{3}MLCT state and the ^{3}MC excited state and, therefore, if this energy-gap is sufficiently increased by an appropriate choice of co-ordinating ligands, it should be possible to prevent photodecomposition of the Ru(II) polypyridyl complexes[28]

There is, however, a problem associated with this approach which has its basis in the energy gap law[29-32] As the emission energy decreases, the

luminescent lifetime also decreases This effect is due to an increase of the nonradiative decay rate (k_{nr})[29] The energy-gap law predicts that radiationless decay rates depend on the energies of the emitting state, namely the lower the energy of an emitting state, the more strongly it couples with the ground state and the larger the value of k_{nr} Hence, the luminescent lifetime decreases

In this chapter, we concentrate on a series of pyridyltriazine ligands and examine the effect of the more electron-withdrawing six-membered ring in comparison with the aforementioned electron-donating five-membered triazole ring Much attention has been focused on effects arising from the effect of substituent changes in the chromophoric ligand in a co-ordination environment, i e , by the addition of electron-withdrawing or electron-donating substituents on the triazine ring The ligands studied are 3-(pyridin-2-yl)-1,2,4-triazine (pt), 5,6-dimethyl-3-(pyridin-2-yl)-1,2,4-triazine (dmpt), 5,6-diphenyl-3-(pyridin-2-yl)-1,2,4-triazine (dppt) and 3,5,6-tris-(pyridin-2-yl)-1,2,4-triazine (tpt) For the structure of these ligands, see Figure 7 1 1 The effect of lowering the ligand π^* level is investigated with respect to the photostability of the Ru(II) polypyridyl complexes.

A number of ruthenium compounds containing the ligands dmpt, dppt and tpt have already been prepared by Hage et al[33] The results suggest that the pyridyltriazine ligands have rather low-lying LUMO levels, and have weaker σ-donor properties than those of 2,2'-bipyridine Furthermore, it was concluded that these ligands do not merely act as spectator ligands, but participate actively in the photophysical processes occurring for these complexes However, no photophysical studies were carried out In this chapter, the photophysical properties of mononuclear Ru(II) polypyridyl complexes containing the ligands pt, dmpt and dppt were investigated

A dinuclear compound containing the pt ligand is also investigated, where one Ru-containing unit is bound bidentately to the triazine ligand and to the N of

the pyridyl ring and the other Ru-containing unit must be co-ordinated in a monodentate fashion to another N at the triazine ring This is quite and unusual compound because of the monodentate nature of one of its ruthenium units and its electronic and electrochemical properties are, therefore, investigated in detail

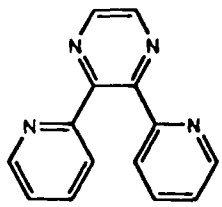

dpp

2,3-bis(2-pyridyl)pyrazine

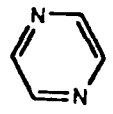

pyrazine

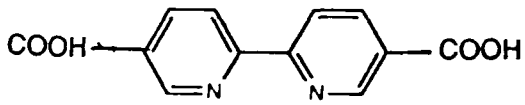

dcbpy

4,4'-di-(carboxy)-2,2'-bipyridine

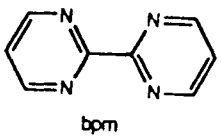

bpm

2,2'-bipyrimidine

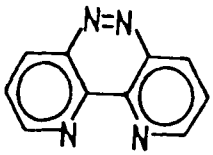

taphen

dipyrido[3,2-c 2',3'-e]pyridazine

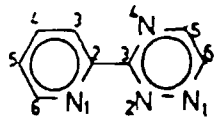

pt

3-(pyridin-2-yl)-1,2,4-triazine

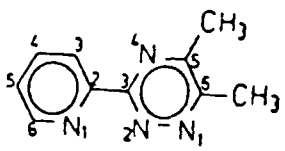

dmpt

5,6-dimethyl-3-(pyridin-2-yl)-1,2,4-triazine

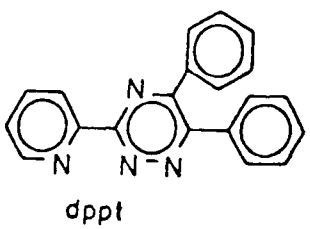

dppt

5,6-diphenyl-3-(pyridin-2-yl)-12,4-triazine

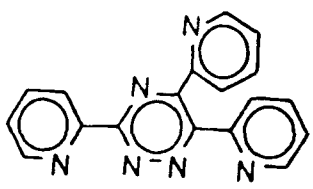

tpt

3,5,6-tris-(pyridin-2-yl)-1,2,4-triazin

Figure 7 1 1

Structure of the ligands cited in the text

7.2 EXPERIMENTAL

7 2 1 *Preparation of the ligands*

The ligands 3-(pyridin-2-yl)-1,2,4-triazine (pt), 5,6-dimethyl-3-(pyridin-2-yl)-1,2,4-triazine (dmpt), 5,6-diphenyl-3-(pyridin-2-yl)-1,2,4-triazine (dppt) and 3,5,6-tris-(pyridin-2-yl)-1,2,4-triazine (tpt) were synthesised by Dr R Hage, Leiden University, The Netherlands cis-$[Ru(bpy)_2Cl_2]$ $2H_2O$ was prepared as mentioned in Section **3 2**

7 2 2 *Preparation of the complexes*

$[Ru(bpy)_2(pt)](PF_6)_2$ **(1)**

520 mg (1 mmol) cis-$[Ru(bpy)_2Cl_2]$ $2H_2O$ was heated under reflux with 2 2 mmol Hpt (350 mg) for 6 hr in 50 cm^3 ethanol water (1 1 v\v) After evaporating the alcohol, an excess of aqueous NH_4PF_6 was added The resulting precipitate was filtered and recrystallised from acetone water (1 1 v\v) Although two isomers are possible for this complex, only one isomer was observed in the HPLC traces in appreciable yields Further purification took place by semi-preparative HPLC, using a mobile phase of 80 20 acetonitrile water containing 0 1 M KNO_3 and a flowrate of 2 5 cm^3/min Yield 70% (560 mg) Found for $C_{28}H_{22}F_{12}N_8P_2Ru$ C, 38 8, H, 2 6, N, 13 0% Anal Calcd C, 39 0, H, 2 6, N, 13 0%

$[Ru(bpy)_2(dmpt)](PF_6)_2$ H_2O **(2)**

This complex was prepared according to literature methods[33] and purified as for compound (**1**) Two isomers formed in the ratio of 4 1 The main fraction was isolated in good yield, but the second isomer was only obtained in small

quantities Therefore, a very limited analysis of this fraction is given Yield 70% (635 mg) for isomer 1 Yield 10% (90 mg) for isomer 2 Found for $C_{30}H_{28}F_{12}N_8OP_2Ru$ (isomer 1) C, 40 1, H, 3 0, N, 12 4% Anal Calcd C, 39 7, H, 3 1, N, 12 4%

$[Ru(bpy)_2(dppt)](PF_6)_2$ **(3)**

This complex was prepared and purified as for compound (**2**), yielding one main fraction Yield 80% (810 mg) Found for $C_{40}H_{30}F_{12}N_8P_2Ru$ C, 47 6, H, 3 1, N, 11 0% Anal Calcd C, 47 4, H, 3 0, N, 11 1%

$[Ru(bpy)_2(tpt)](PF_6)_2\ H_2O$ **(4)**

This compound was again prepared and purified as for compound (**2**) Yield 65% (670 mg) Found for $C_{38}H_{30}F_{12}N_{10}OP_2Ru$ C, 44 0, H, 3 0, N, 13 5% Anal Calcd C, 44 1, H, 2 9, N, 13 6%

$[(Ru(bpy)_2)_2(pt)Cl](PF_6)_3\ 2H_2O$ **(5)**

1 14 g (2 2 mmol) cis-$[(Ru(bpy)_2Cl_2]\ 2H_2O$ and 160 mg (1 mmol) Hpt was heated under reflux for 8 hr in ethanol water (1 1) The resulting complex was isolated by addition of aqueous NH_4PF_6 after evaporation of the ethanol The compound was purified by repetitive recrystallisation from acetone water (1 1 v\v) Yield 45% (670 mg) Found for $C_{48}H_{42}F_{18}N_{12}O_2P_3Ru_2$ C, 38 7, H, 2 7, N, 11 3% Anal Calcd C, 38 6, H, 2 8, N, 11 3%

7.3 RESULTS AND DISCUSSION

7 3 1 *^{1}H NMR spectra*

Table 7 1 lists the ^{1}H NMR resonances obtained for Ru(II) polypyridyl complexes containing the triazine ligands Chemical shifts of the bpy ligands have been omitted because of their similarity to those reported previously for other similar compounds[34-38] In fact, the bpy protons of all four compounds are very similar The complexity of the spectra made it necessary to carry out COSY experiments to assign the peaks[39]

Figure 7 3 1 contains as a representative example, the ^{1}H and COSY NMR spectrum of $[Ru(bpy)_2(pt)]^{2+}$ For the mononuclear $[Ru(bpy)_2(LL)]^{2+}$ complexes (where LL = pt, dmpt, dppt and tpt), H^3 is shifted at least 0 46 ppm downfield compared with the free ligand This is caused by the presence of the metal ion forcing the ligand to adopt a cis-conformation The steric crowding of the H^3 proton and strong Van-der-Waals interactions causes a significant downfield shift of the H^3 proton[40-41] The H^4 and H^5 protons are similarly shifted downfield for all the complexes, again due to their proximity to the metal ion, although the effect is less noticeable for these protons On the other hand, the H^6 proton is shifted by at least 0 49 ppm upfield in comparison with the free ligand This is due to the position of the H^6 proton lying just above a pyridyl ring of an adjacent bpy ligand[42-43] The singlet at 7 35 ppm shows up in the spectra of all of the complexes and is not coupled to any other proton For this reason, it is assumed to be an impurity in the solvent used, i e all NMR spectra were carried out in the same CD_3CN

The co-ordination mode of the pyridyltriazine ligands is expected to be via N2 of the triazine ring and via the pyridine nitrogen atom[33] In this case, much less

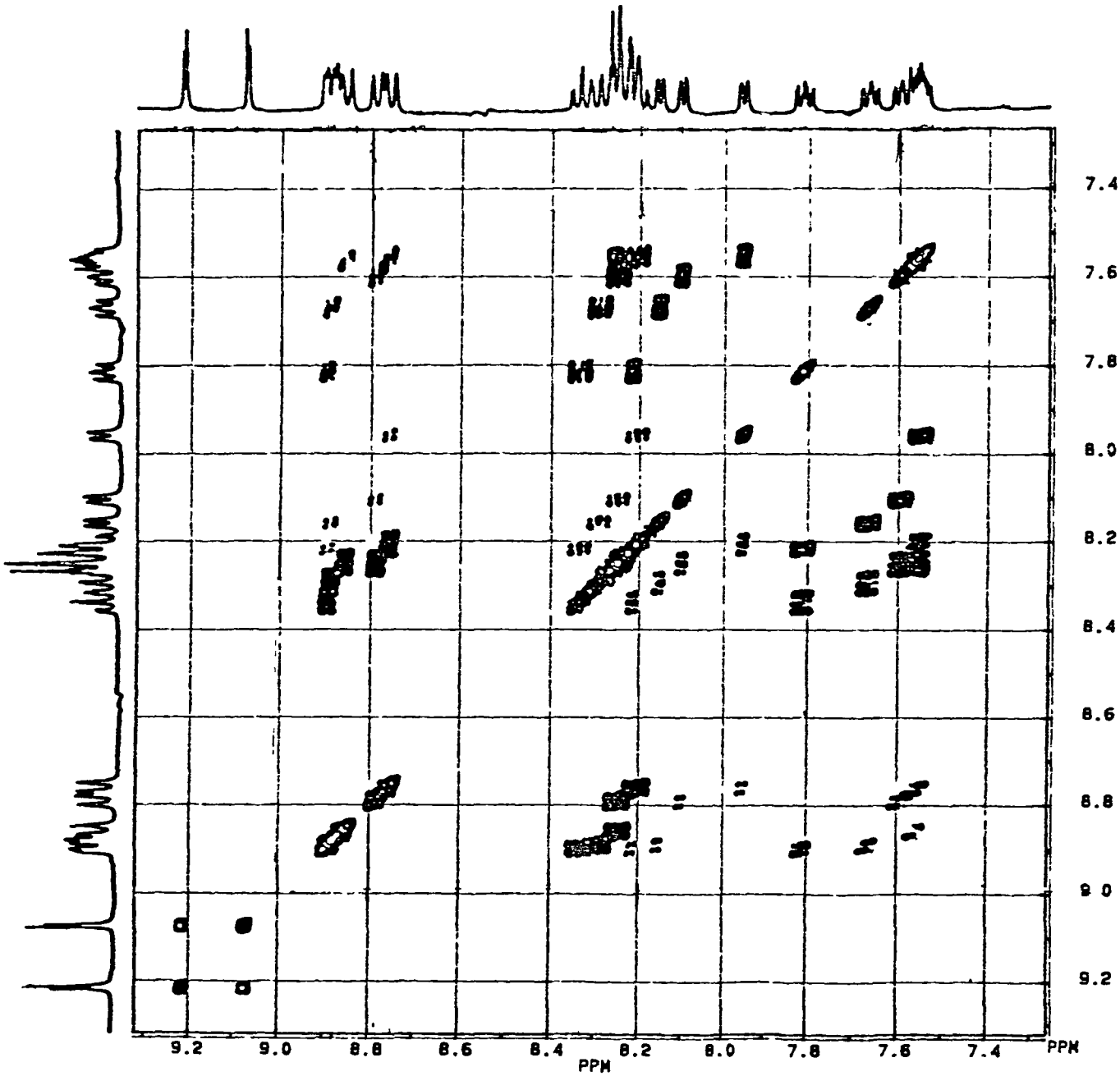

Figure 7 3 1

400 MHz ^{1}H and COSY NMR spectrum of $[Ru(bpy)_2(pt)]^{2+}$ in CD_3CN

Compound	H^3	H^4	H^5	H^6	R
$[Ru(bpy)_2(pt)]^{2+}$	8 88 (d) (-0 57)	8 33 (t) (-0 41)	7 81 (t) (-0 32)	8 21 (d) (+0 49)	9 06 9 21[a] (d) (d)
$[Ru(bpy)_2(dmpt)]^{2+}$ F1	8 78 (d) (-0 42)	8 26 (t) (-0 27)	7 72 (t) (-0 17)	8 12 (d) (+0 64)	2 45 2 70[b] (s) (s)
$[Ru(bpy)_2(dmpt)]^{2+}$ F2	9 02 (-0 66)	8 22 (-0 23)	7 56 (-0 01)	7 65 (+1 11)	2 22 2 55[b] (s) (s)
$[Ru(bpy)_2(dppt)]^{2+}$	9 00 (d) (-0 64)	8 33 (t) (-0 34)	7 80 (t) (-0 25)	8 24 (d) (+0 52)	7 14 - 8 02[c] (m)
$[Ru(bpy)_2(tpt)]^{2+}$	9 05 (d) (-0 46)	8 35 (t) (-0 24)	7 82 (t) (-0 17)	8 27 (d) (+0 60)	7 41 - 8 40[d] (m)
$[(Ru(bpy)_2)_2(pt)Cl]^{3+}$ F1	8 83 (d) (-0 52)	8 26 (t) (-0 34)	7 59 (t) (-0 10)	8 50 (d) (+0 20)	8 23 (d) 10 00 (d)
$[(Ru(bpy)_2)_2(pt)Cl]^{3+}$ F2	8 78 (d) (-0 47)	8 25 (t) (-0 33)	7 66 (t) (-0 17)	8 54 (d) (+0 16)	8 23 (d) 10 00 (d)
pt	8 31 (d)	7 92 (t)	7 49 (t)	8 70 (d)	8 90 9 50 (d)[a]
dmpt	8 36 (d)	7 99 (t)	7 55 (t)	8 76 (d)	2 70 2 60 (s)[b]
dppt	8 54 (d)	8 06 (t)	7 62 (t)	8 84 (d)	7 37-7 89 (m)[c]
tpt	8 61 (d)	8 11 (t)	7 67 (t)	8 88 (d)	7 44-8 37 (m)[d]

Table 7 1

^1H NMR resonances of the triazine complexes in CD_3CN and free ligands in deuterated DMSO (R groups a = H, b = CH_3, c = phenyl, and d = pyridyl) (s = singlet, d = doublet, t = triplet and m = multiplet)

steric hindrance between the R groups and adjacent ligands is present The chemical shifts of the protons of the R groups (H, CH_3, phenyl or pyridyl) are not changed much upon co-ordination, indicating that steric hindrance is not present to a large extent

The dinuclear complex, $[(Ru(bpy)_2)_2(pt)Cl]^{3+}$, has a very complicated ^1H NMR spectrum (see Figure 7 3 2) and consequently no complete assignment of the NMR peaks is possible The spectrum does, however, indicate the presence of two isomers for this complex The presence of these isomers is not expected to affect the physical properties of the complexes and, therefore, no attempt was made to separate them further[44] All future measurements are carried out on this mixture of two isomers

The H^3 proton of the dinuclear complex is shifted downfield to the same extent as with the monomeric complex However, a less dramatic upfield shift of the H^6 proton is observed when a second Ru ion is co-ordinated The presence of the second metal ion causes the steric interaction between the bpy rings and the triazine ligand to increase[45] Also, the sharing of the electron density on the triazine ligand between two metal ions causes a less dramatic downfield shift of the H^3 proton in comparison with the mononuclear situation[44]

The similarities between the resonances observed for the mononuclear and dinuclear complexes suggest that again in the dimeric situation co-ordination of one $Ru(bpy)_2$ unit occurs via N2 of the triazine ring The second $Ru(bpy)_2Cl$ unit must be co-ordinated either via N1 or N4 of the triazine ring Due to steric reasons, N4 is the favoured site of co-ordination Due to the presence of the Cl^- ion, if co-ordination via N2 of the triazine ring was taking place, a large downfield shift of the H^3 proton would be expected due to the effect of the polarised Ru-Cl bond[46] Therefore, it is postulated that the $Ru(bpy)_2$ unit is co-ordinated bidentately via N2 of the triazine ring and the $Ru(bpy)_2Cl$ unit is co-ordinated in a monodentate

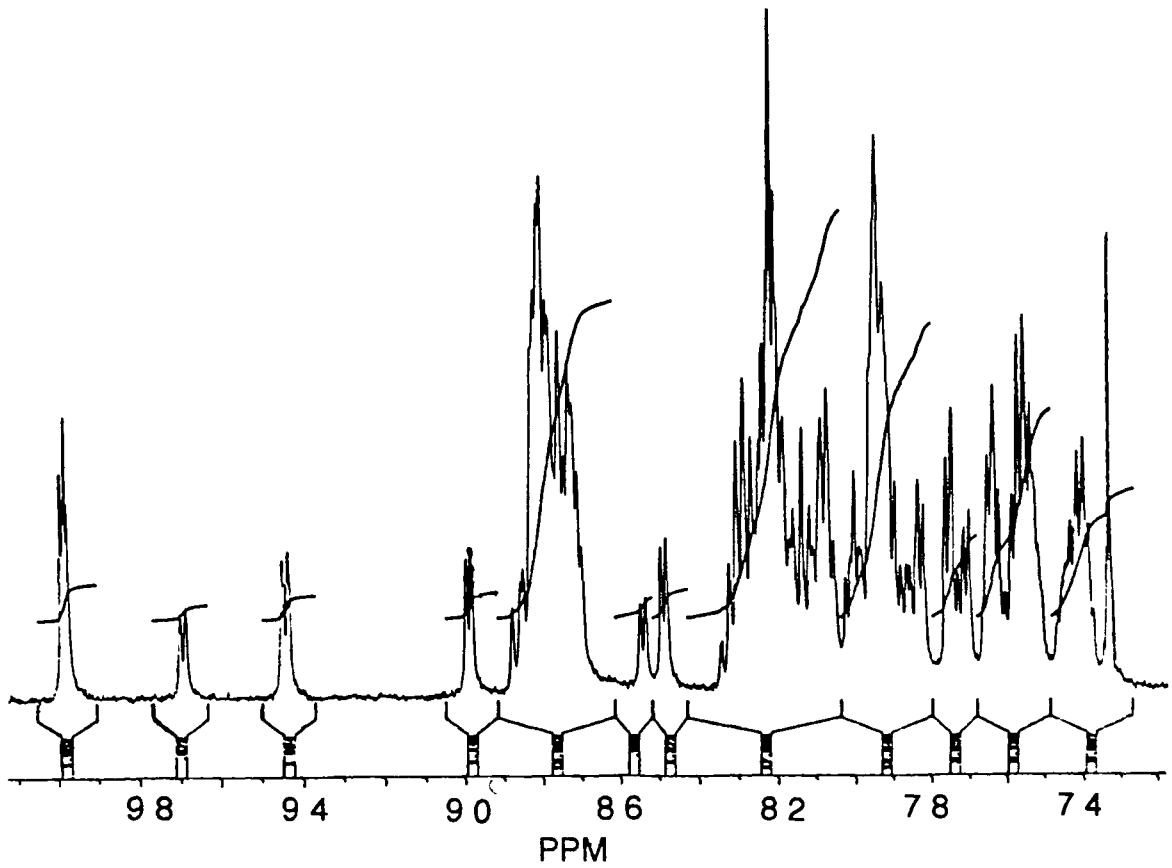

Figure 7 3 2

400 MHz ^1H NMR spectrum of $[(Ru(bpy)_2)_2(pt)Cl]^{3+}$ in CD_3CN

fashion via N4 of the triazine ring In order to elucidate the structure of this compound fully, an X-ray structure would be necessary

7 3 2 *Absorption and Emission properties*

The absorbance and emission maxima of the triazine complexes are presented in Table 7 2 Included in this table are the extinction coefficients and luminescent lifetimes of the complexes

Compared with $[Ru(bpy)_3]^{2+}$, the maximum wavelength of absorption for $[Ru(bpy)_2(pt)]^{2+}$ is only slightly blue-shifted However, the presence of two methyl substituents in the dmpt complex causes a considerable blue shift in the λ_{max} Again a blue shift is observed when the dinuclear $[(Ru(bpy)_2)_2(pt)Cl]^{3+}$ complex is formed In the case of complexes containing the ligands dppt and tpt, a red shift in the λ_{max} is observed Similarly, in the case of the emission maxima, a shift to higher energy is observed for complexes containing dmpt and for the dinuclear complex compared with $[Ru(bpy)_2(pt)]^{2+}$ and a shift to lower energy is seen when the hydrogens are replaced by phenyl or pyridine rings

The differences observed in the λ_{max} of absorption for these complexes compared with $[Ru(bpy)_3]^{2+}$ may be related to the inductive effect of the substituents on the triazine ring, as no shift in the λ_{max} is observed when bpy is replace by pt (the non-substituted pyridyltriazine ligand)[44] The position of these bands are governed by both the σ-donor and π-acceptor properties of the ligand[41] Electron-withdrawing ligands reduce the electron density on the metal ion resulting in a stabilisation of the metal-based t_{2g} level with a consequent blue shift of the MLCT bands Strong σ-donating ligands cause destabilisation of the filled d orbitals and, therefore, the MLCT band shifts to lower energy Similar shifts are observed with the emission maxima at room temperature and at 77 K

The blue shift observed in the absorption and emission maxima upon replacement of the pt ligand with the dmpt ligand has been encountered before for

Compound	[a]Absorption (log ε)		[a]Emission (τ/μs) 298 K		[b]Emission (τ/μs) 77 K	
$[Ru(bpy)_2(pt)]^{2+}$	450	(4 14)	688	(0 084)	632	(5 06)
$[Ru(bpy)_2(dmpt)]^{2+}$ 1	443	(4 16)	663	(0 097)	612	(5 75)
$[Ru(bpy)_2(dmpt)]^{2+}$ 2	435	(---)	654	(0 093)	617	(5 42)
$[Ru(bpy)_2(dppt)]^{2+}$	475	(4 30)	712	(1 08)	651	(10 09)
$[Ru(bpy)_2(tpt)]^{2+}$	485	(4 23)	722	(0 37)	704	(7 26)
$[(Ru(bpy)_2)_2(pt)Cl]^{3+}$	438 597	(4 19) (4 45)	665	(0 096)	611	(4 93)
$[Ru(bpy)_3]^{2+}$	452	(4 11)	608	(0 62)	582	(4 80)

Table 7 2

Absorption and Emission properties of the triazine compounds [a]Measured in acetonitrile [b]Measured in ethanol Lifetime measurements (± 0 02 μs) carried out under argon

complexes containing methyl substituents[48-50] It reflects the decrease in electronic charge occurring on Ru(II) as a consequence of the increased π-acceptor ability and lower σ-donor ability of dmpt relative to pt

Upon co-ordination of a second metal ion, the π-acceptor properties of the triazine ligand now has to be shared between two metal sites, thus causing a shift to higher energy of the MLCT bands[51-52] The low energy band at 597 nm is in agreement with the presence of a $[RuN_5Cl]$ moiety[53] There is a shift to higher energy for the emission maximum compared with the mononuclear case, again due to the sharing of the π-acceptor properties of the pt ligand upon co-ordination

of the second $Ru(bpy)_2$ unit It is very unusual to observe an emission from this type of dinuclear species However, the emission occurs at a different wavelength than that observed for the mononuclear complex and from both HPLC analysis and NMR data no impurity appears to be present in the sample Therefore, it is concluded that the emission observed for this dinuclear species is due to a metal-to-ligand charge transfer transition and not due to an impurity in the sample.

7 3 3 *Acid-Base properties*

For the mononuclear complexes containing the ligands pt, dmpt and dppt, no shift in the λ_{max} was observed upon changing the pH in the pH range 1 5 - 9, due to the absence of an available N-H group on the triazine ring The triazine ligands are considerably more acidic than the 1,2,4-triazole complexes studied previously[54-56]

The only compound to exhibit any pH dependency in its absorption spectrum was $[Ru(bpy)_2(tpt)]^{2+}$ As can be seen from Figure 7 3 3, a shift in the λ_{max} from 495 nm to 523 nm occurs upon changing the pH in the range 7 45 - 1 14 pH units with an isosbestic point being observed at 512 nm Upon further acidification in the pH range 1 14 - 0 00 pH units, the λ_{max} of absorption further shifts from 523 nm to 545 nm with a second isosbestic point being maintained at 555 nm Two separate pK_a steps are occurring Due to the fact that no pK_a steps were detected for the other complexes in this pH region, it is reasonable to assume that these pK_a steps are due to (de)protonation of the two pyridine rings[48] in the tpt ligand, and not due to (de)protonation of the triazine ring Again (de)protonation of the triazine ring occurs outside our range of measurements The pK_a values for (de)protonation of the pyridine rings were calculated to occur at

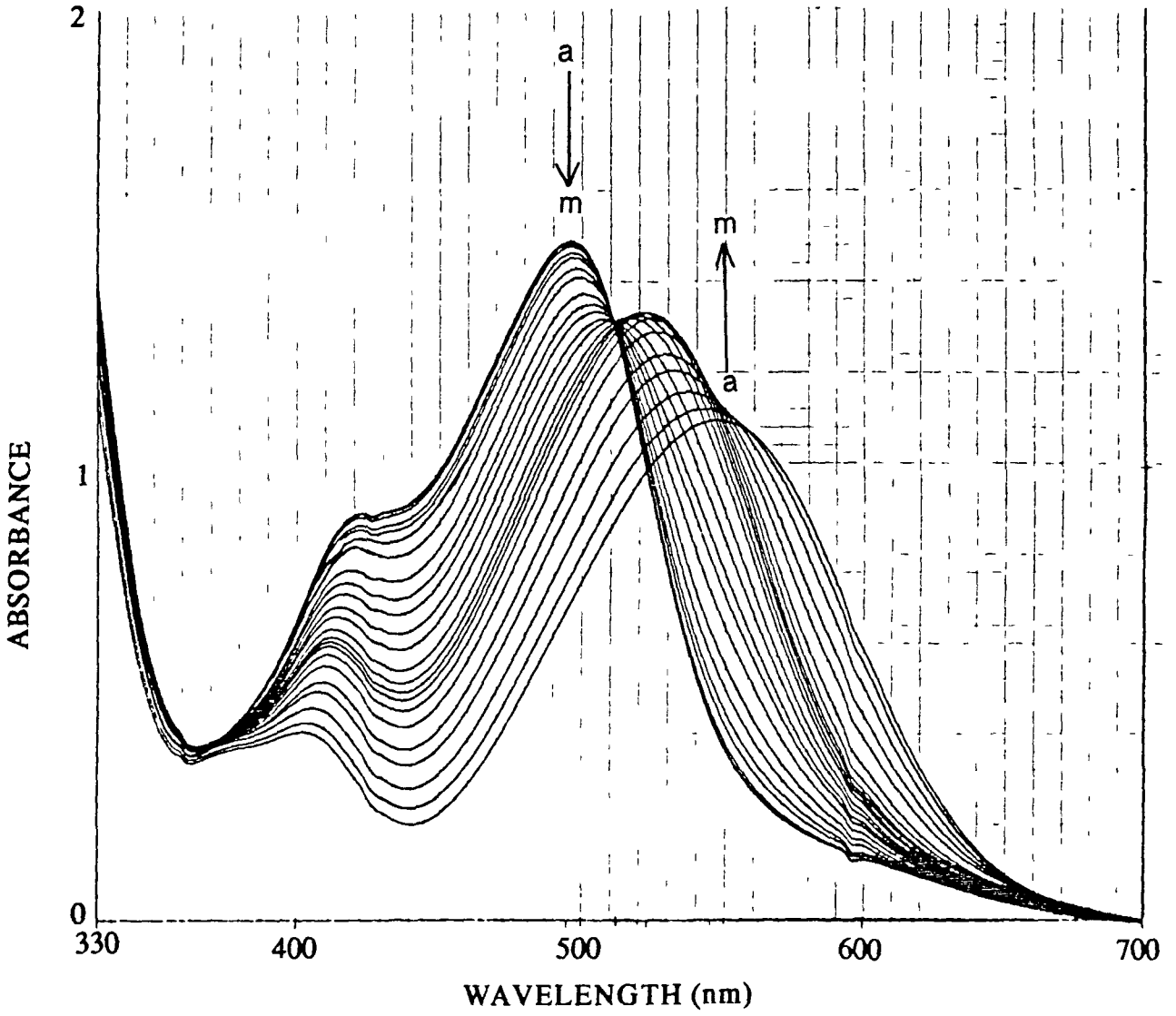

Figure 7 3 3

Changes in the absorption spectrum in MeCN as a function of pH for $[Ru(bpy)_2(tpt)]^{2+}$ (a) pH 7 41 (m) pH 0 00 using H_2SO_4

pH 1 26 and pH 0 6 Both pH dependent steps were found to be reversible

7 3 4 *Electrochemical properties*

The electrochemical properties of the triazine complexes are presented in Table 7 3 For the ruthenium compounds containing dipyridyl or diphenyl substituted pyridyltriazines as ligands and for $[Ru(bpy)_2(pt)]^{2+}$, the $Ru^{II/III}$ oxidation potentials have been shifted to more positive values compared with those of $[Ru(bpy)_3]^{2+}$, while the ligand based reduction potentials have been shifted to less negative values, indicating that the triazine ligands are stronger π-acceptors than bpy[58-60]

A comparison with results obtained by Hage et al[33] suggest that the first reduction potential of $[Ru(bpy)_2(dppt)]^{2+}$ is approximately the same as that of $[Ru(dppt)_3]^{2+}$, while the second reduction potential occurs at the same value as that of the first reduction potential of $[Ru(bpy)_3]^{2+}$, indicating that the first reduction step is dppt-based for this compound

Compared with the analogous dppt, tpt and pt compounds, the oxidation potentials of $[Ru(bpy)_2(dmpt)]^{2+}$ are less positive and the first reduction wave is observed at a much more negative potential This indicates that the difference between the lowest π* level (or LUMO) and the filled d-orbitals (or HOMO) is larger in the case of complexes with dmpt[61-64] and the dmpt ligand is therefore a weaker π-acceptor in comparison with the other triazine ligands The reduction potential is still less negative than the first reduction potential of $[Ru(bpy)_3]^{2+}$, indicating that the triazine ligand is reduced first The second two reduction potentials for all the complexes studied here are bpy-based reductions[65-66] All the results indicated that the lowest π* levels of the complexes are pyridyltriazine based

For the dinuclear compound, two oxidation potentials are observed Figure

Compound	Oxidation Pot. (V)	Reduction Pot. (V)
$[Ru(bpy)_2(pt)]^{2+}$	1 41	-0 80 -1 48 -1 71
$[Ru(bpy)_2(dmpt)]^{2+}$ (1)	1 28	-1 13 -1 50 -1 77
$[Ru(bpy)_2(dmpt)]^{2+}$ (2)	1 30	-1 16 -1 50 -1 77
$[Ru(bpy)_2(dppt)]^{2+}$	1 35	-0 88 -1 57 -1 79
$[Ru(bpy)_2(tpt)]^{2+}$	1 42	-0 78 -1 50 -1 70
$[(Ru(bpy)_2)_2(pt)Cl]^{3+}$	0 92 1 55	-0 66 -1 40
$[Ru(bpy)_3]^{2+}$	1 22	-1 36 -1 53

Table 7 3

Electrochemical potentials (DPP) of the triazine compounds measured in acetonitrile containing 0 1 M TEAP Values in volts versus SCE

7 3 4 shows the CV of $[(Ru(bpy)_2)_2(pt)Cl]^{3+}$ in the potential range 0 - 1 8 V The first oxidation process occurring at 0 92 V is reversible However, the second oxidation process occurring at 1 55 V is irreversible The presence of the chloride ion is also confirmed by the low first oxidation potential observed[67] If it is assumed, therefore, that the first oxidation potential corresponds to a one electron oxidation of the monodentate Ru-containing unit with co-ordinated Cl^- then the second oxidation process is due to the bidentate Ru-containing unit

Further investigation of the redox processes for this complex were carried out using spectroelectrochemistry in the UV/vis region of the absorbance spectrum (see Figure 7 3 5) [68] Upon generation of the mixed-valence $Ru^{III}Ru^{II}$ species i e using an applied potential of 1 30 V, the maxima at 438 nm and 597 nm are shifted to higher energy to 415 nm and 485 nm with a significant reduction of intensity

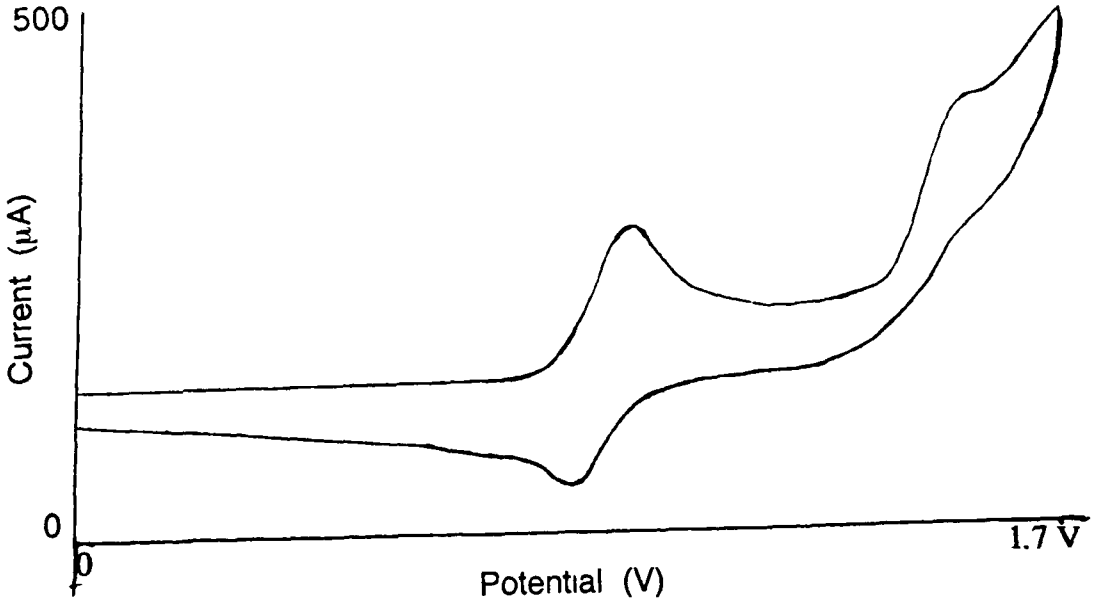

Figure 7 3 4

Cyclic voltammogram of the oxidation processes for $[(Ru(bpy)_2)_2(pt)Cl]^{3+}$ measured in acetonitrile / 0 1 M TEAP Scan rate 100 mV/sec

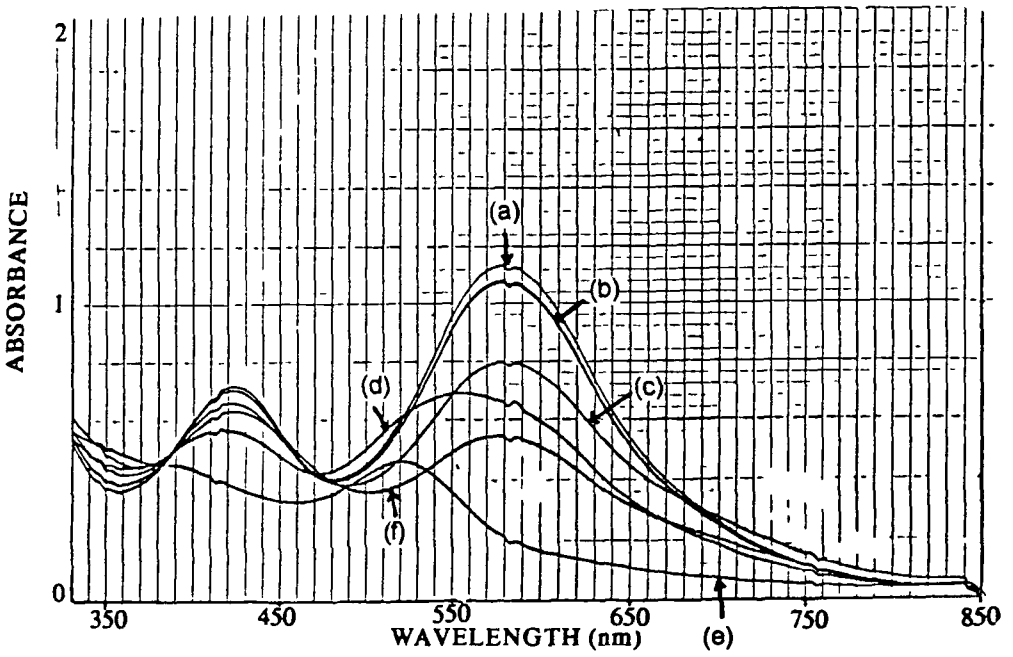

Figure 7 3 5

Spectroelectrochemistry in the UV/vis region of $[(Ru(bpy)_2)_2(pt)Cl]^{3+}$ in MeCN / 0 1 M TEAP Applied potentials are (a) 0 V, (b) 0 9 V, (c) 1 0 V, (d) 1 3 V, (e) 1.6 V, and (f) 0 9 V

When the applied potential is removed, the maxima return to their original values. The peak at 438 nm regains its original intensity and is, therefore, reversible However, the peak maximum at 597 nm has nearly disappeared and the redox process is, therefore, irreversible An electrochemically induced anion loss has occurred leading to this irreversibility as observed previously for $[Ru(bpy)_2(L)Cl]^+$ (where L = pyridine)[69]

Figure 7 3 6 contains the absorption and emission maxima (in eV) versus the difference between the first oxidation and first reduction potentials ($\Delta E_{1/2}$) for the triazine complexes Also included in the plot is a number of ruthenium compounds with pyridyltriazole ligands as reported previously[70-71] The absorption and emission maxima of the ruthenium compounds with dppt, pt and tpt correlate well with the electrochemical measurements, indicating that the same type of orbitals play a role in the absorption and emission processes as well as the oxidation and reduction processes of the complexes[72-73] The two dmpt complexes are not found in the linear region of the graph, suggesting that perhaps different ligands are involved in the absorption and emission processes compared with the electrochemical processes The luminescence does not come from the CT excited state involving the LUMO, but from a higher energy (thermally activated) excited state This phenonomen has been encountered previously for compounds containing the dipyrido-3,2-phenazine (DP) ligand[18]

It is also possible to calculate the excited-state redox potentials of these compounds by calculating the difference between the ground state and the excited state emission energy in eV according to the equations[74-75]

$$E_{1/2}^{3+/2+*} = E_{1/2}^{3+/2+} - E_{em} \qquad \textbf{7.1}$$

$$E_{1/2}^{2+*/+} = E_{1/2}^{2+/+} + E_{em} \qquad \textbf{7.2}$$

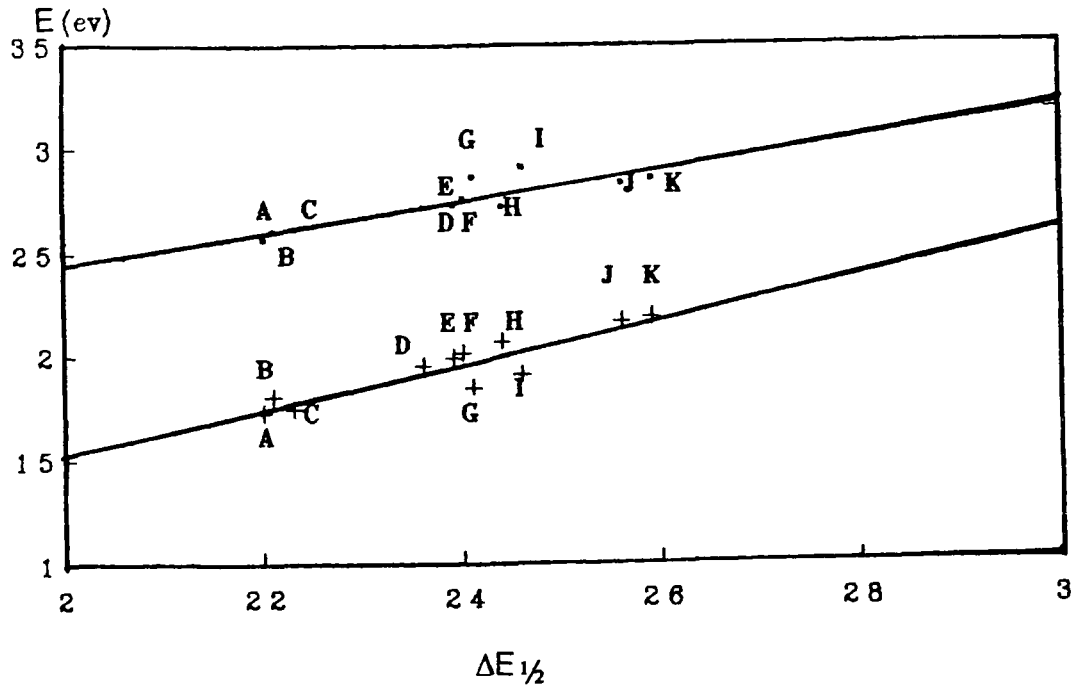

Figure 7 3 6

Plot of the (a) absorption and (b) emission energies versus $\Delta E_{1/2}$ for (a) $[Ru(bpy)_2(tpt)]^{2+}$,(b) $[Ru(bpy)_2(pt)]^{2+}$, (c) $[Ru(bpy)_2(dppt)]^{2+}$, (d) $[Ru(bpy)_2(3Mpztr)]^{2+}$, (e) $[Ru(bpy)_2(pztr)]^{+}$ isomer 2, (f) $[Ru(bpy)_2(1M5pztr)]^{2+}$, (g) $[Ru(bpy)_2(dmpt)]^{2+}$ isomer 1, (h) $[Ru(bpy)_2(pztr)]^{+}$ isomer 1, (i) $[Ru(bpy)_2(dmpt)]^{2+}$ isomer 2, (j) $[Ru(bpy)_2(1M3pztr)]^{2+}$ and (k) $[Ru(bpy)_3]^{2+}$

These values are presented in Table 7 4 The values are lower limits, since the luminescence energy contains a contribution from vibrational distortion between ground and excited states[19] The excited-state potentials indicate that the metals can behave as both photooxidants and photoreductants[28] As photoreductants, the triazine compounds have approximately the same driving force ($E_{1/2}^{3+/2+*}$ = 0 4 V) (with the exception of the dmpt compound and the dinuclear pt species),

Compound	$E_{1/2}^{3+/2+*}$	$E_{1/2}^{2+/+*}$
$[Ru(bpy)_2(pt)]^{2+}$	-0 39	+1 00
$[Ru(bpy)_2(dmpt)]^{2+}$ F1	-0 59	+0 74
$[Ru(bpy)_2(dppt)]^{2+}$	-0 39	+0 86
$[Ru(bpy)_2(tpt)]^{2+}$	-0 30	+0 94
$[(Ru(bpy)_2)_2(pt)Cl]^{3+}$	-0 94	+1 20
$[Ru(bpy)_3]^{2+}$	-0 77	+0 48

Table 7 4

Excited-state redox potentials of the triazine compounds calculated according to equations 7 1 and 7 2

whereas the photooxidants potentials vary in the order pt > tpt > dppt > dmpt E_{em} changes more rapidly than $E_{1/2}^{2+/+}$ as the ligands are changed[28] The results indicate that the triazine complexes are stronger photooxidants but weaker photoreductants than $[Ru(bpy)_3]^{2+}$, except for $[(Ru(bpy)_2)_2(pt)Cl]^{3+}$ which is both a weaker photooxidant and a weaker photoreductant than $[Ru(bpy)_3]^{2+}$. Therefore, it is possible that excited-state redox potentials may be varied systematically over a wide range of compounds of ruthenium(II) by the appropriate combination of ligands This has the benefit of extending the possible range of excited-state photocatalytic applications for Ru(II) polypyridyl compounds

7 3 5 *Luminescent lifetime properties*

All mononuclear complexes containing pyridyltriazine ligands exhibited photostability, i e , no appreciable photodecomposition was detected after five hours irradiation The dinuclear $[(Ru(bpy)_2)_2(pt)Cl]^{3+}$ complex showed partial photostability with a decomposition rate of ca 20% in 5 hours

The luminescent lifetimes of these compounds at room temperature and at 77 K are represented in Table 7 2 The lifetimes increased in the order of pt > dmpt > tpt > dppt A surprisingly long lifetime is observed at room temperature for the $[Ru(bpy)_2(dppt)]^{2+}$ complex The tris compound, $[Ru(dppt)_3]^{2+}$, was also prepared For this complex, which was not isolated sufficiently pure, a lifetime of 0 69 μs at room temperature was obtained Because of the relatively long luminescent lifetime of this complex, the emitting state of the mononuclear species was investigated in detail using temperature dependent luminescent lifetime measurements

The activation energies and exponential prefactors for the pt, dmpt and dppt compounds are presented in Table 7 5 The values obtained for $[Ru(bpy)_2(pt)]^{2+}$ and $[Ru(bpy)_2(dmpt)]^{2+}$ are the same within experimental error, suggesting that similar excited-state processes are occurring for these triazine ligands irrespective of the substitutions on the ligand However, the activation energy for $[Ru(bpy)_2(dppt)]^{2+}$ was significantly lower than for the other two complexes The low activation energies and prefactors of all the complexes are indicative of photostable species and suggest that thermally activated surface crossing to the ^3MC excited state cannot occur i e the energy gap between the ^3MLCT and ^3MC excited states is quite large[76-78]

Figure 7 3 7 shows the $\ln(1/\tau)$ versus $1/T$ plot obtained for these compounds As can be seen, there are significant differences in their temperature

Compound	E_a (cm^{-1})	A (s^{-1})
$[Ru(bpy)_2(pt)]^{2+}$	1356	9 67 x 10^8
$[Ru(bpy)_2(dmpt)]^{2+}$ isomer 1	1398	1 75 x 10^9
$[Ru(bpy)_2(dppt)]^{2+}$	1057	1 06 x 10^9

Table 7 5

Activation parameters and kinetic parameter for the triazine compounds as measured in ethanol methanol (4 1 v\v) Errors ± 10 %

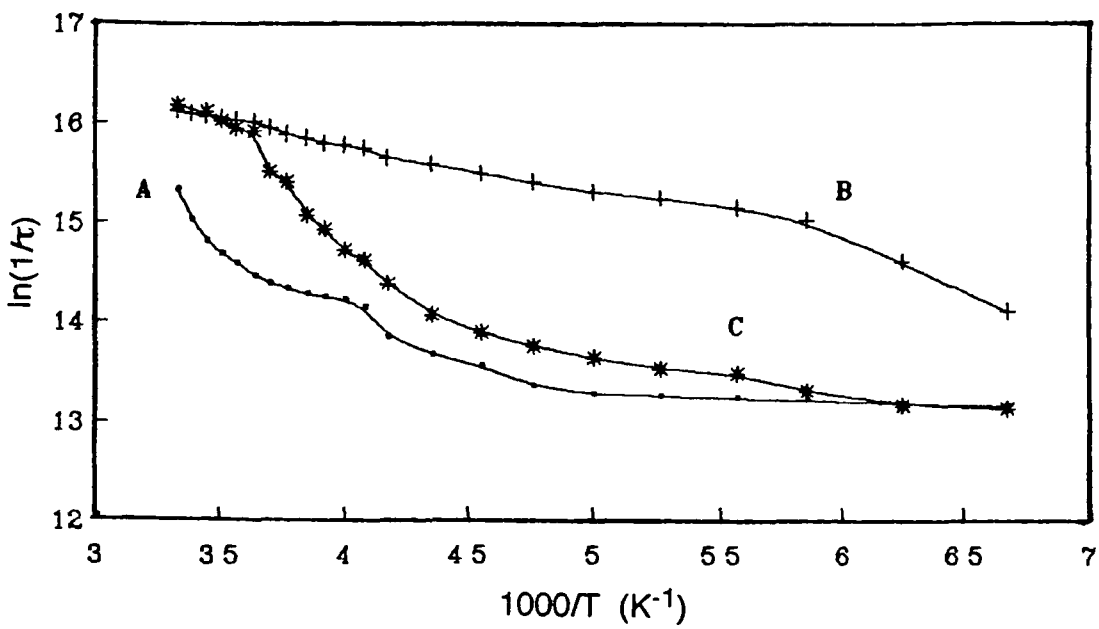

Figure 7 3 7

Plot of the ln(1/τ) versus 1/T for (a) $[Ru(bpy)_2(pt)]^{2+}$, (b) $[Ru(bpy)_2(dmpt)]^{2+}$ and (c) $[Ru(bpy)_2(dppt)]^{2+}$ in ethanol methanol (4 1 v/v) at temperatures > 150 K

dependent profiles A step occurs around 200 K for $[Ru(bpy)_2(pt)]^{2+}$ and $[Ru(bpy)_2(dppt)]^{2+}$, which is absent in the temperature dependence of $[Ru(bpy)_2(dmpt)]^{2+}$

Such a two-step behaviour, however, has a precedent in the case of $[Ru(bpy)_2(bpt)]^{+}$, where the second step was attributed to reorientation of the solvent molecules Such a reorientation is required by the strong change in the dipole moment caused by the Ru ----> bpy CT excitation and can only take place when the solvent has acquired the property of a non viscous fluid[79] We already know from the electrochemical data that the LUMO is pyridyltriazine based in these complexes Perhaps, the Ru ----> pyridyltriazine CT produced upon excitation also causes a strong change in the dipole moment which requires a reorientation of the solvent molecules

It is not clear why this step is absent in the $[Ru(bpy)_2(dmpt)]^{2+}$ complex The dmpt ligand is a weaker π-acceptor than the pt or dppt ligands and, therefore, it is possible that the dipole moment effect is not as pronounced Thus, the solvent molecules do not required the same degree of reorientation

The energy gap between the ground state and ^{1}MLCT excited state for $[Ru(bpy)_2(pt)]^{2+}$ and $[Ru(bpy)_2(dppt)]^{2+}$ was calculated to be 10850 cm^{-1} and 10164 cm^{-1} respectively The relative ground state energies are obtained from the Ru(II/III) potentials, while the approximate ^{1}MLCT state energies are obtained from the room temperature absorption maxima[80] However, the energy gap for $[Ru(bpy)_2(dmpt)]^{+}$ was found to be significantly larger (12250 cm^{-1}) Similarly, the energy gap between the ground state and the ^{3}MLCT excited state (calculated from the room temperature emission maxima) is larger for the complex containing the dmpt ligand This indicates that the excited state properties of this complex are different to those containing the other pyridyltriazine ligands, in agreement with the electrochemical data which suggests that this ligand is a weaker π-acceptor

The kinetic parameters for the three monomeric complexes have also been calculated and are presented in Table 7 6 The radiative rate constant, k_r, was found to increase in the order tpt < dppt < pt < dmpt Similarly, the same order was found for the non-radiative rate constant, k_{nr} As neither k_r or k_{nr} are constant throughout the series of compounds, this implies that the emitting state is different in each of the complexes[81-82] In other words, if the emitting state was the same for each of these compounds, the values of the radiative and non-radiative rate constants would likewise be similar Since the lowest π^* level involved in the emission process is based on the triazine ligand for all these complexes, this implies that the presence of a substituent on the pyridyltriazine ligand significantly effects the position of the LUMO

Compound	k_r (s^{-1})	k_{nr} (s^{-1})	ϕ_{em}
$[Ru(bpy)_2(pt)]^+$	3 53 x 10^3	1 94 x 10^5	1 58 x 10^{-4}
$[Ru(bpy)_2(dmpt)]^+$ isomer 1	1 53 x 10^4	1 59 x 10^5	9 43 x 10^{-4}
$[Ru(bpy)_2(dppt)]^+$	2 79 x 10^3	9 63 x 10^4	2 72 x 10^{-4}
$[Ru(bpy)_2(tpt)]^+$	2 10 x 10^3	1 36 x 10^5	2 52 x 10^{-4}
$[(Ru(bpy)_2)_2(pt)Cl]^{3+}$	1 28 x 10^4	1 90 x 10^5	8 14 x 10^{-4}

Table 7 6

The kinetic parameters for the triazine complexes ϕ_{em} w r t $[Ru(bpy)_3]^{2+}$, error ± 10% Rate constant error ± 5%

7.4 Conclusion

The nature of the lowest unoccupied molecular orbital (LUMO) is still of interest for these type of Ru(II) polypyridyl complexes as it controls, to a certain extent, the photochemical and photophysical properties of the compounds It is clear that replacement of the five-membered 1,2,4-triazole ring (as studied previously) by a six-membered 1,2,4-triazine ring, significantly alters the properties of the resulting complexes In fact, for 1,2,4-triazines the higher oxidation potentials and lower reduction potentials, suggest that the LUMO is triazine-based in these complexes The 1,2,4-triazine ligands can be placed in the class of stronger π-accepting and weaker σ-donating ligands compared to bpy

The increased photostability and long emission lifetimes observed for the 1,2,4-triazine complexes, even in the dinuclear complex, compared with previously studies bridging ligand, ensures that these complexes are of interest in the search for suitable photochemical molecular devices, as stability is a major requirement for a good photocatalyst

The observance of relative long lived emitting states for $[(Ru(bpy)_2)_2(pt)Cl]^{3+}$ is very interesting as normally in this sort of complex emission does not occur This coupled with the increased stability of this complex compared with $[Ru(bpy)_3]^{2+}$ ensures that the pyridyltriazine ligands are an important class of ligands with novel photophysical and photochemical properties

7.5 References

1 E M Kober and T J Meyer, *Inorg Chem*, **1984**, *23*, 3877

2 E M Kober, J L Marshall, W J Dressick, B P Sullivan, J V Caspar, and T J Meyer, *Inorg Chem*, **1985**, *24*, 2755

3 D P Rillema, D G Taghdiri, D S Jones, C D Keller, L A Worl, T J Meyer, and H A Levy, *Inorg Chem*, **1987**, *26*, 578

4 R Hage, R Prins, J G Haasnoot, J Reedijk, and J G Vos, *J Chem Soc, Dalton Trans*, **1987**, 1389

5 R Hage, A H J Dijkhuis, J G Haasnoot, R Prins, J Reedijk, B E Buchanan and J G Vos, *Inorg Chem*, **1988**, *27*, 2185

6 R Hage, J G Haasnoot, D J Stufkens, T L Snoeck, J G Vos, and J Reedijk, *Inorg Chem*, **1989**, *28*, 1413

7 B E Buchanan, R Wang, J G Vos, R Hage, J G Haasnoot, and J Reedijk, *Inorg Chem*, **1990**, *29*, 3263

8 R Hage, J G Haasnoot, J Reedijk, R Wang, E M Ryan, J G Vos, A L Spek, and A J M Duisenberg, *Inorg Chim Acta*, **1990**, *174*, 77

9 R Hage, J G Haasnoot, J Reedijk, and J G Vos, *Chemtracts - Inorg Chem*, **1992**, *4*, 75

10 C H Braunstein, A D Baker, T C Strekas, and H D Gafney, *Inorg Chem*, **1984**, *23*, 857

11 R M Berger, *Inorg Chem*, **1990**, *29*, 1920

12 G Di Marco, A Bartolotta, V Ricevuto, S Campagna, G Denti, L Sabatino, and G De Rosa, *Inorg Chem*, **1991**, *30*, 270

13 G Denti, S Serroni, S Campagna, V Ricevuto, and V Balzani, *Inorg Chim Acta*, **1991**, *182*, 127

14 P A Lay, R H Magnuson, and H Taube, *Inorg Chem*, **1988**, *27*, 2364

15 J T Hupp, G A Neyhart, and T J Meyer, *J Am Chem Soc*, **1986**, *108*, 5349

16 Md K Nazeeruddin and K Kalyanasundaram, *Inorg Chem*, **1989**, *28*, 4251

17 K Kalyanasundaram, Md K Nazeeruddin, M Gratzel, G Viscardi, P Savarino, and E Barni, *Inorg Chim Acta*, **1992**, *198-200*, 831

18 F Barigelletti, A Juris, V Balzani, P Belser, and A von Zelewsky, *Inorg Chem*, **1987**, *26*, 4115

19 D P Rillema, G Allen, T J Meyer, and D Conrad, *Inorg Chem*, **1983**, *22*, 1617

20 G H Allen, R P White, D P Rillema, and T J Meyer, *J Am Chem Soc*, **1984**, *106*, 2613

21 T S Akasheh, P C Beaumont, B J Parsons, and G O Phillips, *J Phys Chem*, **1986**, *90*, 5651

22 S D Ernst and W Kaim, *Inorg Chem*, **1989**, *28*, 1520

23 F Barigelletti, A Juris, V Balzani, P Belser, and A von Zelewsky, *J Phys Chem*, **1986**, *90*, 5190

24 A Juris, P Belser, F Barigelletti, A von Zelewsky, and V Balzani, *Inorg Chem*, **1986**, *25*, 256

25 R J Crutchley and A P B Lever, *J Am Chem Soc*, **1980**, *102*, 7129

26 R J Crutchley and A P B Lever, *Inorg Chem*, **1982**, *21*, 2276

27 K R Barqawi, A Llobet, and T J Meyer, *J Am Chem Soc*, **1988**, *110*, 7751

28 D P Rillema, C B Blanton, R J Shaver, D C Jackman, M Boldaji, S Bundy, L A Worl, and T J Meyer, *Inorg Chem*, **1992**, *31*, 1600

29 M Furue, K Maruyama, T Oguni, M Naiki, and M Kamachi, *Inorg Chem*, **1992**, *31*, 3792

30 S F McClamaham, R F Dallinger, F J Holler, and J R Kincaid; *J Am. Chem Soc*, **1985**, *107*, 4853

31 G Denti, S Serroni, L Sabatino, M Ciano, V Ricevuto, and S Campagna, *Gazz Chim Ital*, **1991**, *121*, 37

32 T J Meyer, Prog *Inorg Chem*, **1983**, *30*, 389

33 R Hage, J H van Diemen, G Ehrlich, J G Haasnoot, D J Stufkens, T L. Snoeck, J G Vos, and J Reedijk, *Inorg Chem*, **1990**, *29*, 988

34 R P Thummel and Y Jahng, *Inorg Chem*,, **1986**, *25*, 2527

35 C J Fitzpatrick, H A Goodwin, A Launikonis, A W H Mau, and W H F Sasse, *Aust J Chem*, **1983**, *36*, 2169

36 J M Kelly, C Long, C M O'Connell, J G Vos, A H A Tinnemans, *Inorg Chem*, **1983**, *22*, 2818

37 P J Steel, F Lahousse, D Lerner, and C Marzin, *Inorg Chem*, **1983**, *22*, 1488

38 P J Steel and E C Constable, *J Chem Soc, Dalton Trans*, **1990**, 1389

39 R Hage, A H J Dijkhuis, J G Haasnoot, R Prins, J Reedijk, B E Buchanan, and J G Vos, *Inorg Chem*, **1988**, *27*, 2185

40 F E Lytle, L M Petrosky, and L R Carlson, *Anal Chim Acta*, **1971**, *57*, 239

41 E C Constable and J Lewis, *Inorg Chim Acta*, **1983**, *70*, 251

42 B D J R Fennema, R Hage, J G Haasnoot, J Reedijk, and J G Vos, *Inorg Chim Acta*, **1990**, *171*, 223

43 P B Hitchcock, K R Seddon, J E Turp, Y Z Yousif, and J A Zora, E C Constable, and O Wernberg, *J Chem Soc, Dalton Trans*, **1988**, 1837

44 R Hage, Thesis, **1991**, The Netherlands

45 W Tang, D Chen Z Liu, and A Dai, *Sci China, Ser B*, **1991**, *34*, 8, 897

46 J D Birchall, T D O'Donaghue, and J R Wood, *Inorg Chim Acta*, **1979**, *37*, L461

47 A Juris, V Balzani, F Barigelletti, S Campagna, P Belser, and A von Zelewsky, *Coord Chem Rev*, **1988**, *84*, 85

48 J P Collin and J P Sauvage, *Inorg Chem*, **1986**, *25*, 135

49 M T Indelli, C A Bignozzi, A Marconi, and F Scandola, *J Am Chem. Soc*, **1988**, *110*, 7381

50 E V Dose and L J Wilson, *Inorg Chem*, **1978**, *17*, 9, 2660

51 M Haga, *Inorg Chim Acta*, **1983**, *75*, 29

52 A M Bond and M Haga, *Inorg Chem*, **1986**, *25*, 4507

53 S M Geraty and J G Vos, *J Chem Soc, Dalton Trans*, **1987**, 3073

54 C Long and J G Vos, *Inorg Chim Acta*, **1984**, 125

55 J G Vos, *Polyhedron*, **1992**, *11*, 18, 2285

56 H A Nieuwenhuis, J G Haasnoot, R Hage, J Reedijk, T L Snoeck, D J Stufkens, and J G Vos, *Inorg Chem*, **1991**, *30*, 48

57 R Wang, J G Vos, R H Schmehl, and R Hage, *J Am Chem Soc*, **1992**, *114*, 6, 1964

58 D Sandrini, M Maestri, V Balzani, U Maeder, and A von Zelewsky, *Inorg Chem*, **1988**, *27*, 2640

59 R Hage, J G Haasnoot, J Reedijk, R Wang, and J G Vos, *Inorg Chem*, **1991**, *30*, 3263

60 K J Takeuchi, M S Thompson, D W Pipes, and T J Meyer, *Inorg Chem*, **1984**, *23*, 1845

61 S Ernst and W Kaim, *Inorg Chem*, **1989**, *28*, 1520

62 D P Rillema and K B Mack, *Inorg Chem*, **1982**, *21*, 3849

63 J V Caspar and T J Meyer, *Inorg Chem*, **1983**, *22*, 2444

64 D P Rillema, G Allen, T J Meyer, and D Conrad, *Inorg Chem*, **1983**, *22*, 1617

65 D P Rillema, R W Callahan, and K B Mack, *Inorg Chem*, **1982**, *21*, 2589

66 A Kirsch-De Mesmaeker, L Jacquet, A Masschelein, F Vanhecke, and K Heremans, *Inorg Chem*, **1989**, *28*, 2465

67 G Denti, S Serroni, S Campagna, V Ricevuto, A Juris, M Ciano, and V Balzani, *Inorg Chim Acta*, **1992**, *198-200*, 507

68 B E Buchanan, P Degn, J M P Velasco, H Hughes, B S Creavan, C Long, J G Vos, R Howie, R Hage, J H van Diemen, J G Haasnoot, and J Reedijk, *J Chem Soc, Dalton Trans*, **1992**, *7*, 1177

69 B P Sullivan, D Conrad, and T J Meyer, *Inorg Chem*, **1985**, *24*, 2640

70 J V Caspar and T J Meyer, *Inorg Chem*, **1983**, *22*, 2444

71 E S Dodsworth and A B P Lever, *Chem Phys Letts*, **1985**, *119*, 1, 61

72 E S Dodsworth and A B P Lever, *Chem Phys Letts*, **1984**, *112*, 6, 567

73 E S Dodsworth and A B P Lever, *Chem Phys Letts*, **1986**, *124*, 2, 152.

74 C M Elliot, R A Freitag, and D D Blaney, *J Am Chem Soc*, **1985**, *107*, 4647

75 D P Rillema, J K Nagle, L F Barringer, and T J Meyer, *J Am Chem. Soc*, **1981**, *103*, 56

76 F Barigelletti, A Juris, V Balzani, P Belser, and A von Zelewsky, *Inorg. Chem*, **1983**, *22*, 3335

77 J Van Houten and R J Watts, *J Am Chem Soc*, **1976**, *98*, 16, 4853

78 T J Meyer, *Pure & Appl Chem*, **1986**, *58*, 9, 1193

79 F Barigelletti, L De Cola, V Balzani, R Hage, J G Haasnoot, J Reedijk, and J G Vos, *Inorg Chem*, **1989**, *28*, 4344

80 B E Buchanan, R Wang, J G Vos,R Hage, J G Haasnoot, and J Reedijk, *Inorg Chem*, **1990**, *29*, 3263

81 G H Allen, R P White, D P Rillema, and T J Meyer, *J Am Chem. Soc*, **1984**, *106*, 2613

82 E M Kober, J V Caspar, R S Lumpkin, and T J Meyer, *J Phys Chem*, **1986**, *90*, 3722

CHAPTER 8

FINAL REMARKS AND FUTURE WORK

In this thesis, the photochemical, photophysical and electrochemical properties of a wide range of Ru(II) diimine complexes containing substituted 1,2,4-triazoles has been investigated Several new Ru(II) and Os(II) complexes containing pyridyl- and pyrazyltriazole ligands have been synthesised and characterised Some novel complexes containing pyridyltriazine ligands have also been made Their photophysical properties have been analysed and, in particular, the temperature dependent luminescent lifetime measurements of a number of complexes has been studied in detail The most interesting results obtained in this work are as follows

The isolation of a monodentate photolysis product:

To obtain a ruthenium complex containing a potentially chelating pyridyltriazole ligand bound in a monodentate fashion, both thermal as well as photochemical methods were employed For both types of species, complexes which contained the monodentate co-ordinated ligands bound through a non-chelating nitrogen of the triazole ring Where the second chloride atom is strongly co-ordinated to the metal centre, steric considerations prevail A photochemically induced slippage of the co-ordination bond from the N2 to the N1 atom of the ligand occurs This change in co-ordination site can be reversed by photochemical as well as thermal means Normally, photolysis of ruthenium diimine complexes leads to loss of ligands, the regeneration of a bidentate co-ordination mode has not so far been observed

The photostability of Ru(II) complexes containing triazoles:

Photostability has been observed for a number of Ru(II) complexes containing triazoles These include both isomers of $[Ru(bpy)_2(pztr)]^+$,

$[Ru(bpy)_2(bpt)]^+$, $[Ru(bpy)_2(bpzt)]^+$, both isomers of $[Ru(bpy)_2(ppt)]^+$, all of the pyridyltriazine complexes and all of the osmium species

This is a very interesting property as it is essential for the fundamental application of these species as photosensitizers in solar energy conversion systems Although over 300 different Ru(II) complexes have been synthesised in the past few years, only a very small number of these are found to be stable Most of these photoinert complexes contain at least one good π-acceptor ligand 1,2,4-triazole ligands are good σ-donors and, therefore, these type of compounds are relatively rare It is also interesting to note that protonation / deprotonation can control the photochemical reactivity of these complexes as seen with compounds containing the Hpztr ligand

Photoinduced linkage isomerism

Photoinduced linkage isomerism has been observed for the two isomers of $[Ru(bpy)_2(Hpztr)]^{2+}$ Such behaviour has only been noted previously for complexes containing the analogous Hptr ligand and is, therefore, quite novel

The nature of the emitting state in mixed polypyridyl complexes:

Using time resolved resonance Raman spectroscopy the nature of the emitting state in mixed bpy/phen compounds was found to be bpy-based This is a particularly interesting observation, as neither the ligand-based reductions nor the ground-state resonance Raman spectra could discriminate between the ^{1}MLCT levels of the two polypyridyl ligands The nature of the emitting charge transfer states is solely determined by the nature of the polypyridyl ligand, but the location of the first metal-based oxidation is controlled by the asymmetry of the bpt^- ligand

pH control of the nature of the emitting state:

It has already been found that for a series of Ru(II) compounds containing pyrazyltriazole ligands, such a Hpztr and Hbpzt, it is found that the LUMO is bpy-based when the triazole ring is deprotonated, but upon protonation the emitting state becomes pyrazyltriazole-based This switch-over to bridging ligand based emission also occurs upon formation of a dinuclear complex It is interesting to note that in the highly asymmetric Hppt ligand, the emission also becomes bridging ligand based upon formation of a dinuclear species or upon protonation of the pyrazine-bound mononuclear species (Upon protonation of the pyridine-bound mononuclear complex the emission remains bpy-based) This suggests that for this ligand, the pyrazine ring significantly lowers the π^* level of the ppt^- ligand and, therefore, dominates the emission process

Complexes with strong π-acceptor ligands:

The Ru(II) compounds containing the strong π-acceptor ligands were all found to be photostable In addition, the luminescent lifetimes of these complexes were comparable to those obtained for $[Ru(bpy)_3]^{2+}$ In fact, $[Ru(bpy)_2(dppt)]^{2+}$ was found to have a room temperature luminescent lifetime of the order of 1 µs This complex could, therefore, become increasingly important for its application as a photosensitizer in solar energy conversion systems

A number of questions have arisen in this thesis which have not been fully clarified These questions are as follows

1. Why is there a linear relationship between the activation energies and the number of phen ligands in a complex?

The properties of phen and bpy polypyridyl ligands are very similar It is unclear why the phen ligands have much smaller activation energies compared to their bpy analogues

2. Why is the lifetime of $[Ru(phen)_2(bpt)]^+$ longer lived than that of $[Ru(bpy)_2(bpt)]^+$, but the lifetime of $[(Ru(phen)_2)_2(bpt)]^{3+}$ is significantly shorter than that of $[(Ru(bpy)_2)_2(bpt)]^{3+}$?

Upon formation of a dinuclear species, the lifetime decreases by a factor of four for the bpy-containing species, but by a factor of twenty for the phen-containing complexes The addition of a second $Ru(bpy)_2$ (or $Ru(phen)_2$) moiety makes the deactivating ^3MC excited states accessible at room temperature, due to a decreased σ-donor ability of the bridging ligand However, it is unclear why the effect is so large for phen-containing complexes Other factors must be playing a role in decreasing the lifetime of the dinuclear species

3. Why are the photochemical properties of the dinuclear complexes containing the three structurally similar bridging ligand bpt^-, ppt^-, and $bpzt^-$ so different?

Although, some theories as to why the photochemical properties of these three complexes are so different, it is still unclear how the pyrazine-ring is effecting the photochemical properties of these complexes

1. Why is there a linear relationship between the activation energies and the number of phen ligands in a complex?

The properties of phen and bpy polypyridyl ligands are very similar It is unclear why the phen ligands have much smaller activation energies compared to their bpy analogues

2. Why is the lifetime of $[Ru(phen)_2(bpt)]^+$ longer lived than that of $[Ru(bpy)_2(bpt)]^+$, but the lifetime of $[(Ru(phen)_2)_2(bpt)]^{3+}$ is significantly shorter than that of $[(Ru(bpy)_2)_2(bpt)]^{3+}$?

Upon formation of a dinuclear species, the lifetime decreases by a factor of four for the bpy-containing species, but by a factor of twenty for the phen-containing complexes The addition of a second $Ru(bpy)_2$ (or $Ru(phen)_2$) moiety makes the deactivating ^3MC excited states accessible at room temperature, due to a decreased σ-donor ability of the bridging ligand However, it is unclear why the effect is so large for phen-containing complexes Other factors must be playing a role in decreasing the lifetime of the dinuclear species

3. Why are the photochemical properties of the dinuclear complexes containing the three structurally similar bridging ligand bpt^-, ppt^-, and $bpzt^-$ so different?

Although, some theories as to why the photochemical properties of these three complexes are so different, it is still unclear how the pyrazine-ring is effecting the photochemical properties of these complexes

4. Why are the temperature dependent profiles of the three triazine complexes so different?

The only difference between the ligands pt, dmpt and dppt lies in the presence of substituents on the pyridine ring Although, it is expected that the inductive effects of the substituents should effect their excited-state lifetimes, it is not clear why the profiles are so totally different for these three complexes

Further work:

More detailed investigations are needed in order to find possible answers to some of these questions

It would be interesting to synthesise phen-containing complexes with the ligands bpzt$^-$ and ppt$^-$ and to investigate their photophysical properties and, in particular, to see if these complexes show similar excited-state behaviour as was found for the bpt$^-$ complexes It may also be interesting to synthesise mixed-ligand polypyridyl complexes of the ppt$^-$ ligand in order to investigate if the pyrazine ring in the bridging ligand or the presence of different auxiliary polypyridyl ligands would dominate its excited-state properties

A much more detailed investigation of the pyridyltriazine complexes is necessary, especially a detailed photophysical study of the unusual dinuclear complex It would be interesting to examine further the effect of substituents on the physical properties of these complexes

Furthermore, a single crystal structure of the dinuclear $[(Ru(bpy)_2)_2(ppt)]^{3+}$ species is crucial for confirming the co-ordination mode for this complex Also, a single crystal structure of the dinuclear $[(Ru(bpy)_2)_2(pt)Cl]^{3+}$ complex is necessary in order to investigate its mononuclear co-ordination mode

The complexes containing the ppt$^-$ ligand have very unusual excited-state properties It would be necessary to carry out more detailed resonance Raman

studies on all of these complexes In particular, time resolved resonance Raman spectroscopy may enable some insight into the excited-state processes occurring for these compounds